Smart formulation for precise crop protection

Steven James Banks

Submitted in fulfilment of the requirement for the degree of Doctor of Philosophy

December 2019

Abstract

Post-emergence selective herbicides are an important part of the management of competitive weed species within crops, with delivery through the use of formulation being a key factor in their effective use. As a result of increasing environmental concern and stricter regulation on herbicide usage, there is a progressive move away from solvent based herbicide formulations to more environmentally friendly water-based systems, such as suspension concentrates (SC). Effective delivery of the active ingredient is often a major limitation to SC formulations, being highly dependent on chemical additives known as adjuvants. In this project we have examined the effect of varying the adjuvant chemistry on the delivery of SC formulated herbicides using wheat (*Triticum aestivum*) as the crop and blackgrass (*Alopecurus myosuroides*) and ryegrass (*Lolium multiflorum*) as the weeds targeted for control. The herbicides selected for the study were cyhalofop-butyl, diuron, metolachlor, flufenacet and propyzamide. Several biomarkers of primary herbicide delivery were assessed, including stress-inducible genes as determined using qPCR, and absorbed active ingredient and immediate detoxification products, monitored by liquid chromatography coupled to mass spectroscopy (LCMS). Changes in the expression of the stress-responsive genes catalase, GST23, GSTF1, gstu2, HSP90, RGA4, and ATP synthase over the timescales of interest (0 – 16 hours post treatment) proved unreliable. Instead, emphasis was placed on identifying primary detoxification products of herbicides effectively formed spontaneously on uptake *in planta*.

Of the five herbicides tested, metolachlor and flufenacet proved the most tractable, as both undergo spontaneous conjugation with glutathione when taken up into plant cells, with the conjugates being readily detectable by LCMS. With further refinement of the analytical technology, this approach focussed on flufenacet, a herbicide of increasing importance in grass weed control, which following its glutathionylation is then processed into a sequential series of catabolites of the conjugate notably glutamyl-cysteine, cysteinyl-glycine and cysteine flufenacet conjugates. By monitoring the levels of these flufenacet metabolites over time, it proved possible to measure the uptake, bioavailability, and metabolism of the herbicide as a dynamic process.

Wheat, blackgrass, and ryegrass were treated with flufenacet formulations containing 10% (w/w) of a “Tween” and “Tween L” series of adjuvants. Herbicide uptake and metabolism

were greater in both blackgrass and ryegrass than in wheat with all adjuvants tested. Whereas varying adjuvant type had little effect on flufenacet uptake in wheat, with the weeds, the Tween series showed a step-wise change in uptake rate correlating with the level of ethoxylation, with Tween 22 (8 repeat units of polyethylene glycol) resulting in the greatest uptake and Tween 20 (20 repeat units of polyethylene glycol) resulting in the least.

To explain these results, the droplet properties of the applied formulations were observed by looking at contact angle, surface tension, dry down distribution, and drying time, to determine influence on uptake. Additionally, the surface characteristics of leaves of each plant were explored looking at the composition of the waxy cuticle by gas chromatography coupled mass spectroscopy (GC-MS) and gas chromatography couple flame ionisation (GC-FID). Wheat tended to have higher chain length compounds composing the waxy cuticle, giving rise to a more hydrophobic surface and a reduced contact angle of applied herbicides. Both blackgrass and ryegrass shared several similarities in waxy chemical composition, such as 1-Hexacosanol being the predominant chemical within each, giving rise to similar levels of contact angle regression on herbicide application.

Using metabolite formation as a highly sensitive marker of the initial stages of herbicide uptake our studies demonstrate that varying Tween adjuvant chemistry can enhance delivery in grass weeds, while having no significant effects on the crop. This differential uptake can be explained by differences in the formulated herbicide's behaviour on the surface of these grasses, which are in turn dependent on surface hydrophobicity. Further refinements in adjuvant chemistry show new potential in enhancing grass weed control in wheat using existing selective herbicides. With further study these results could be applied to additional actives and weed species to best optimise herbicide formulations for delivery and control.

Table of Contents

List of Figures

List of Tables

Declaration and copyright

The material presented here is the result of the author's work, except where explicitly stated. Contributions to this work by others or references to others' work have been duly acknowledged. This material has not been submitted for any other degree at Newcastle University or any other institution.

Acknowledgements

Firstly, I would like to thank my supervisor Professor Rob Edwards. Your continued insight, support and understanding has been imperative to the completion of this project. I've managed to learn so much over the last four years and I can't thank you enough for that.

I would like to thank all the members of the RE group, old and new, for all the help and guidance both in the lab and in the long and arduous write up process. I would like to acknowledge Melissa Brazier-Hicks for all her help getting started in the lab prior to your move to Syngenta, and Nawaporn Onkokesung for taking over this role and continuing to offer me help and support. I would also like to extend my thanks to Sara Ortega who, despite being a more recent addition to the RE group, has helped immensely in the proof reading and formatting of my thesis. Best of luck to both Stewart and Gabby in your final couple of years.

Phil and George, it's been a long four years and somehow, we don't now hate each other. Congratulations to both of you for making it through and thanks for being there through the good and the bad. Additional thanks to James for drinking endless amounts of tea with me and Mac for his life coaching skills.

Thank you to Newcastle University for hosting my research and to BBSRC and Croda for providing sponsorship. I would like to thank everyone at Croda for being so helpful and accommodating during my visits there. In particular, I would like to offer my thanks to Kathryn Knight, my Croda supervisor, as well as Marie-Capucine and Amy Dyde for your help and supervision during my time in the lab at Croda.

Last but not least I would like to thank my family and friends for your unwavering support and encouragement. Thanks go to my parents for putting up with my PhD ramblings and encouragement during some trying times. Thank you to Beth for being able to take my mind off my ever-consuming PhD and provide some respite.

1 Introduction

1.1 Overview

Weeds are among the most important biological constraints on cropping efficiency, competing with crop plants for nutrients, water, light and space, as well as harbouring pathogens and insect pests (Iqbal et al., 2019). Weed management is an essential part of modern agriculture, being used within crop production systems across the world (Gage et al., 2019). Herbicides are chemical compounds designed to kill or supress plants by affecting one or more process vital to plant survival. Herbicides have become a staple of modern agriculture over the last 70 years providing effective, economical weed control estimated to prevent the loss of up to 45% of food crops worldwide (Hilz et al., 2013). Herbicides have replaced less effective weed control measures such as manual and mechanical weeding, and in combination with better agricultural practices have let to large increases in yields (Heap, 2014). Herbicides can be classified in several ways based on use, chemistry, mode of action, selectivity, and application timing. Based on application timings herbicides fall into one of two categories, pre-emergence, or post-emergence. Pre-emergence herbicides are applied prior to the emergence of weeds and are soil mobile acting on germinating weed seedlings before any significant growth can occur. Post-emergence herbicides are applied directly once the weed has emerged from the soil and are taken up by absorption through foliar tissues (Z. Li et al., 2017). Often herbicides will be best suited to being used in one case or the other however there are several chemistries which can be used both pre and post emergence, often formulated with differing co-formulants depending on intended application. Herbicides may be further classified as selective or non-selective (Case et al., 2005). Non-selective herbicides will indiscriminately affect both weed and crop plants (Ye et al., 2019). Selective herbicides only affect weeds but are often used with safeners to enhance their selectivity and reduce crop damage (Case et al., 2005). There are several ways by which this selectivity may be achieved, such as an inability of the herbicide to bind the target enzyme within the crop, the crop having an innately higher ability to detoxify the enzyme, or a lesser propensity for uptake within the crop plant (Carvalho et al., 2009).

1.2 Herbicide formulation

Herbicide formulation is an essential part of active delivery by enhancing a number of properties, namely optimising biological activity, improving long term stability, reducing

waste and environmental impact, and reducing required active dosage (Tominack et al., 2000). A wide variety of formulation types have been developed, with many actives having the potential to be formulated in multiple ways (Cush, 2006). As the development of new active ingredients has slowed in recent years and is considered financially high risk by many companies, the novel use of formulations opens up a potential means of extending the usability of available actives (Knowles, 2006). There are several factors which must be taken into consideration when deciding on the type of formulation and nature of co-formulants to be used. The physiochemical properties of the active ingredient will have a large impact on formulation and is commonly the major determinant in how the active will be formulated. As most actives are not water soluble, it is especially important to add supplementary components to allow dilution in water prior to spraying. Additional factors such as environmental impact, mode of action, and means of application are also taken into consideration during formulation (Pontzen, 2007).

There are four primary ways by which herbicides may be formulated: as a solution, a suspension, an emulsion, or by sorption onto a solid surface. A solution consists of a solid or liquid active dissolved in a solvent. Once mixed, a solution will require no agitation and components cannot be mechanically separated. A suspension consists of solid particles dispersed within a liquid medium, usually water. The particles do not dissolve within the liquid and are instead held in suspension with the use of surfactants and wetting agents. Suspensions also have the potential for particles to settle and so must be kept under agitation to maintain an even particle distribution (Tominack & Tominack, 2000). An emulsion is made up of two immiscible liquids, with one dispersed as a droplet within the other. The active is soluble and dissolved in whichever liquid forms the dispersed droplets within the emulsion (Manthey et al., 1989). Sorption is the adhering of a liquid active onto a solid surface such as clay. This can be achieved by one of two mechanisms; adsorption, a chemical or physical attraction between the active ingredient and the surface of the solid in question, or absorption, the entry of the active into pores of the solid (Martin et al., 2011).

1.2.1 Solid formulations

Herbicides formulations can be divided into two principle categories, solid and liquid formulations. Solid formulations can be further divided into those which are either ready to use or must first be mixed with water and applied as a spray. There are several dry, solid

formulation types such as dusts, granules, wettable powders, water dispersible granules, and soluble powders (Ferrell, 2004).

Dust formulations consist of a dry powder made by sorption of an active ingredient, usually at a rate of 1 - 10% w/w, on a very finely ground, inert, dry carrier particle such as clay or chalk. Dusts are ready to use and applied as dry formulations providing good coverage due to the small particle size. This small particle size however makes dust formulations very susceptible to drift, as well as posing an inhalation hazard during both manufacture and use (Martin et al., 2011). Despite the potential draw backs of dust formulations, dusts are cheap to manufacture, do not involve the use of solvents, and can be made from a range of actives so remain a popular formulation type (Knowles, 2006).

Granular formulations are solid, ready to use, preparations used for pre-emergence control, typically containing 1-40% w/w active depending on the chemistry used. Granular formulations are produced similarly to dusts, with the sorption of the active onto an inert solid. Unlike dusts they utilise larger, inert carrier particles, having the largest particle size of all solid formulations. This aids greatly in drift reduction with much reduced loss of the applied agrochemical when compared to powder or liquid based formulations. This large particle size however also results in lower efficacy and the need for greater active loading, as well as resulting in difficulty attaining uniform application compared to other formulation types. After application, granules are free-flowing and disintegrate into the soil to release a soil mobile active able to act pre emergence. Alternatively, some granular formulations may be dissolved or dispersed in water, referred to as water dispersible granules. Water dispersible granules form a suspension upon addition to water and are sprayed as a liquid formulation, allowing both pre and post emergence applications. Although offering a number of advantages such as increased stability, easy spillage recovery, and being easier to pour and measure than other solid formulations, granular formulations are a much more costly means of herbicide formulation (Martin et al., 2011; Wiwattanapatapee et al., 2009).

Wettable powders provide an avenue for formulating actives which are insoluble in both water and oil. Wettable powders consist of a dry, finely ground, inert carrier particle upon which an active is adsorbed or absorbed. They are formulated with dry surfactants to act as wetting and dispersing agents, allowing for wetting of the active bound particles and even dispersion of particles upon addition to water. Wettable powders differ from dust

formulations in that they are diluted in water where a suspension is formed, which can be applied as a spray (Sinha et al., 2016; Zimdahl, 2018). Wettable powders result in large particle size on addition to water, resulting in lower efficacy compared to many other formulation types, and therefore often use higher active loading than other formulation types. This large particle size helps to prevent spray drift, but also makes particles prone to sedimentation and so continual agitation is required during use to maintain an even suspension (Gray et al., 2017). This large particle size also makes wettable powders among the most abrasive formulation types on spray equipment where they are prone to causing blockages. This, alongside new formulation technologies, has resulted in a decrease in the frequency with which wettable powders are used (Zimdahl, 2018).

Soluble powders are among the more uncommon formulations types due to reliance on active ingredients with high water solubility. Soluble powders are added to water wherein they form a solution which can be applied by spraying. Soluble powders confer much of the same benefits as wettable powders, however, due to their solubility in water they do not require constant agitation once within the tank mix. Much like any fine powder, there is a risk of inhalation during both manufacturing and pouring, as well as a limited number of actives being available to be used in this way (Westra, 1998).

1.2.2 Liquid formulations

Liquid formulations make use of either a liquid active ingredient or solid active which is dissolved or dispersed within a liquid medium. Liquid formulations are either solvent based such as emulsifiable concentrates (EC) and oil-in-water (EW)/water-in-oil emulsions (WO), or water based such as suspension concentrates (SC) (Fenn et al., 1989).

Although unlikely to phase out entirely due to ease of formulation and comparatively high levels of efficacy, there has been a general move away from solvent based formulations due to increasing environmental concerns. Suspension concentrates (SC) are water-based formulations in which small particles of the water insoluble active are held in a stable suspension within an aqueous medium. Suspension concentrates are made by mixing the active with wetting and dispersing agents within an aqueous solution, followed by wet milling to attain a small particle size (range 1-10 μm). During milling, particle size is reduced to the desired range where the dispersing agent becomes adsorbed onto the particles of active to maintain the achieved size (Knowles, 2006; Pontzen, 2007). After milling, the active particles

will irreversibly flocculate due to Van der Waals forces, the rate of which being dependent on particle size distribution and active used. Dispersing agents are used to provide a contrasting force to maintain particle size and formulation stability. There are two means by which this repulsive force is achieved, through either electrostatic repulsion or steric hindrance. Electrostatic repulsion makes use of ionic surfactants wherein particles will be repelled from one another due to the shared charge of the surface adsorbed surfactants. Steric hindrance relies on the use of non-ionic surfactants in which a long, hydrophilic chain is adsorbed onto the particle. When two particles come within close proximity a repulsive force is exuded when these chains interact, preventing flocculation. Oftentimes these surfactant types are used in conjunction to provide greater long term stability (Khan et al., 2019; Xiaojing Li et al., 2016; Paria et al., 2004). Due to the hydrophobic nature of most active compounds, wetting agents are required to keep the surface of the milled particles wetted (Cush, 2006).

As shown in Figure 1, Emulsions are either formulated as an oil phase suspended within an aqueous phase (oil in water), or aqueous phase suspended within an oil phase (water in oil). Both make use of an immiscible solvent or oil, alongside surfactants and stabilising agents to form a stable emulsion. Water in oil emulsions comprise a water soluble active being dissolved in an aqueous phase, the droplets of which are suspended within an oil phase. Oil in water emulsions are the reverse, consisting of a solvent or oil soluble herbicide dissolved in the oil phase and suspended in an aqueous phase. Oil in water emulsions are becoming increasingly more popular due to the need to reduce solvent loading within formulations (Y. Li et al., 2019).

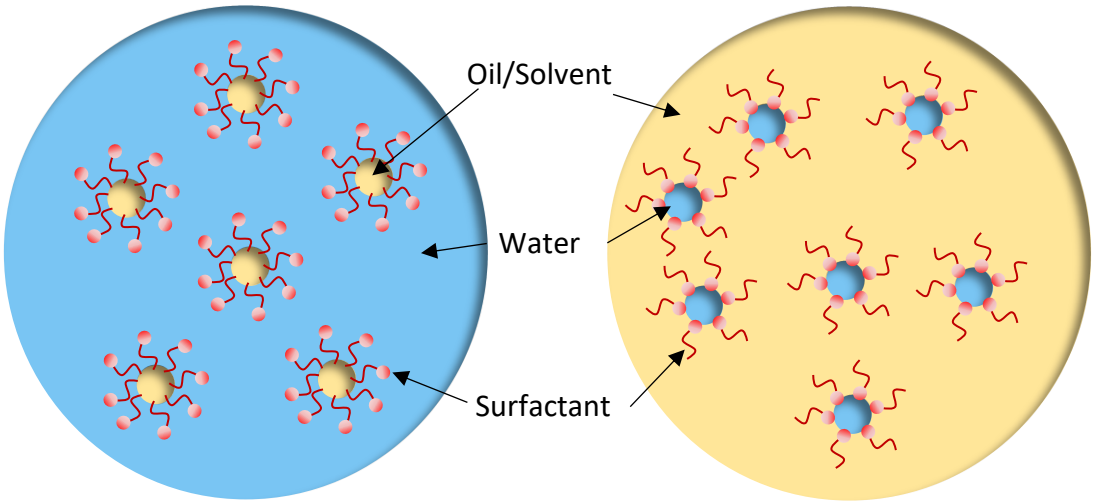

Figure 1. Oil in water with the lipophilic tail of the emulsifying agent within the oil droplet and the hydrophilic head within the water phase maintaining an evenly spread emulsion. The water in oil emulsion is the reverse with the lipophilic tails within the oil phase and hydrophilic heads the aqueous droplets.

Emulsifiable concentrates are among the most widely used herbicide formulations, accounting for an estimated 40% of global herbicide usage (Pontzen, 2007). Emulsifiable concentrates are formulated by dissolving a solid active within a water insoluble, oil or organic solvent alongside emulsifying agents, or adding emulsifying agents to a liquid active. Upon dilution in water, a spontaneous emulsion is formed with a droplet size range of 0.1 to 10 µm and water acting as a carrier, much like an oil in water emulsion. Due to the high level of solvent used within emulsifiable concentrates this poses a risk to both users and manufactures as well as the potential to cause greater environmental impact than water based formulations (Pontzen, 2007; Wiwattanapatapee et al., 2009).

1.3 Adjuvants

An adjuvant is a chemical additive within the herbicide formulation to help facilitate the mixing, application, or improve efficacy of the herbicide. Many adjuvants are already present within herbicide formulations although some may be added to the tank mix prior to application (Hazen, 2000). Adjuvants act in a number of ways and are typically categorised as either activator or utility adjuvants. Activator adjuvants act by enhancing uptake and effectiveness of the herbicide, such as increasing wettability and spreading across the application surfaces, whereas others function by enhancing penetration through the cuticular wax (Grant et al., 2008;Tu et al., 2003). Alternatively, utility adjuvants do not directly enhance

herbicide uptake but instead alter herbicide spray properties such as reducing spray drift or acting as an antifoaming agent. Adjuvants can be further categorised based on specific effects and chemistry (Basi et al., 2013).

1.3.1 Surfactants

Surfactants are surface active agents and are among the most widely used adjuvants. Surfactants can affect many herbicide spray properties such as the dispersing, spreading, sticking and wetting properties of the herbicide formulation. Surfactants cause a reduction in surface tension of the herbicide droplets, allowing for increased spreading of the herbicide across the application surface. This in turn reduces beading and run off of spray droplets, as well as increasing the contact area of active on the plant tissue. In addition, surfactants can also disrupt the crystalline structure and morphology of cuticular wax. This phenomenon known as plasticization, is thought to induce changes in the structural and mechanical properties of the leaf surface, facilitating herbicide uptake. Although not fully understood, it is thought the use of adjuvants may cause an increase in the fluidity of the amorphous wax layer. The result is a reduction in the tortuous nature of the diffusion pathway, creating a shorter route over which the herbicide must diffuse, thereby resulting in greater rates of diffusion (Burghardt et al., 2006; Grant et al., 2008). Surfactants can be further categorised based on charge, with non-ionic surfactants being the most prevalent. Non-ionic surfactants carry no net charge, are hydrophilic, and compatible with a wide range of active ingredients. They are generally biodegradable with many considered inert making them ideal for use in herbicide formulations. Ionic surfactants are either cationic (positive charge) or anionic (negative charge) and can be readily paired with herbicides of the opposite charge, increasing the solubility of polar herbicides within water (Curran et al., 1999). Ionic surfactants however may complex with other compounds within the formulation disrupting stability, and a number have been demonstrated as showing phytotoxicity to both weeds and crop species (Tu & Randall, 2003).

1.3.2 Oil Adjuvants

Oil adjuvants are used alongside formulations containing oil-soluble herbicides and are typically added separately to the tank mixture at 1% of the total spray volume. Due to the hydrophobic nature of oil, a surfactant emulsifier must be added to the tank mix alongside the oil so that droplets are evenly distributed throughout the mix. The exact means by which

oil adjuvants increase herbicide performance is not fully understood, however, several observations have been made: Oil adjuvants have been found to reduce formulation surface tension, thereby increasing surface contact of the herbicide and plant tissue and increasing the area over which the herbicide may diffuse. It has also been proposed that oil adjuvants may increase the fluidity of the cuticular wax, thereby increasing the rate of diffusion, as well as increasing droplet drying time, allowing the herbicide to remain as a mobile droplet for longer (Hazen, 2000).

1.3.3 Wetting and spreading agents

Wetting and spreading agents are largely encompassed within the surfactants category and act by lowering surface tension of the spray mix. This reduced surface tension allows for greater spreading across the plant tissue, increasing the area over which the herbicide has direct contact with the leaf surface for diffusion (Knowles, 2006). There is also evidence to support these adjuvants increasing uptake through stomatal infiltration or flooding (Hazen, 2000). Although wetting and spreading agents are often non-ionic surfactants, there are a number of wetting and spreading agents that only affect the spray droplet properties with no further influence such as disruption of the waxy cuticle and as a result are separately categorised (Knowles, 2006).

1.3.4 Drift control and foaming agents

As most herbicides are applied as a spray, drift can pose a serious problem to pedestrians, terrestrial and aquatic ecosystems, and other crops. Particularly in cases where a fine spray is used, herbicide droplets can easily be carried away from the target area by wind. It has become apparent that one of the biggest ways by which herbicides contribute to environmental pollution is via spray drift into none target areas. There are a few ways by which spray drift can be reduced, such as timing of herbicide application and the use of spray drift controlling adjuvants (Hilz & Vermeer, 2013). Drift control agents create a coarser spray, increasing the spray droplet size and weights. As small droplet sizes are much more prone to being carried by wind to non-target locations, increasing spray droplet size decreases the number of potentially windborne droplets. Drift control agents are commonly classified as either thickening agents, which increase viscosity of the tank mix, or deposit/sticker agents which reduce formulation loss from the target by enhancing droplet retention on the plant surface (Curran et al., 1999).

1.4 Herbicide uptake and barriers to foliar entry

The first major barrier for weed control is the initial application of the herbicide. It has been found that in extreme cases, as little as 1% of the originally applied active makes it to its intended target, with large amounts of this loss arising during spraying (Parween et al., 2016). Many plants prove difficult to wet and so droplets can be prone to beading and falling off the leaf surface, in addition to the potential losses from spray drift. As previously mentioned, the use of adjuvants can help alleviate both spray drift and increase droplet retention considerably (Knowles, 2006). When on the leaf surface, water and solvent of the droplet will progressively evaporate leaving a herbicide deposit, the bioavailability of which is dependent on several factors. Firstly, the distribution of active and coverage across the leaf surface will have a large effect on uptake levels, with greater coverage providing a greater area over which the active may diffuse into the plant. The physical state of the active upon the surface may have large effects, being either solubilised or crystalline. If the active crystallises on the surface there will be a large reduction in bioavailability due to reduced mobility of the active. Conversely, if the active is solubilised within the deposit, a much greater level of mobility will be conserved, allowing for greater diffusion of the active into the plant (Tu & Randall, 2003). Active loading within the formulation also has a large bearing on application activity, with higher concentrations allowing for a greater diffusion gradient into the plant, and longer lasting uptake due to the greater reserves of active. This however also increases the amount of active lost from the deposit to the environment via evaporation and rain wash off, as well as that lost upon initial spraying (Hartzler, 2019; Knowles, 2006).

Once applied to the plant, herbicides must first pass through the cuticle prior to reaching the plant tissue. The plant cuticle is the outermost layer of the plant covering the leaves, fruit, stems, and flowers of higher plants. The cuticle protects the plant against drought, UV radiation, mechanical and pest injuries, pathogen infection and chemical attack, such as that by herbicides. Herbicides must diffuse through the cuticle which consists of multiple barriers for entry into plant cells, namely extra and intra-cuticular wax, and the cutin, prior to reaching plant cell walls and cell membrane (Ziv et al., 2018). The rate at which the herbicide can diffuse into cells is dependent upon a multitude of factors. The most influential of these is the diffusion coefficient of the herbicide across each barrier it must cross (herbicide deposit, wax, cutin, cell wall, cell membrane) as shown in Figure 2. In addition, factors such as concentration

gradient from the herbicide deposit to plant cell and permeance of the herbicide within each cuticular compartment can greatly affect their bioavailability (Hess et al., 2000).

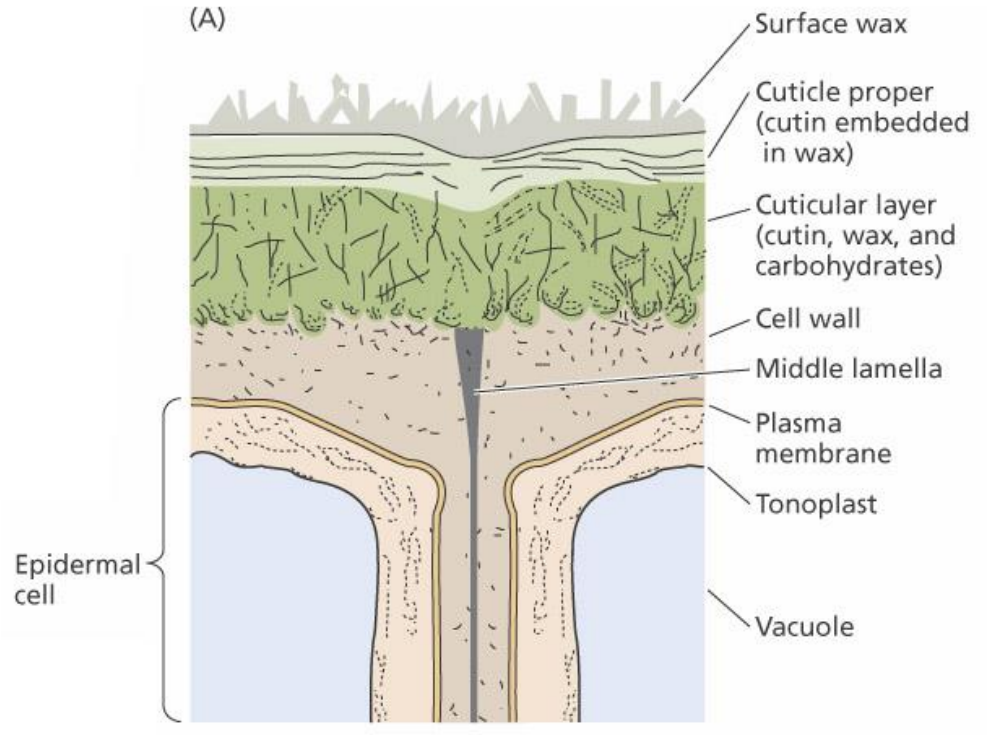

Figure 2. Each barrier to herbicide entry into the epidermal cells. The surface wax, cuticle proper and cuticular layer all constitute the plant cuticle with the cell wall and plasma membrane providing additional barriers for entry. Image: (Taiz et al., 2015)

Outside of the plant cuticle, surface features such as trichomes can affect uptake (Figure 3). Trichomes on the leaf surface can intercept spray droplets prior to contact with the epidermal surface, preventing herbicide diffusion into plant tissue. The level of branching and number of trichome can also reduce the number of spray droplets in contact with the leaf, and thereby uptake. Even at low density, non-branching trichomes can result in reduced uptake. The use of surfactants can help to minimise such effects by allowing the spray to break into smaller droplets upon contact with the trichome, or allow spreading of the droplets off the trichomes and onto the leaf surface (DiTomaso, 1999).

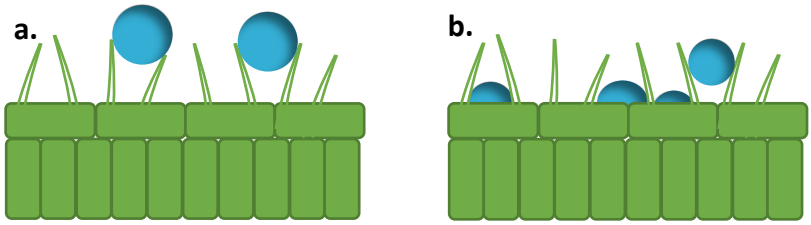

Figure 3. The possible effects of trichome on droplet applications. a. Demonstrates droplet application without the use of surfactants whereas b. represents application with surfactants.

1.4.1 Leaf wax

The outer epidermal cells of plants are covered in a layer of wax which acts as the interface between living plant tissue and the surrounding atmosphere. This waxy layer is lipophilic and non-polar, preventing water from penetrating into the underlying cells, and comprises one of the biggest barriers for entry of pathogens and herbicides (Sadler et al., 2016). Cuticular waxes are semi-crystalline in nature and result in a much-reduced solubility and diffusion coefficient for herbicides compared to the amorphous cutin polymer layer (Burghardt et al., 2006). The leaf consists of two wax layers, the epicuticular wax which is considered the most significant barrier to water soluble herbicides due to its hydrophobic nature, and intracuticular or embedded wax, an amorphous mixture of lipids embedded into the cutin. Both epicuticular and intracuticular wax consists of a wide range aliphatic compounds derived from very long chain fatty acids (VLCFAs) (Buschhaus et al., 2011; Trivedi et al., 2019). As shown in Figure 4, C16 and C18 fatty acids are synthesised within the plastid using malonyl CoA as a precursor molecule, to which the stepwise addition of two carbon acetyl units is performed by fatty acid synthase (FAS). These fatty acids are then transported to the cytosol and further elongated by a multienzyme fatty acid elongase complex within the endoplasmic reticulum to form VLCFAs. These VLCAFs are further modified into the very long chain aliphatic hydrocarbons which make up leaf wax, either through the acyl reduction pathway giving rise to even chain primary alcohols, or the decarboxylation pathway giving rise to odd chain alkanes, aldehydes and ketones (Baker, 1982; Jeffree, 2006).

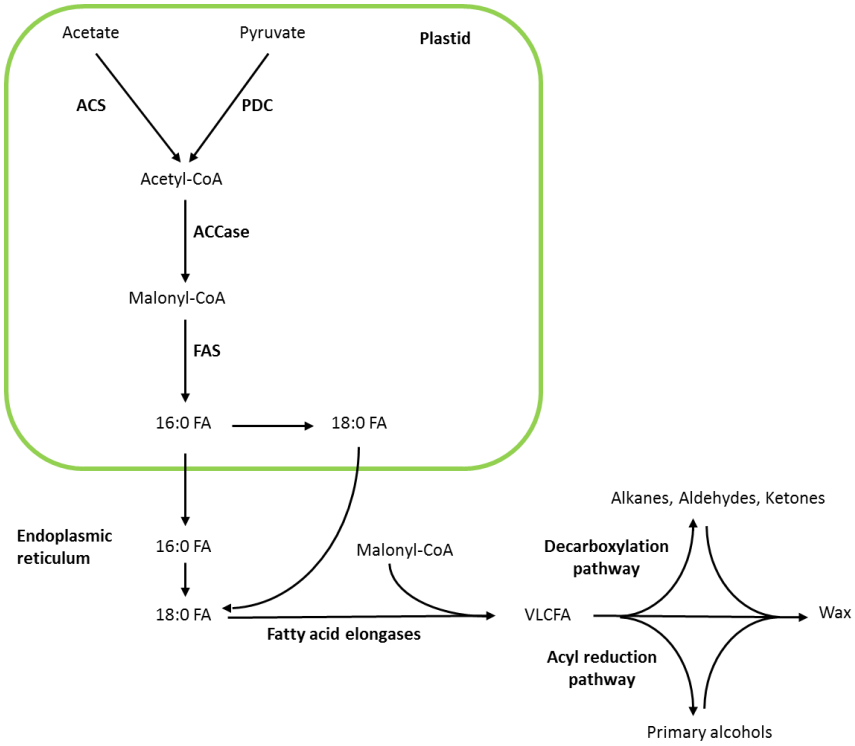

Figure 4. The pathway through which very long chain fatty acids are synthesised and modified to form the constituents of leaf wax. 16:0 and 18:0 fatty acids may be directly incorporate into cutin or undergo hydroxylation prior to incorporation. Abbreviations: ACS Acetyl-Coa synthetase, PDC Pyruvate dehydrogenase complex, ACCase Acetyl-CoA carboxylase, FAS Fatty acid synthase, VLCFA very long chain fatty acids.

The ratios of wax components can vary greatly between species and have a large bearing on both the chemical properties of the leaf surface as well as the physical structure of the wax. It has been found that many crystalline wax structures result from one dominant chemical component, with differing structures arising from different aliphatic hydrocarbons. (Buschhaus & Jetter, 2011; Kirkwood, 1999). Based on previous literature, Buschhaus (2011) theorised epicuticular wax thickness could range from 50 – 375 nm and intracuticular wax from 10 – 375 nm. Although plant species or populations within the same species may have variations in wax thickness, it has previously been demonstrated this has little bearing on cuticular permeability, with the physiochemical properties being the largest determinant. It has also been noted that the presence of greater amounts of wax do not coincide with the occurrence of wax crystals on the leaf surface, highlighting the large influence of wax chemical composition on leaf surface properties (Buschhaus & Jetter, 2011; Sadler et al., 2016).

1.4.2 Cutin and the cuticle

In addition to wax, the herbicide must diffuse through the cutin before it is able to reach the plant cell wall. The cutin acts as a barrier to control movement of water, gases, and solutes, as well as protecting the plant from biotic and abiotic stresses. The “cuticle proper” of most plants consists primarily of a matrix of cutin in which the intercuticlar wax is embedded. Cutin is the primary constituent of the cuticular layer which sits beneath the cuticle proper and above the cell wall. This layer consists of cutin, and carbohydrates embedded within the cell wall, as well as wax, albeit at a reduced abundance relative to the cuticle proper (Pollard et al., 2008). As with cuticular wax, the components of the cutin are fatty acid derived, consisting primarily of a matrix of insoluble, linked, oxygenated and esterified fatty acids (Ziv et al., 2018). Cutin monomers consist of hydroxy acids which are esterified to one another by their primary hydroxyl and carboxylic acid groups to form a long chain, linear polyester. These polyester chains form a branched, cross linked structure through the esterification of the carboxyl group of one fatty acid and the secondary hydroxyl group of another, or to the hydroxyl group of glycerol (Figure 5). The resulting structure has much reduced lipophilicity compared to leaf wax, although the exact three-dimensional structure of the cutin remains unknown (Pollard et al., 2008).

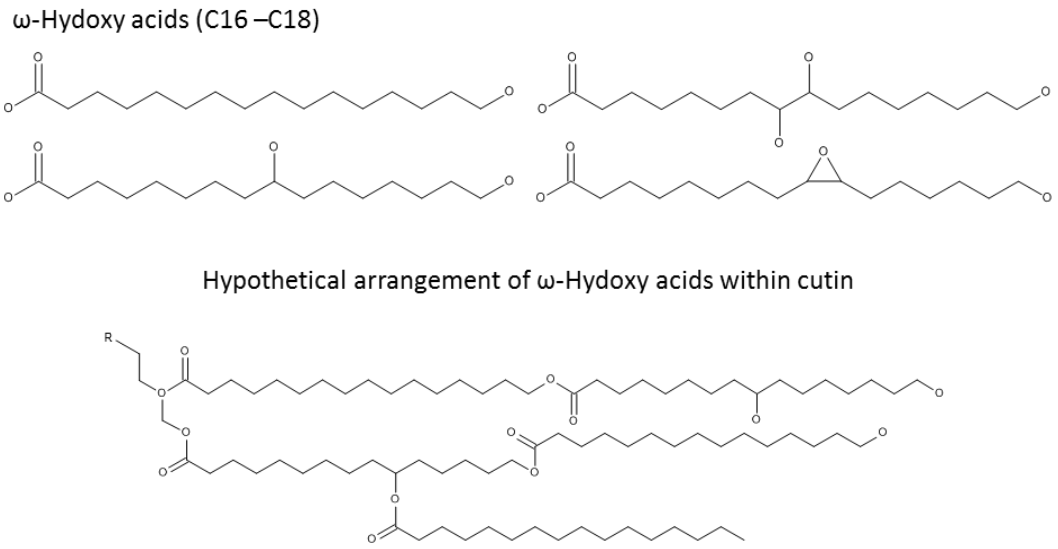

Figure 5. Individual monomers of cutin consist of ω-hydroxy acids and substituted ω-hydroxy acids. Cutin monomers are esterified to one another between the carboxylic acid group and primary alcohol with a branched structure forming from esterification with secondary hydroxyl groups.

1.4.3 Cell wall and membrane

Although not considered part of the cuticle, the cell wall spans the area between the cuticle and epidermal cell membrane and acts as a further barrier to herbicide penetration. Plant cell walls consist of a complex fibrous matrix composed primarily of cellulose, hemicellulose, pectin and lignin (Matsunaga et al., 2004; Cornuault et al., 2018). The plant cell wall helps maintain cell shape, support plant growth, and protect against biotic and abiotic stresses (Matsunaga et al., 2004). Cellulose is the most prominent component of the cell wall, consisting of β-1,4-linked glucan chains interacting via hydrogen bonds to form a crystalline micro-fibril (Keegstra, 2010). In addition to cellulose, lesser molecules in the form of pectin and hemicellulose are also present within the cell wall. Hemicellulose is a heterogeneous polysaccharide composed of various branched sugars such as xylose, glucose, or mannose, linked by a β-1, 4 backbone (Matallana-González et al., 2019; R. Sun, 2010). Hemicelluloses generally constitute 20-30% of total cell wall components, though the exact composition can vary greatly between species (Whistler, 1993). Hemicellulose are known to tightly bind cellulose micro-fibril through hydrogen bonding where they act to fill the void between cellulose fibrils, functioning as a supporting material within the cell wall, as well as providing coupling to lignin (Ebringerová, 2005; Spiridon et al., 2005).

Pectin is amongst the most complex macromolecules in nature consisting of 17 potential monomers with more than 20 linkages. Pectin makes up a small percentage of the overall cell wall structure, being present predominantly in the primary cell wall and middle lamella. Due to its complexity, how pectin is incorporated into the cell wall and its overall role are less well understood compared to other components. Pectin is thought to play an important role within initial cell wall formation and so is only found within the outermost cell wall. Pectin is also thought to influence porosity of the primary cell wall, as well as surface charge, pH, and ion balance, playing a role in ion transport into the cell (Harholt et al., 2010; Voragen et al., 2009). Herbicide penetration of the cell wall occurs by diffusion through what is a hydrophilic layer, with diffusion rate being dictate by pH outside and inside the cell, and water solubility of the active.

The cell membrane provides the final barrier for entry of herbicides into the plant cell, wherein herbicidal activity can occur. The cell membrane is comprised of lipids and acts as lipophilic barrier for herbicide entry. Passive diffusion is the most common means by which herbicide uptake occurs, with a concentration gradient being established due to the greater concentration outside the cell (Figure 6). Lipophilic herbicides tend to diffuse more freely across the cell membrane due to the hydrophobic nature of the membrane, although will often prove slower to diffuse through the cell wall. Although less common, some herbicides utilise active transport to move into cells against a concentration gradient. Herbicides such as sulfonyl ureas are weak acids due to the presence of a carboxylic acid group. As the pH outside the cell (~5) is lower than that found within the cell (~7.5), weak acids outside the cell become protonated (COOH) resulting in a lack of charge, and a greater degree of lipophilicity. Once within the cell, the hydrogen is lost due to the higher pH, resulting in a negatively charged herbicide (COO^-). This molecule is more water soluble, and so is less able to diffuse back across the lipophilic cell membrane. As the concentration of uncharged, lipophilic herbicide molecules remains greater outside of the cell membrane, continuous diffusion into the cell occurs (Hartzler, 2019; Sterling, 1994).

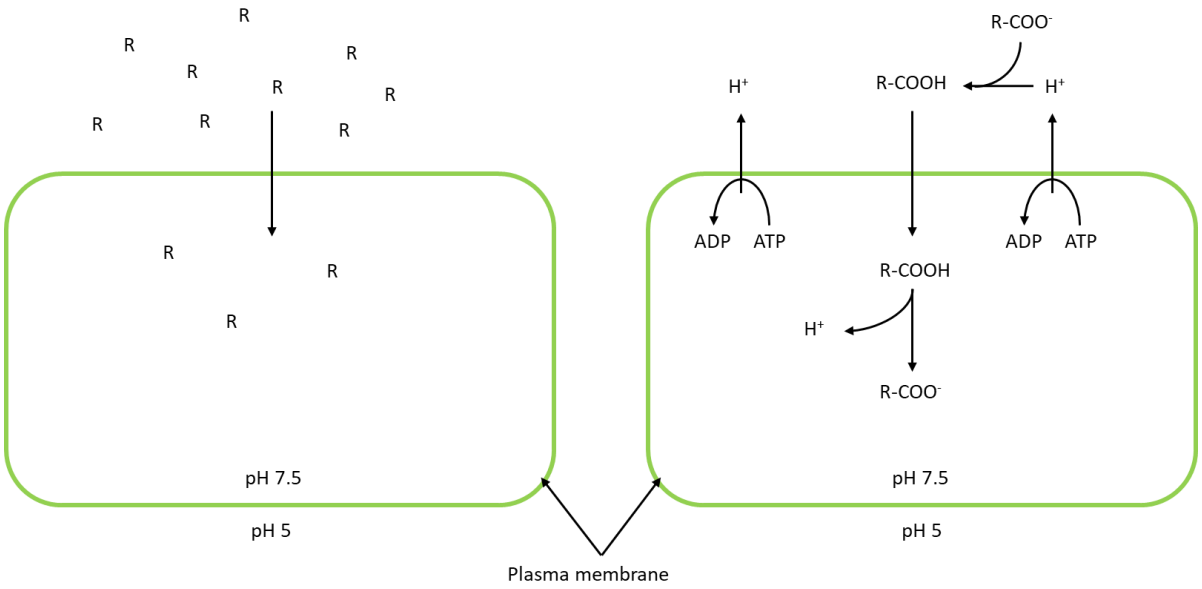

Figure 6. a. Diffusion across a concentration gradient with a higher concentration of herbicide outside the cell than within, resulting in continual uptake of the herbicide into the cell. b. Active transport of weak acid herbicides where in the differing pH outside and within the cytosol can be exploited to drive a concentration gradient between the protonated and un-protonated herbicide.

Regardless of the route taken by the herbicide during diffusion, it must overcome both hydrophilic and lipophilic layers prior to reaching plant cells. Lipophilic herbicides are readily absorbed into the epicuticular wax wherein they easily move through the embedded intracuticular wax to the cutin and pectin layer. At this point, the diffusion rate of lipophilic herbicides will be reduced due to the increased hydrophilic nature of the cutin and pectin layer of the cuticle.

1.5 Herbicide metabolism and resistance

Herbicides function by inhibiting key functions in normal plant physiology essential for growth or survival. For example, cyclohexanedione herbicides act by inhibiting Acetyl Coenzyme A Carboxylase (ACCase). The ACCase enzyme is essential for fatty acid synthesis, the inhibition of which prevents the synthesis of phospholipids needed for the formation of lipid bilayers required for cell structure and function, ultimately resulting in plant death (Sherwani et al., 2015). Due to the large benefits conferred by using herbicides over past methods of weed control, there has been a worldwide increase in usage and reliance upon herbicides. This has in turn resulted in a selective pressure on weed populations to develop means of alleviating herbicide toxicity, with over 300 herbicide resistance biotypes having been reported

worldwide (Burns et al., 2018; Patzoldt et al., 2006). There are two primary means by which herbicide resistance is categorised, target site resistance (TSR) and non-target site or enhanced metabolism mediated resistance (NTSR) (Devine et al., 2000).

Herbicides must reach concentrations within plant cells at which a lethal dose is attained. At such concentrations, the inhibitory effect upon vital enzymes will be such that key physiological process will be disrupted resulting in plant death. Target site resistance arises from a point mutation of the amino acid sequence of the target enzyme, either by deletion or substitution. The result is a structural change within the enzyme at the site of action, reducing the binding affinity of herbicides. The target enzymes function is still maintained, although often with an associated "fitness" cost causing a degree of reduction in function, however results in resistance to herbicides targeting the altered enzyme (Comont et al., 2019; Vila-Aiub et al., 2009).

TSR may arise by one of two means, the first of which being a substitution mutation. A number of herbicides act as photosystem II (PS II) inhibitors such as triazine, which was reported as one of the first herbicides to which resistance had been found. These herbicides bind the plastoquinone-binding site of the D1 protein within the photosynthetic electron chain. The binding of herbicides to the D1 protein results in a shortage of NADPH required for CO_2 fixation. The result is the formation of oxygen derived free radicals and oxidative damage to cells, ultimately leading to cell and plant death. Multiple instances of resistance have been found towards PS II inhibiting enzymes, with most seeming to arise from a mutation of Ser_{264} to Gly within the D1 protein. With the herbicide having reduced binding affinity towards the plastoquinone binding site and therefore an inability to inhibit the D1 protein, electrons may still be transferred from the PS II reaction centre to the cytochrome b_6/f complex, although with an associated fitness cost (Devine & Shukla, 2000; Vila-Aiub et al., 2009).

Although much rarer, TSR may arise from the deletion of an amino acid at the target site of the herbicide (Patzoldt et al., 2006). Protoporphyrinogen oxidase (PPO) is an enzyme involved in tetrapyrrole biosynthesis pathway which produces some of the most abundant macromolecules within plants such as heme and chlorophyll. Although synthesis of heme and chlorophyll is differentially compartmentalised, in both instances PPO catalyses the removal of six electrons of protoporphyrinogen IX to form protoporphyrin IX (Xianggan Li et al., 2005; A. S. Richter et al., 2013). When susceptible plants are treated with a PPO inhibitor,

protoporphyrinogen IX accumulates and is exported in the cytoplasm from plastids and mitochondria, the sites of heme and chlorophyll synthesis respectively. Here peroxidase-like enzymes which remain unaffected by PPO inhibitors convert protoporphyrinogen IX to protoporphyrin IX. This in the presence of light induces the formation of singlet oxygen and oxygen derived radicals, causing oxidative damage to the cell membrane and ultimately cell death (Xianggan Li & Nicholl, 2005). It has been found within a population of *Amaranthus tuberculatus* that resistance has arisen due to the presence of *PPX2L*, a gene encoding PPO containing a codon deletion. The codon deletion within *PPX2L* results in the deletion of Gly_{210} within PPO and is suspected to encode both mitochondrial and plastids isoforms of the PPO enzyme. The resulting enzymes have reduced binding affinity for PPO inhibitors resulting in much increased tolerance (Patzoldt et al., 2006).

Plants have evolved a chemical detoxification system towards xenobiotics such as herbicides and it is through this detoxification system by which Non-target site resistance arises (Brazier-Hicks et al., 2018). Non-target site resistance is a much more complex means of resistance with any resistance arising not at the target site being classified as such. The exact mechanism by which NTSR arises and acts to reduce herbicide susceptibility has yet to be fully elucidated due to the polygenic, complex mechanisms underlying NTSR resistance. Although most herbicides can be detoxified by plants to some extent, the ability of many plants is insufficient to prevent herbicide effectiveness, and it is through this difference that selectivity is established within several herbicides. Herbicide metabolism arises from the coordinated involvement of enzymes involved in transport and metabolise, collectively termed the "xenome". Multiple large protein families are utilised during herbicide detoxification such as glutathione transferases (GSTs), cytochrome P450s (CYPs) and glycosyltransferases (UGTs) and play major roles in catalysing the detoxification of xenobiotics (Brazier-Hicks et al., 2018; Cummins et al., 2013). The xenome comprises a multi-phase system (Figure 7) through which xenobiotics are transported, conjugated, and undergo metabolism and are re-incorporated into macromolecules (Gershater et al., 2007). It is the increased action of the xenome that is thought to underpin NTSR mediated herbicide resistance, resulting from enhancement in herbicide metabolism, sequestering and compartmentalisation, or a reduction in uptake (Burns et al., 2018).

1.5.1 Xenome metabolism

Herbicide metabolism is a multiphase system utilising many enzymes that detoxify xenobiotics. Phase I of the xenome involves cytochrome P450 monooxygenases (CYPs) mediated transformation of the xenobiotic through dealkylation or oxidative reactions (Van Eerd et al., 2003). CYPs are predominantly membrane associated proteins localised on the endoplasmic reticulum. They utilise reduced nicotinamide adenine dinucleotide phosphate (NADPH) and atmospheric oxygen to catalyse the insertion of oxygen within the xenobiotic. CYPS can catalyse hydroxylation, oxidation, demethylation, dealkylation and desaturation of the xenobiotic (Schuler et al., 2003). This exposes or adds a functional group, increasing reactivity of the xenobiotic and helping facilitate phase II of the xenome, conjugation. These reactive functional groups can be conjugated to hydrophilic molecules, typically sugars or thiols like the tripeptide glutathione (GSH). Conjugation is mediated by two enzymes, glycosyltransferases (GTs) for sugar conjugation and glutathione S-transferases (GSTs) for glutathione conjugation (Cummins et al., 2011; Kreuz et al., 1996). GTs can be further subdivided based on the functional group to which the sugar is conjugated, O-glycosyltransferases for -OH or -COOH, and N- glycosyltransferases for -NH_2 (Bowles et al., 2005). The resulting conjugate has both reduced phytotoxicity due to the removal of reactive centres, and increased water solubility helping to facilitate phase III. There are however many xenobiotic compounds which do not undergo phase I metabolism and instead are able to be directly conjugated within phase II without any prior processing (Cummins et al., 2011). Phase III facilitates the active transport of the now water-soluble xenobiotic conjugates from the cytosol to vacuole or to extracellular spaces. This occurs by one of two mechanisms depending on what molecule is used in conjugation; glutathione conjugated xenobiotics are transported via ATP-binding cassette transporters (ABCs) with glycosylated xenobiotics being transported by ATP dependent transporters (Rea, 2007; Schulz et al., 2006). Within the vacuole additional metabolism may occur, such as glutathione conjugated xenobitics being further processed by cleavage of glycine and glutamate to form a xenobic-cysteine conjugate. The final phase, phase IV, involves compartmentalisation of the xenobiotic derived metabolites into the plant cell wall (Brazier-Hicks et al., 2008).

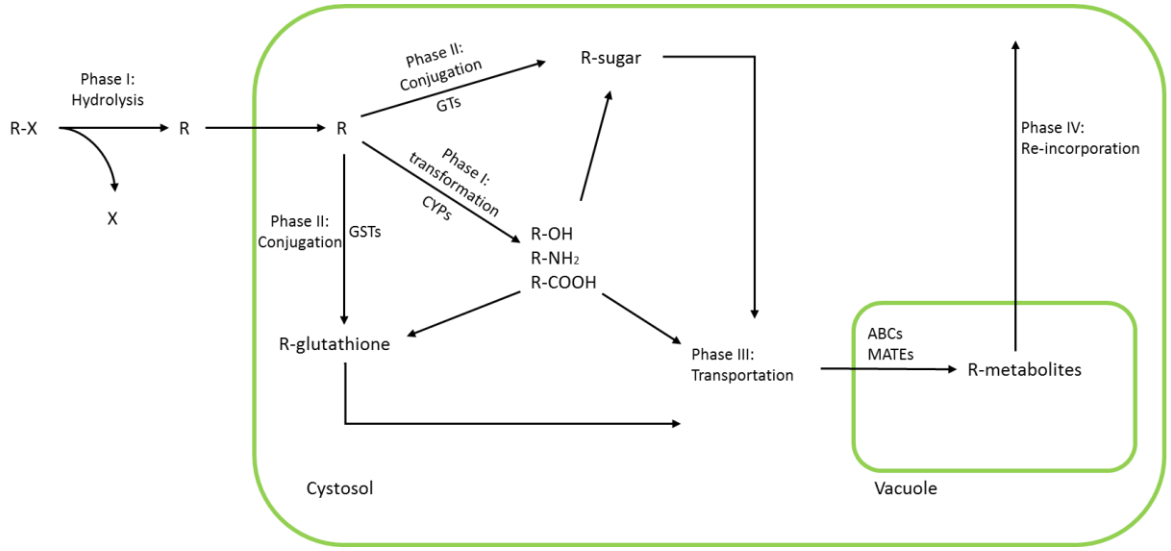

Figure 7. Generalised plant xenome highlighting the phases through which xenobiotics are metabolised. Xenobiotics firstly undergo CYP mediated transformation in which a reactive group is added or exposed, allowing for conjugation, typically with a sugar or thiol molecules. The conjugate is then transported into the vacuole where it undergoes further metabolism prior to reincorporation into the cell.

1.5.2 Herbicide resistance in blackgrass

Blackgrass (*Alopecurus myosuroides)* is an annual diploid grass weed prevalent across the UK and Europe. Blackgrass seeds geminate across late summer and early autumn during which time sowing of winter crops begin (S. R. Moss et al., 2010). Due to the large populations, widespread distribution, high reproductive capacity, allogamous reproduction and genetic and phenotypic plasticity, the formation of resistant populations is an ever increasing problem (Powles et al., 1995). The repeat exposure of blackgrass to the same chemicals, as well as under dosing of herbicides, has resulted in several populations evolving both NTSR and TSR resistance traits. Blackgrass was first identified as displaying traits now known as NTSR in 1984 in Peldon, Essex. This population of blackgrass was found to have the ability to resist the toxic effects of four herbicides across three modes of action, showing resistance had not arisen solely through TSR. This population was termed as multiple herbicide resistant (MHR), also referred to as NTSR, due to its innate capacity to metabolise and display resistance to multiple classes of herbicide (Cummins et al., 2013). Such resistance has since been reported in multiple plant species including *Lolium Sp,* with resistance being associated with up-regulation of CYPs and GSTs, key xenome enzymes.

Many resistant blackgrass populations have been associated with an increase in the expression levels of *Am*GSTF1, a plant specific phi class GST. AmGSTF1 has become a reliable marker for the presence of NTSR within blackgrass having been found at levels 20 times higher in resistance populations than wild type susceptible populations, however is not thought to be involved directly in the metabolism of herbicides (Cummins et al., 2011; Cummins et al., 2013). The exact role of AmGSTF1 in herbicides resistance has not yet been established, having been demonstrated to have only limited herbicide detoxifying capabilities. It has been shown however that *Arabidopsis thaliana* transformed with *AmGSTF1* developed tolerance towards chlorotoluron, alachlor and atrazine. This resistance was found not to result from changes in gene expression, but changes in regulatory control of protective compounds leading to an accumulation of glutathione, anthocyanins and flavonoids (Cummins et al., 1999). It has also been found that NTSR mediated resistance can lead to resistance to herbicides to which the plant has had no previous exposure (Délye et al., 2005). For example, a blackgrass population with repeated exposure to pendimethalin, a cell division and elongation inhibitor, has been found to have developed resistance to multiple additional herbicides of differing chemical classes, despite no previous exposure (Tétard-Jones et al., 2018). In addition, weed populations exhibiting NTSR can often be found with TSR, further increasing the difficulty of re-establishing weed control (Cummins et al., 2013). There are several know ways by which blackgrass may develop TSR with most arising from amino acid substitutions of which 2 and 12 point mutations have been established within ACCase and ALS enzymes respectively (Jang et al., 2013; Tranel & Wright, 2002).

1.6 Genetically modified crops

Genetic modification is the process of manipulating the genetic material within a living organism, enabling them to perform specific functions often unattainable through conventional selection breeding (Raman, 2017). Over recent years, the weed populations in farmland has been progressively increasing, resulting in an increased reliance on herbicide usage. Several herbicides have been shown to negatively impact crop species, resulting in weed control at the expense of lost crop yield (Shi, et al, 2020).

Although resistance within weeds poses a great issue to crop yields and food security, the use of genetic engineering has allowed for exploitation of these mechanisms of herbicide tolerance, by artificially introducing them into crop plants (Shi, et al, 2020; Zhang, 2016).

Particularly prevalent within the United States, the introduction of herbicide tolerance to crop species has allowed for the use of chemical actives which would otherwise negatively impact crop yields, or allowed increase active dose rates to be used, which would otherwise impact crop health. The use of GM crops provides a much broader means through which to deal with weed species, and can help reduce the chances of herbicide resistance development by proving a greater chemical arsenal which can be utilised on a particular crop (Anderson, et al, 2019). Although the use of genetically modified crops has many benefits, their use is also filled with controversy and potential risks. A recent example has involved issues with dicamba spray drift, causing potentially sever damage to sensitive crops. A second, and potentially worse issue is arising in the form of resistant weed species emerging due to repeated, low dose exposure to active chemicals via spray drift. Weed exposed to herbicides via spray drift have been associated with being dosed at the optimum level of exposure for herbicide resistance selection. Although the use of genetically modified crops has clear benefits, their use is not the "be all end all" of crop management and must be appropriately incorporated into a broader crop protection scheme (Bruno, et al, 2020). The use of herbicide formulation can help to account for factors such as spray drift and provide more targeted delivery to minimise the risk of resistance development (Hilz & Vermeer 2013).

1.7 Project aims, objectives, and hypotheses

Herbicides are of great importance within crop production systems, however with decreased discovery rates of new actives and increasing reports of herbicide resistance, maintaining weed control is becoming progressively harder. Herbicide formulation has the potential to greatly enhance herbicide effectiveness and offers a potential means of extending the usable life span of herbicides.

The primary focus of this project was to investigate the effect of adjuvants upon a base herbicide formulation and investigate differing formulation interactions between a crop species, wheat, and two associated weed species, blackgrass and ryegrass. In the first instance, a herbicide formulation needed to be created to which adjuvants could easily be incorporated.

It was then important to establish a biomarker system from which uptake could be measured. It was hypothesised that a potential marker of bioavailable herbicide could be established as a proxy for determining herbicide uptake. To identify such a marker, a three-tier omics system

was used to initially explore means of monitoring herbicide uptake without the use of radio-chemicals:

- At the genetic level looking for differences in gene expression among several stress related gene markers established in previous research.
- Expression levels of GSTs through the use of western blotting as GSTs are directly involved in glutathione mediated herbicide detoxification
- Metabolic profile through which differences in herbicide metabolites could be established with levels of metabolite being dependent upon the amount of herbicide with bioavailability within the plant.

After establishing a usable biomarker, uptake comparison studies testing differing adjuvants could be performed to observe the effects upon uptake rates. As the adjuvants selected had a “step-wise” change in chemistry, it was hypothesised that a link could be established between uptake rates, the chemical nature of the adjuvant used and the surface properties of the leaf surface to which the formulation was applied. Using biomarkers it was possible to investigate the reason for differences in uptake observed between formulations and plant species. The characteristics of each formulation was measured in the form of dry down distribution, drying time, surface tension, and contact angle. In addition, the physiochemical properties of blackgrass, wheat, and ryegrass were investigated through SEM imaging and chemical profiling by GCMS/FID.

2 Materials and methods

2.1 Materials and regents

Winter wheat (*Triticum aestivum, var. Corial*) was supplied by KWS and used for all wheat experiments. Sensitive model weed species, Ryegrass (*Lolium multilorum*) and Black grass (*Alopecurus myosuroides*) were purchased from cotswoldseeds and herbiseed respectively.

Herbicides for formulation creation (diuron, flufenacet, propyzamide, cyhalofop-butyl, and metolachlor), were provided by Croda at commercial grade (>97%). Formulation components, Atlox 4913, Atlox 4914, Atlox 4838B, Atlox 4894, Atlas G-5002L, Etocus 10, Etocus 35 were all provided by Croda. Additional formulation components Proxel GXL and silcolapse 5000 were purchased from Arch and Elkem respectively. Xanthan gum and glycerine were purchase from Sigma-aldrich. All adjuvants, Tween 20, Tween 22, Tween 23, Tween 24, Tween L-1505, Tween L-1010, Tween L-0515, Atplus DRT 100, Synperonic 127, AL2575, Symprolam 35, Atplus 242, Atplus 310, Atplus UEP 100, and Atplus PFA were provided by Croda.

Organic solvents acetonitrile and methanol were of LCMS grade with aqueous dilutions performed with LCMS grade water, all of which were purchased from Fisher Scientific. Chloroform of GCMS grade was also purchased from Fisher Scientific.

2.2 Herbicide formulation

2.2.1 Suspension concentrate

Three suspension concentrate formulations were made up for the herbicidal active components diuron (650 g/l), propyzamide (300 g/l), and flufenacet (500 g/l). In each instance, the active surfactants, continuous phase, and antifoaming agents were weighed out together as shown in Table 1. The formulation was initially mixed by spatula until a slurry like consistency was obtained and then homogenised using a T25 Ultra-Turex homogeniser at 9500 rpm for 1 minute. The formulation was then milled for 15 minutes to attain a small particle size. While milling, glycerine and xanthan gum were weighed out, mixed by spatula, and allowed to swell for 10 minutes. After milling, the amount of formulation remaining was weighed and from this value the amount of glycerine/xantham gum to be added was calculated to be in line with the initial intended composition. The formulation was homogenised one last time as described above.

The formulations were checked for particle size to ensure small size (d90 < 15µm) and that only one peak was present (multiple peaks would suggest agglomeration of particles and a lack of long-term stability). Particle size readings were taken using a malvern mastersizer 2000 with a stirrer speed of 2500 rpm and the refractive index set to 1.606 nm for diuron, 1.538 nm for flufenacet, and 1.549 nm for propyzamide.

Table 1. The composition of SC formulations for each herbicide. In each instance, the active, surfactants, continuous phase and antimicrobial and antifoaming agents were mixed and milled prior to the addition of pre-mixed glycerine and xanthan gum

Diuron 650 g/l

Component	Purpose	% Assay	Density (g/ ml)	g/100 ml	Volume (ml)
Diuron	Active	98	1.48	66.33	44.8
Atlox 4913	Non-ionic surfactant	100	1.00	6	6
Atlas G-5002l	Non-ionic emulsifier	100	1.00	2	2
Proxel GXL	Antimicrobial agent	100	1.00	0.1	0.1
Silcolapse 5.001	Antifoaming agent	100	1.00	0.1	0.1
Water	Continuous phase		1.00	42.78	42.78
Glycerine	Thickening agent	100	1.26	5	3.97
Xanthan gum	Stabiliser	100	1	0.25	0.25

Flufenacet 500 g/l

Component	Purpose	% Assay	Density (g/ ml)	g/100 ml	Volume (ml)
Flufenacet	Active	98	1.45	51.02	35.19
Atlox 4913	Non-ionic surfactant	100	1	4	4
Atlox 4894	Non-ionic surfactant	100	1	1	1
Proxel GXL	Antimicrobial agent	100	1	0.1	0.1
Silcolapse 5.001	Antifoaming agent	100	1	0.1	0.1
Water	Continuous phase		1	53.41	53.41
Monopropylene glycol	Thickening agent	100	1.04	6	6
Xanthan gum	Stabiliser	100	1	0.2	0.2

Propyzamide 300 g/l

Component	Purpose	% Assay	Density (g/ ml)	g/100 ml	Volume (ml)
Propyzamide	Active	97	1.33	30.93	23.15
Atlox 4913	Non-ionic surfactant	100	1	1.5	1.5
Atlox 4894	Non-ionic surfactant	100	1	1.5	1.5
Hydravance 100	Non-ionic surfactant	100	1	6	6
Proxel GXL	Antimicrobial agent	100	1	0.1	0.1
Silcolapse 5.001	Antifoaming agent	100	1	0.1	0.1
Water	Continuous phase		1	67.65	67.65
Glycerine	Thickening agent	100	1.26	5	3.97
Xanthan gum	Stabiliser	100	1	0.25	0.25

2.2.2 Oil in water emulsion

Cyhalofop-butyl was formulated as an oil in water emulsion at 100 g/l. The oil phase was made up with cyhalofop-butyl being added to solvesso and then dissolved by sonication in an XUBA3 sonication water bath (set to 35 KHz). The surfactants were added to the oil phase as shown in

Table 2, then homogenised as described when formulating SCs. The water phase was made up separately and placed onto a magnetic stirrer set to 1000 rpm. The oil phase was then added dropwise to prevent phase inversion and provide a stable emulsion. The particle size was once again checked using the mastersizer.

Table 2. The composition of both the oil phase and water phase for the cyhalofop-butyl oil in water emulsion. Each phase was made up separately and the oil phase slowly added to the water phase.

Cyhalofop-butyl 100 g/l
Oil Phase

Component	Purpose	% Assay	Density (g/ ml)	g/100 ml	Volume (ml)
Cyhalofop-butyl	Active	98	1.17	10.2	8.7
Solvesso ND150	Solvent phase	100	1	40	40
Atlas G-5002l	Non-ionic surfactant	100	1	4	4
Atlox 4914	Non-ionic surfactant	100	1	1	1

Water Phase

Component	Purpose	% Assay	Density (g/ ml)	g/100 ml	Volume (ml)
Water	Continuous phase		1	40	40
Proxel GXL	Antimicrobial agent	100	1	0.1	0.1
Silcolapse 5.001	Antifoaming agent	100	1	0.1	0.1
Monopropylene glycol	Thickening agent	100	1.04	6	6
Xanthan gum	Stabiliser	100	1	0.2	0.2

2.2.3 Emulsifiable concentrate

Metolachlor was formulated as an emulsifiable concentrate due to being liquid in its native form. The formulation was created using a triangle screening process utilising 3 different surfactants; Atlox 4838B, Etocus 10, and Etocus 35. The highlighted triangle points were selected for initial screening and directed the varying surfactant ratios shown

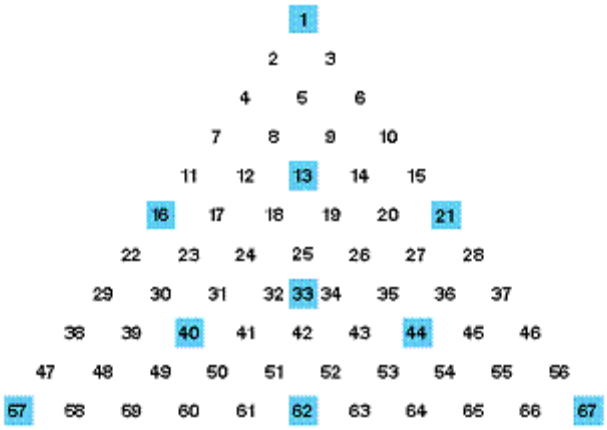

Figure 8 The triangle screening process used. Each corner represents 100% of a particular surfactant, point 1 being Atlox 4838B, point 57 being Etocas 10 and point 67 being Etocas 35. Differing points within the triangle represent different ratios of adjuvants. For example, point 62 will consist of 50% Ecotas 10, and 50% Etocas 35. Point 33 will consist of each adjuvant in equal quantities. (further information available at https://cropformulating.crodadirect.com/Brochure.aspx).

Each mixture was tested for stability following a 20 times dilution in water containing 342 ppm Ca^{2+}. Formulations were left for 1 hour and observed to check for sedimentation, or agglomeration, within the solution. From these initial trials, point 67 performed the best and so was made into a full 500 ml formulation.

Table 3. The composition of each of the triangle points screened with each corner (1, 57, 69) representing one of the three surfactants accounting for 100% of the surfactant added. Moving away from these points begins to factor in other surfactants while reducing that of each corner point

	Triangle number									
Component (%)	**1**	**13**	**16**	**21**	**33**	**40**	**44**	**57**	**62**	**67**
Metolachlor	90	90	90	90	90	90	90	90	90	90
Atlox 4838B	10	6	5	5	3.3	2	2	0	0	0
Etocas 10	0	2	5	0	3.3	6	2	10	5	0
Etocas 35	0	2	0	5	3.3	2	6	0	5	10

2.3 Plant growth conditions and treatment

2.3.1 Plant growing conditions

Seeds were germinated in petri dishes on glass fibre filter paper soaked in distilled water and were germinated in growth chambers. All plants were grown in a Sanyo versatile environmental test chambers (growth chambers) with a day cycle from 6:00-22:00 (16 hours) and night cycle from 22:00-6:00 (8 hours). During the day cycle, plants were exposed to a light

intensity of 125-150 µmol m^2s^{-1} Photosynthetic photon flux density (PPFD), and a temperature of 18°C. The night cycle was at and a temperature of 16°C with no light. Germinated seeds of similar size were selected and transferred to pots containing John Innes No. 2 soil. Plants were then grown in the growth chambers until the 2-leaf stage of growth (12 on Zadoks scale of cereal growth, 2-3 week old).

2.3.2 Herbicide treatment

Aliquots of the flufenacet SC formulation were top treated with each adjuvant at 10% w/w. Flufenacet herbicide formulations were then diluted in d.i. water at a rate of 2.4 mg formulation per ml, or, 1.2 mg active per ml, comparable to application rates of commercial formulations during field application. For other actives to which no adjuvants were added, herbicides were diluted to levels comparable to those found within tank mixes. Diuron was diluted to 2mg formulation per ml, or 1.1 mg active, cyhalofop butyl to 6.2 mg/ml (0.62 mg/ml active) Propyzamide to 5.9 mg/ml (1.68 mg/ml active), and metolachlor to 5 mg/ml (4.5 mg/ml active) The formulations were distributed across the flag leaf of plants using a 10 µl repeat pipette set to dispense 25 0.4 µl droplets as displayed in Figure 9.

Figure 9. SC Formulation having just been applied to the leaf of a 3-leaf stage wheat plant (left) and 2 hours after drying.

5 plants within each sample pot equated to 5 treated leaves per replicate resulting in a total application of 0.06 mg, or 165 nmol of flufenacet per pot. Plants were placed back into the growth chamber under the same conditions under which they were grown and left to incubate over a 16 hour time course with harvests taking place at 30 minutes, 1, 2, 3, 4, 6, and 16 hours after application. At each time point, the flag leaves from one pot were cut from the plants, pooled together and then weighed. The pooled samples were ground in liquid nitrogen and stored in a 15 ml falcon tube until extraction. Extraction was performed by the addition of 80% methanol at 10x v/w. The samples were quickly vortexed and then placed on an end over end rotator at 4^{o}C for 1 hour. The samples were centrifuged at 2500xg for 5 minutes and the supernatant retained for analysis. Samples were stored at -20^{o}C for further analysis.

2.4 Gene expression studies

2.4.1 Extraction of total RNA

Leaf tissue was harvested and ground under liquid nitrogen. Less than 100mg of plant tissue was then transferred to a pre-microfuge tube and RNA was extract using a Quiagen Rneasy plant mini kit in accordance with the manufacturer's instructions. Samples were treated with RNase-free DNase I as an additional step as specified in the manufacturer's instructions. Samples were quantified and checked for purity using a Nanodrop ND1000 spectrometer then stored at -80^{o}C until use.

2.4.2 Reverse transcription for synthesis of cDNA

Reverse transcription was used to obtain cDNA from the RNA extract which could then be used for quantitative polymerase chain reaction (qPCR). Reaction mixtures were made up with 5 µg RNA, 1 µl oligo dT primers at a concentration of 10µM, 1 µl 10 mM dNTP mix, 4 µl 5xRT buffer, 1 µl ribosafe RNAse inhibitor, 1 µl tetro reverse transcriptase and topped up to 20 µl with DEPC treated water. Samples were mixed by gentle pipetting and PCR was performed by incubation at 45^{o}C for 30 minutes. The reaction was terminated by incubation at 85^{o}C for 5 minutes and cDNA stored at -20^{o}C until use.

2.4.3 Primer selection and validation

Primers were designed and ordered from IDT (Table 4). The primers were diluted in de-ionised water to make a 100 mM stock containing both the forward and reverse primers of each

primer pair. A 48 well plate was used and into each well a total reaction mixture of 15 µl was added with a final composition of 7.5 µl 2x SYBR green, 0.6 µl primer mix, 3.75 µl of cDNA and 3.15 µl of d.i water. The plate was spun in a chilled centrifuge at a temperature of 4^{o}C and speed of 2000xg for 2 minutes. qPCR was performed on a Roche light cycler 96 under the following parameters:

- Pre incubations: 1 cycle at 95^{o}C for 600 seconds
- 2 step amplification: 45 cycles at 95^{o}C for 10 seconds followed by 60^{o}C for 30 seconds
- Melt: 1 cycle at 95^{o}C for 10 seconds, 65^{o}C for 60 seconds, 95^{o}C for 10 seconds

Table 4. 7 Primer sets which had been optimised to look at expression of various stress response genes in wheat.

Description	**Gene bank number**	**Forward primer**	**Reverse primer**
Actin (Housekeeping)	AB181991.1	CCCAGCAATGTATGTCGCAA	TCACCAGAGTCGAGCACAAT
Catalase	X94352.1	CCGGAGAGTCTGCACATGTT	GCCTTTCCATCCCTGCTGAT
GSTF1	AJ440796.1	AGATCAAGAACGTGCTGGCA	GAGATGCGTAGGGTGTAGCC
ATP synthase	M16843.1	AGGCACAGATCCTCCACAAA	GGACTTGATTTCGTTGCCCA
HSP 90	JN052206.1	ACAAGGAAGAGTACGCTGCT	ACTCAAGCTGACCCTCAACA
RGA4	AF087521.1	CCGCCGTTACCTAGAGAAGA	TATCCGACCAAGTTTGCCAC
GST23	JX051003.1	TGAAGGTGTTTGGCATGTGG	TTCTTGGTCACCGGGTTGT
GSTU2	AJ414700.1	CCCAGCAATGTATGTCGCAA	ACGGACTCAGACACACACAA

2.5 Protein extraction and methodology

2.5.1 Plant extraction

Plant tissue was weighed upon harvesting, ground in liquid nitrogen, and stored in 15 ml falcon tubes prior to use. Beakers were chilled on ice with 3x V/W extraction buffer (50 mM Tris-HCl, 2 mM EDTA, 1 mM DTT, pH 7.5), as well as PVPP at 50 g/l extraction buffer. Upon addition of the ground plant tissue, the sample was mixed thoroughly using a spatula and filtered through a double layer of miracloth (22-25 µm pore size). The filtrate was transferred

to Oakridge centrifuge tubes which were centrifuged at 10000xg for 15 mins at a temperature of 4^{o}C. The protein containing supernatant was decanted and retained for use.

2.5.2 Protein quantification

Protein extracts were quantified using a Thermo Scientific Pierce BSA Protein Assay Kit. A working reagent was made up by combining 50 ml reagent A (sodium carbonate, sodium bicarbonate, bicinchonic acid and sodium tartrate in 0.1 M sodium hydroxide) and 1 ml reagent B (4% copper sulphate pentahydrate).

Each standard contained 1 ml of working reagent as well as 50 µl bovine serum albumin which was used to generate a standard curve from 2000 µg/ml to 0 µg/ml. Standards were incubated at 37^{o}C for 30 minutes and absorbance readings were taken using a Shimadzu UV-1800 spectrophotometer at a wavelength of 562 nm.

Protein extracts were diluted in extraction buffer at a 1 in 10 dilution and 50 µl then added to 1 ml working reagent prior to incubation as previously described and used to determine the concentration of the extract.

2.5.3 Sodium dodecyl sulphate polyacrylamide gel electrophoresis (SDS-PAGE)

12% gels were used for all SDS-PAGE. The resolving layer of each gel was made up by mixing 3.2 ml 40% acrylamide solution, 2.5 ml 4x resolving buffer (1.5M Tris-HCl pH 9, 0.4% tetramethylethylenediamine (TEMED), 0.4% SDS), and 4.2 ml D.I water. The solution was degassed, and 0.1 ml APS was added to the solution and quickly mixed to induce polymerisation of the acrylamide. The resolving layer of the gel was then pipetted into a pre-assembled gel cast until it reached within 1 cm from where the well comb would lie. A layer of H_2O saturated butan-1-ol was added to the gel to help with levelling and the gel was left to set for 30 minutes. The layer of butan-1-ol was then washed off with water. The stacking layer of the gel was made up from 0.5 ml 40% acrylamide solution and 4.5 ml 1.11x stacking buffer (0.14M Tris-HCl pH 6.8, 0.11% TEMED, 0.11% SDS) followed by degassing. 0.5 ml APS was added, and the solution quickly mixed before transfer into the gel cast. A comb of the required number of wells was added into the cast and the gel allowed to set for 30 minutes.

Protein samples were prepared by the addition of 2x SDS loading buffer (100 mM Tris-HCl, 20 % (v/v) glycerol, 4 % (w/v) SDS, 0.2 M DTT, 0.2 % (w/v) bromophenol blue, pH 6.8) and boiled for 5 minutes. The gel was placed into a Bio-Rad electrophoresis chamber which had been

assembled in accordance with the manufacturer's instructions. 700 ml of running buffer was made up from 140 ml 5x SDS-PAGE running buffer (125 mM Tris, 0.96M glycine, 0.5% SDS) and 560 ml D.I water and added to the tank. The gel comb was removed and 15 µl protein sample in loading buffer was then added to each well. For reference, 10 µl of pre-stained Precision Plus protein ladder solution was added. 100 V was applied to the gel tank until the dye front had moved through the stacking layer, at which point the voltage was increased to 200 V and run until the dye front exited the bottom of the gel.

2.5.4 Western blotting

After their separation by SDS-PAGE, polypeptides were transferred to a PVDF (polyvinylidene difluoride) membrane of 0.2 µm pore size with a protein-binding capacity of 240 µg/cm^2, using an iBlot 2 transfer stack. This was carried out according to manufacturers' instructions. Once transferred, the membrane was immersed in 50 ml blocking buffer (1xTBS, 3% w/v milk powder) and left to shake for 1 hour at room temperature. The buffer was removed, and a fresh 20 ml blocking buffer was added. The primary antibody had previously been raised by the Edwards group towards *Alopecurus myosuroides*' protein GSTF1, otherwise known as *Am*GSTF1, and was added at a 1/1000 dilution (20 µl) and placed on a shaker at room temperature for 1 hour. The membrane was washed twice in 50 ml 1xTBS, 0.05% Tween 20 with each wash lasting 5 minutes, before a final wash with 50 ml 1xTBS for 5 minutes. The membrane was placed in 20 ml TBS containing 3% milk (w/v) and the secondary antibody, anti-rabbit IgG whole molecule alkaline phosphate, at a 1/5000 dilution (4 µl). The membrane was then washed twice in 50 ml 1xTBS, 0.05% Tween 20 for 5 minutes, with a final wash of TBS for 5 minutes. The membrane was finally washed in 20 ml 100 mM Tris-HCl buffer of pH 9.5 for 2 minutes. The protein blot was developed by the addition of 10 ml developing buffer (100 mM Tris-HCl pH 9.5), 33 µl nitro blue tetrazolium (NBT), and 33 µl BCIP (5-bromo-4-chloro-3-indoyl phosphate) and incubated in darkness for 15 minutes. Once developed and the immunoblotted proteins visible, the membrane was transferred to water and left in darkness for an additional 30 minutes. The membrane was then dried with cool air and visualised.

2.5.5 1-Chloro-2,4-dinitrobenzene (CDNB) glutathione transferase activity assay

900 µl of assay buffer (0.1 M potassium phosphate, pH 7.5) along with 25 µl 40 mM CDNB were added to cuvettes and incubated at 30^{o}C for 5 minutes. 25 µl of protein extract was

added alongside 50 µl 100 mM glutathione to give a total reaction volume of 1 ml. The cuvette was placed into a spectrophotometer and absorbance readings were taken every 0.5 seconds for 30 seconds at a wavelength of 340 nm. A non-enzyme control was used to account for the spontaneous rate of conjugation.

2.5.6 Flufenacet activity assay

To an Eppendorf tube, 20 µl 1M Tris-HCl (pH 7.5), 10 µl of 20 mg/ml BSA and 50 µg protein extract were added and made up to 170 µl with water. The reaction mixture was then incubated at 30^{o}C for 3 minutes and 10 µl of 10 mM flufenacet and 20 µl of 10 mM glutathione added to the reaction. At selected time points of 10, 20, 30, and 40 minutes, 10 µl of 3M HCl was added to stop the reaction and the samples stored at -20^{o}C overnight to precipitate the protein. Samples were centrifuged at maximum for 3 minutes and the supernatant analysed by liquid chromatography coupled to mass spectroscopy (QDa) as described in section 2.6.3.

2.5.7 Glutathione concentration assay

Plant tissue was ground under liquid nitrogen and 100 mg – 300 mg aliquots taken and added to pre-chilled microfuge tubes. 5% sulfosalicylic acid (SSA) was made through dilution of SSA in assay buffer (provided in kit). 3x v/w 5% sulfosalicylic acid (SSA) was added to each tube, which were then vortexed for 20 seconds. An additional 7x v/w 5% SSA was then added (10x total). Cells were lysed by sonication at 40kV for 5 minutes, vortexed, and then centrifuged at 10000x g at 4^{o}C to precipitate proteins. Measurements of both oxidised and reduced glutathione were taken for each plant species using an Invitrogen™ Glutathione Fluorescent Detection Kit in accordance with manufacturer's instructions. Colorimetric detection readings were taken using a Hidex sense microplate reader.

2.6 Herbicide uptake studies

2.6.1 Metabolite synthesis

In order to quantify proposed glutathione and cysteine conjugates of flufenacet, these metabolites had to be synthesised as none were commercially available. The synthesis reaction was performed by reacting 17.5 µmol of flufenacet with 500 µl of either glutathione (100 µmol/ ml) or cysteine (200 µmol/ ml). 562.5 µl of 1:1 acetonitrile:ethanol was added to the reaction which was made to pH 9 with trimethylamine to encourage spontaneous conjugation. The total reaction was made up to 1.5 ml by topping up with water and left at

room temperature for 48 hours. The reaction mixtures were then diluted, and LCMS used to confirm the reaction had run to completion with no unreacted flufenacet remaining or to quantify any residual parent, as well as to confirm the identity of metabolites.

2.6.2 Liquid chromatography coupled mass spectrometry (LCMS)

Liquid chromatography coupled mass spectrometry (LCMS) was used to analyse for herbicide parent compounds and metabolites. Prior to processing of samples, propachlor was added to each sample at a concentration of $1x10^{-3}$mg/ ml as an internal standard. Samples were prepared for LCMS by centrifugation at 10000xg for 30 seconds and 100 µl of sample transferred to a 300 µl Chromacol fixed insert vial.

For analysis, two LCMS systems were used, a quadrupole time of flight (QTOF) instrument for metabolite identification, and a quadrupole Dalton (QDa) for metabolite quantification. During identification, the ultra-performance liquid chromatography (UPLC) instrument used was a Waters aquity I class (FTN) coupled to a Waters Xevo GZ-XS quadrupole time of flight (QTOF) mass spectrometer (MS). For each sample, an injection volume of 5 µl was taken from the 100 µl sample. A 3-minute run time was used for separation by UPLC with a flow rate of 0.5 ml/min. A solvent gradient with LCMS grade water and LCMS grade acetonitrile, each containing 0.1% formic acid, was used for sample separation. Sample separation was performed using a C18 1.7µm reverse phase column of dimensions 1.2 mM x 50 mM. A gradient was run with an initial concentration of 95% water and 5% acetonitrile over the course of 2 minutes and then maintained at 95% acetonitrile for 30 seconds. When using negative ionisation, a capillary voltage of 2kV was used with 3kV used for positive ionisation. A source temperature of 120^{o}C with a desolvation temperature of 600^{o}C and a gas flow rate of 800L/hr were employed. The identities of metabolites were confirmed by LC-MS/MS. Fragmentation patterns were obtained for each of the identified metabolites over a mass range of 100-1000 Da using a scan time of 0.1 sec and collision energy ramp of 20-40eV.

Quantification of flufenacet and its metabolites was carried out with the same instrumentation used for initial identification with the use of an Aquity QDA in place of the QTOF. The same run conditions and column were used as within the initial identification process with all screening taking place in positive ionisation mode with a cone voltage of 15V.

Standard curves for flufenacet, glutathione-flufenacet conjugate, and cysteine-flufenacet conjugate of known concentrations were made by 3x serial dilution for quantification of samples and allowed for quantification of samples ranging from 0.7 nmol to 55 nmol for flufenacet, and 0.015 nmol to 11.2 nmol for both the glutathione and cysteine conjugates. Data analysis was carried out using MassLynx V4.1.

2.7 Wax profiling analysis

2.7.1 Scanning electron microscopy (SEM)

Samples were prepared for SEM by firstly drying leaf within a desiccator for 1 week. Samples were mounted onto an aluminium mount using double coated carbon conductive tabs, and then gold coated. Images were taken using a Tescan Vega 3LMU SEM coupled with a Bruker Xflash 6 | 30 detector for energy dispersive X-Ray spectroscopy (EDS) analysis.

2.7.2 Wax extraction and derivatization

Extraction of wax was performed on 5g of leaf tissue from either wheat, blackgrass or ryegrass, with the flag leaf used in each instance. The leaves were submerged in 50 ml of GCMS grade chloroform for 30 seconds. The leaves were submerged two times each in 50 ml of fresh chloroform and the two chloroform extracts combined. The extract was evaporated down using a rotary evaporator until a volume of 5 ml had been obtained. A 1 ml aliquot of each extract was taken and to it tetracosane was added at a concentration of 0.1 mg/ ml to serve as an internal standard. The 1 ml sample was placed in a rotary evaporator until all solvent had been evaporated and no further loss of weight detected. Prior to analysis, extracts were also derivatised for GC analysis. This was done to increase volatility, stability at high temperatures and to improve peak shape to help with the identification of hydroxyl-containing compounds. Trimethylsilylation was carried out using 20 µl N,O-Bis-(trimethyl)-trifluoro-acetamide and 180 µl pyridine to catalyse the reaction. The reaction was left at room temperature for 24 hours after which, the samples were rotary evaporated until dry. The samples were then dissolved to a concentration of 1 mg/ ml wax in chloroform, and analysed be either gas chromatography coupled to mass spectroscopy (GC-MS) or gas chromatography coupled to flame ionisation detection (GC-FID).

2.7.3 GCMS analysis

Both derivatised and underivatised wax was dissolved in chloroform at a concentration of 1 mg/ ml with tetracosane added as an internal standard at a concentration of 0.1 mg/ ml. GCMS analysis was carried out using a 5977B GC/MSD system. Separation was achieved using Phenomenex capillary column ZB-5HT 30m x 0.25 mM I.D. with a 0.25 µm film thickness. Helium was used as a carrier gas with a flow rate of 2.2 ml/min in constant flow mode. The oven temperature was programmed from 50°C to 340°C at a rate of 6°C.min with a 22 minute hold at 340°C. 1 µl of sample was injected using a 1:10 split mode and an injector temperature of 300°C. The mass spectrometer was run with an electron impact mode of 70eV and a source and quadrupole temperature of 300°C and a scanning range of 30 – 1200 amu per second.

2.7.4 GC-FID analysis

Separation was achieved using a Phenomenex capillary column ZB-5HT 30m x 0.25 mm I.D. X 0.25 µm film thickness. Helium was used as a carrier gas with a flow rate of 2.2 ml/min in constant flow mode. The oven temperature was programmed from 50 °C to 340 °C at a rate of 6 °C/min with a 22 minute hold at 340°C. 1 µl of sample was injected using a 1:10 split mode and an injector and FID temperature of 300°C. Quantification of wax components was carried out using authentic standards representative of the chemical classes found in leaf wax. The standards used were stigmasterol for sterols, tetracosane for alkanes, octacosanol for fatty alcohols, stearic acids for fatty acids and stearyl palmitate for wax esters. Standards for hydroxyl-containing standards were derivatised as described prior to their quantification.

2.8 Herbicide droplet analysis

2.8.1 Droplet dry down distribution

In order to observe the distribution of actives within applied droplets, a dry down distribution reading was taken. Formulations were diluted to 2.4 mg/ml in d.i water and 0.5 µl droplets pipetted onto glass microscope slides which had been cleaned with an acetone-soaked fibre free cloth. Once the droplet had dried, imaging was performed on a BX51 microscope using polarised light with a grid of images taken to include the entirety of the droplet. This was done by taking images in order, as shown in Figure 10, and leaving 20% overlap between each image to allow for subsequent stitching of images together. 5 droplets for each formulation were imaged and stitched together to form a complete droplet image using the software image J.

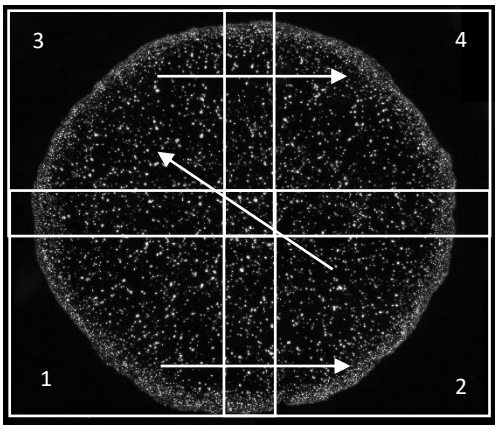

Figure 10. A droplet of the SC formulation with no additional adjuvant demonstrating the order in which images were taken. Overlap was left between each image to allow for image stitching to provide a complete image

Dried Droplet Analysis (DDA) software was used to analyse images. Images were analysed to look at the ratio of distribution of active within the droplet as compared to that distributed at the edge of the drop, referred to here on in as the beta value. A beta value of 1 indicated a uniform deposit, with deposition at the outer edges of the droplet resulting in a greater beta value the more pronounced the outer deposition becomes. The DDA software was used to calculate the particle distribution along a number of lines centred within the droplet, in this instance, 500 lines were used. Increasing line thickness was used to make the calculated distribution less noisy, with 5 pixels used as the thickness for each line.

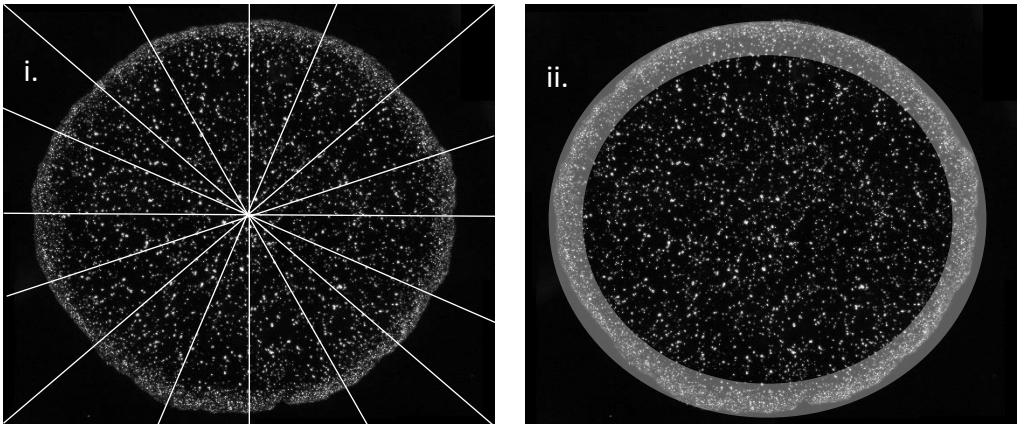

Figure 11 i. demonstrates how lines are distributed throughout the droplet to calculate the particle distribution. ii. Shows where the outer deposit lies with regard to the rest of the droplet, it is the ratio between the highlighted ring and the rest of the drop which is used to calculate the beta value.

2.8.2 Droplet contact angle

The contact angle of droplets was taken for flufenacet formulations applied to four different surfaces, parafilm, to act as a model surface, and the leaves of wheat, black grass and ryegrass respectively. The formulations were diluted down to 2.4 mg/ml with deionised water, and 9 µl droplets applied to surface using a DS 500/GT gas tight 500 µl syringe with an attached SNS xx dosing needle. The contact angle was measured with an OCA 15EC contact angle measuring system at both the left and right side of the droplet and averaged across multiple droplet applications. The droplet angle was taken upon leaf application and then again after 1 minute to observe the change over time. All contact angle measurements were performed at a controlled temperature of 20 ^{o}C and controlled humidity of 40%.

2.8.3 Surface tension

The equilibrium surface tension of adjuvant containing flufenacet formulations was measured using a sigma 700 tensiometer. Formulations were diluted down to 2.4 mg/ml in d.i water and rolled for an hour to ensure mixing. Water was used as a reference to ensure the instrument had been adequately cleaned between runs and runs were only performed when water gave a reading between 70 and 74 mN/m to ensure accuracy and no carry over from previous tests.

2.9 Statistical analysis

To detect statistical differences between two groups, a t-test was carried out provided that all its assumptions (the data are continuous, the data follow a normal distribution, the variance of the two populations are equal, the two samples are independent) were satisfied.

In instances where three of more groups were present, ANOVA tests were carried out, provided all assumptions were satisfied (data is normally distributed, variance is homogenous, each sample is independent). One-way ANOVA was carried out where the relationship between an independent and dependant variable is of interest. A two-way ANOVA was used in the assessment of the interrelationship of two independent variables on a dependent variable.

Both these statistical tools assume that residuals are normally distributed, with a mean 0, and a constant variance. Normality of residues was assessed by visual inspection of QQ plots, which arranges the data collected against the theoretical values for a normally distributed population. A Shapiro-Wilk test was conducted on the residuals to further determine the normality of the data. In instances where a p-value is less than or equal to 0.05, the data is determined to not fit a normal distribution with 95% confidence. In instances where this assumption may be violated, a non-parametric Mann Whitney was considered.

All statistical analysis was carried out using Prism version 8, with P values for each test represented as follows: not significant (n/s) = >0.05, * = ≤0.05, ** = 0.01, *** = ≤ 0.001

3 Herbicide formulation and biomarker identification

3.1 Introduction

All important crop species throughout the world are subject to losses from pests, pathogens, and weeds. The application of herbicides is one of the most economically viable and effect means by which to deliver yield, by suppression of competitive weed species (Pan et al., 2019). While the benefits of herbicides are apparent and a requirement in modern agriculture, the negative impacts of herbicides cannot be ignored. An estimated 4.6 million tonnes of herbicide are sprayed annually worldwide and in the most extreme cases it is estimated that as little as 1% of the active ingredient reaches its intended target, with the majority transferred to soils, water bodies and the atmosphere (W. Zhang et al., 2011). With such a small amount of herbicide affecting its intended target, improved herbicide formulations offer a potential avenue to reduce both active loading of herbicide formulations, as well as the total amount applied by facilitating increased uptake and translocation to the site of action.

The efficacy of applied herbicides depends on a number of factors, one of the most impactful being the way in which they are formulated. Appropriate herbicide formulations aim to match the physiochemical characteristics of active ingredients and make considerations of the physiology of crop and weed plants (Mesnage et al., 2018; Satchivi et al., 2014). Herbicide formulations consist not only of the active, but a number of co-formulants (or inerts) including surfactants, dispersants, adjuvants, and in many cases solvents. There is currently a general move away from environmentally harmful formulations such as solvent based emulsions, to those which are water based, such as suspension concentrates (Pan et al., 2019). In this project a range of actives have been selected for initial formulation and testing, which comprise different herbicide chemistries acting on different modes of action (Figure 12). The compounds were cyhalofop-butyl, typically formulated as an emulsion, diuron, propyzamide and flufenacet typically formulated as suspension concentrates, and metolachlor, typically formulated as an emulsifiable concentrate.

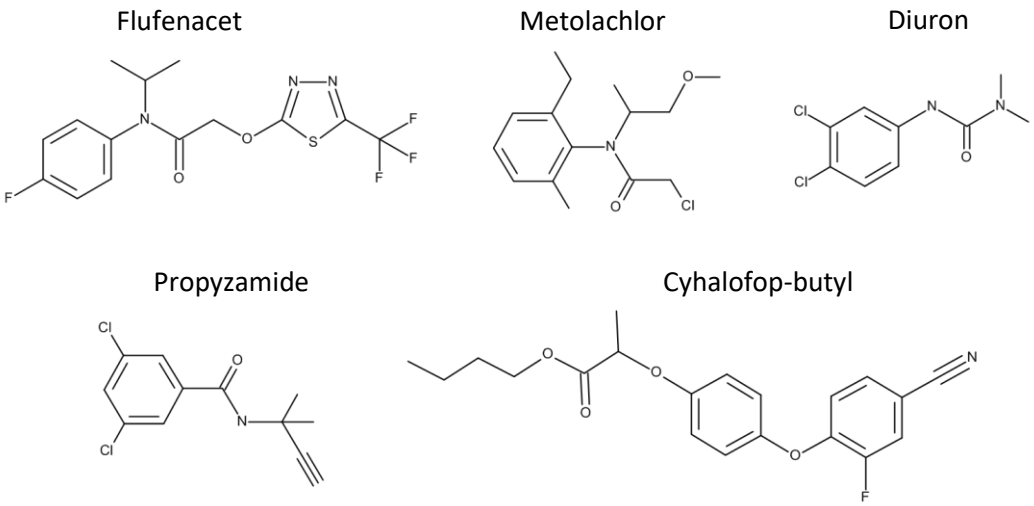

Figure 12. Chemical structure of each of the herbicides used in the process of biomarker identification

Cyhalofop-butyl is an aryloxyphenoxypropionate herbicide which is typically used within rice fields for the post emergence control of grass weeds, primarily barnyard grasses (*Echinochloa spp*) and silver top grass (*Austrodanthonia spp*). Cyhalofop-butyl is a systemic herbicide able to move through both the xylem and phloem of treated foliage. The herbicide accumulates in meristem tissues where it acts as an Acetyl-CoA carboxylase (ACCase) inhibitor, preventing fatty acid biosynthesis and causing a lack of cell, organ, and tissue growth, which eventually results in plant death (J.-D. Wang et al., 2010; Ottis et al. ,2005;Ruiz-Santaella et al., 2006). Cyhalofop-butyl is a pro-herbicide in which metabolism to the herbicidally active cyhalofop-acid occurs rapidly in susceptible weeds (Ottis et al., 2005; J. Wu et al., 2014). Selectivity is derived through two means, firstly, in crop plants there is a lack of functionality of esterases able to metabolise cyhalofop-butyl to its acid form, resulting in slow formation of the acid (Ruiz-Santaella et al., 2006). Secondly, the low concentration of acid which is formed is more quickly metabolised to inactive metabolites such as cyhalofop-diacid in none target plants (Ottis et al., 2005).

Metolachlor is a chloroacetanilide herbicide commonly used for control of broadleaf grasses in maize, sugar beets, sorghum, soybean and other crops (Al-Khatib et al., 2002; Stara et al., 2019). Metolachlor acts by inhibiting plant growth and development by targeting fatty acid elongases, interfering with plant development such as leaf and flower growth, and stem elongation. Typically, damage resulting from metolachlor is stunting of plant growth followed by plant death. Metabolism of metolachlor is primarily by glutathione conjugation, and

further downstream processing to the malonyl-cysteine conjugate, as well as other sulphur linked metabolites, with oxidative metabolism also observed (Al-Khatib et al., 2002).

Diuron (3-(3,4-dichlorophenyl)-1,1-dimethylurea) is a photosystem II (PSII) inhibitor acting within aerial parts of the plant and moving primarily through the Xylem. Diuron blocks photosynthetic electron transfer conversion by competing with electrons for binding to the D1 quinone-binding site of the secondary plastoquinone (QB-site) (Lichtenthaler et al., 2013; Pascal-Lorber et al., 2010). As a consequence, photosynthetic electron flow from the primary plastoquinone (QA-site) to the secondary QB-site is inhibited. This leads to a reduction in the rate of synthesis of ATP and NADPH, both of which are required for fixation of CO_2. (Lichtenthaler et al., 2013; Svyantek, 2016). In addition, the interrupted electron flow results in the formation of oxygen derived radicals such as $^1O_2$, H_2O_2, and OH (Flors et al., 2006; Svyantek et al., 2016). This result is photo-oxidation of cellular components such as chloroplast, resulting in cellular degradation and eventual plant death (Shukla et al., 2008).

Propyzamide (3,5-dichloro-N-(1,1-dimethylprop-2-ynyl)benzamide) is a benzonitrile amide herbicide which is used for both pre and post emergence for the control of perennial and broad-leaf weeds. Propyzamide acts by inhibiting tubulin polymerisation and thus disrupts mitosis in dividing cells within the shoots and roots (Travlos et al., 2017; Zhao et al., 2015; P. Wu et al., 2019).

Flufenacet (N-(4-Fluorophenyl)-N-isopropyl-2-{[5-(trifluoromethyl)-1,3,4-thiadiazol-2-yl]oxy}acetamide) is an oxyacetanilide herbicide which is used primarily for the control of grass weeds and has been found to provide effective control in maize, soybean, potato and wheat (Rasool et al., 2019). Flufenacet is applied pre or early post emergence and acts by inhibiting the biosynthesis of very-long-chain fatty acids. This results in inhibition of cell division in newly growing tissue, causing stunting of the plant and eventual death. The direct target of flufenacet however has yet to be elucidated (Lechelt-Kunze et al., 2003).

This chapter focuses on the ways by which these actives can be formulated and tested for stability, as well as ways by which these formulations affect uptake in crops (wheat) and weeds (blackgrass and ryegrass. This chapter aimed to look at gene expression, protein expression, and metabolite levels as a means of determining uptake levels of herbicide. Due to the phytotoxic nature of herbicides it would be expected that a stress response would be

induced within the plant in response to herbicide treatment. It was hypothesised the concentration of bio-available herbicide would therefore correlate to the level of gene induction, protein induction, and metabolite concentration levels found within each plant, providing a proxy measure for herbicide uptake.

3.2 Herbicide formulation and initial stability testing

Formulation of herbicides is necessary for several reasons, namely improved stability, delivery, operator safety, and reduction in environmental impact (Roechling, 2018). Of the selected actives, metolachlor is liquid in its native form, whereas the others are solid powders. The particle size of solid herbicides after formulating can have a significant effect on both the efficiency and stability of the herbicide formulation and so was determined after formulating. Selection of the formulation type is highly dependent on the physiochemical properties of the active used. Of these solid formulations, diuron, propyzamide and flufenacet were formulated as suspension concentrates (SC) in which insoluble solid particles are suspended within an aqueous continuous phase. This is done using surfactants such as wetting and dispersing agents, which help maintain the smaller particle sizes achieved following milling. After milling, particles will otherwise progressively flocculate irreversibly because of van der Walls forces, leading to a progressive increase in particle size and an unstable formulation (Schmitt et al., 2014). There are two ways by which this can be avoided; through the use of electrostatic repulsion, or by steric hindrance. Ionic surfactants will be adsorbed onto the particle surface during milling and produce electrostatic repulsion between dispersed particles and prevent agglomeration. Alternatively, non-ionic surfactants with no net electric charge may be used such that the hydrophobic head of the surfactant adsorbs onto the solid particle, while the hydrophilic tail sits within the aqueous solution. When particles approach one another, the hydrophilic tails repel one another and prevent agglomeration (Terescenco et al., 2019).

Particle size readings were taken for each of the formulated solid actives to ensure uniformity and stability of the formulation. This was done using a Mastersizer 2000 which utilises laser diffraction with a red-light source of 632.8 nm and a blue light source of 470 nm as described in 2.2.1. As particle size has such a large effect on herbicide efficacy, it was important to ensure that the herbicide formulations were within an acceptable range of size distribution (0.1 µm – 15 µm). Smaller particles evenly distributed within the formulation increase coverage of the active across the leaf surface and therefore enhance uptake. Particles which

are too small however are more likely to react with other formulation components, be light sensitive, or show crystal growth, resulting in an unstable formulation (Roechling, 2018).

Due to its lack of water solubility and therefore low stability in water-based formulations, cyhalofop-butyl was formulated as an oil in water emulsion. Cyhalofop-butyl along with non-ionic surfactants, were dissolved in aromatic hydrocarbon solvent Solvesso™ ND150, to act as the oil phase. This oil phase was then added dropwise to an aqueous phase, such that the lipophilic head of the surfactants sits within the oil droplet and the hydrophilic tail in the aqueous phase, maintaining the oil droplets as a suspension. The first cyhalofop-butyl formulation (Figure 13. d.) had a d(0.9) of 10.498 µm falling within the desired range of particle size. There was however a secondary peak which showed particles as large as 100 µm. This would indicate instability in the formulation and progressive agglomeration of oil droplets, causing a shift to much larger particle sizes during long term storage. This resulted from an overloading of the oil phase, meaning that the repulsive forces of the surfactants on the oil droplets were not able to maintain droplet size. Upon reducing the ratio of the oil phase, a much more stable formulation was produced with only one peak and a d(0.9) of 9.931 µm (Figure 13. e.).

The propyzamide formulation showed the lowest particle size distribution, but also had a second minor peak showing uneven distribution (Figure 13 a.). Initial diuron formulation (Figure 13 b.) showed a broad range of particle sizes with the largest having a diameter of 2 mm. This initial diuron formulation was prepared at 800 g/L, comparable to commercial formulations for this herbicide. This loading however was not compatible with the formulation components used, with coagulation of the active occurring. As the aim was for have a d(0.9) of less than 15 µm (90% of particles less than 15 µm), and to have only one peak, the formulation was further refined by reducing the loading of active to 650 g/L. By reducing the load of the active the d(0.9) of the diuron formulation was reduced to 6.301 µm with only one peak present (Figure 13 c). This indicated a more uniform particle size, and as only one peak was present, a reduced risk of coagulation and better formulation stability.

Propyzamide

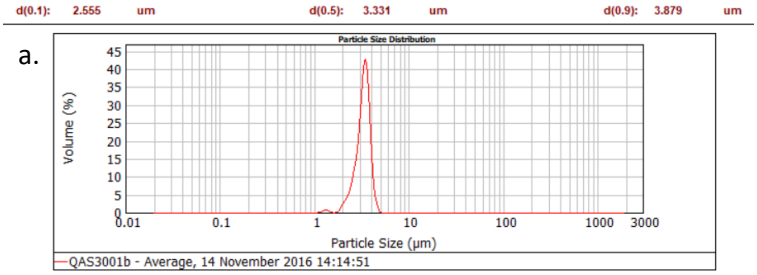

Diuron

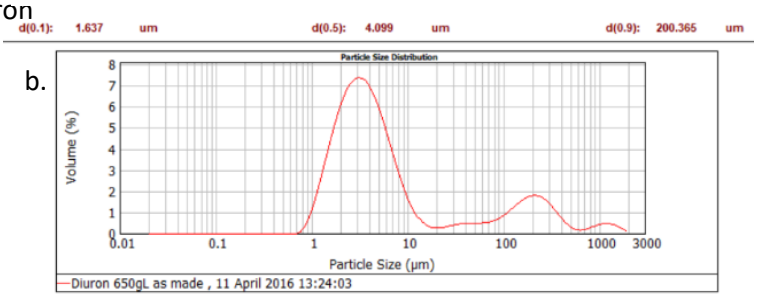

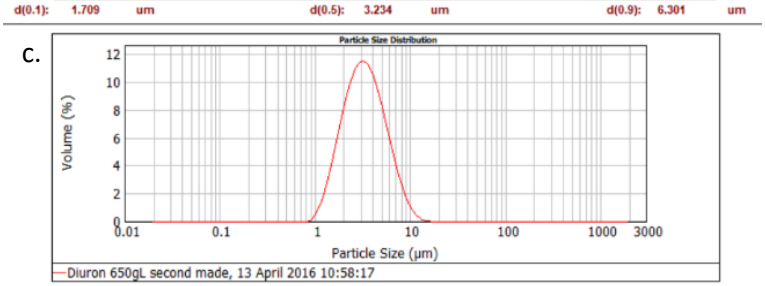

Cyhalofop-butyl

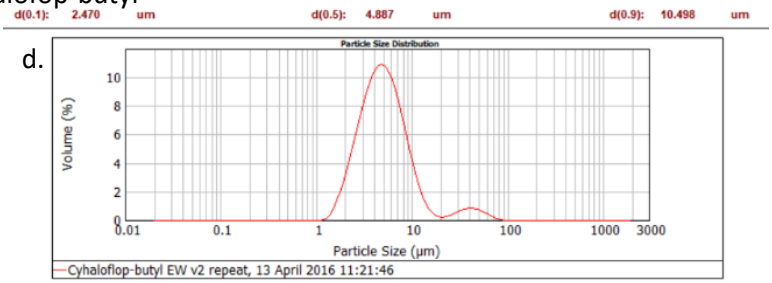

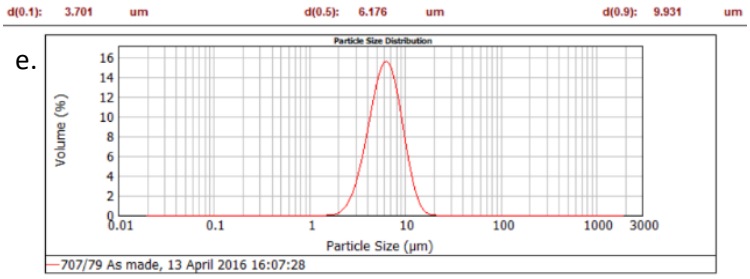

Flufenacet

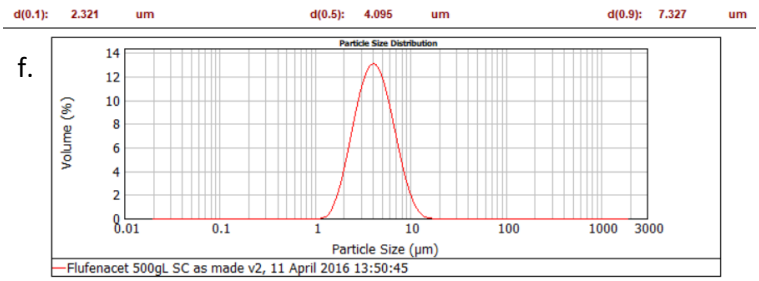

Figure 13.Particle size readings taken for each of the solid based formulations. Each peak represents the average particle size found within the formulation with the width showing the particle size distribution. b. and d. are examples of unsuccessful formulations with a., c., e., and f. representing the final formulations

Metolachlor is a liquid in its native form and was formulated as an emulsifiable concentrate (EC). An EC consists of a liquid active ingredient, optimally combined with solvent and surfactants, allowing stable emulsion formation upon addition to water. This is achieved by balancing water and active soluble surfactants at the water/active interface to allow for a stable emulsion to be formed. Metolachlor EC formulations were tested by dilution in water to look for spontaneous blooming, and then left for a period of 30 minutes. After 30 minutes had passed, formulations were checked for sedimentation. As seen in Figure 14, formulations 1, 13, and 16 had notable sedimentation, indicating instability. Upon closer inspection, all formulations aside from point 67 (90% metolachlor and 10% Etocas 35) resulted in a degree of sedimentation, indicating an incompatibility with the formulation. For this reason, point 67 was used for final formulation creation and testing.

Figure 14. Metolachlor formulations were made based on the triangle points previously demonstrated. The formulations were diluted 1 in 10 in water and left for 30 minutes to check for instability through sedimentation formation.

3.3 Identification of herbicide metabolites using liquid-chromatography tandem mass-spectrometry.

As it was not possible to use radio labelled herbicides due to the quantities required, alternative means of identifying active uptake had to be established. As many herbicide metabolites are only produced *in planta*, this provided a potential avenue through which to establish levels of uptake. Plant metabolites were identified by looking at previous literature and finding known metabolites of each active, as well as looking for potential metabolites based on the metabolic pathways of similar actives. Herbicide formulations were applied to leaf surfaces, incubated, and the metabolites and parent extracted as described in section 2.6.1. These extracts were then screened by liquid-chromatography coupled to mass-spectrometry, allowing for the detection and identification of molecules based on mass to

charge ratio after ionisation. Due to the nature of biological extracts, a number of co-extractants were present alongside the molecules of interest. For this reason, chromatography was important to reduce the negative effects of direct infusion such as ion suppression. Thus, while using direct infusion or with inadequate chromatography, the electrospray response of compounds of interest may be suppressed by biological components which compete for ionisation (Cajka et al., 2014; Jemal et al., 1999). After chromatographic separation of compounds, mass spectrometry was used to separate individual molecules based on their mass to charge ratio after ionisation (Figure 15). When first performing metabolite identification, quadrupole time of flight mass spectroscopy (QTOF) was used due to its high resolution and ability to confirm metabolite identification by tandem mass spectrometry (MS-MS). Using quadrupole based identification, molecules are transformed into gas phase ions and through the use of electric and magnetic fields, the response of each ion, and therefore mass can be determined (Fenn et al., 1989). The time of flight aspect relies on measuring the time taken for the ion to fly through a field free region, with mass being proportional to the time to reach the detector (L. H. J. Richter et al., 2019). The QTOF instrument is a hybrid of both quadrupole and time of flight resolution, allowing selected ions to be filtered out in the quadrupole, fragmented, and separated by *m/z* in the TOF detector to allow high resolution detection (Pan et al., 2019).

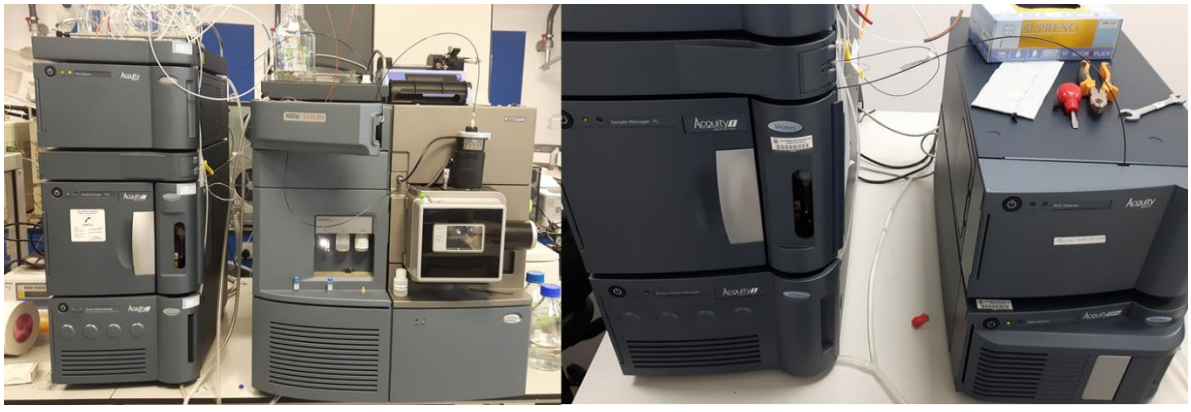

Figure 15. (left) QTOF system used for initial metabolite screening and MSMS for confirmation of identity. (right) QDa system used for metabolite quantification using authentic standards

Raw MS data was acquired and analysed using the Mass Lynx software. Mass Lynx was used to look for H^+ ions of the proposed metabolites in order to obtain retention times, observe mass accuracy, and to extract the peak areas of potential metabolites. Metabolites with an

observed m/z of over 20 ppm deviation from the theoretical m/z were discarded, while those within the appropriate range underwent MS-MS to confirm identity. MS-MS data was again analysed by Mass Lynx, where a fragmentation profile was assigned to observed peaks based on the structure of the metabolite found.

3.3.1 Cyhalofop-butyl

Cyhalofop-butyl is a pro-herbicide with differential metabolism being the means by which control and selectivity are derived. As such, the metabolic pathway is well established, as shown in Figure 16. Cyhalofop-butyl firstly undergoes de-esterification to form cyhalofop-acid, which has been shown to be the herbicidally active form of cyhalofop-butyl (Ruiz-Santaella et al., 2006). Cyhalofop-acid is then metabolised to the inactive amide metabolite by oxidation of the cyanide group. Further downstream catabolism to the inactive cyhalofop di-acid occurs following hydroxylation of the amino group (Khare et al., 2014).

A second pathway by which cyhalofop-butyl has been found to be metabolised is the hydrolysis of the propionic acid group of cyhalofop-acid, or the butyl propanoate group of cyhalofop-butyl, to form cyhalofop-DP. Further metabolism by the removal of the hydroxyl group has been proposed (Ruiz-Santaella et al., 2006). Blackgrass, wheat and ryegrass samples treated with cyhalofop-butyl were screened for each of the proposed metabolites.

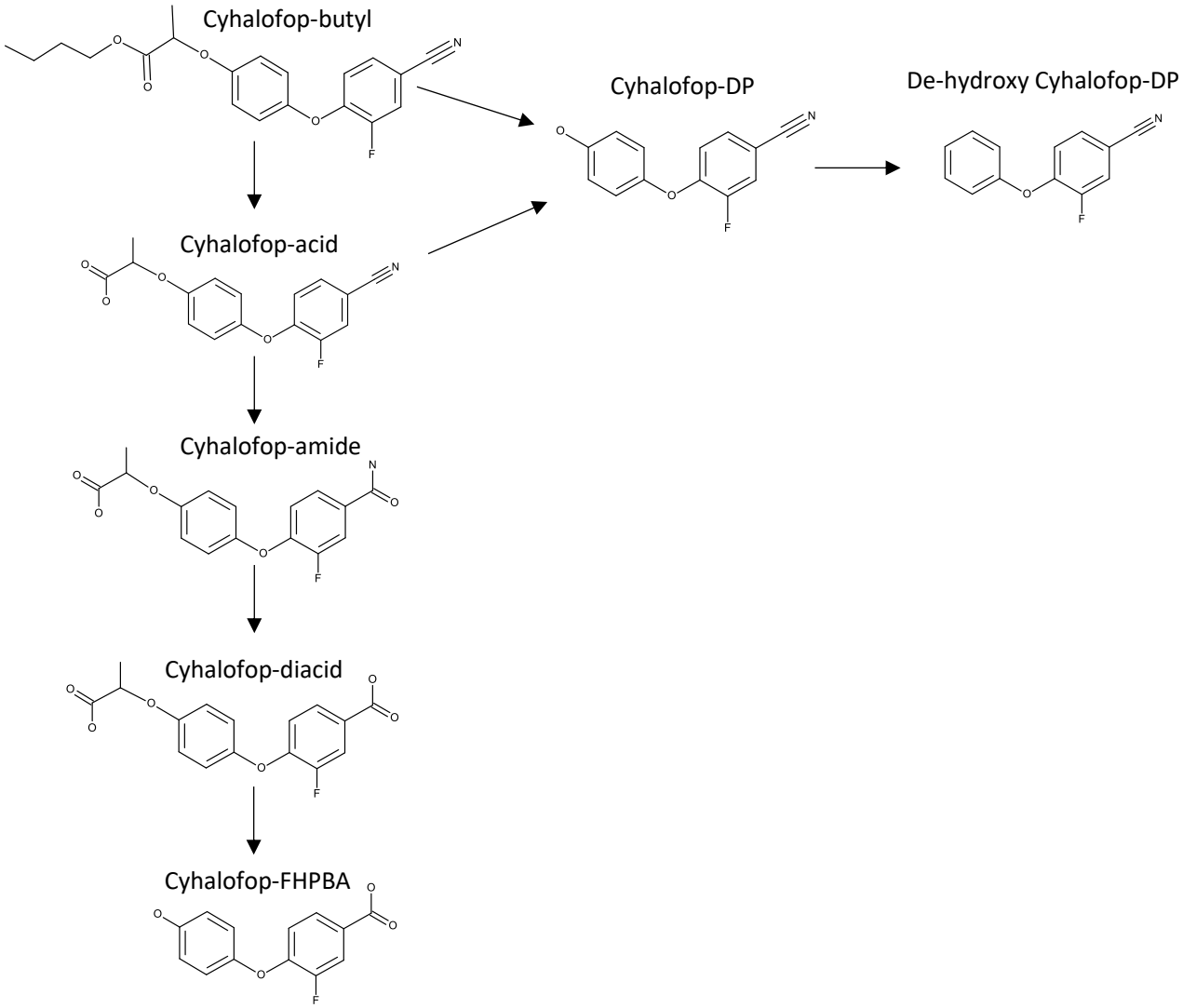

Figure 16.Proposed metabolic pathway of cyhalofop-butyl in plants

As shown in Figure 17, cyhalofop-butyl was detectable in all plant extracts with a retention time of 3.81 min and a m/z of 358.1464 (predicted 358.1455) when positively ionised. Cyhalofop-acid was found to be present in only wheat and blackgrass with a retention time of 4.17 min and m/z of 302.0832 (predicted 302.0829) and none detected in ryegrass. As shown in Table 5, there were several key differences in the way by which cyhalofop-butyl was metabolised within each plant. Cyhalofop-acid, the metabolite of most herbicidal activity, was found predominantly in black grass, with 10% of this level found in wheat and none detected in ryegrass extracts. The None herbicidally active cyhalofop-diacid was found primarily in wheat with lower levels also detectable in black grass, indicating further downstream metabolism from the cyhalofop-acid. Although cyhalofop-DP was present in only small

amounts, the deoxygenated variant of cyhalofop-DP was present at much greater levels in all plants indicating rapid dehydroxylation cyhalofop-DP within each plant species.

Table 5. Peak area per gram fresh weight of plant tissue from each of wheat, blackgrass, and ryegrass, showing the comparative amounts of cyhalofop-butyl and its metabolites within each species. Detectable amounts were displayed as peak area units per gram of fresh weight of leaf tissue.

	PkA/g FW		
Metabolite	**Wheat**	**Blackgrass**	**Ryegrass**
Cyhalofop-butyl	22691.18	114606.90	53198.41
Cyhalofop-acid	1090.69	11441.38	0.00
Cyhalofop-amide	384.80	3282.76	3023.81
Cyhalofop-diacid	3708.33	2393.10	0.00
Cyhalofop-FHPBA	1112.75	0.00	0.00
Cyhalofop-DP	75948.53	0.00	25039.68
Dehydroxy cyhalofop-DP	865.20	0.00	0.00

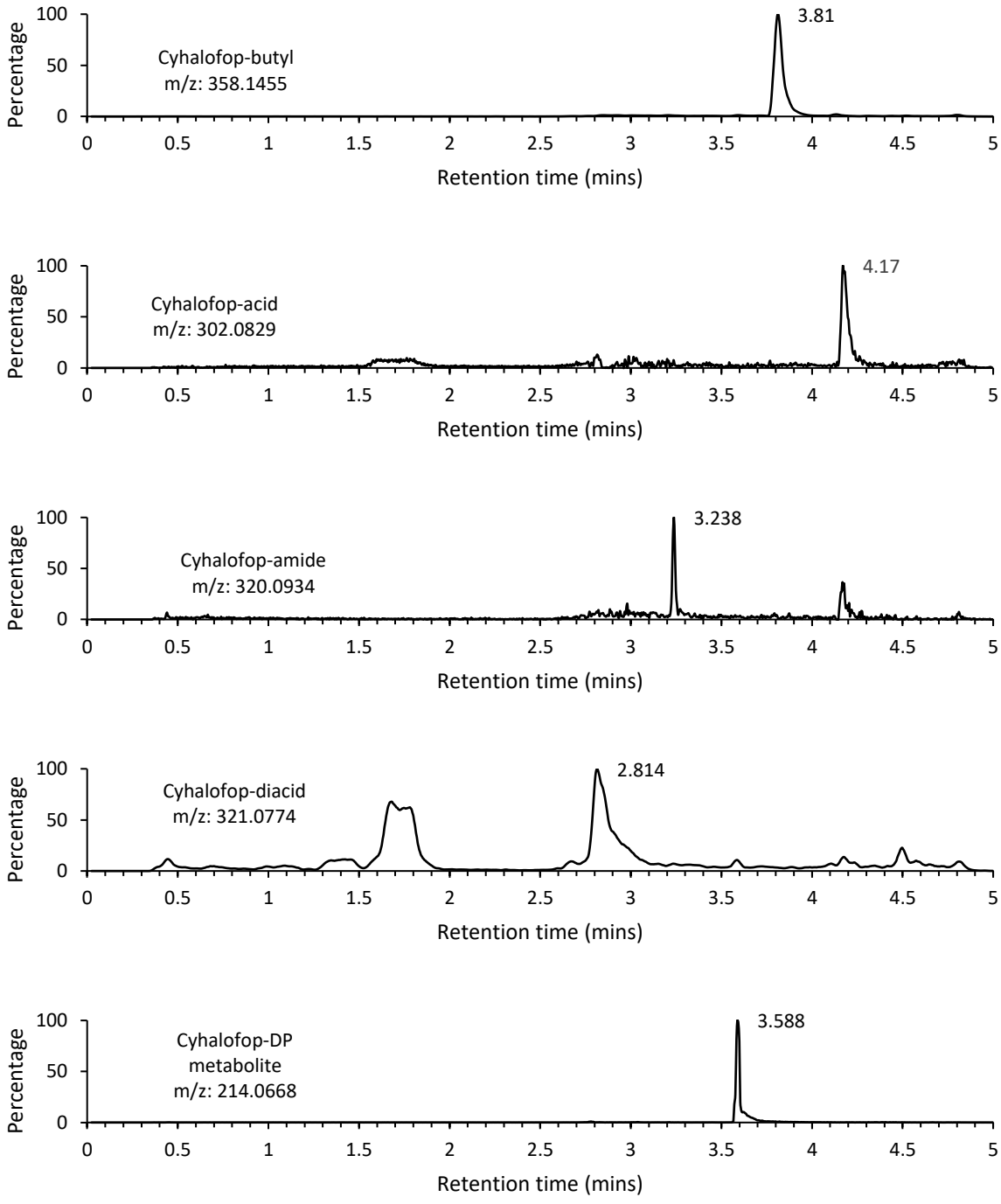

Figure 17. Retention time and m/z of cyhalofop-butyl and the detectable metabolites across all plant species

3.3.2 Diuron

The metabolic profile of Diuron in wheat has previously been described by Pascal-Lorber 2010, (Figure 18). LC-MS was used to look for these metabolites in diuron treated samples of wheat, ryegrass, and blackgrass. Samples were positively ionised, and the mass ions of proposed metabolites screened for in each sample

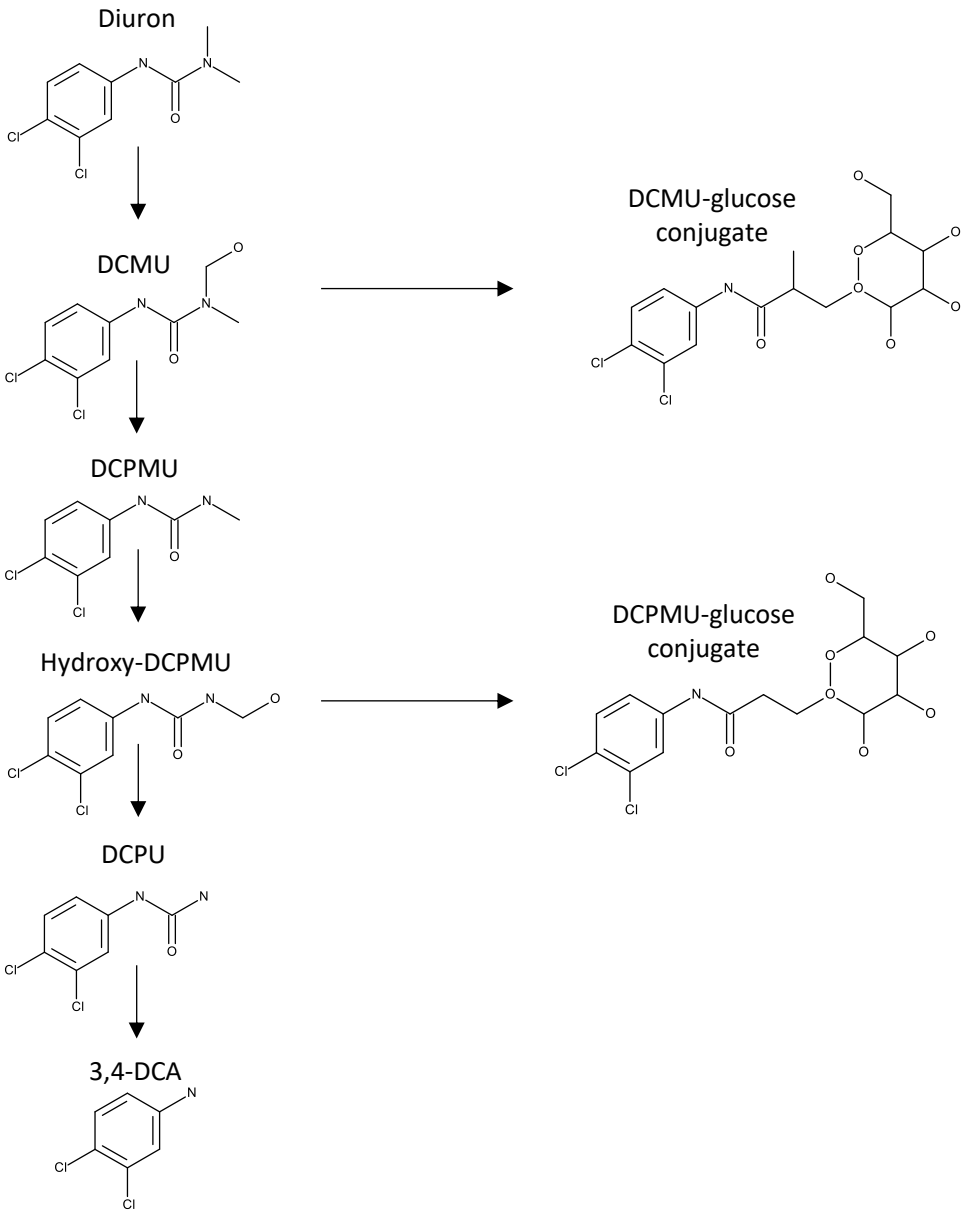

Figure 18. The metabolic pathway of diuron within plant as proposed by Pascal-Lober (2010)

As highlighted in Figure 19 and Table 6, upon searching for the parent compound, diuron was detectable in all plant samples with a retention time of 3.515 minutes and a mass of 233.0249 (predicted 233.0248). The identification of diuron was confirmed with the use of an authentic

standard which showed the same retention time as that found within the samples. For diuron, three mass ions were present (233.0248, 235.0215, 237.0202) resulting from isotopes of the two chlorine atoms found within diuron. Chlorine isotopes are present at levels of 76% ^{35}Cl and 24% ^{37}Cl resulting in ~6% of diuron atoms consisting of two ^{37}Cl isotopes, ~36% consisting of one ^{35}Cl and one ^{37}Cl isotope, and ~58% of molecules consisting of two ^{35}Cl further supporting identification. Diuron was found within each plant species however only one downstream metabolite, DCMU, was found in blackgrass and ryegrass, with none detected in wheat (Table 6). DCMU was found to have a retention time of 3.706 and a mass of 219.0090 (predicted 219.0092), as well as masses of 221.0061 and 221.0044 resulting from chlorine isotopes. DCMU was found to be in low abundance indicating either slow metabolism of diuron or poor detection by LCMS. It was also found that the level of diuron present within wheat was lower than that determined in either blackgrass or ryegrass, where it was found at similar levels. This would suggest that diuron was either taken into the wheat at a reduced level compared to weed species, that the herbicide was metabolised by a yet unidentified metabolic pathway or that the downstream metabolites were not detectable by LCMS.

Table 6. Peak area per gram fresh weight for diuron in wheat, blackgrass and ryegrass. Only one metabolite, DCMU was detectable across all species.

	PkA/g FW		
Metabolite	**Wheat**	**Blackgrass**	**Ryegrass**
Diuron	43805.16	323020.73	449360.66
DCMU	0.00	3134.72	0.00

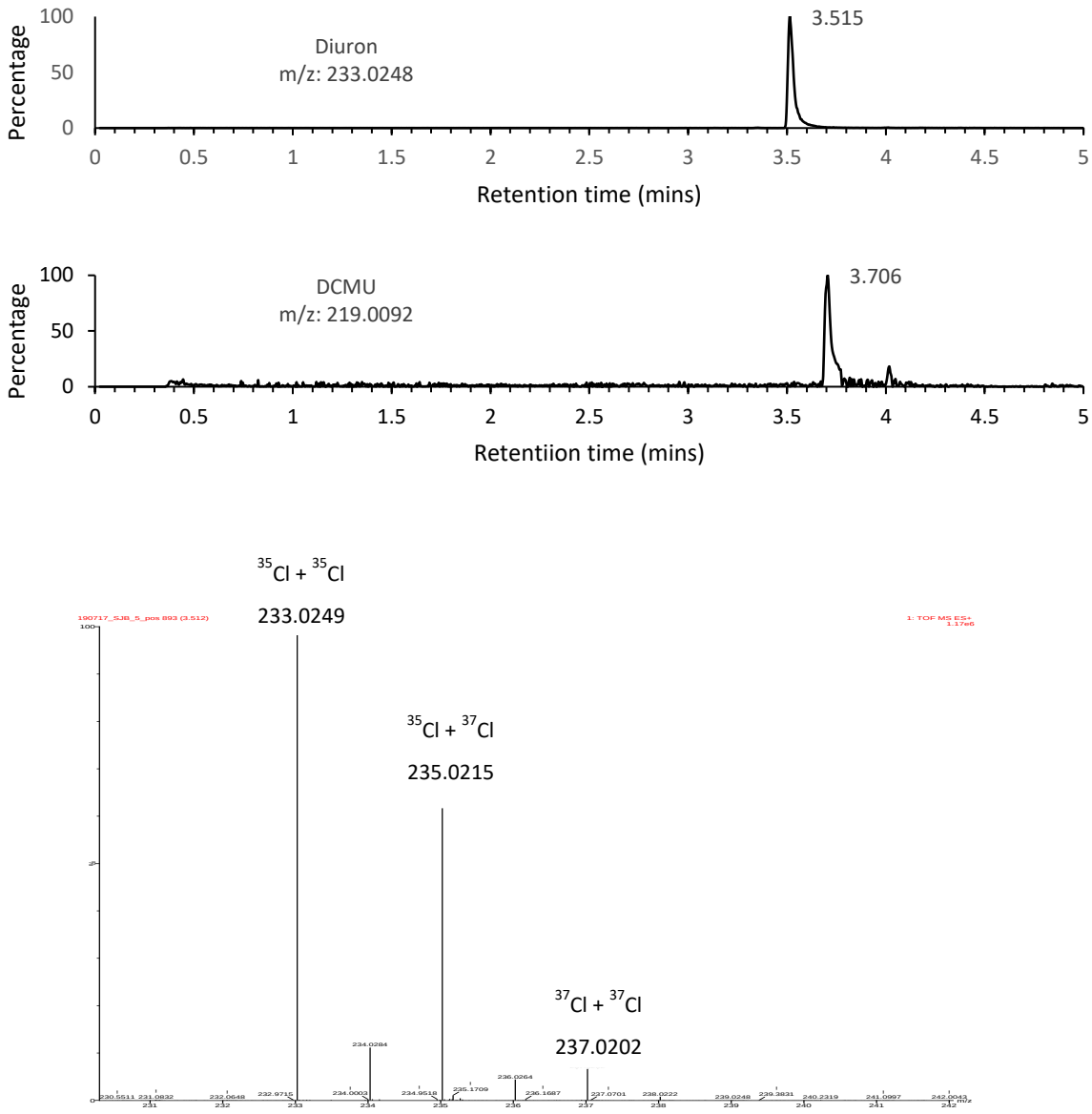

Figure 19. LCMS profiles of m/z = 233.0348 (Diuron) and m/z = 219.0092 (DCMU) as well as the detected isotopic masses of diuron

3.3.3 Flufenacet

Flufenacet metabolism has been previously described by Bayer and is thought to occur by two distinct pathways (Figure 20). Glutathione mediated metabolism involves glutathione conjugation of flufenacet and subsequent downstream processing. Further downstream metabolism of the glutathione-flufenacet conjugate occurs by hydrolysis of either the glutamine or glycine residue, upon which further hydrolysis of the remaining amino acid can occur yielding a cysteine-fluenacet conjugate. Dücker et al (2019) has proposed three

pathways by which the cysteine conjugate may be further metabolised; namely that the cysteine conjugate is processed by either direct conjugation with malonate or hydrolysed to the lactic acid conjugate (Dücker et al., 2019). The lactic acid conjugate may then be conjugated with malonate or glucose. Alternatively, oxidation of the sulphur may occur. No metabolites downstream of the cysteine-flufenacet conjugate were detected in the current study. The second pathway proposed involves the hydrolysis mediated cleavage of flufenacet to flufenacet-alcohol which will then undergo further oxidation into flufenacet oxalate.

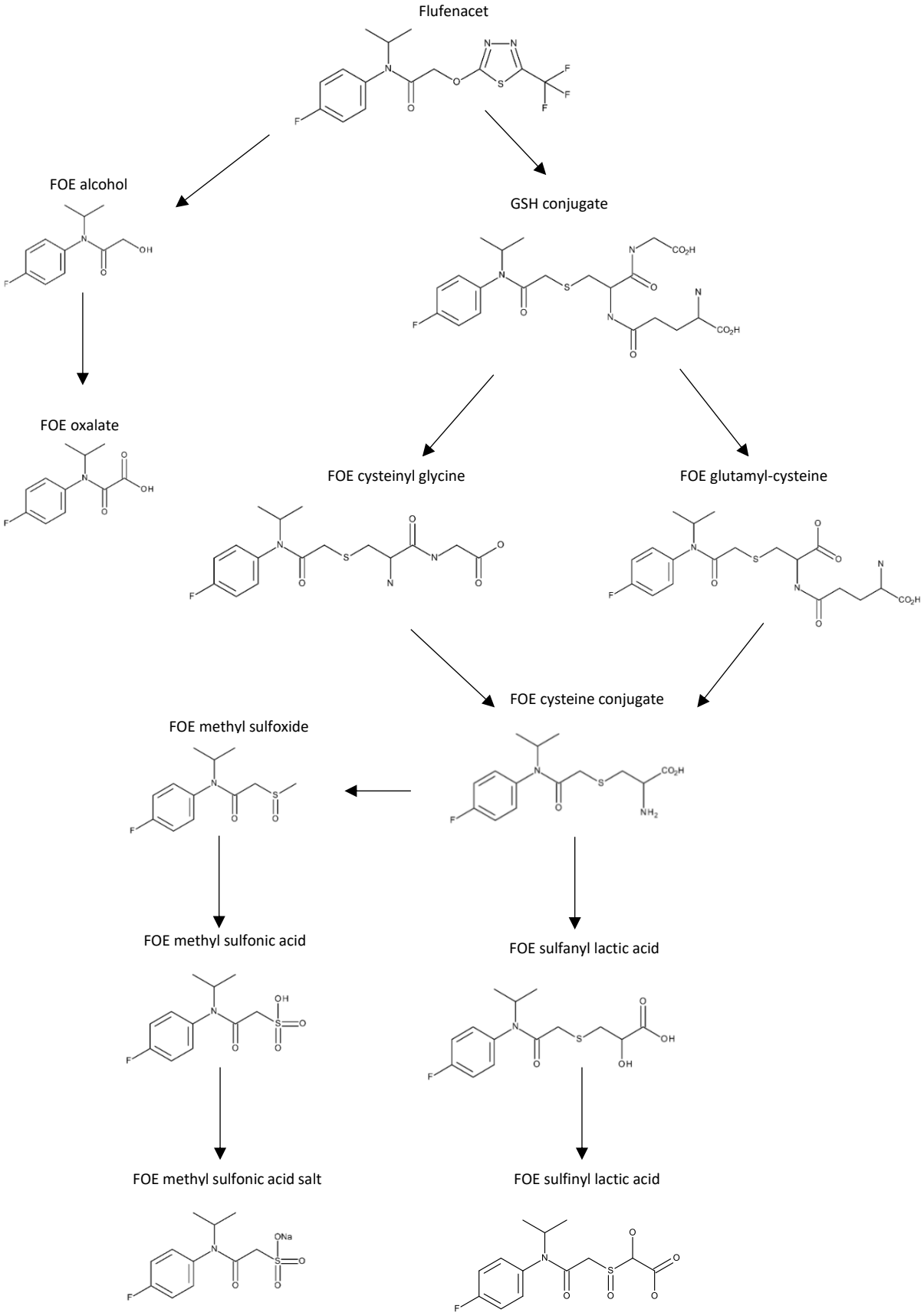

Figure 20. Proposed oxidative (left) and glutathione (right) mediated detoxification pathways for flufenacet.

Treated samples of wheat, blackgrass, and ryegrass were screened for each of the proposed metabolites by LCMS with both positive and negative ionisation. Glutathione and L-cysteine conjugated standards of flufenacet were synthesised and authenticated using electrospray ionisation mass spectroscopy as described in section 2.6.2 and 2.6.3 respectively. Utilising positive ionisation, glutathione and cysteine conjugates of flufenacet were identified in both standards and samples, with a mass of 501.1816 and 315.1173 respectively (predicted masses 501.1819 and 315.1179). As shown in Figure 21, additional intermediate and further downstream metabolites were identified within samples, namely flufenacet-glutamyl cysteine and flufenacet-cysteinyl glycine were found. Both the cysteinyl-glycine and glutamyl-cysteine conjugate were identified in wheat, blackgrass, and ryegrass with masses of 444.1605 and 372.1393 respectively. The primary route of metabolism from glutathione to cysteine conjugates varied between blackgrass, ryegrass, and wheat. In both blackgrass and ryegrass, the herbicide was primarily metabolised to flufenacet cysteinyl-glycine with only small levels of the metabolite found in wheat, where the glutamyl-cysteine conjugate was the dominant intermediate metabolite. It was also noted that levels of flufenacet and metabolites were lower in wheat than in either blackgrass or ryegrass, indicating a lower level of herbicide uptake overall.

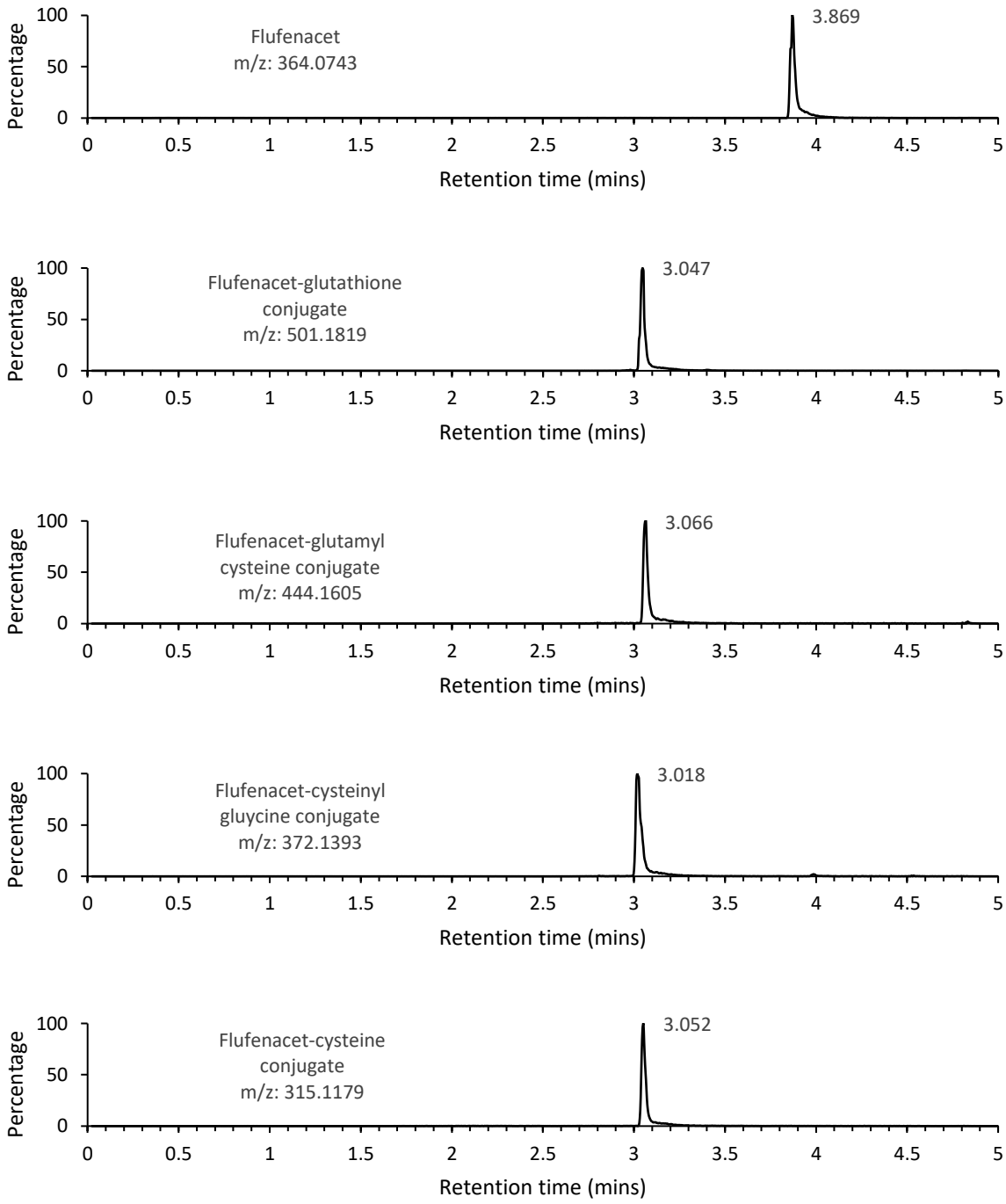

Figure 21. The retention times and peaks obtained when searching for the masses of flufenacet and its corresponding glutathione-like metabolites.

To support initial metabolite identification, MSMS was used as a means of observing the fragmentation profile of each metabolite and parent compound (Figure 22). The fragmentation profile of flufenacet has been well documented, with the observed mass ions corresponding to those previously ascertained. Flufenacet-glutathione and its further

downstream metabolites were fragmented to verify identification. All Glutathione based metabolites resulted in two peaks of mass 192.0822 Da and 226.0702 Da arising from cleavage of the two thioether bonds in the cysteine moiety. The glutathione-flufenacet metabolite resulted in a fragment of 129 Da less than the fragmented molecule (372.1393 Da), characteristic of the loss of a glutamyl moiety from the glutathione conjugate (Brazier-Hicks et al., 2008). A mass of 426.1497 Da was also detected, resulting from the loss of the glycine residue. The most prominent fragment occurred with a mass of 226.0702 resulting from the α-cleavage of the glutathione molecule with sulphur remaining bound to the original flufenacet molecule. The same profile was also found with authentic glutathione standards further supporting identification of the glutathione-flufenacet conjugate.

The glutamyl-cysteine conjugate also resulted in a fragment of 129 Da less than the original molecule resulting from the loss of glutamate (315.1178 Da), as well as retaining other characteristic fragment masses present within the glutathione conjugate (192.0822 Da, 226.0702 Da, 269.1122 Da). Both the flufenacet-cysteine and cysteinyl-glycine conjugates shared similar fragmentation profiles. Distinction was made based on slightly differing LC retention times, differing masses, and by referencing with the synthesised cysteine-flufenacet conjugate standard. The cysteine-flufenacet conjugate showed a distinct peak of mass 299.1024 resulting from N- cleavage within the cysteine moiety.

Flufenacet MS-MS fragmentation

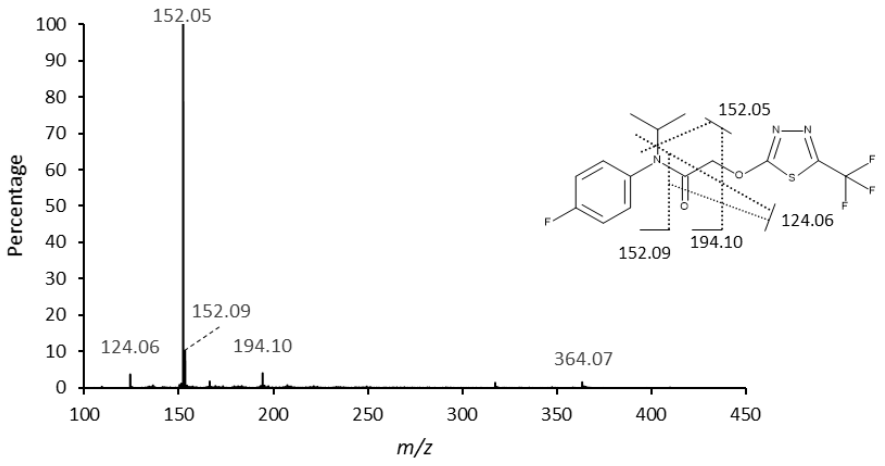

Glutathione-Flufenacet conjugate MS-MS fragmentation

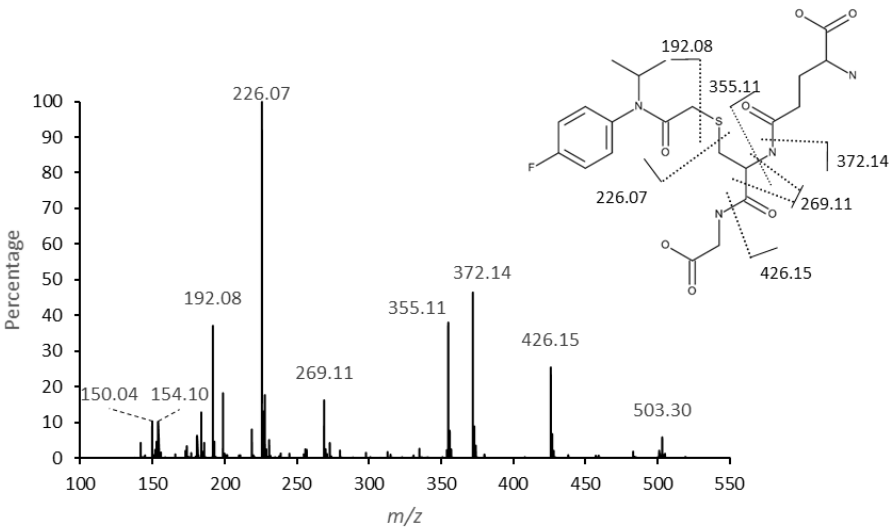

Cysteinyl-glycine conjugate MS-MS fragmentation

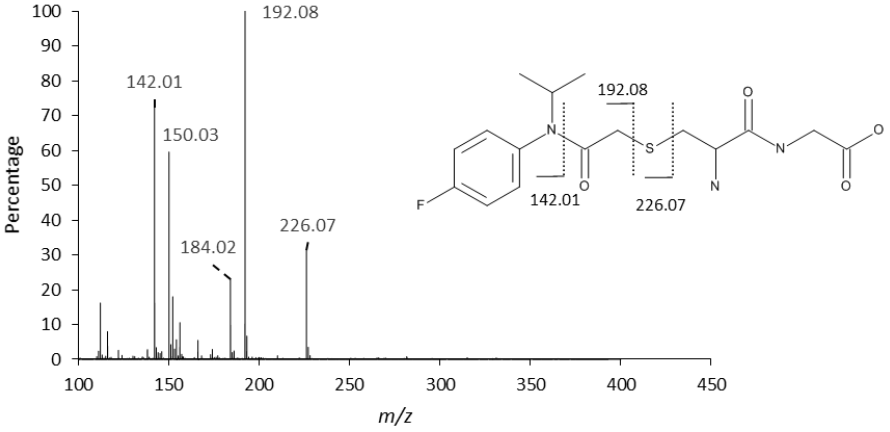

Glutamyl-cysteine conjugate MS-MS fragmentation

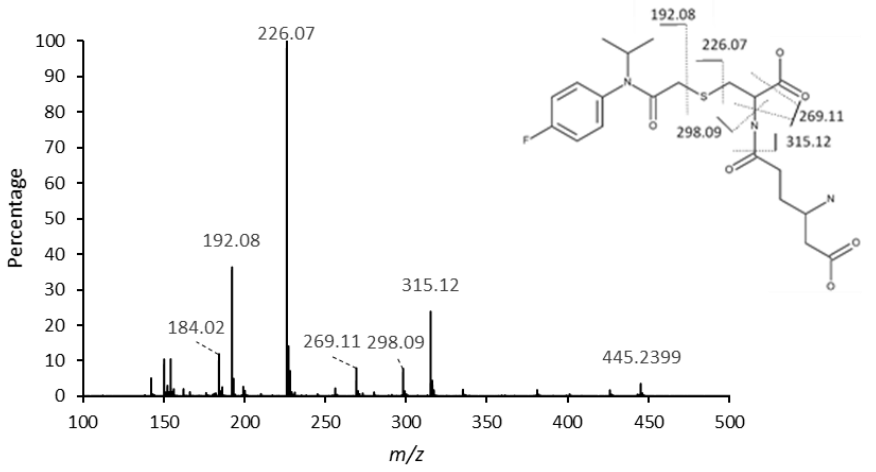

Cysteine conjugate MS-MS fragmentation

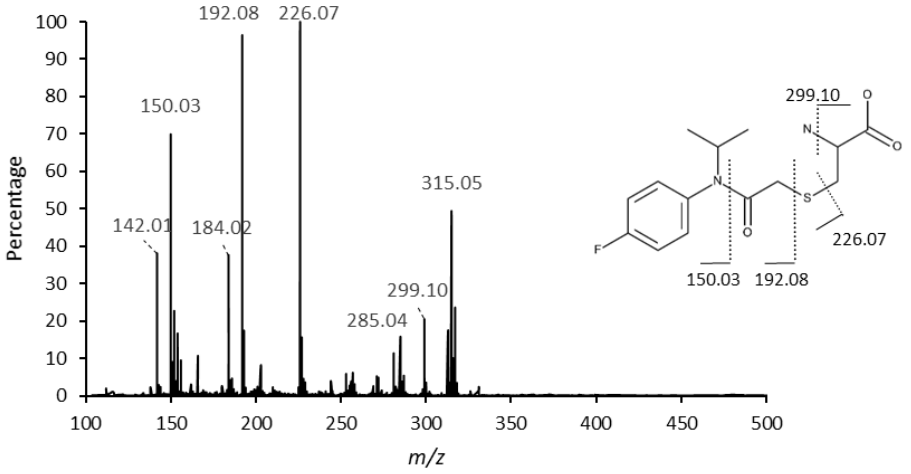

Figure 22. MSMS fragmentation profile of flufenacet and each of the identified flufenacet metabolites. Molecular fragments corresponding to prominent peaks have been assigned to support initial identification

3.3.4 Metolachlor

Metolachlor undergoes multiple metabolic pathways as shown in Figure 23, notably via glutathione conjugation, demethylation, hydroxylation and dealkylation. All three pathways were explored within these experiments.

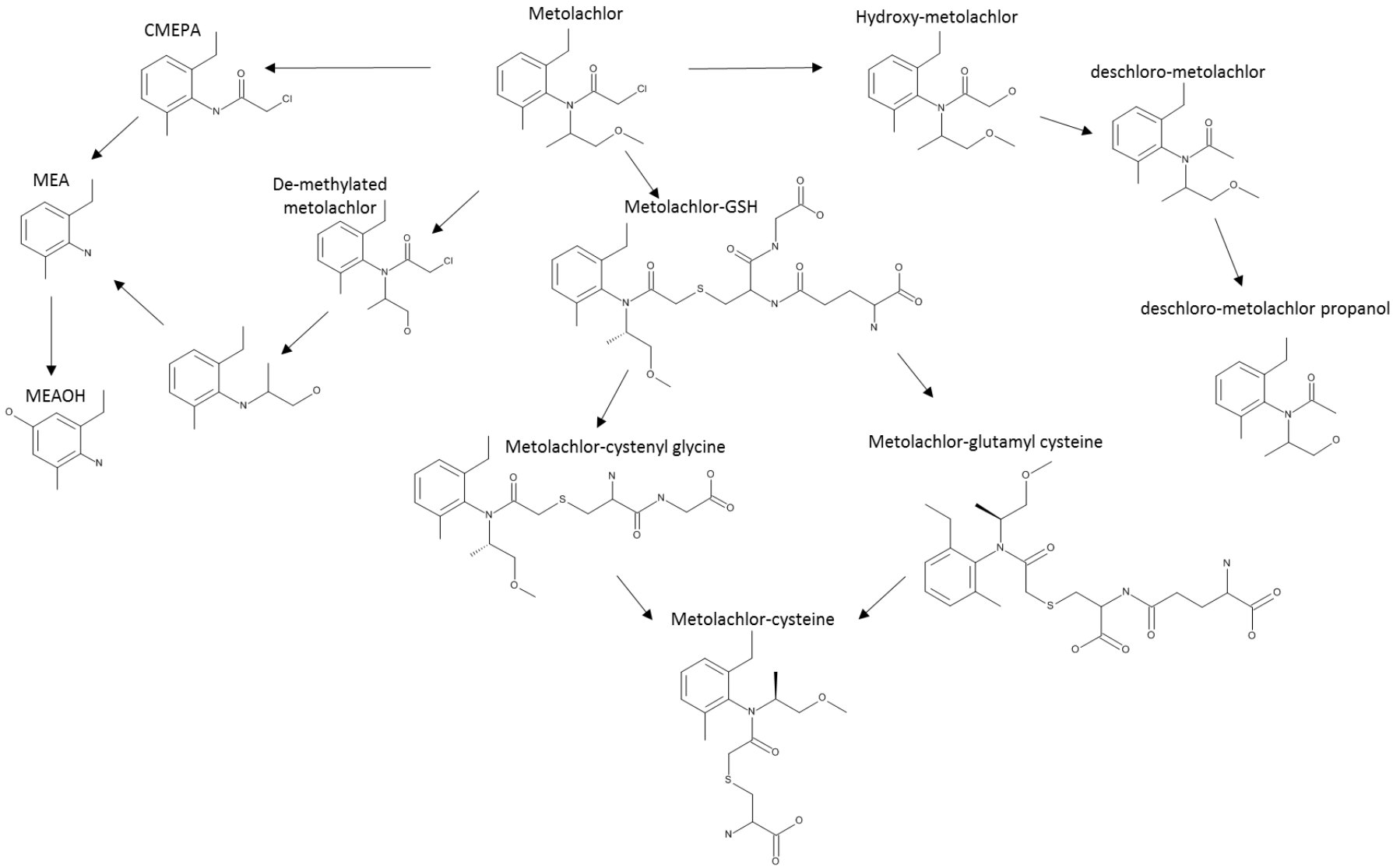

Figure 23.Metolachlor metabolic pathways by glutathionylation, demethylation, hydroxylation and dealkylation

As with the other herbicides, the parent compound was detectable in all instances with a retention time of 3.905 minutes and mass of 284.1417 (predicted 284.1417) (Figure 24). It was also once again noted that due to the presence of chlorine within metolachlor, a second, less prominent isotopic mass was found of m/z 286.1394, arising from ^{37}Cl. Within the oxidative pathway, one of the initial metabolites, CMEPA, was found in great abundance in each plant species which has previously been shown to be derived from cytochrome P450 mediated metabolism (S. Coleman et al., 2000). Outside of CMEPA however, the oxidative pathway yielded few results, with only noisy spectra associated with possible metabolites in which identification would be hard to confirm. Although these compounds could not be directly quantified due to a lack of standard, it was concluded that oxidation is unlikely the primary pathway by which metolachlor undergoes metabolism in wheat, blackgrass, or ryegrass due to the inability to detect any late stage downstream metabolites.

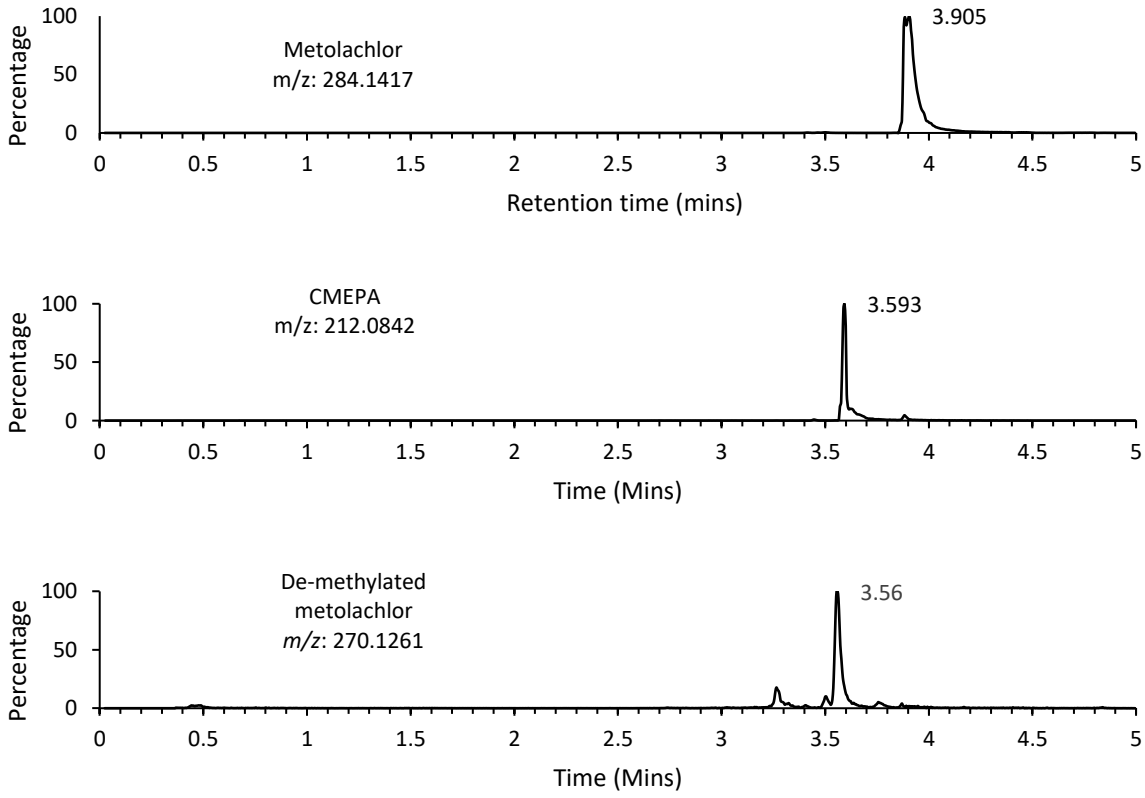

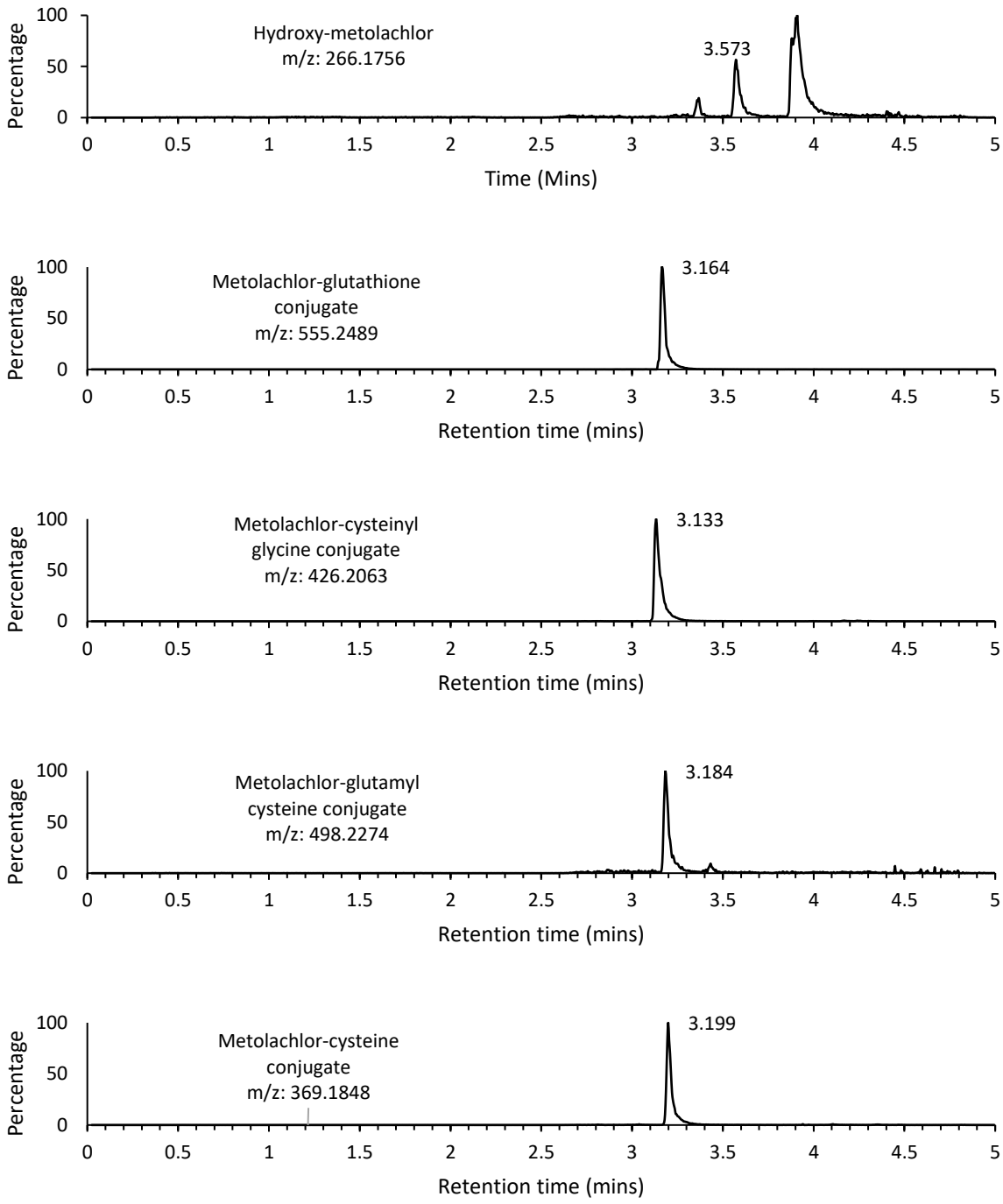

Figure 24. LC-MS peaks and retention times resulting from filtering by M^+ of metolachlor and proposed metabolites

Figure 14 shows the distribution of metabolites found within extracts from wheat, blackgrass, and ryegrass. Glutathione conjugation was seen to occur to the greatest extent, with much higher levels of glutathione conjugated metolachlor and its downstream metabolites detected in all plants compared to other pathways. Wheat extracts contained lower levels of

the glutathione conjugate and its downstream metabolites compared to both weed species. Additionally, it was found that the pathway by which the glutathione conjugate was further metabolised varied between plants. Within black grass, the glutathione conjugate was primarily processed by cleavage of glutamate to result in a cysteinyl-glycine conjugate and free glutamate. This cleavage is thought to result from the action of the gamma-glutamyl transferase (GGT) enzyme, which hydrolyses the peptide bond between cysteine and glutamate (Hanigan, 2014). GGT enzymes are thought to be present in both the vacuole as well as the cytosol, it has been found however that the rate of vacuole sequestering of the glutathione conjugate is much greater than the rate by which cytosolic GGT's are able to hydrolyse glutathione conjugates. It is therefore thought the majority of this processing occurs in the vacuole (Hanigan, 2014; Ohkama-Ohtsu et al., 2007)

Within wheat only low levels of cysteinyl-glycine were detected, with formation of a glutamyl-cysteine conjugate appearing to be the first step in downstream metabolism to a cysteine conjugate. This process is thought to be mediated by another cytosolic enzyme, dipeptidase, which cleaves the glycine residue and results in the formation of a glutamyl-cysteine conjugate (Kumada et al., 2007). Glutathione conjugated metabolites have been found to result in rapid cytosolic accumulation due to increased water solubility. With both enzymes proposed to be cytosolic, it would be reasonable to assume this difference results from differing enzyme levels as opposed to differential compartmentalisation of the glutathione conjugate.

Table 7. Peak area per gram fresh weight attained for metolachlor and its metabolites in wheat, blackgrass, and ryegrass. Results were attained by the pooling of five treated plants.

	PkA/g FW		
Metabolite	**Wheat**	**Blackgrass**	**Ryegrass**
Metolachlor	440431.5	4285317	934664.7
Metolachlor-GSH	34637.06	1427066	2617796
Metolachlor-cysteinyl glycine	8187.817	413431.7	454089.8
Metolachlor-glutamyl cysteine	80901.02	25535.52	316515
Metolachlor-cysteine conjugate	5911.168	196541	68377.25
CMEPA	184055.8	55983.61	597012
De-methylated metolachlor	2454.315	55316.94	12712.57
Hydroxy metolachlor	532.9949	0	0

MSMS fragmentation was used to help confirm the identity of metabolites and parent (Figure 25). Two peaks were present with an m/z of 252.11 and 254.11 resulting from the presence of ^{35}Cl and ^{37}Cl isotopes respectively. Two other notable peaks were detected with an m/z of 134.10 and 176.14 following cleavage of the Cl, resulting in no isotopic variation in each instance.

Fragmentation profiles of glutathione-like conjugates had several similar traits to those found within flufenacet conjugates. Within the metolachlor-glutathione conjugate two distinct peaks arose from the cleavage of each of the glutamyl and glycine motif. Cleavage of the glycine resulted in the loss of 129 Da and a fragment of m/z 426.11 whereas the cleavage of glutamate resulted in a loss of 75 Da and fragment of m/z 480.22.

Metolachlor MS-MS fragmentation

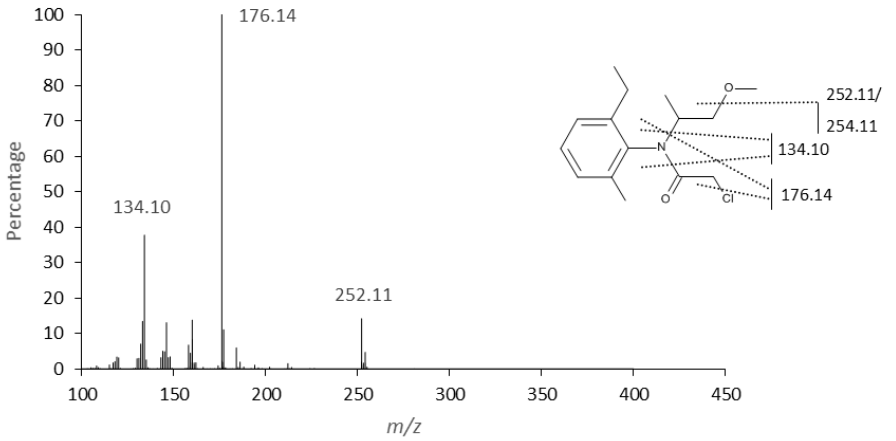

Metolachlor-Glutathione conjugate MS-MS fragmentation

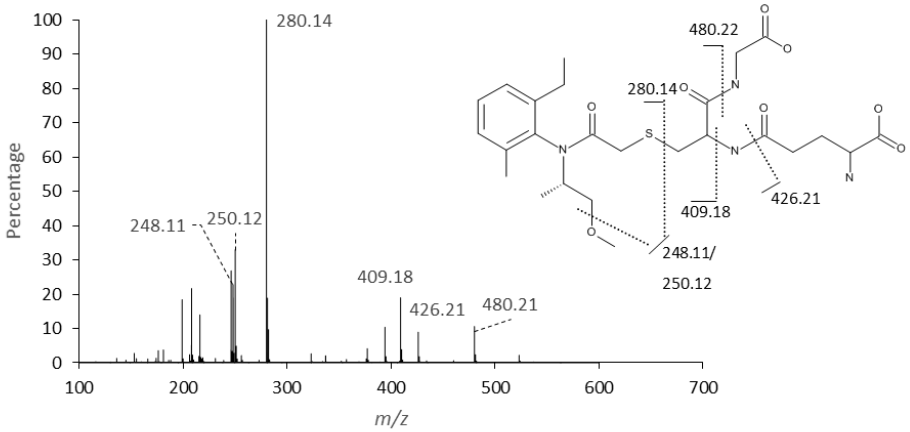

Metolachlor-cysteinyl-glycine conjugate MS-MS fragmentation

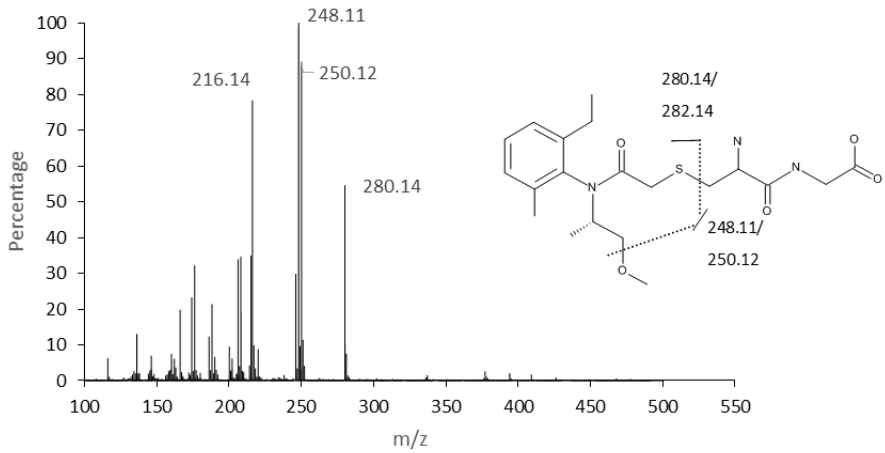

Metolachlor-glutamyl-cysteine conjugate MS-MS fragmentation

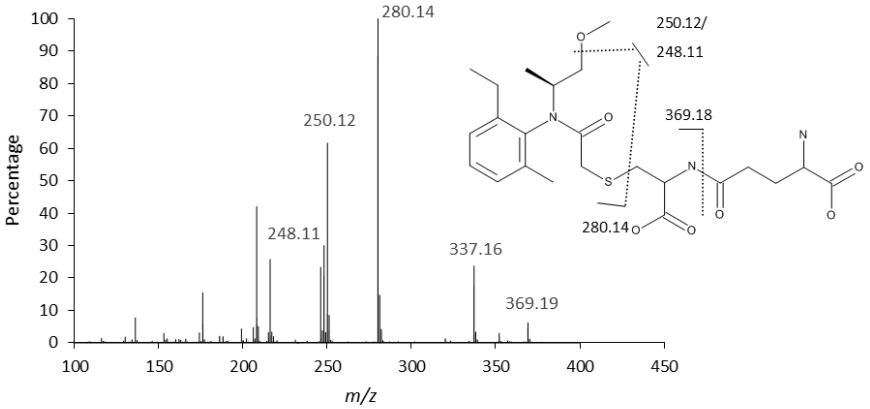

Metolachlor-cysteine conjugate MS-MS fragmentation

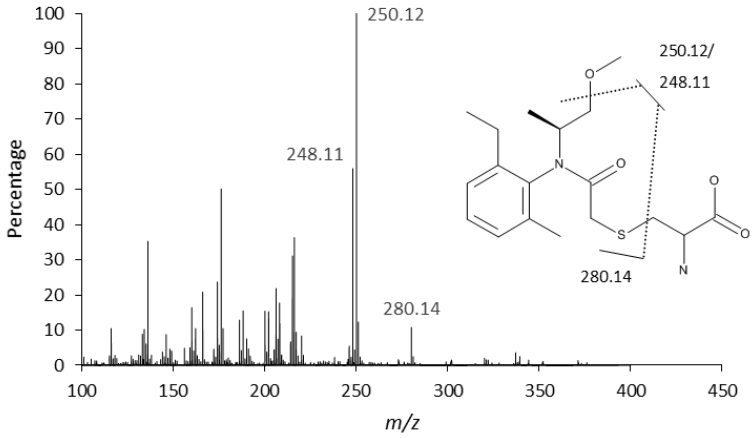

Figure 25. MS-MS fragmentation of metolachlor and downstream metabolites with proposed fragmentation structures

3.3.5 Propyzamide

Propyzamide is a benzamide herbicide that acts by inhibiting cell division in target plants. It is used as a systemic post emergence herbicide for the control of many broadleaf and grass weeds, primarily within fruit and root crops. Propyzamide was the fifth and final herbicide screened for its metabolic profile within wheat, blackgrass and ryegrass.

Screening of propyzamide by LCMS resulted in the detection of only the parent compound with no metabolites detectable. As seen in Figure 26, propyzamide was found to have a retention time of 3.785 minutes and m/z of 256.0303 (predicated 256.0296). Much like

diuron, propyzamide contains two chlorine atoms resulting in the presence of three isotopic masses of 256.0303, 258.0274, and 260.0246, supporting initial identification.

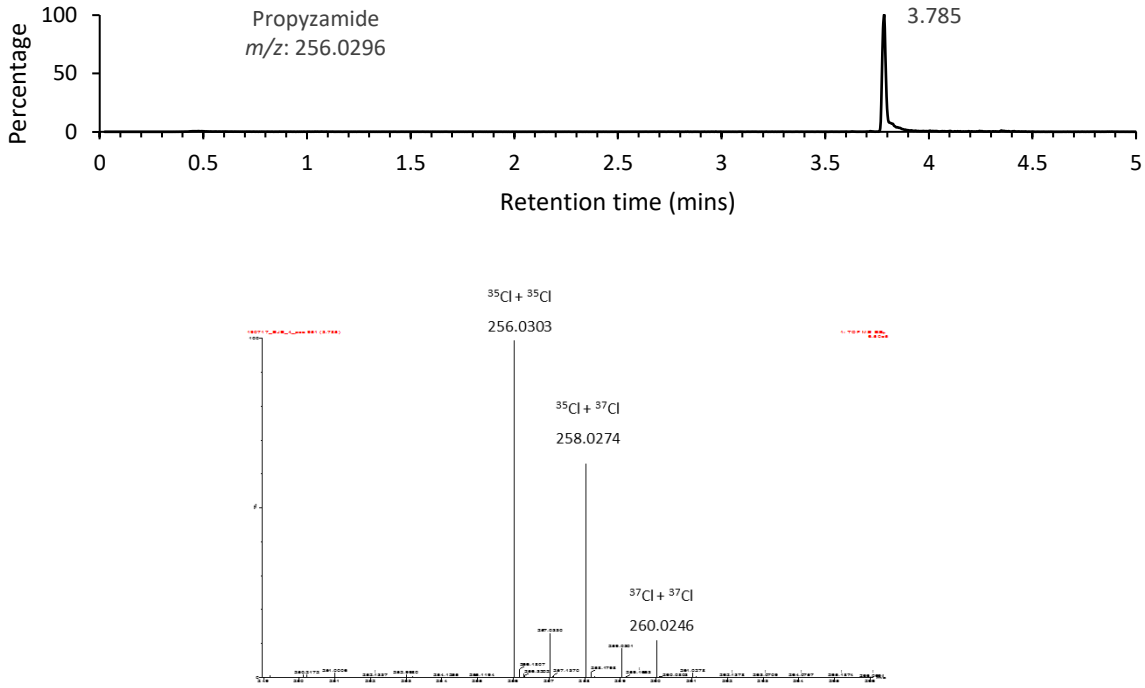

Figure 26. The peak and retention time obtained from searching for the m/z 256.0296, the H^+ ion of propyzamide, as well as the isomeric masses attained due to the presence of chlorine.

MSMS fragmentation of propyzamide resulted in two prominent peak sets Figure 27. One at 144.96 and 146.96 resulting from cleavage of the chlorinated benzene, and a second set at 172.96 and 174.96 resulting from α-cleavage prior to the nitrogen group. In both instance 3 peaks are present resulting from isotopic Cl with two major peaks and one minor resulting from Cl^{37}.

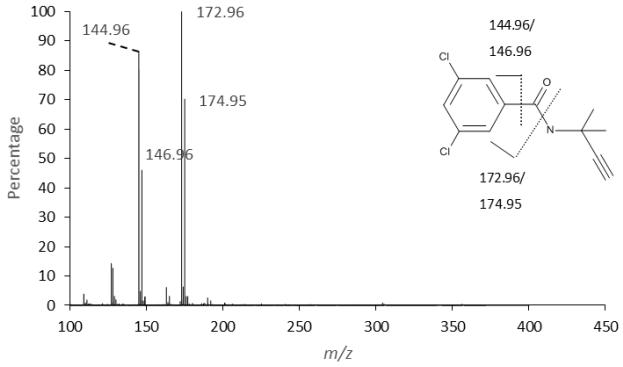

Figure 27. The MS-MS fragmentation profile of propyzamide used in confirmation of identity

3.4 Assessing the expression of GSTF1 after herbicide treatment

GSTF1 has been found to play a role in oxidative stress tolerance, as well as the detoxification of xenobiotic compounds, although the exact method by which this occurs remains unknown. *Am*GSTF1 been found to be upregulated within non-target site resistant populations of blackgrass, and although not thought directly involved in herbicide metabolism, is used as a marker of enhanced metabolism. It was therefore proposed that levels of GSTF1 may increase in response to herbicide stress.

Two populations of blackgrass were screened by immuno-blotting detection by western blot, along with the cordial wheat population (five leaves pooled per replicate from plants at the three-leaf growth stage). Two black grass populations were selected, a multiple herbicide resistant population (Peldon 05), and wild type susceptible population (Rothamsted 09). Plants were treated with each of the 5 herbicide formulations at the respective dosage as described in 2.3.2. Immuno-blotting by western blot was used to screen samples for changes in GSTF1 using an antibody raised towards black grass (*Am*GSTF1-1) which also showed cross reactivity within wheat.

Figure 28 b. shows the expression of a 27 kDa protein within the black grass MHR population with much reduced levels detectable within the WTS population. There are however no notable differences between the treated and untreated samples within each population indicating no effect on expression levels of *Am*GSTF1 when herbicide treatment is applied. The same was true of wheat, with no notable differences between treated and untreated samples. Wheat was however found to express two distinct polypeptides of masses 27 kDa and 28 kDa thought to be two isoforms of the GSTF1 protein.

Although able to highlight differences in expression between the susceptible and resistant populations of black grass, the use of immuno-blotting did not show potential in elucidating any differences that might arise resulting from herbicide stress.

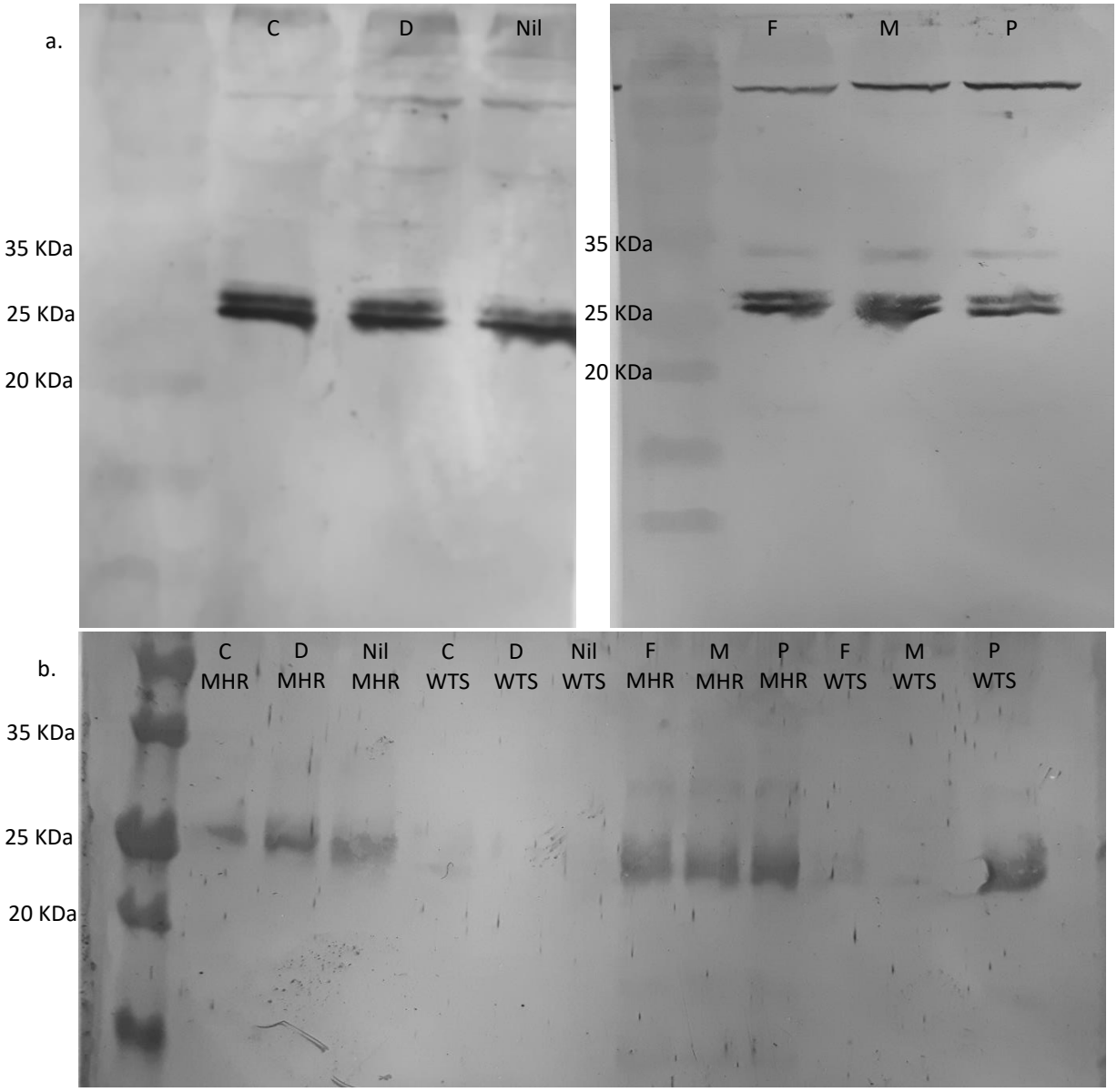

Figure 28 Western blots performed upon treated wheat and blackgrass samples. Plants were grown to the three-leaf stage with treatment by droplet application to the flag leaf of each plant. Five leaves were pooled for each replicate. a. shows the relative expression levels within treated wheat samples whereas b. shows relative expression levels within MHR and WTS blackgrass. Well labels represent herbicide treatments; C = cyhalofop-butyl, D = Diuron, F = Flufenacet, M = Metolachlor and P = Propyzamide, while Nil represents the negative control.

3.5 Gene expression study

As western blotting did not yield any significant results as to GST induction following herbicide exposure, gene expression was looked at as an alternative route to inducible biomarkers. Gene expression studies were performed in wheat due to genetic uniformity between plants, as well as extensive testing of housekeeping and stress response genes. Primers were

designed to cover multiple potential housekeeping and previously identified stress response genes provide coverage of a multitude of pathways.

3.5.1 Housekeeping gene validation

Several factors can influence RNA amounts present in samples when performing extractions for qPCR. Things such as tissue mass, treatment, and RNA extraction efficiency can all influence RNA recovery (Schmittgen et al., 2000). When analysing qPCR data these variables can impact on sample readings, which must therefore be referenced to an internal control gene known as a housekeeping gene. The most important factor when selecting a house keeping gene is consistent expression throughout treated and untreated samples so that data may be normalised (Jain et al., 2018). Although selected housekeeping genes are often involved in basic cellular functions and constitutively expressed, it has been found that these genes may be prone to change in expression under certain conditions (Schmittgen & Zakrajsek, 2000). It was therefore important to test a range of housekeeping genes and establish if any changes in expression were noted upon herbicide treatment. Housekeeping genes were selected based on those described in the literature, the expression of which is thought to remain constant namely Actin, Alpha tubulin, and CYP18-2 (Primers shown in Table 8) (Schmittgen & Zakrajsek, 2000; Thellin et al., 1999).

Table 8. Forward and reverse primers selected to be tested for potential housekeeping genes

Gene	Gene bank number	Forward			Reverse			Product length (bp)
		Sequence (5'-3')	Tm (°C)	GC%	Sequence (5'-3')	Tm (°C)	GC%	
Actin	AB181991.1	CCCAGCAATGTATGT CGCAA	58.91	50	TCACCAGAGTCGAGC ACAAT	59.03	50	84
Alpha tubulin	U76558.1	TTTCCTCCTATGCCC CAGTG	59.08	55	AGACAGCAGGCCATG TACTT	59.01	50	154
CYP18-2	AY456122.1	AAGTTCGTCCACAAG CACAC	58.99	50	GGACGGTGCAGATGA AGAAC	58.92	55	94

Primers were initially tested for replication efficiency to ensure linear replication of cDNA with increasing concentration, and the melt curve observed to determine if any nonspecific primer binding was occurring. As seen in Table 9, each of the tested housekeeping primers showed an efficiency close to 2, indicating doubling of DNA copy number after each cycle of qPCR. An efficiency range of 10% is generally accepted allowing for an efficiency of 2.00 ± 0.2, a margin of error in which all tested housekeeping genes fell (Jain et al., 2018, Svec, 2015). The slope is

determined by the Cq value of each of the dilutions within the standard curve. If the concentration of cDNA is diluted 1 in 10, it will take an additional 3.33 qPCR cycles to reach the same level of florescence as the undiluted sample (Svec et al., 2015). As seen in Table 9, the slope was close to 3.33 for each primer set, indicating that this was the case in each of the tested housekeeping primers and is the value from which the efficiency is derived. The gradient of the standard curve would be expected to have an R^2 value close to one, indicating correct dilution and consisted ratio between Cq and cDNA concentration. A range of $R^2 = 0.95 – 1.00$ was applied which each of the house keeping genes fit within.

Table 9. Housekeeping primers tested within wheat samples. Each sample was tested using a three times serial dilution of cDNA to determine efficiency.

Gene	Efficiency	Slope	R^2
Actin	2.00 ± 0.15	-3.32	0.99
Alpha tubulin	2.03 ± 0.05	-3.26	1.00
CYP18-2	2.03 ± 0.05	-3.26	1.00

A melting curve was used to observe fluorescence across a temperature gradient. As temperature is increased, double stranded DNA dissociates into single strands causing a decrease in fluorescence. When only one cDNA product is present, dissociation will occur within a narrow temperature range giving rise to a single, uniform peak which is consistent throughout samples. Melt curves were observed to look for singular, uniform peaks within samples and found to consistently show only one peak within each tested housekeeping gene.

With all housekeeping genes meeting the selection criteria, genes were tested upon herbicide treated samples to determine if there was any influence on the levels of gene expression. In each case, a one-way ANOVA was used as a means of determining significance of differing Cq values for each housekeeping gene. As highlighted in Figure 29, both CYP18-2 and alpha-tubulin were found to have significant differences between treated and untreated samples. In all treatments there was a significant difference in Cq of alpha tubulin when compared to the nil treatment with all Cq values being lower indicating a higher level of expression. This was also the case within CYP18-2 apart from flufenacet treated samples. Actin showed no significant variation between treated and untreated samples and was therefore selected as a reference marker going forward.

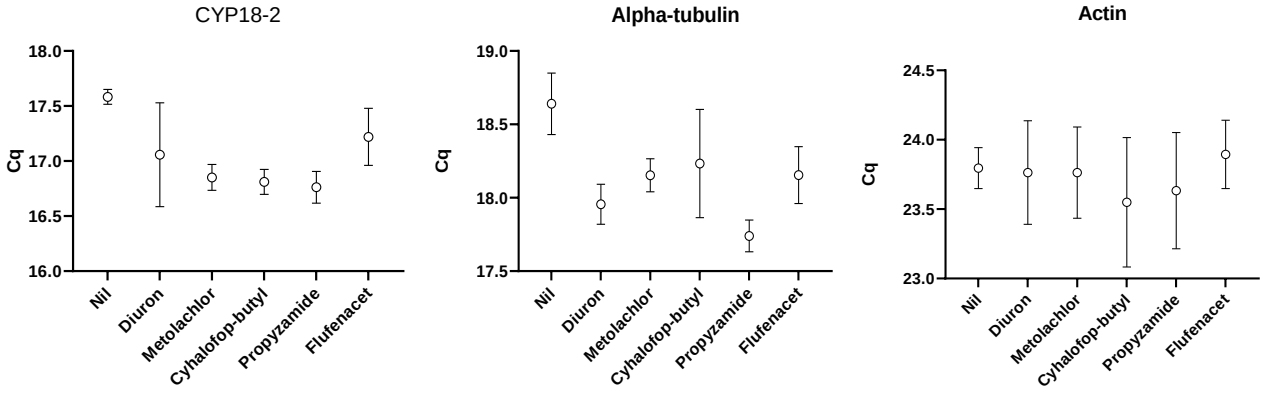

Figure 29. The Cq values of CYP18-2, Alpha-tubulin, and Actin within Nil (negative control) and herbicide treated samples after 3 hours. Actin was found to have the least differentiation between mean values, and no treatments were significantly different from the Nil or the other treatments (based on one-way ANOVA)

3.5.2 Stress response gene testing

After establishing actin as the house keeping gene, a range of stress response genes were selected to check for changes in expression upon application of the various herbicides. Due to the polygenic response of plants to xenobiotic toxicity, and multiple modes of action being used in initial screening, a variety of biotic and abiotic stress markers were tested (Table 10). These genes underwent an initial screen to check efficiency and consistency of the melt curve, and a final selection was made based on the criteria applied to the house keeping primers.

As herbicides such as diuron induce oxidative stress as a means of causing plant damage, catalase (CAT), peroxidase (POD), and superoxide dismutase (SOD2) were selected for initial screening due to their role in diminishing oxidative damage (Alici et al., 2016). The action of catalase in reducing oxidative stress is well documented, with the enzyme catalysing the conversion of cellular hydrogen peroxide into water and hydrogen (Nandi et al., 2019). In addition, ATP synthase was selected due to the ability of photosystem II inhibiting enzymes to prevent ATP synthesis (Pansook et al., 2019). Multiple GST enzymes were also screened due to their role in glutathione mediated detoxification in many xenobiotics. It has been shown that differing GST classes are more specific towards differing herbicides with many having been shown to be safener inducible (Dixon et al., 2003; Thom et al., 2002). Additional common stress response genes such as heat shock protein 90 (HSP90), Late embryogenesis abundant 5 (LEA5), and C-repeat/DRE-Binding Factor (CBF14) genes were selected as general broad range markers (Naot et al., 1995; Novák et al., 2015; G. F. Wang et al., 2011).

Table 10.A range of stress response genes were selected for initial screening covering a wide range of response pathways. Table 10 shows tested stress response genes including efficiency and slope. Primers with an efficiency 10% outside of 2.00 (i.e <1.80 or > 2.20) were discarded.

Gene	Response	Gene bank number	Forward			Reverse			Product length (bp)	Efficiency	Slope	R^2
			Sequence (5'-3')	Tm (°C)	GC%	Sequence (5'-3')	Tm (°C)	GC%				
CAT	Oxidative stress	X94352.1	CCGGAGAGTCTGCACATGTT	60.04	55.00	GCCTTTCCATCCCTGCTGAT	60.11	55.00	119	2.04 ± 0.10	-3.24	1
GST1	Detoxification	AF184059.1	AGATCAAGAACGTGCTGGCA	59.96	50.00	GAGATGCGTAGGGTGTAGCC	59.97	60.00	135	2.02 ± 0.11	-3.28	1
ATP synthase	Drought	M16843.1	AGGCACAGATCCTCCACAAA	58.93	50.00	GGACTTGATTTCGTTGCCCA	58.76	50.00	122	2.04 ± 0.14	-3.36	0.99
HSP90	Heat shock protein	JN052206.1	ACAAGGAAGAGTACGCTGCT	59.03	50.00	ACTCAAGCTGACCCTCAACA	58.87	50.00	96	2.04 ± 0.06	-3.24	1
GST 23	Drought	JX051003.1	TGAAGGTGTTTGGCATGTGG	58.96	50.00	TTCTTGGTCACCGGGTTGT	59.08	52.63	145	2.01 ± 0.05	-3.30	0.98
GSTF1	Safener inducible	AJ440796.1	GCTACACCCTATGCGTCTCT	58.97	55.00	GCACACACCTCGGCTTATTT	58.83	50.00	159	1.97 ± 0.11	-3.39	1
GSTU2	Safener inducible	AJ414700.1	CCGACAAGATGCTCGAGTTC	58.73	55.00	ACGGACTCAGACACACACAA	59.18	50.00	128	1.96	2.2	0.99
RGA4	Fungal infection	AF087521.1	CCGCCGTTACCTAGAGAAGA	58.61	55.00	TATCCGACCAAGTTTGCCAC	58.18	50.00	112	2.02 ± 1.53	-3.28	0.59
POD	Oxidative stress	X56011.1	CGCAGTGTGGGACCTTTAAG	58.84	55.00	CCCCTTCTGTGACATGAGGT	59.01	55.00	182	1.26 ± 0.25	-.2.3	0.85
SOD2	Oxidative stress	FJ890987.1	CTACAAGCCGCTCAACCTCA	60.04	55.00	CTTGGCTGGGAGACTGGAAG	60.04	60.00	89	32.95 ± 1.65	-0.66	0.05
LEA5	Drought/salt/heat	KJ502295.1	AGAACCAGGCGAGCTACATG	59.82	55.00	GGTCTTCTCCTGCACAACGA	59.97	66.00	156	1.26 ± 2.54	-10.11	0.85
RuBisCO	Wounding	AY328025.1	CCGTTTTGTCTTTTGTGCCG	58.80	50.00	TCTTCACATGTACCCGCAGT	59.03	50.00	99	1.59	-6.23	0.58
CBF14	Cold stress	AY785901.1	TGAATGAGCACTGGTTTGGC	59.04	50.00	CGAACAAGTAGCTCCATGGC	58.99	55.00	141	2.66 ± 0.70	-2.35	0.79
COR14b	Cold stress	AF207546.1	CGATGGCTTCTTCTTCCGTG	59.00	55.00	CGTTAGCAGGAGTCGCTCTA	58.98	55.00	171	1.84 ± 0.11	-3.79	1

Selected primers were used to screen herbicide treated plants at field rates as described in 2.11. Samples were harvested and screened for differential gene expression 3 and 16 hours after herbicide treatment. As shown in Figure 30, overall there was a greater level of gene response 3 hours after treatment than 16 hours, with most inducible genes returning to a level close to that of the nil treatment by 16 hours. There were however exceptions to this, with *TaRGA* and *TaGST23* continuing to rise in flufenacet treated samples, *catalase* and *TaGST23* continuing to rise within propyzamide treated samples, and *TaGSTU2* continuing to rise in metolachlor treated samples.

The most frequently induced genes were *TaGSTU2* and *TaRGA4*, both of which were induced within all treated samples by 3 hours. *TaGSTU2* has been previously studied in soybean and shown to exhibit a broad range of specificity towards xenobiotics and various biotic stresses. This would suggest an overarching role within stress response and catalytic flexibility to numerous stimuli (Skopelitou et al., 2017). It is therefore unsurprising to see induction arising from each of the herbicide treatments. *TaRGA4* was induced within all treatments by 3 hours, decreasing back to base level in all treatments by 16 hours, with the exception of flufenacet. Within flufenacet treated wheat, *TaRGA4* continued to rise to a 10-fold induction level by 16 hours.

Within diuron treated samples *TaATP synthase*, *TaRGA4* and *TaGSTU2* were found to be induced by 3 hours with 1.77, 2.15 and 2.92-fold levels of induction respectively. As diuron acts as a photosystem II inhibitor, thereby inhibiting the production of ATP, this initial increase in ATP synthase may be a direct response to decreasing ATP levels. In all cases however, levels of induction had decreased to base levels by 16 hours. Metolachlor had also shown an increase in *TaATP synthase* induction by 3 hours, reaching 2.61 times expression. *TaGSTF1* was found to be upregulated 2.22-fold by 3 hours within flufenacet treated samples. This was the only treatment within which any change in expression of *TaGSTF1* was noted and had decreased to base levels by 16 hours.

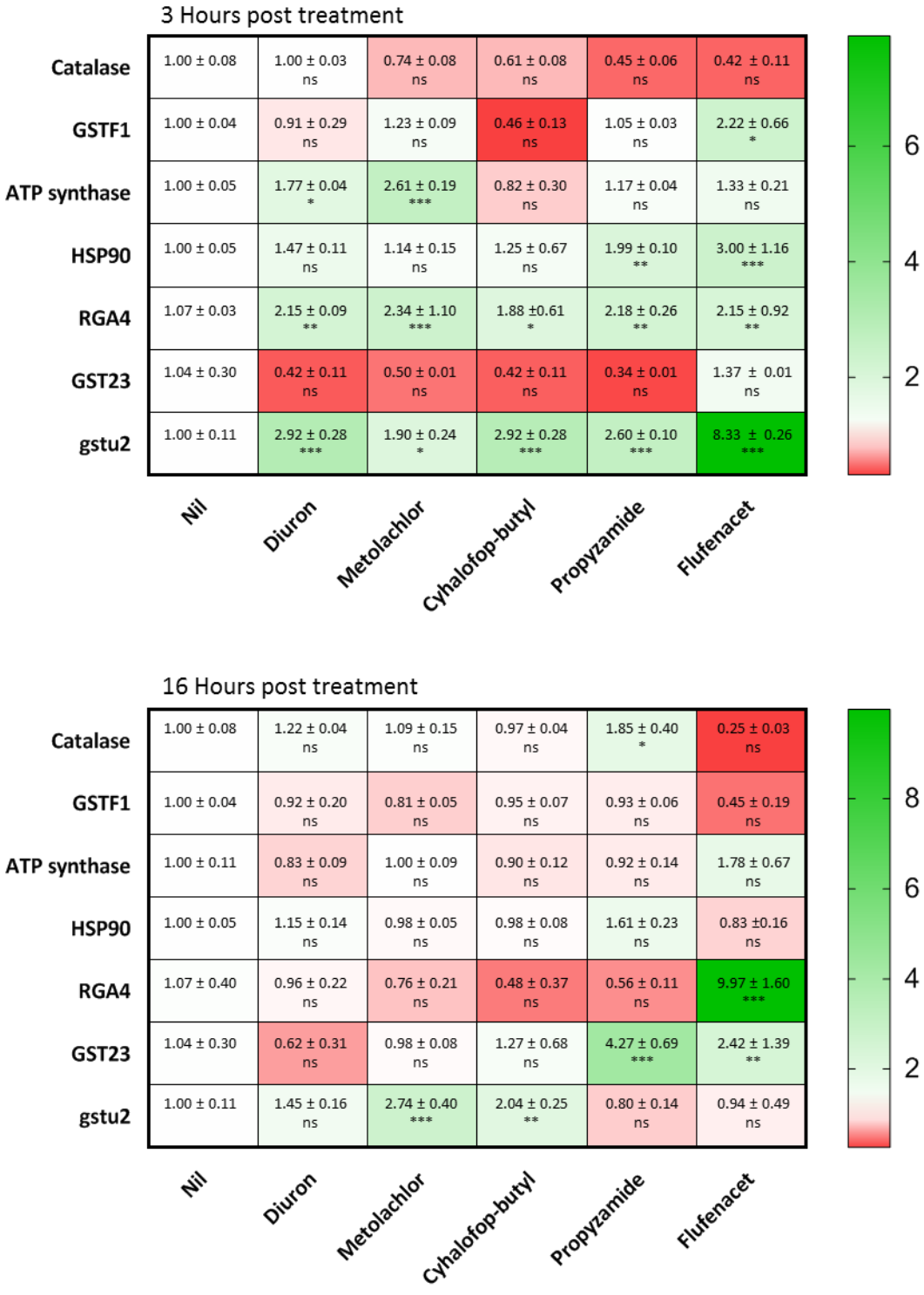

*Figure 30. Heat map showing wheat gene response 3 and 16 hours after herbicide treatments for selected stress response genes. Actin was used as the house keeping gene against which gene responses were normalised. Wheat was treated with by droplet application at the three-leaf stage, with RNA being extracted from 100 mg of pooled tissue samples (3 plants per pooled sample). Significance of difference from the nil treatment was conducted using a multiple t-test in which all treatments were compared to the nil treatment. Significance is represented by ns = not significant, * = P ≤ 0.05, ** = P ≤ 0.01, *** = P ≤ 0.001.*

3.6 Flufenacet time course study

Having established potential markers in the form of metabolites and response genes, a single herbicide formulation was selected into which adjuvants could be added to test their effects upon uptake. The flufenacet formulation was selected for several reasons; Initial herbicide trials had been conducted on wheat as a model crop species, and blackgrass and ryegrass as model weed species. Flufenacet is often used in the pre and early post emergence treatment of wheat to control grass weeds such as blackgrass and ryegrass (Dücker et al,. 2019). As the flufenacet formulation was made as a suspension concentrate, adjuvants have the potential to confer the greatest increases in efficacy due to their comparatively poor performance against solvent-based formulations. Flufenacet treatment also resulted in a number of notable changes in gene expression, as well as having easily detectable metabolites, of which the flufenacet-cysteine and flufenacet-glutathione conjugates could be synthesised.

An initial screening was performed using the base SC formulation to observe changes in gene expression across an extended time course within wheat. Expression of the previously examined genes were observed 1, 2, 3, 4, 6, and 16 hours post treatment. As shown in Figure 31, induction of gene expression was found to be greater at earlier times with a number of notable changes across time. *TaGSTU2* had the greatest levels of overall induction with gene expression increasing 13.5-fold by 1 hour when compared to the nil treatment. Expression of gstu2 then progressively decreased over time, reaching a 2-fold expression levels by 6 hours, and decreasing back to base expression levels by 16 hours. All other tested genes were found to have slower rates of induction, reaching maxim levels of expression at later points. Both *TaATP synthase* and *TaGST1* were found to increase 3- and 2-fold respectively by 4 hours, and progressively decreasing until reaching a base level of expression by 16 hours. *TaRGA4* was the only gene found to have significantly increased levels of expression by 16 hours. Expression of *TaRGA4* remained consisted across the first 6 hours, increasing to 10 time's greater expression than the nil treatment by 16 hours. *TaGST23* was found to increase at a consistent rate until reaching a maximum level of expression by 6 hours with a 9-fold induction.

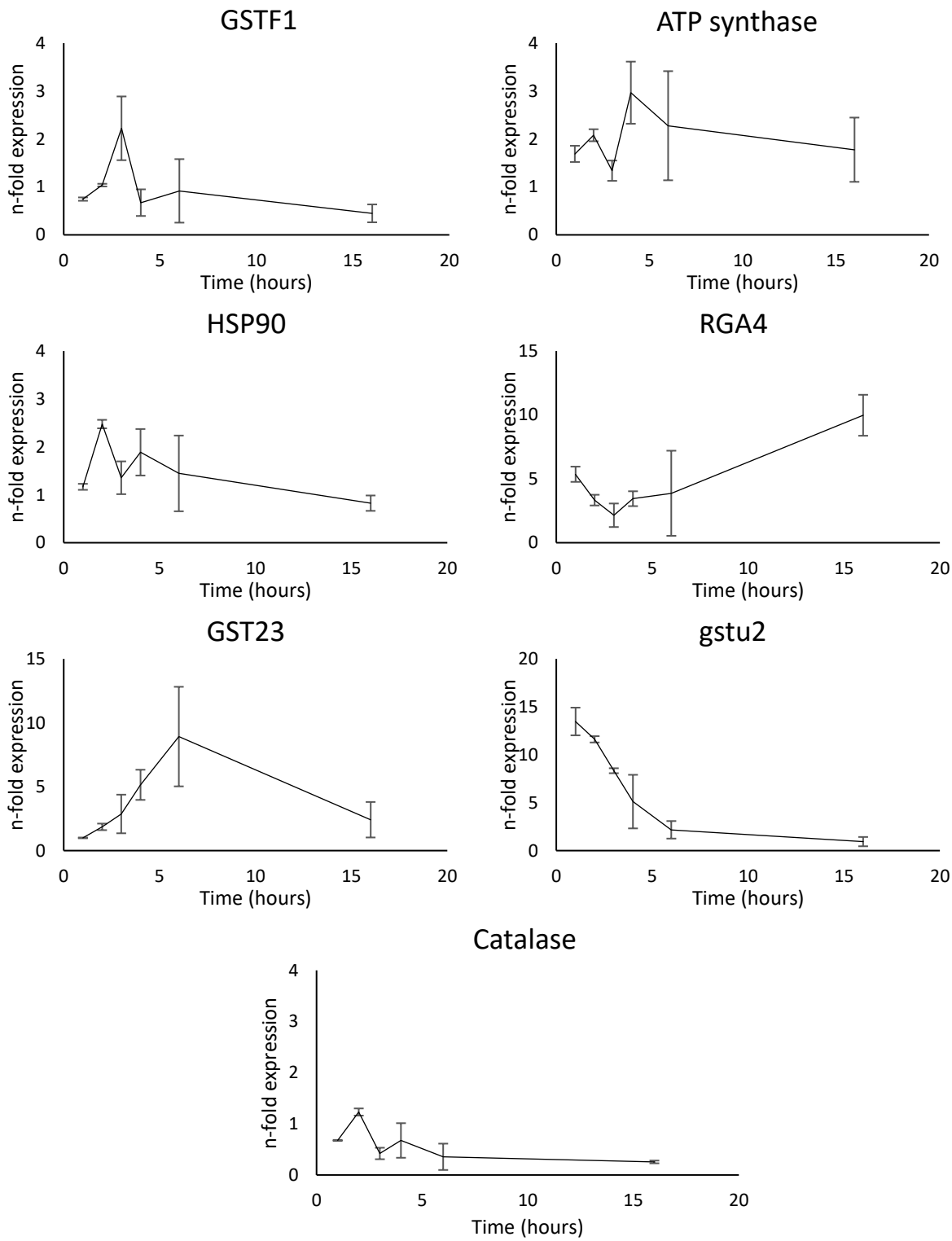

Figure 31. Gene expression across a 16 hour time course (1, 2, 3, 4, 6, and 16 hours) of selected stress response genes in flufenacet (165 µmol) treated wheat at the three leaf stage (each sample consisted of three pooled leaves). Actin was used as the house keeping gene against which other genes were normalised, with changes in gene expression based on expression levels found in untreated wheat. Data points are presented as the mean with standard deviation indicating variance.

In addition to gene expression, the levels of flufenacet and glutathione derived metabolites were monitored over time. As seen in Figure 32, by 30 minutes flufenacet as well as the glutathione conjugate were detected within the plant extracts, although had yet to be metabolised to cysteine at a detectable level. By 1 hour, the point by which *TaGSTU2* had the highest level of expression, metabolism to the cysteine conjugate can be detected and the glutathione conjugate is present at its highest level of 0.025 nmol. This level remained consistent until 4 hours, by which time the rate of metabolism to each of the cysteinyl-glycine, glutamyl-cysteine, and cysteine conjugates had rapidly increased. This was coupled with decreasing levels of glutathione-flufenacet indicating downstream metabolism. The level of flufenacet within the plant continued to increase until 6 hours, at which point a progressive decrease was seen by 16. This decrease in both flufenacet and its corresponding glutathione conjugate was coupled with a progressively rising level of cysteine-flufenacet and glutamyl-cysteine conjugate, suggesting no further uptake was occurring by 16 hours and the remaining flufenacet present was being metabolised.

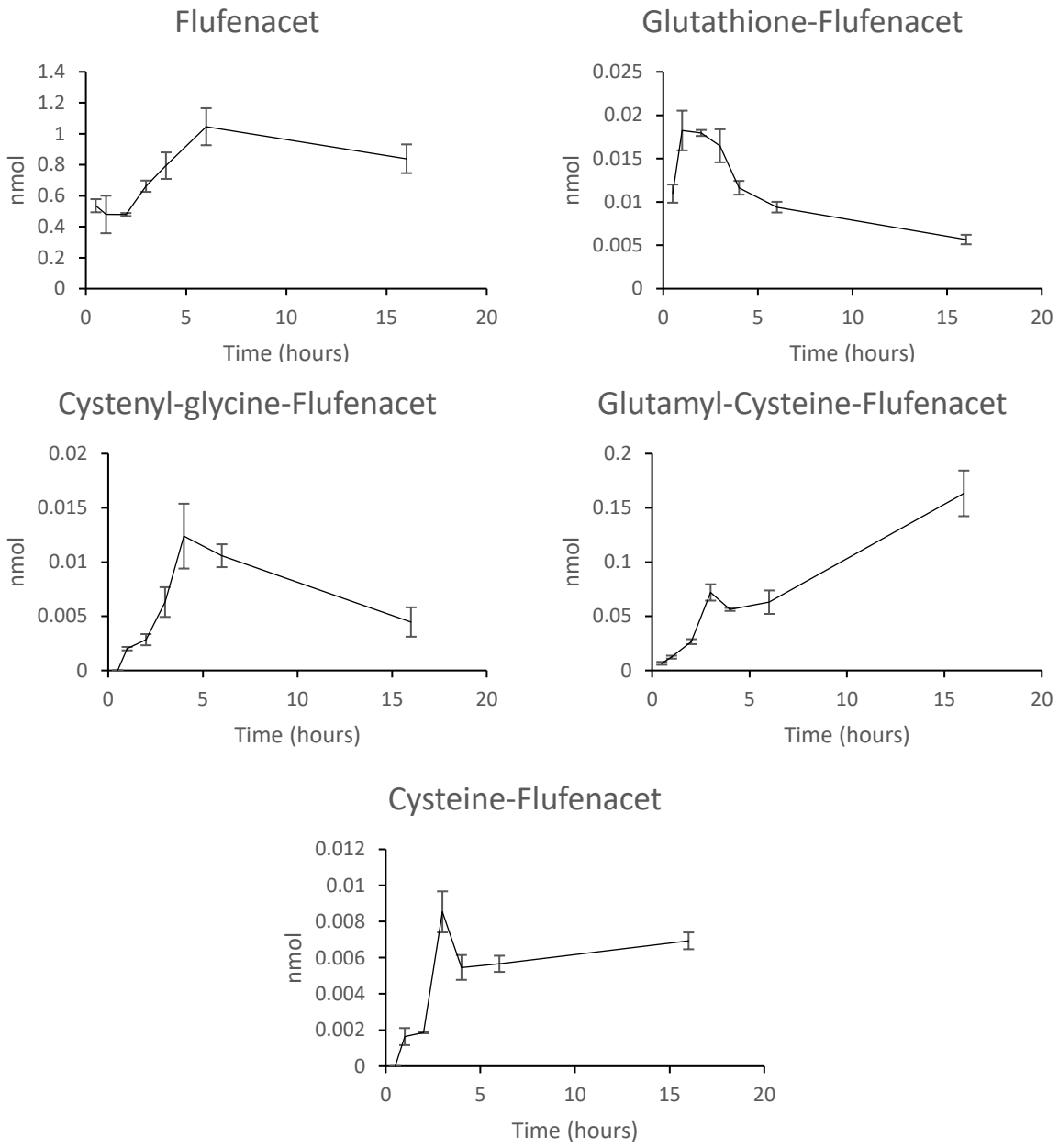

Figure 32. Levels of flufenacet and downstream glutathione-like conjugates within flufenacet treated wheat (165 µmol of flufenacet applied in 0.4 µL droplets to 3 leaf stage wheat. Each sample consisted of three pooled leaves) extracts across a 16 hour time course (30 minutes, 1, 2, 3, 4, 6, 16 hour time points). Data points are presented as the mean with standard deviation showing variance.

3.7 Discussion

Although herbicide uptake is often measured with the use of radiochemicals, such tags were not feasible at the concentration and quantity at which herbicide formulations are typically made and applied. Additionally, due to a lack of access to radiochemicals, more thorough method validation methods were not available. As such, alternative means of measuring delivery were investigated using three “omics” level approaches; namely looking at herbicide metabolism, changes in protein or gene expression, all as potential markers herbicide exposure *in planta*.

The metabolic profiles of cyhalofop-butyl, diuron, metolachlor, flufenacet and propyzamide were investigated in wheat, blackgrass and ryegrass. Herbicide formulations were initially tested for two reasons; to be sure the parent and metabolites were detectable by available LCMS equipment, and that the herbicide formulations were effectively facilitating uptake. Of the tested formulations, diuron and propyzamide showed low levels of parent and metabolite being detected. Diuron treatment resulted in the first stage metabolite DCMU being detected, however with no further downstream metabolites detected. As both these herbicides were formulated as water-based SC formulations with no additional adjuvants, a low level of uptake might be expected due to the hydrophobic nature of the leaf surfaces. Flufenacet was also formulated as an SC, however, metabolite detection proved much easier with this herbicide. Flufenacet has been previously demonstrated to be metabolised by conjugation with glutathione and further catabolism of the conjugate. Flufenacet-glutathione and related downstream metabolites; cysteinyl-glycine, glutamyl-cysteine and cysteine flufenacet conjugates all proved easily detectable and identifiable by LCMS within each plant extract.

Both metolachlor and cyhalofop-butyl were formulated as an EC and EW preparations respectively. Metolachlor has been demonstrated to undergo glutathione mediated detoxification much like flufenacet. The respective metabolites were also easily detectable and identifiable with distinct MSMS fragmentation spectra. Cyhalofop-butyl resulted in detection of several metabolites with cyhalofop-acid, cyhalofop-amide, and cyhalofop-diacid being detectable across the different plant species. Cyhalofop-butyl metabolites were detected at only low concentrations, indicating either low content or poor sensitivity of detection by LCMS. Due to this, quantification would prove difficult resulting from interference from background noise. There were however a few notable differences between

each species with the di-acid form being most prevalent in wheat, only small amounts detectable in blackgrass, and none at a detectable level within ryegrass. The herbicidal cyhalofop-acid was also found in greatest abundance within blackgrass extracts with lower levels present in both wheat and ryegrass. This would indicate a degree of differential metabolism between each species, with wheat having the greatest ability to metabolise herbicidal cyhalofop-butyl and cyhalofop-acid to its inactive cyhalofop-diacid form.

The levels of the protein *Am*GSTF1-1 were measured by western blot within herbicide treated blackgrass samples, with the antibody also detecting an immunoreactive ortholog in wheat. There were no notable differences in the levels of this protein after herbicide application, despite being a marker of herbicide resistance within blackgrass. Although differences in levels of *Am*GSTF1 between MHR and WTS blackgrass could be seen, there was a lack of direct response to herbicide uptake. Due to this lack of response, qPCR was used as a means of looking for differing levels of response from stress genes in herbicide treated samples. A number of stress response genes were tested to provide coverage of a range of potential pathways, out of which *TaGSTU2* and *TaRGA4* were found to be the most responsive. Both *TaGSTU2* and *TaRGA4* were found to be upregulated 3 hours post treatment within all treatments, indicating that despite the low level of metabolite in diuron and lack of in propyzamide, herbicide uptake and resulting plant stress was occurring. GSTU2 has previously been found to having binding affinity and catalytic activity towards multiple herbicides (Skopelitou et al, 2017) as well as being present at greater levels within several NTSR populations of black grass suggesting an important role in both herbicide detoxification and herbicide resistance (Tétard-Jones et al., 2018). RGA4 is a pathogen response protein and was also upregulated in all treatments. RGA4 is a constitutively expressed protein which induces cell death if not for the inhibitory action of RGA5 (Césari et al., 2014). Although not thought to be directly involved in herbicide detoxification, it has been proposed that the application of exogenous herbicides may increase plant susceptibility to disease, resulting in an indirect response (Andersen et al., 2018). There are a two means proposed by which this may occur; disruption of the rhizospheres bacterial ecology, resulting in a decrease in beneficial bacteria and increase in opportunistic pathogenic bacteria; and disruption of uptake, translocation, and utilisation of essential minerals thereby disrupting normal physiological disease resistance (Martinez et al., 2018). As these trials were performed by controlled leaf

application, any disruption to rhizosphere bacterial colonies would not have been an influencing factor. It could therefore be reasonably assumed this change resulted from a general disruption to the plants native physiology.

In conclusion, flufenacet offered the best herbicide in which adjuvants could be incorporated for formulation testing. As both the parent and metabolites were easily detectable by LCMS and could be synthesised, this would allow for direct quantification when looking at the influence of adjuvants. Uptake of flufenacet could therefore be monitored through metabolite formation. Although gene response proved telling of herbicide uptake, establishing a direct link between response levels and uptake would be difficult due to the short time frame in which the genes are induced in relation to how long the herbicide is present. Direct quantification of herbicide metabolites by LCMS was therefore the chosen method by which future adjuvant studies would be performed.

4 Chapter 4: Flufenacet uptake and plant profiling

4.1 Introduction

Within chapter 3, cyhalofop-butyl, diuron, metolachlor, flufenacet, and propyzamide herbicides were screened for potential markers of uptake through gene and protein expression, and metabolite formation. Although differences in gene expression were seen upon formulation application, up regulation of genes occurred over a short time frame and so establishing a link between herbicide uptake in the plant and levels of overexpression would prove difficult. Flufenacet was chosen as it undergoes rapid metabolism *in planta* in the presence of glutathione through a combination of spontaneous and catalysed conjugation. Moving forward, it was therefore decided to use LCMS and glutathione related metabolites as a means of determining uptake of flufenacet. Although not as optimal as using radio-chemicals for overall quantification, levels of flufenacet conjugates would be directly related to how much flufenacet was present and bioavailable within the cell, allowing for a comparative study of adjuvant effectiveness in compound delivery.

Adjuvants are non-herbicidal chemical additives added to formulations in order to improve the action of the principle active ingredient. Adjuvants can improve formulation characteristics such as wetting and spreading, droplet retention, or reduce surface tension (Hao et al., 2019). Adjuvants fall under several classifications, namely oils, surfactants, spray modifiers and utility modifiers (Pacanoski, 2014). Oil based adjuvants increase the retention time of the active upon the leaf, allowing for greater uptake. By incorporating oil into water-based formulations, evaporation will take longer to occur, and the herbicide will remain mobile in a liquid suspension for a longer period of time (Xu et al., 2010). Oil based adjuvants are often co-formulated with surfactants to allow for stable formation of an emulsion when mixed with water and further improve formulation properties. Surfactants are surface active agents which can act as adjuvants. Some surfactants can improve pesticide dispersion, spreading, and foliar penetration (Izadi-Darbandi et al., 2019). Surfactants are characterised based on the charge they carry; Non-ionic surfactants carry no charge and are generally water-soluble compounds. These surfactants act by reducing the surface tension of the water molecules within the herbicide formulation, allowing for greater spreading and therefore coverage of the leaf surface. Non-ionic surfactants are generally thought to have s lesser

impact on crop health compared to ionic surfactants. Many non-ionic surfactants are considered inert, and so are generally favoured over potentially phytotoxic ionic surfactants. Anionic surfactants improve spreading, however, have the potential to cause foaming under agitation, as well as some being thought to cause a degree plant stress. Cationic surfactants are positively charged and often very toxic to plants due to disruption of the ionic charge across the membrane. As such, cationic surfactants are not considered suitable for use within crops (Czarnota et al., 2010; Hull, 1982; Westra). Surfactants are the most frequently used adjuvants within herbicide formulations, particularly non-ionic surfactants, with some having been found to enhance glyphosate uptake 65% compared to a none adjuvant containing formulation (de Ruiter et al., 1998; Pacanoski, 2014). Adjuvants have the potential to greatly increase herbicide efficacy towards weed species, and through improved uptake offer the potential for lower active loadings within formulations, and lower active application rates. Alongside this, increased herbicide uptake has the potential to re-establish a degree of control within resistant populations by delivering herbicide levels within the plant beyond its metabolic capabilities for detoxification (Castro et al., 2018; Nakka et al., 2019).

The interaction between formulation, in which the adjuvant properties are paramount, and leaf surface, can greatly influence factors such as wetting and spreading, or enhance the formulations ability to plasticise the leaf wax. It was thought that the differing chemical nature of the selected adjuvants would lead to varying levels of uptake, as seen by metabolite concentrations within plant extracts. It is understood that selecting adjuvants of similar Log P to that of the herbicide can increase uptake rates over other, more dissimilar adjuvants. It was therefore hypothesised that of the Tween series, tween 22 would result in the greatest levels of uptake (Tween 22 Log P = 1.9, flufenacet Log P = 3.5) and Tween L10-10 would result in the greatest uptake of the tween L series of adjuvants (Log P = 4.63).

4.2 Adjuvant screen

Adjuvants were initially tested for their effect on flufenacet uptake via monitoring formation of glutathione and cysteine conjugates. As these conjugates had been synthesised, it allowed for their quantification using reference standards along with determining flufenacet levels. The different formulations were applied to leaves as described in section 2.6.1 and incubated for 16 hours prior to extraction. The adjuvant screen was performed with the aim of narrowing down the number of adjuvants for in depth study. Factors such as uptake, potential

environmental impacts, and any potential harm to the crop plant would be taken into consideration when selecting these adjuvants. Screening was carried out in cordial wheat as a model crop species and herbicide susceptible blackgrass (Rothamsted population) as a model weed species. Levels of flufenacet as well as its glutathione and cysteine conjugates were determined 16 hours post application (Figure 35).

A range of adjuvants were initially selected to cover multiple chemistries and differing charges as shown in Table 11. The Tween series consists of ethoxylated sorbitan esters with varying levels of ethoxylation. The Tween series investigated comprised Tween 20, 22, 23 and 24, each differing in chain length of polyethylene glycol repeats as shown in Table 12. With increase in the number of polyethylene glycol repeats, the Tween series follows a progressive change in physiochemical properties. Increasing the length of the polysorbate chain results in an increase in the hydrophilic-lipophilic balance (HLB). The HLB is a measure of the degree to which surfactants are either hydrophilic or lipophilic. Many surfactants contain both hydrophobic and hydrophilic regions, with the effective balance of these regions being assigned an HLB value (Pasquali et al., 2008). Higher HLB values (>10) represent surfactants which are progressively more water soluble, with lower values (<10) being hydrophilic and becoming more oil soluble. Known as hydrophilic and lipophilic pathways, It has been proposed that higher HLB, in general, will enhance penetration of water soluble herbicides and may facilitate movement through the plant cutin and into cells (Popp et al., 2005). A lower HLB surfactant will generally enhance uptake of less water soluble compounds helping penetrate the epicuticular wax at a greater rate but then may be slower in moving through the cutin compared to more water soluble actives (Hagedorn et al., 2017).

The Tween L series consists of two chemical modifications, with varying levels of ethoxylation and propoxylation across the series. The foremost number represents the level of ethoxylation with the latter the level of propoxylation. For example, Tween L-0515 consists of 5 units ethylene oxide and 15 units propylene oxide per molecule. The Tween L series also follows a progressive change in physiochemical properties with HLB again increasing with increasing levels of ethoxylation. This however occurs at a reduced rate compared to the Tween series highlighting the influence of propoxylation in reducing the hydrophilic-lipophilic balance (HLB).

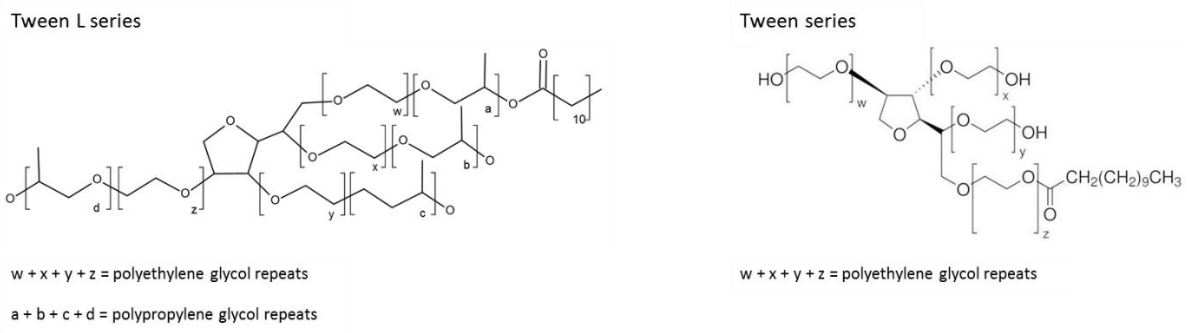

Figure 33. Structure of Tween and Tween L series adjuvants based on molecules of ethylene and propylene as dictate by Table 12

In addition to the Tween and Tween L series, several "Atplus™" adjuvants were investigated. The Atplus series consists of a range of alkoxylated molecules in which an expoxide has been added to an alcohol in the case of Atplus PFA and 242, and a polyol ester within Atplus UEP 100.

Table 11. The range of adjuvants used in initial screening, with charge, chemical class, and HLB where available.

Adjuvant	Chemical class	Surfactant type	HLB
Atplus 310	Phosphoric acid ester	An-ionic	
Atplus UEP 100	Alkoxylated polyol ester	N/A	
Atplus PFA	Alkoxylated alcohol		
Atplus 242	Alkoxylated alcohol	Non-ionic	
Atplus DRT 100	Emulsifier blend	Surfactant blend	
Tween 20	Polyoxyethylene (20) sorbitan monolaurate ester	Non-ionic	17
Tween 22	Polyoxyethylene (8) sorbitan monolaurate ester	Non-ionic	14.8
Tween 23	Polyoxyethylene (12) sorbitan monolaurate ester	Non-ionic	15.8
Tween 24	Polyoxyethylene (16) sorbitan monolaurate ester	Non-ionic	16.5
Tween L-0515	Ethoxylated and propoxylated sorbitan ester	Non-ionic	5.3
Tween L-1010	Ethoxylated and propoxylated sorbitan ester	Non-ionic	8.8
Tween L-1505	Ethoxylated and propoxylated sorbitan ester	Non-ionic	12.7
AL-2575	C8-10 Alkyl polysaccharide	Non-ionic	13
Synprolam 35X15	Amine ethoxylate	Non-ionic	15
Synperonic PE/F 127 (Poloxamer 407)	Polyalkylene oxide block co-polymer	Non-ionic	18-23

Table 12. Levels of ethoxylation and propoxylation within the Tween and Tween L series of adjuvants, alongside log P and HLB. Log P and HLB provide insight into the hydrophobicity of the adjuvant, with higher HLB and lower log P indicating a more hydrophilic compound.

Adjuvant	Units of ethylene oxide (EO)	Units of Propylene oxide (PO)	Log P*	HLB
Tween 20	20	0	-0.55	17
Tween 22	8	0	1.9	14.8
Tween 23	12	0	1.08	15.8
Tween 24	16	0	0.26	16.5
Tween L-0515	5	15	7.44	5.3
Tween L-1010	10	10	4.68	8.8
Tween L-1505	15	5	1.92	12.7

*Calculated using Molinspiration

The addition of adjuvants resulted in an increase in levels of both parent and metabolite determined within both wheat (Figure 35) and blackgrass in most instances (Figure 36). Within wheat, low levels of both parent and conjugate were detected relative to the amount applied. Addition of Tween L-1505 yielded the largest combined levels of parent and metabolite containing around 2.5 nmol of the applied 165 nmol. Within AL257, Synprolam™ 35X15, and Synperonic™ PE/F 127, there was no significant increase in uptake compared to the base SC formulation, with the levels of both flufenacet and conjugates being found in similar quantities. The Tween series showed a progressive change with the stepwise addition of ethylene oxide, although these were not significantly different from one another. Tween 20 promoted the greatest levels of both flufenacet as well as conjugates (~2.5 nmol total) in plant tissue among the Tween series, with Tween 22 giving the lowest levels (~1.25 nmol total). Based on this initial study, it would appear increasing the level of ethylene oxide content resulted in an increase in flufenacet uptake within wheat. This trend however was not maintained within the Tween L series. Tween L-1505 contains the highest level of ethylene oxide within the Tween L series, however the formulation promoted lower levels of both cysteine and glutathione conjugate (~0.5 nmol conjugate) compared to Tween L-1010 (~0.6 nmol conjugate). Tween L-1505 shares a similar HLB and log P with the Tween 22 formulation, however resulted in greater uptake, indicating HLB and log P are not the sole determinants of uptake. As Tween L-1010 resulted in the greatest level of uptake, this would suggest a possible increase in uptake resulting from the increased levels of propylene oxide. Although this trend did not continue within the Tween L-0515 formulation (15 molecules PO), it was noted that this adjuvant appeared somewhat unstable within the formulation and would result in a

degree of precipitation of flufenacet unless constantly agitated. The incorporation of UEP 100 within the formulation resulted in a significant increase in levels of flufenacet as well as the flufenacet-glutathione and flufenacet-cysteine conjugates over the base formulation. The levels of each were found to be similar to those found within the Tween L-1505 extract.

Within blackgrass extracts there was an overall higher level of both flufenacet and its conjugates when compared to wheat. The addition of adjuvants conferred an increase in both metabolite and parent in all cases except for Atplus 242, AL-2575, and Synperonic PE/F 127, all of which showed no significant difference from the base formulation. The Tween series once again followed a stepwise progression albeit following the opposite trend to that seen in wheat. Within blackgrass, assessing the Tween series, Tween 22 resulted in the greatest levels of both conjugates (~9 nmol) with Tween 20 (~5.5 nmol) showing the lowest. Within blackgrass it would therefore seem that greater uptake of flufenacet occurs when applied in conjunction with an adjuvant bearing lower levels of ethoxylation. Within the broader alkoxylated Tween series, Tween L-1010 once again resulted in the greatest level of uptake when compared to the remaining Tween L series, however, was not too dissimilar from Tween L-1505. Tween L-0515 once again resulted in the lowest uptake level of the Tween L series, likely owing to the lack of stability previously mentioned.

It was observed in both blackgrass and wheat that in several instances the levels of the flufenacet parent did not correlate with the levels of conjugate when compared to other treatments. This disassociation may arise as some adjuvants are able to cause plasticisation of the waxy cuticle, causing a greater level of fluidity within the amorphous phase of the waxy cuticle (Gitsopoulos et al., 2018). In addition, it has also been observed that the size and number of crystalline platelets present on the leaf surface can be reduced by the addition of adjuvants (Figure 34). Both factors are thought to decrease the tortuous nature of active diffusion across the cuticle, increasing uptake levels. Without wax plasticisation, diffusion is much slower and it is possible for the active to become immobile or diffuse much more slowly through the cuticle (Knowles, 2006). This would therefore give an artificially high level of flufenacet within the extract, which is not bioavailable. It is for this reason that the level of conjugate was used as a primary means of assessing uptake.

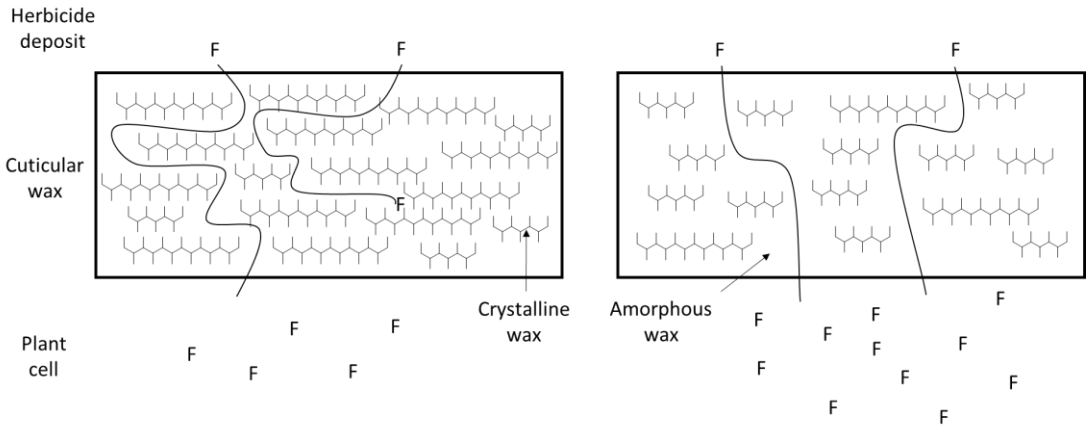

Figure 34. A demonstration of the potential effects of adjuvants upon leaf wax. In the presence of a plasticising adjuvant (shown right), there is a decrease in the size of the crystalline platelets and increase in the fluidity of the amorphous phase, allowing for a less tortuous diffusion pathway and therefore greater diffusion.

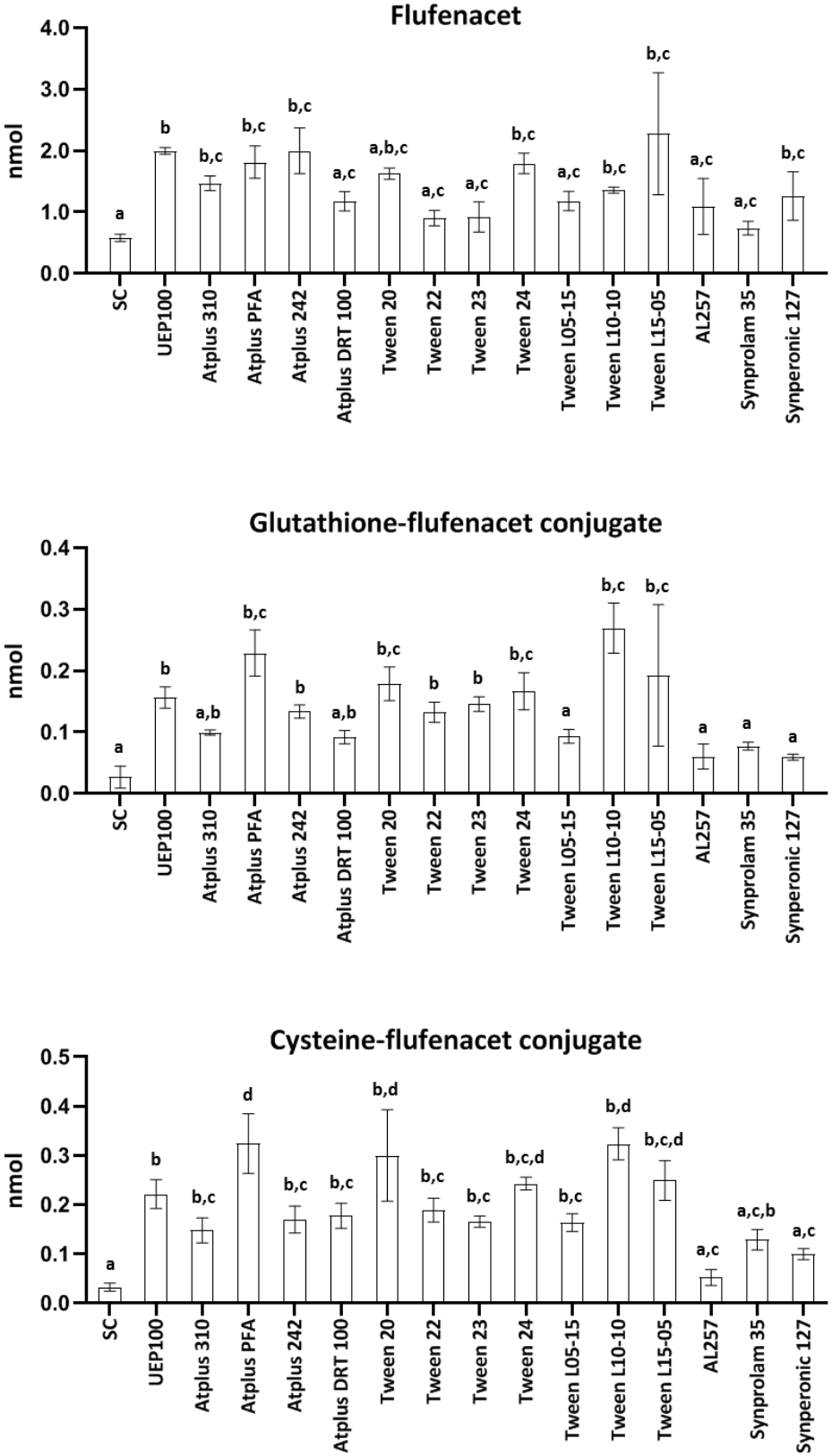

Figure 35 Flufenacet, glutathione, and cysteine conjugate levels within wheat extracts treated for 16 hours with flufenacet formulations with various adjuvants Data are presented as the mean of three samples (SD). Significance was assessed utilising a two-way ANOVA in which all treatments were compared. Lettering represents statistical significance, e.g. bars denoted with "a" are significantly different from those not denoted with a.

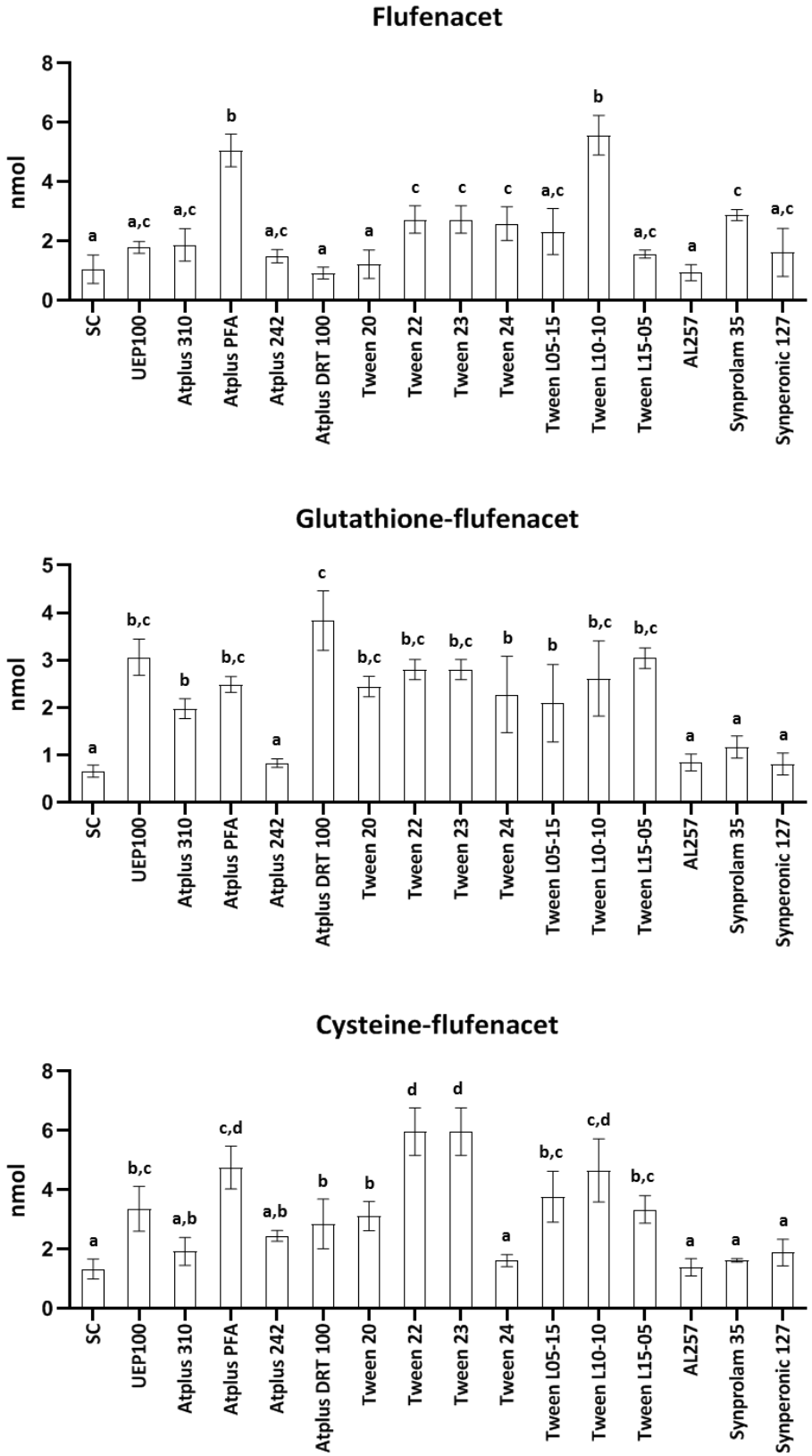

Figure 36. Flufenacet, glutathione, and cysteine conjugate levels within blackgrass extracts treated for 16 hours with flufenacet formulations with various adjuvants. Data are presented as the mean of three samples (SD). Significance was assessed utilising a two-way ANOVA in which all treatments were compared. Lettering represents statistical significance, e.g. bars denoted with "a" are significantly different from those not denoted with a.

Having looked at uptake in the presence of a number of adjuvants, the formulations were narrowed down to a smaller selection for more in depth study. Those selected for further study consisted of the Tween and Tween L series of adjuvants. These were selected for a number of reasons: They are both non-ionic, innert surfactants and so would not be expected to have a toxic effect upon the plant when correctly dosed (Agnello et al., 2015; Czarnota & Thomas, 2010). The Tween and Tween L series adjuvants are well characterised and follow a stepwise change in physical and chemical properties to allow potential elucidation of factors influenacing uptake. Additionally, Tween 20 is among the most frequently used non-ionic surfactants because of its inert nature, low cost, and ability to reduce surface tension at low concentrations, making it viable across a number of industries (Parr et al., 1965). These are traits shared with other Tweens, making them ideal for further study. Although the use of UEP 100 and Atplus PFA resulted in significant increases in both parent and conjugate formation, they did not provide a sequential change in chemistry and physiochemical properties, and so the Tween and Tween L series were seen as the most ideal set of adjuvants for further study.

4.3 Flufenacet time course studies

In order to better assess the effects of adjuvants upon herbicide uptake, formulations were applied to leaves of the plants of interest, and harvested across a time course of 0.5, 1, 2, 3, 4, 6, and 16 hours. Flufenacet and its metabolites were extracted from samples and analysed by LCMS to allow for detection and quantification as described in section 2.6.2. Although standards were only synthesised for the glutathione and cysteine-flufenacet conjugates, due to the similar readings produced by both standards, it was assumed that the intermediary metabolites, cysteinyl-glycine and glutamyl-cysteine, would also behave as such. These two metabolites were therefore quantified based on the standard curve produced for the flufenacet-glutathione conjugate.

Within wheat there was a notable increase in uptake with all adjuvant-containing formulations when compared to that seen with the base SC as shown in Figure 37. The effects of adjuvants upon uptake rates can be seen as early as 30 minutes post treatment, with all adjuvants resulting in higher levels of uptake compared to the base formulation. With the exception of Tween L-0515 and Tween 22, all adjuvants resulted in conjugate levels in the leaf over 10 times greater than those seen with the base formulation by 16 hours. All adjuvants

also promoted greater levels of the flufenacet parent compound being detected within the plant. However, this increase above the base formulation of the parent was less notable than was seen with conjguate levels. This likely stems from the ability of adjuvants to help facilitate not only transport across the waxy cuticle, but also delay drying of the droplet, and thus maintain the mobility of flufenacet over a longer period of time at the leaf surface. Additionally, adjuvants have been suggested as disrupting the epicuticular wax allowing for greater levels of diffusion (Hagedorn et al., 2017). As the base SC formulation does not benefit from such disruption, it is likely a larger portion of diffusing flufenacet becomes trapped within the waxy cuticle, and is therefore not bioavailable. Most adjuvant treatments showed similar trends of both conjugate and parent across the time course, with conjugate levels continuing to rise up to 16 hours as levels of flufeneacet decreased. This would suggest that uptake of flufenacet was no longer occuring and the remaining herbicide within the plant being metabolised, or that flufenacet was being taken up at a much reduced rate and/or metabolised faster than it was diffusing into cells. This is supported by looking at the individual metabolites, where the first stage metabolite, glutathione-flufenacet, can be seen to decrease as the levels of further downstream metabolties rise. Additionally, it was found that the residual flufenacet within the leaf wash was significantly greater in the SC formulation than within the adjuvant containing treatments. This would indicate less herbicide having been taken into the plant cells and epicutiular wax, and remaining on the surface. Despite a detectable difference between the base SC formulation and those containing adjuvants, no statistical difference in flufenacet levels could be detected in the leaf wash between the differing adjuvant treatments.

Within the Tween L series of adjuvants, a progressive trend can be seen as levels of ethylene oxide increase and levels of propylene oxide decrease. Tween L-0515 (5 units EO : 15 units PO) showed the lowest levels of overall conjugate formation with 1.5 nmol detectable by 16 hours. Tween L-1010 (10 units EO: 10 units PO) was found to contain 2.1 nmol of metabolite with Tween L-1505 (15 units EO: 5 units PO) containing 2.4 nmol. Although levels found in L15-05 were greater than in L-1010, this was not statistically significant and when comparing earlier time points it was found that both L10-10 and L15-05 yielded similar levels of both metabolite and parents across the entirety of the time course. Tween 22 and Tween L-0515 showed similar levels of conjugate formation (1.6 and 1.5 nmol respectively) and resulted in

the lowest levels of conjugate of all adjuvant treatments. Although this was a large increase compared to that seen with the SC formulation, all other adjuvants had a statistically higher level of conjugate formation by 16 hours.

The Tween series showed a similar trend to that observed within the Tween L series, with increasing levels of ethylene oxide resulting in a higher levels of uptake. Tween 20 had the highest level of ethoxylation of all tested adjuvants with 20 units ethylene oxide, and was found to have the highest level of uptake of the Tween series of adjuvants with 2.4 nmols of metabolite detected 16 hours post treatment. Tween 24 (16 units ethylene oxide) showed the second lowest levels of uptake, with 1.9 nmol of metabolite formed by 16 hours. Both Tween 23 and 22 (12 and 8 units ethylene oxide respectively) showed higher levels of uptake compared to both Tween 24 and Tween 20, however no significant differences were noted between the two.

Within most formulations a peak level of flufenacet was reached within the first few hours, after which point a decrease was seen up to 16 hours. This would indicate the herbicide droplet had dried on the leaf surface and the active had reduced mobility, resulting in slower diffusion into the plant. Overall there were few differences between treatments. All adjuvants resulted in an increase in uptake compared to the SC formulation, most adjuvants promoted similar increases in both parent and metabolite levels. Both Tween L-1010 and Tween L-1505 showed increased uptake levels over Tween 22, but at comparable levels to that of Tween 20, 23, and 24. As differences were only noticed at the extremes of selected adjuvants, i.e Tween 20 (20 mols polysorbate) and Tween 22 (8 mols polysorbate), it becomes apparent that much larger changes in adjuvant chemistry are required to induce large changes in uptake within wheat.

SC

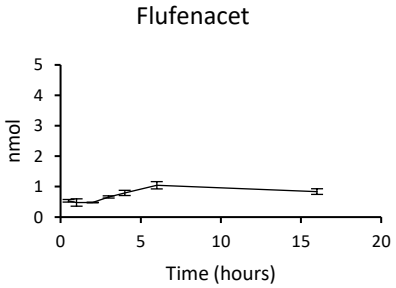

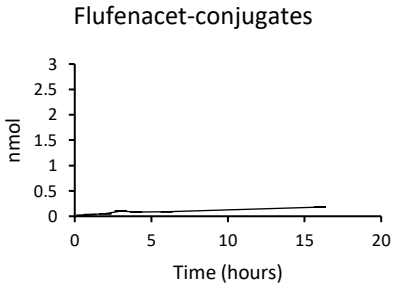

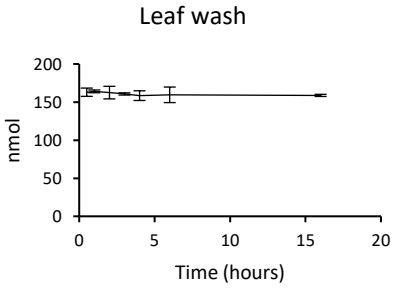

Tween L-0515

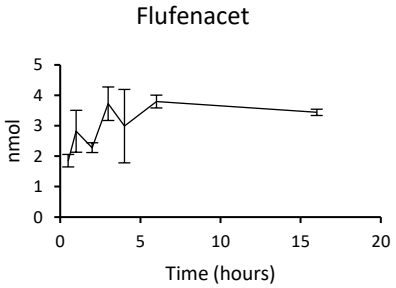

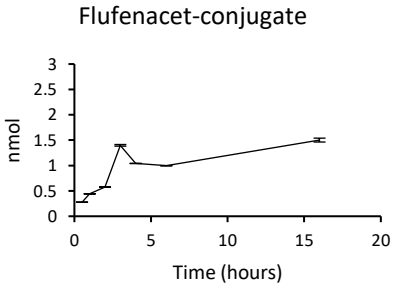

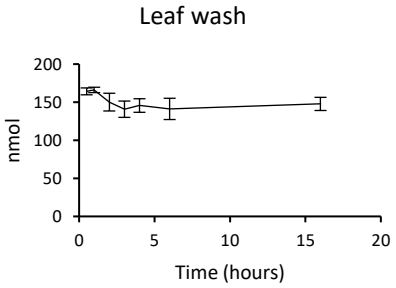

Tween L-1010

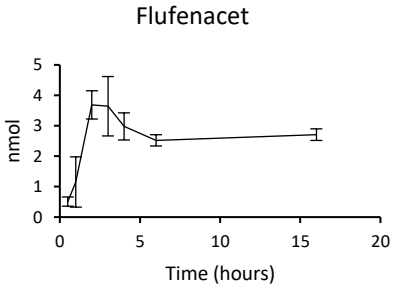

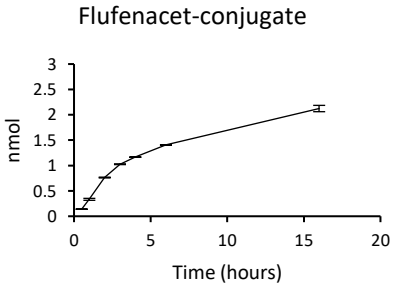

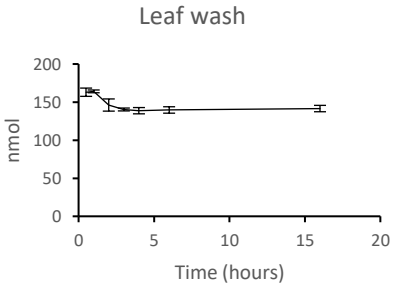

Tween L-1505

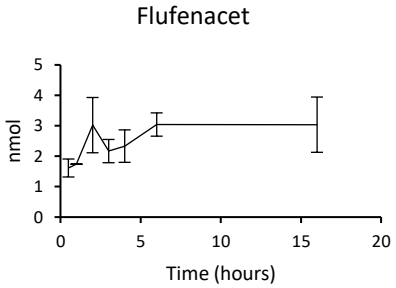

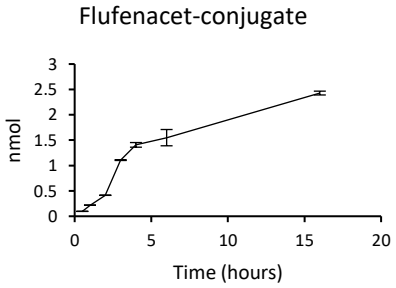

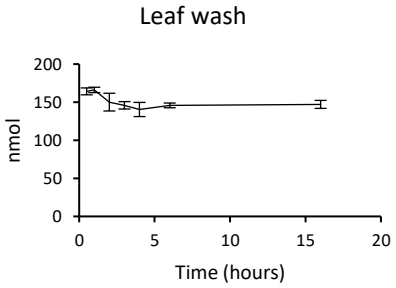

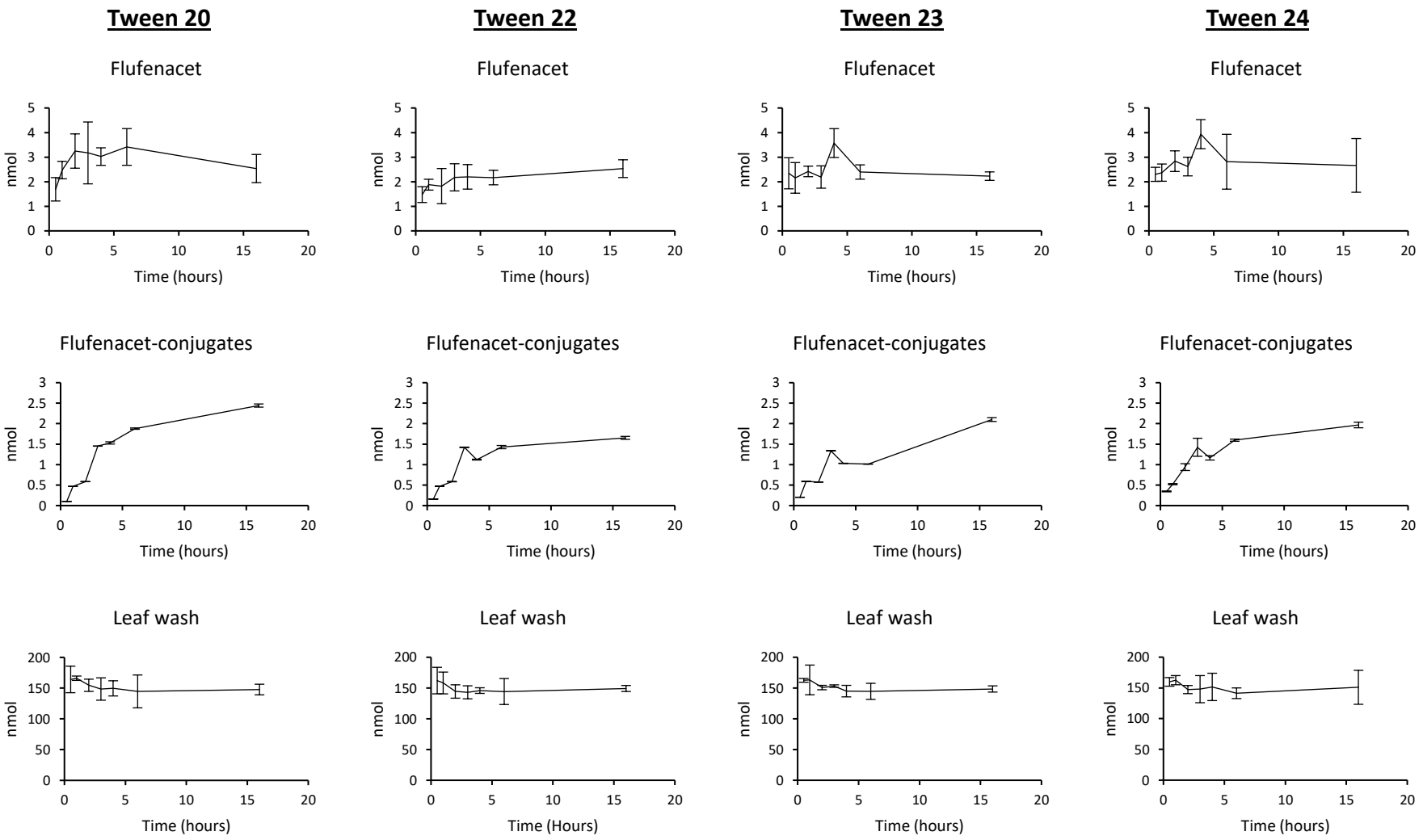

Figure 37. Levels of flufenacet and cumulative flufenacet conjugate levels (glutathione, cysteine, γ glutamyl-cysteine and cysteinyl-glycine) found within wheat extracts across a 16-hour time course. Each series shows the effect of different adjuvants added to the base SC formulation with the column denoted as "SC" showing conjugate and parent levels when no adjuvant is added. Data are presented as the mean of three pooled samples (5 treated leaves per pooled sample) with standard deviation denoting variance.

As with wheat, there was a notable increase in levels of both flufenacet and total conjugate levels when adjuvant containing formulations were applied to blackgrass (Figure 38). This increase above that seen with the base SC formulation was notable by 30 minutes and became increasingly apparent across the remainder of the time course. The lowest performing adjuvant, Tween L-1505, resulted in 3.9 nmol of conjugate formation by 16 hours compared to 1.8 nmol with the base SC, a 46% increase. Of the tested adjuvants, Tween 22 and Tween L-1010 resulted in the greatest increase in levels of flufenacet and metabolites over the base SC formulation. By 16 hours, total conjugate levels had reached 12.5 nmol within Tween 22 treated samples, and 9.2 nmol in samples containing Tween L-1010. It was noted that levels of flufenacet did not directly relate to conjugate levels, with Tween L-1010 promoting significantly higher levels of parent compared to Tween 22. Both Tween L-0515 and Tween L-1505 also resulted in levels of parent that did not correlate with the level of conjugate observed in the Tween series. As all Tween L series adjuvants resulted in a lower level of conjugate than would be expected as compared with the parent extracted, it was concluded that this has arisen from flufenacet accumulating within the waxy cuticle and not being bioavailable.

It had been noted in application of Tween L adjuvant containing formulations that a degree of particulate coagulation occurred upon addition to water, increasing the overall particle size and therefore resulting in a less mobile active. Despite this, levels of conjugate within the Tween L-1010 formulation were markedly higher than those observed within both Tween 20 and Tween 24 formulations. This would suggest that although a degree of active was becoming trapped within the cuticle, the delivery of active to cells was still greater in Tween L-1010 than in Tween 20 or Tween 24. Of the Tween formulations Tween 22 delivered the greatest levels of both parent and metabolite. A stepwise progression was observed with lower levels of ethoxylation resulting in higher levels of flufenacet and its metabolites. Of the Tween formulations, Tween 20 resulted in the lowest level of both conjugate and parent with 5.7 and 1.3 nmol respectively, being detected by 16 hours. Tween 22 resulted in the highest level with 12.5 nmol of conjugate and 3.3 nmol of parent detected by 16 hours. It was also noted that within the Tween 22 and 23 formulations, the same large dip in detected flufenacet by 16 hours seen in other formulations was not observed. This would suggest a more continuous, although reduced level of delivery beyond the initial “spike” in parent. This

is supported looking at the levels of individual metabolites, wherein levels of glutathione conjugate are seen to continue increasing at 16 hours, although at a reduced rate.

Within most treatments a peak level of detectable flufenacet was observed between 3 and 6 hours, with continuous uptake up until this point. Beyond 6 hours, the herbicide droplet would begin to dry with flufenacet becoming less mobile, slowing the rate of diffusion into the plant. This is usually followed by a progressive decrease in flufenacet and increase in levels of downstream metabolites, indicating the flufenacet within the plant is being metabolised and not replaced at the same rate by further herbicide diffusing in. It was found that most adjuvants did not alter the time by which flufenacet levels had peaked when compared to the SC formulation. All adjuvants except for Tween 22 and Tween 23 resulted in a peak level of flufenacet by 3 hours, compared to the 4 hours for the aforementioned formulations. This would demonstrate that many of the adjuvants had little impact on the initial drying time of the droplet, with this remaining similar to that of the SC formulation (further investigated in chapter 5). Despite decreases in active mobility in the droplet occurring at the same time, these peaks in flufenacet levels still remained significantly higher than that of the SC. This would indicate the rate of diffusion of flufenacet was much higher during the period the active was in solution.

SC

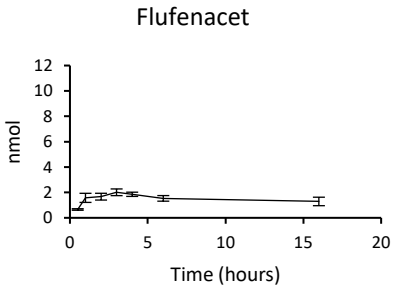

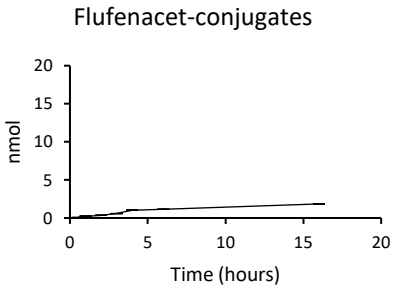

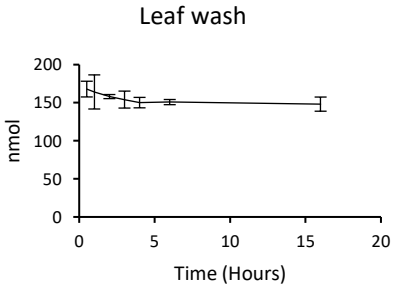

Tween L-0515

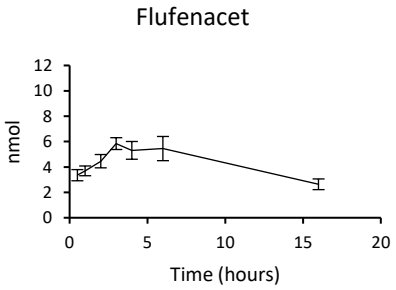

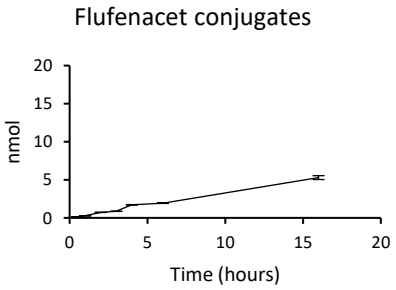

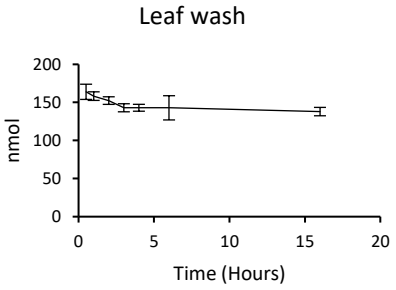

Tween L-1010

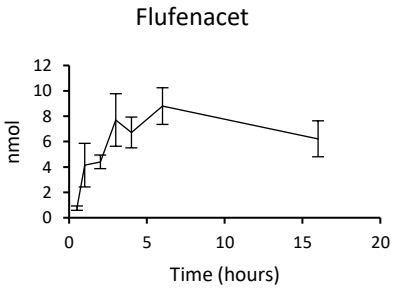

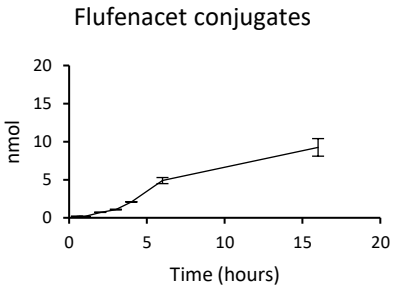

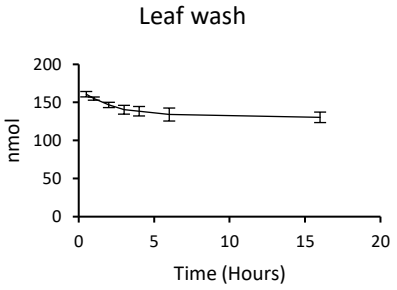

Tween L-1505

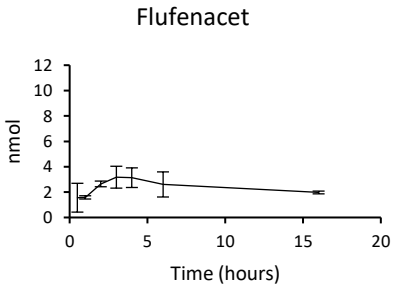

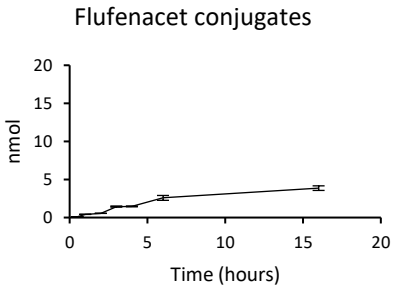

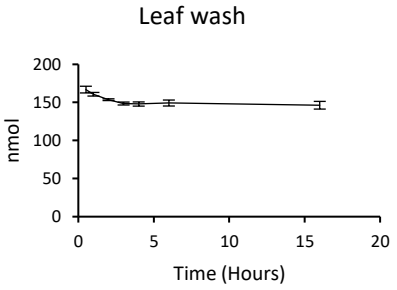

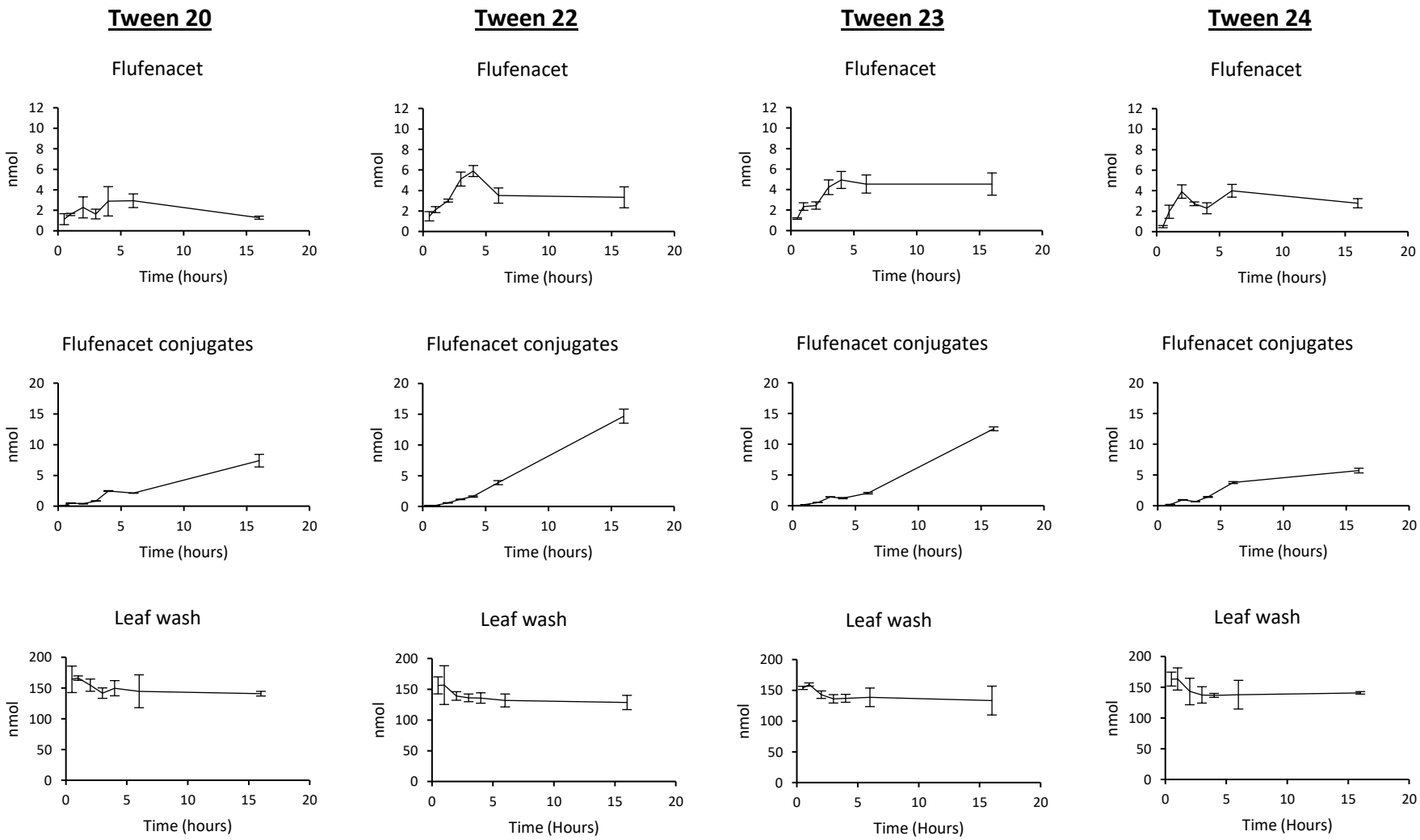

Figure 38. Levels of flufenacet and cumulative flufenacet conjugate levels (glutathione, cysteine, γ glutamyl-cysteine and cysteinyl-glycine) found within blackgrass extracts across a 16-hour time course. Each series shows the effect of different adjuvants added to the base SC formulation. Data are presented as the mean of three pooled samples (5 treated leaves per pooled sample) with standard deviation denoting variance.

Having establish levels of flufenacet uptake in both wheat and blackgrass, ryegrass was also investigated to see if similar levels of uptake were observed in a second grass weed. As a stepwise trend had been established within the Tween series, Tween 23 and 24 were omitted from the study, with only the longest and shortest chain length polysorbates of Tween 20 and Tween 22 included. As had been previously observed, all adjuvants resulted in a significant increase in both the amount of flufenacet and its metabolites detected compared to the base SC formulation.. Metabolite levels within the sample prepared using Tween 20 reached a peak of 2.5 nmol at 3 hours post treatment. Beyond this, a decrease to 2 nmol was seen by 6 hours, a level which was maintained until 16 hours, which, in conjunction with decreasing flufenacet levels, showed that uptake of the herbicide had slowed. The application of Tween 22 resulted in greater uptake of flufenacet compared to when Tween 20 was applied, with 3.8 nmol of flufenacet detected after 3 hours. The levels of metabolite were also found to continue increasing until the 16 hour time point with 6.2 nmol of metabolite detectable. It was found that despite higher levels of flufenacet detected in plants treated with either Tween L-0515 or L10-10 containing formulations as compared to those containing Tween L-1505 or Tween 22, the level of metabolites was similar in all cases. It was therefore concluded that the maximum rate at which ryegrass was able to metabolise flufenacet via glutathione mediated detoxification had been reached, and despite the presence of more flufenacet, metabolism was saturated.

Although it had been noted that the Tween L series of adjuvants were not stable over longer periods of time, and flufenacet was potentially accumulating within the waxy cuticle, there were still notable differences in metabolite levels within wheat and blackgrass samples treated with Tween L formulations. It was also noted that the decrease in flufenacet from 6 hours to 16 hours within each of these samples remained consistent, with a ~1 nmol decrease determined during this time. The decrease seen in flufenacet levels did not correlate with the larger rise in metabolite levels, indicating that uptake was continuing beyond the peak level of flufenacet, although at a reduced rate. This is also supported by the levels of flufenacet attained within the leaf wash which can be seen to continue to decrease up until 16 hours.

Overall, it was found that applying Tween L-0515 and Tween L-1010 to the formulation resulted in the greatest level of uptake within ryegrass, based on levels of both parent and metabolite detected. Both adjuvant containing formulations resulted in a peak level of

flufenacet at 4 hours with 4.7 nmol being detected in the extract in each instance. The overall level of metabolite also remained the same within the treatments across the time course. As previously mentioned however this remained in line with treatments which showed lower flufenacet uptake, suggesting the plant had reached its maximum detoxification rate.

SC

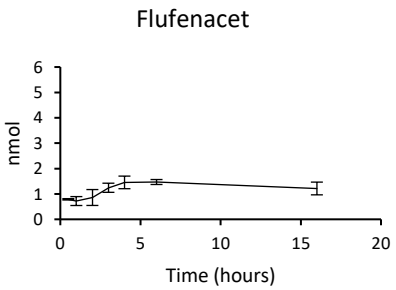

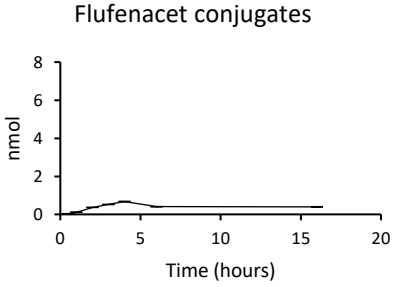

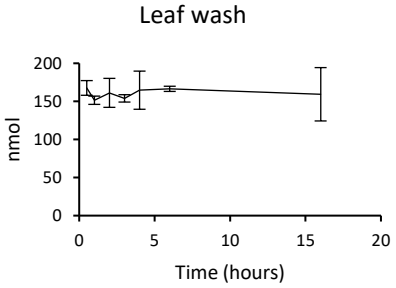

Tween L-0515

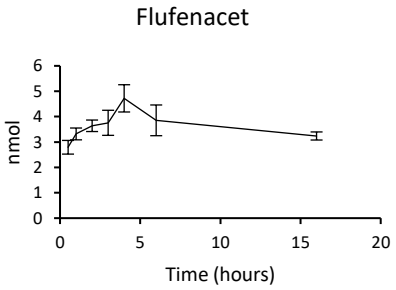

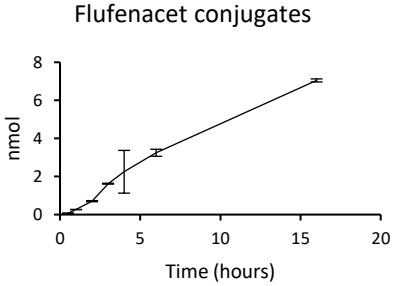

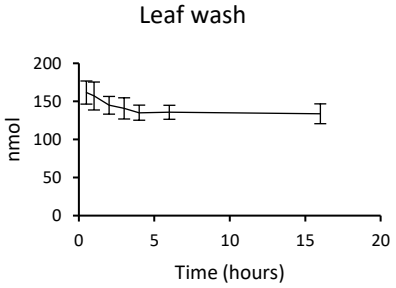

Tween L-1010

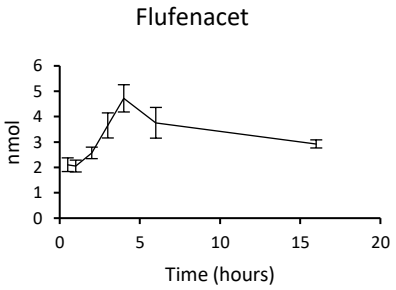

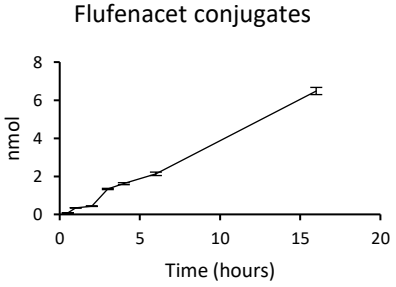

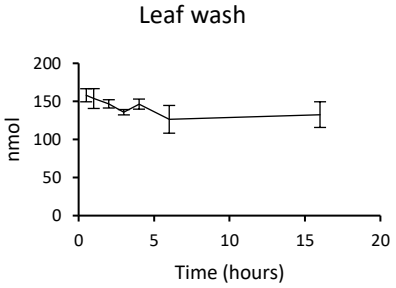

Tween L-1505

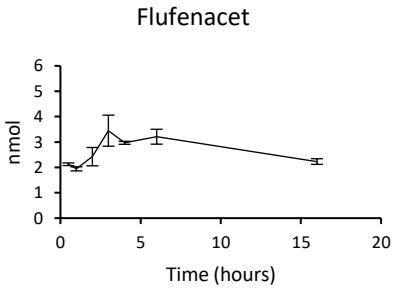

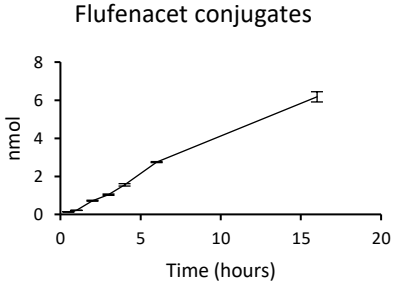

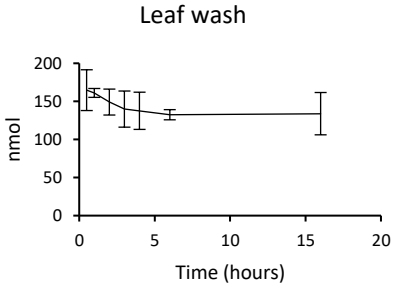

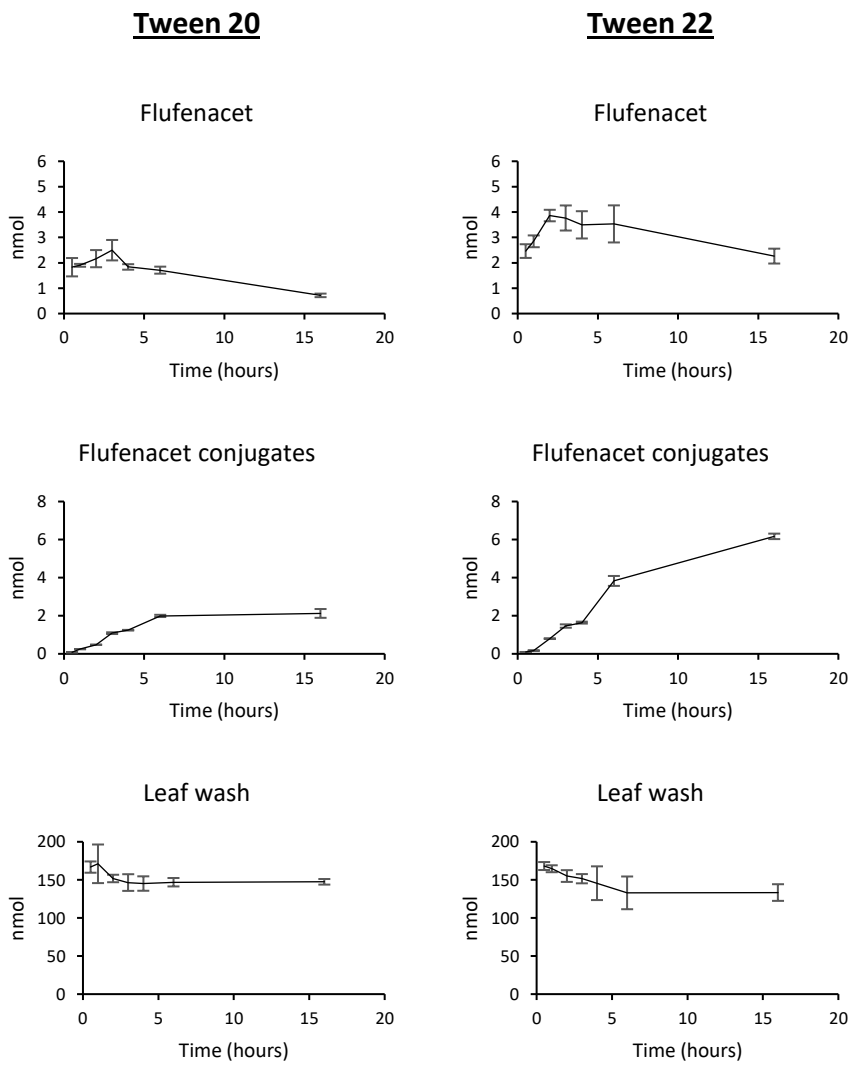

Figure 39. Uptake observed within ryegrass treated with the base SC formulation and adjuvant containing formulations consisting of Tween 20, Tween 22, Tween L-0515, Tween-L1010, and Tween L-1505. Three replicates consisting of five plants per replicate were harvested across a 16 hour time course (30 minutes, 1, 2, 3, 4, 6, and 16 hours). For each treatment, the total conjugate observed (top), flufenacet within the plant (middle) and flufenacet washed off the plant (bottom) have been presented. Results are displayed as the mean value with the standard deviation indicating variance

Although the uptake studies allowed for easy cross comparison of adjuvants within individual plant species, comparing different plant species based solely on metabolite production would prove much more difficult. This is due to differing physiology within each plant, leading to different rates and pathways of metabolism, meaning the same level of flufenacet in one plant might give rise to a much greater level of metabolite than another.

The composition of total conjugated metabolites was therefore compared in more detail using the Tween 22 formulation applications shown in Figure 40. In addition to the differences in overall metabolite detected within each plant (2 nmol in wheat, 10 nmol in blackgrass, and

6 nmol in ryegrass by 16 hours) there were notable differences in the levels of each glutathione-based metabolite. By 16 hours, wheat was found to have the overall lowest level of glutathione-flufenacet metabolite, with only 0.3 nmol detected compared to the 1.5 nmol of blackgrass and 3 nmol of ryegrass. This would suggest either a much-reduced level of flufenacet present within wheat, or a much slower rate of metabolism to the glutathione conjugate compared to the weed species. Within ryegrass the rate of production for each conjugate reached a plateau between 6 and 16 hours, indicating a maximum rate of metabolism had been reached, as previously discussed. The glutathione conjugate is sequestered into the vacuole where it undergoes further metabolism to form the flufenacet-cysteine conjugate. This can occur by one of two routes, by cleavage of the gluytamyl residue to form cysteinyl-glycine, or cleavage of glycine to form glutamyl-cysteine conjugates (Brazier-Hicks et al., 2008). There were notable differences in which pathway was the most prevalent within each species. Within wheat only low levels of cysteinyl-glycine were present, with a peak level of 0.1 nmol by 4 hours which progressively decreased by 16 hours. Conversely, the levels of cysteinyl-glycine were much higher in both blackgrass and ryegrass, with 1.5 and 1 nmol being extracted respectively. The reverse was true of the glutamyl-cysteine conjugate with 1.5 nmol being present within wheat by 16 hours, compared to the 0.06 nmol of blackgrass and 0.5 nmol of ryegrass. Within wheat, the level of cysteine conjugate was also significantly lower (0.3 nmol) than detected in blackgrass (5 nmol) and ryegrass (1.5 nmol). As levels of the glutamyl-cysteine within wheat, and cysteinyl-glycine conjugates within blackgrass and ryegrass are all found at similar levels, this would suggest differing rates of conversion to the cysteine conjugate within each plant. Based on levels of the cysteine conjugate precursors within each species compared to the level of cysteine conjugate found, it is clear that blackgrass has the greatest ability to process downstream metabolites.

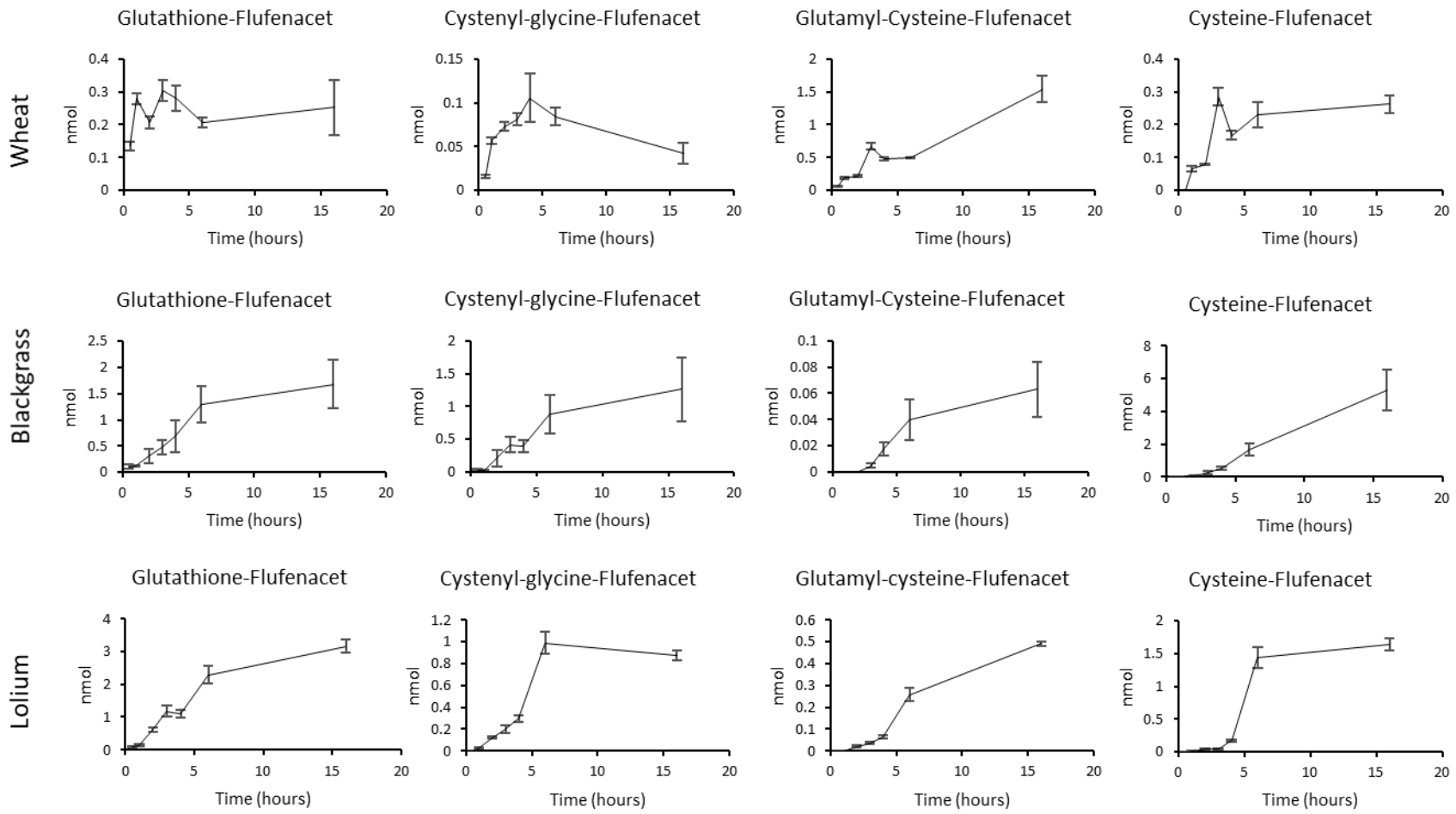

Figure 40.Typical Distribution of glutathione-based metabolites within flufenacet treated wheat, ryegrass, and blackgrass. The show example is from the Tween 22 (10% w/w) containing formulation using three replicates of treated leaf samples from 3 leaf stage plants. After treatment, samples were harvested across a 16 hour time course at 30 minutes, 1, 2, 3 ,4, 6, and 16 hours. Data are presented as the mean of three pooled samples (5 treated leaves per pooled sample) with standard deviation denoting variance.

4.4 Plant physiological profiling

Although intraspecies variation between adjuvant treatments is easy to determine and clear trends can be established, determining differences in uptake between plant species provides a much greater challenge. As has already been established, the pathway by which the glutathione conjugate is further catabolised to the cysteine conjugate varies between each species. In addition to this, factors such as metabolic rate, and glutathione availability may greatly affect the ability of plants to detoxify xenobiotics via glutathione mediated metabolism. It was therefore important to establish the enzymatic ability of each plant to conjugate flufenacet to glutathione to further elucidate different uptake levels between species

4.4.1 CDNB activity assay

The focus of this chapter has been to look at the uptake of various flufenacet formulations with the respective glutathione conjugate being an indicator of flufenacet bioavailability within plant cells. In the first instance, GST activity within crude protein extracts was measured based on its catalytic ability to substitute glutathione for the chlorine group of CDNB (Figure 41) which can be posteriorly quantified by colorimetric detection. The glutathione-DNB conjugate absorbs at 340nm and thus the rate at which the conjugate is formed, and therefore rate of increased absorbance at 340nm, is directly proportional to the GST activity within the sample when spontaneous conjugation is accounted for (Habig et al., 1974) This was done on the assumption of being able to quantify relative GST mediated xenobiotic-detoxifying activity within wheat, black grass, and ryegrass, which may correlate to levels of flufenacet metabolism levels.

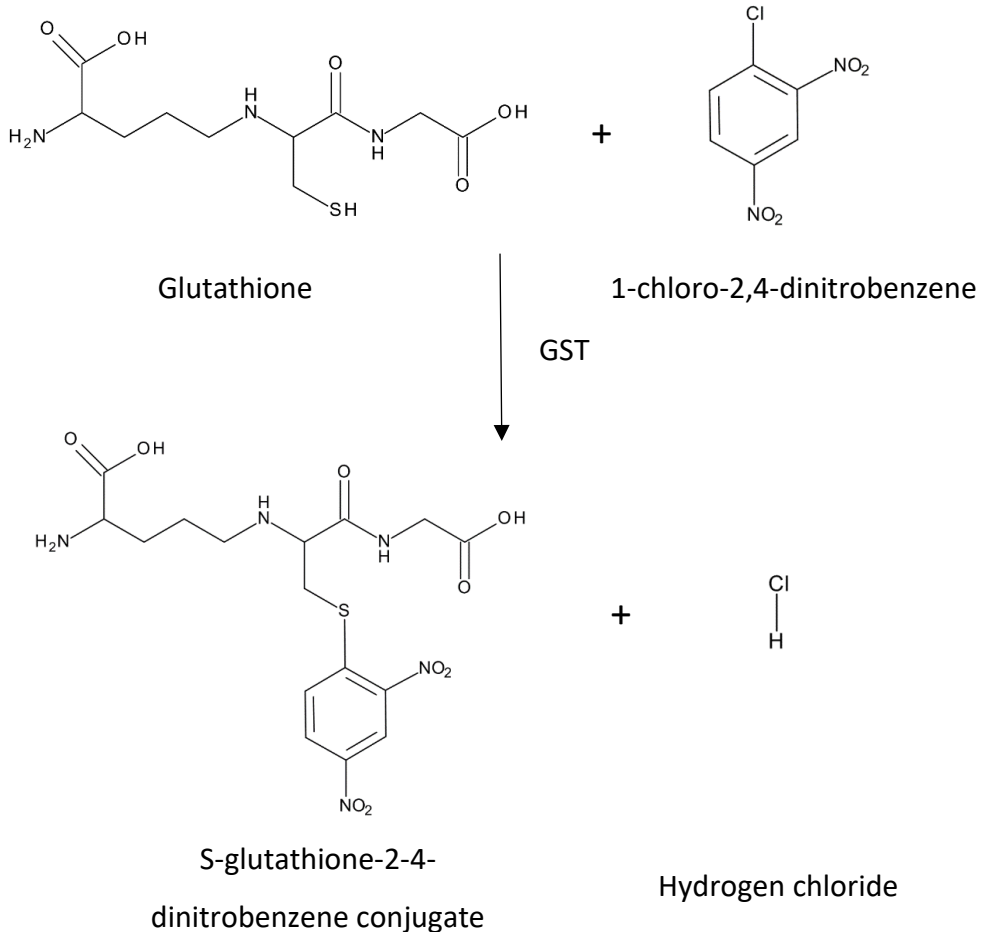

Figure 41.The reaction pathway of the CDNB assay. The product of the reaction, S-glutathione-2-4-dinitrobenzene conjugate, absorbs at 340 nm allowing for quantification based on absorbance.

The CDNB assay was used to look for differing levels of GST activity in wheat, blackgrass, and ryegrass. Looking at Table 13, there was no statistically significant difference in enzyme activity towards CDNB within the weed species. Activity levels were found to be around 30% lower in wheat than blackgrass and ryegrass, with activity of 0.70 nKat/mg crude protein extract in wheat compared to the 0.92 nKat/mg of blackgrass and 0.94 nKat/mg of ryegrass. Although differing levels of activity were observed in the two weed species compared to wheat, this did not correlate with the overall levels of flufenacet related conjugates despite similar conjugating ability towards CDNB. Several possible reasons for this have been proposed; the levels of parent able to penetrate the leaf surface may vary between each species with the differing concentrations in conjugate arising from different levels of flufenacet available within the cell or, the enzymes involved in the conjugation of CDNB are not be the same as those involved with glutathione conjugation of flufenacet. Spontaneous

conjugation with glutathione may provide a key role in glutathione mediated metabolism of flufenacet.

Table 13. Activity levels of crude protein extracts of wheat, blackgrass and ryegrass towards CDNB (calculated levels based on 3 replicates. each being extracted from 5 g of leaves from 3 leaf stage plants).

Plant	Specific Activity (nKat/mg)
Wheat	0.702 ± 0.08
Blackgrass	0.916 ± 0.06
Ryegrass	0.944 ± 0.041

4.4.2 Flufenacet activity assay

Having established GST activity was detectable within the crude protein extracts by CDNB assay, it was important to establish enzymatic activity towards flufenacet at physiological pH. As the flufenacet-GSH conjugate absorbance coefficient has not been established, an alternative method of looking for GST activity towards flufenacet was developed. The flufenacet activity assay was carried out in each species over a time frame of 40 minutes. Samples were taken every 10 minutes and the reaction stopped by the addition of 10µl 3M HCl, preventing both spontaneous and enzymatic conjugation. After freezing and centrifugation to precipitate the protein within the sample, analysis was performed by LCMS, looking at the levels of glutathione-flufenacet conjugate formation over time. The time course follows a linear trend from 10 to 30 minutes at which point the rate of increase in glutathione-flufenacet conjugate begins to slow (Figure 42). This decrease in the flufenacet conjugate may be as a result of the protein in the crude extract beginning to degrade and losing functionality, or that a large portion of the glutathione and flufenacet had been conjugated, whether spontaneously or enzymatically. Therefore, when calculating the enzymatic rate only the first three time points (10, 20, and 30 minutes) were used.

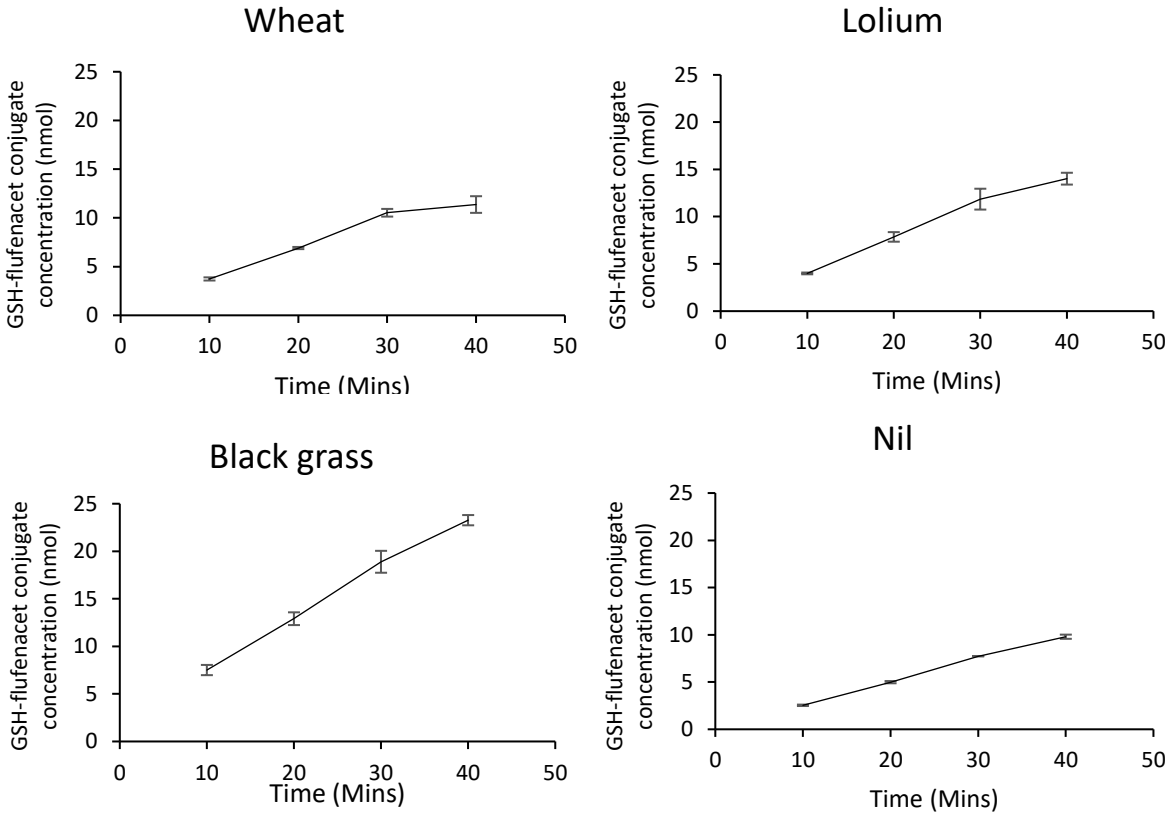

Figure 42. This figure displays the concentration of glutathione-flufenacet conjugate across a time course of 10, 20, 30 and 40 minutes. Crude protein extracts from wheat, lolium, and black grass were used to conduct CDNB assays with three replicates per time point. A negative control containing no enzyme was used to establish the spontaneous rate of conjugation and normalise results.

By removing the spontaneous rate of conjugation, the enzymatic rate of flufenacet-glutathione conjugation of the crude extracts could be calculated (Table 14). Wheat was found to have the lowest enzymatic activity towards flufenacet with 0.0178 nKat/mg of crude protein extract. Ryegrass had a much greater rate of 0.039 nKat/mg, but was still much lower than the 0.079 nKat/mg of blackgrass. This was unexpected as the means by which herbicical selectivity is derived is often through differing rates of metabolism of the herbicide (Carvalho et al., 2009). This however did correlate with levels of conjugate found during uptake trials, with blackgrass containing the greatest levels of conjugate overall, and wheat the least. This also supported the notion that ryegrass may have reached its maximum rate of metabolism within several hours of the treatments, as the level of activity is much lower compared to that of blackgrass.

Despite the comparativly high enzymatic activity within blackgrass, levels of glutathione conjugate found were comparable to those found within ryegrass. There was however much

greater levels of downstream metabolites within blackgrass which continued to increase up until 16 hours. It was therefore deduced that the further downstream processing ability of blackgrass was much greater than that within ryegrass (Cummins et al., 2009).

Although a lower level of activity of flufenacet-glutathione conjugation was observed within wheat, the levels of glutathione conjugate formation were comparably much lower than this would suggest. This likely stems from an overall lower level of flufenacet uptake within wheat, with control being confered by a lesser ability to absorb the active rather than differential metabolism between crop and weed. Although often coupled with differential metabolism, a lesser degree of uptake and translocation of herbicides has been observed within maize (*Zea mays*) (Grossmann et al., 2002).

Table 14. Activity of crude protein extracts towards flufenacet based on conversion to the glutathione-flufenacet conjugate. This value was calculated by the rate of conversion of flufenacet to the glutathione-flufenacet conjugate across the 10, 20, and 30 minute time points after accounting for the spontaneous rate attained in the nil. Extracts were attained from the pooling of five leaf samples per replicate, with three replicates used at each time point.

Plant	Specific Activity (nKat/mg)
Wheat	0.0178 ± 0.002
Blackgrass	0.079 ± 0.0017
Ryegrass	0.039 ± 0.002

4.4.3 Glutathione concentration assay

Due to the high levels of spontaneous conjugation observed under physiological pH during the flufenacet activity assay, it was thought that a degree of conjugation would therefore be spontaneous and dependent on the concentration of glutathione present within the cell. The concentration of both reduced and oxidised glutathione was therefore looked at in wheat, blackgrass and ryegrass.

As shown in Table 15 ryegrass extracts were found to contain significantly less glutathione (both reduced and oxidised), compared to the similar amounts found in wheat and blackgrass (468.94 and 513.64 nmol/gFW respectively). Despite similar levels of glutathione within

wheat and blackgrass, the formation of the glutathione-flufenacet conjugate was much lower in wheat. It was also noted that in each instance oxidised glutathione accounted for around 10% of the total glutathione content. This would suggest that enzymatic activity has a much greater impact on conjugation than any spontaneous effect.

Table 15. Levels of both oxidised (GSSG) and reduced glutathione (GSH) in blackgrass, wheat, and ryegrass extracts. Glutathione was extracted from five pooled leaves per sample, with three replicates per plant. Data are displayed as the mean with standard deviation indicating variance.

Plant	GSSG (nmol/gFW)	GSH (nmol/gFW)	Total (nmol/gFW)
Wheat	43.03 ± 4.40	405.91 ± 19.09	448.94 ± 23.20
Blackgrass	53.27 ± 7.81	460.37 ± 44.20	513.64 ± 51.26
Ryegrass	13.05 ± 0.40	118.76 ± 15.51	131.82 ± 15.91

4.5 Blackgrass population study

Herbicide resistance is a globally prevalent problem and poses a great threat to the sustainability of agriculture with once susceptible weed populations no longer controlled by particular herbicides (Baucom, 2019). Herbicide resistance within blackgrass is an ever increasing problem, and with 5% yield losses at just 10 plants per m^2, has the potential to cause large scale crop losses (S. Moss, 2017). Although resistance to flufenacet has not been widely reported in blackgrass, it is thought to be gradually emerging due to its use in targeting populations resistant to other herbicides. There are two types of resistance found within blackgrass, non-target site resistance (NTSR), and target site resistance (TSR). TSR resistance stems from a mutation within the herbicides target enzyme. The result is an enzyme which is still functional, however with reduced binding affinity for the herbicide reducing control (Neve et al., 2014). NTSR is less well understood, with any mechanism conferring resistance not by target site alterations being considered NTRS. NTSR gives rise to resistance to multiple herbicides, with a multitude of genes having been found as potentially involved (Baucom, 2019; Tétard-Jones et al., 2018). Identified genes are generally broad-spectrum with involvement in herbicide translocation and detoxification, such as ABC transporters, GSTs, and CYPs. Due to the wide degree of genetic variation within NTSR populations, and the

various mechanisms by which it has been proposed to occur, it has proven difficult to elucidate the exact means by which this increased tolerance occurs (Baucom, 2019).

Eight blackgrass populations (Table 16), exhibiting various physiological differences were screened to look for variations in metabolism compared to a WTS population, Roth 09, which had no previous exposure to herbicides. Several populations exhibiting herbicide resistance were available from previous studies and originated from Rothamsted research. The Peldon 05 population is often used as a reference population for non-target site resistance (NTSR) and has been shown to have enhanced levels of both *Am*GSTF1 as well as *Am*GSTU2. Resistance to both ALS and ACCase targeting herbicides have been observed, with mutations in ALS determined, indicating TSR to this target site. No such mutation is present within ACCase however, indicating resistance to this class of herbicide is derived by other means, such as enhanced metabolism (Stephen R. Moss et al., 2003). Two target site populations were selected, Notts 05, which exhibits target site mutations within both ACCase and ALS, and low levels of *Am*GSTF1, and Hor 08, containing a mutation of ACCase. Both populations have been found to express low levels of *Am*GSTF1 thereby potentially lower levels of metabolism towards herbicides they do not display TSR towards. Three field collected populations were also screened, Suffolk 09, Kent 02, and Warren 09, each of which have exhibited NTSR resistance and have been found to overexpress *Am*GSTF1 and *Am*GSTU2. A final population, Pend 14 was also investigated, which has been selected from a blackgrass population repeatedly exposed to pendimethalin over a period of 8 years. Evolved resistance to pendimethalin has been found to result from enhanced metabolism with this population containing elevated levels of *Am*GSTF1 (Tétard-Jones et al., 2018).

Table 16. Various blackgrass populations and relative levels of AmGSTF1 and AmGSTU2 compared to the Roth 09 WTS population. ↑ represents increased expression with ↓ indicating a decrease compared to Roth 09. Multiple populations contained either ALS or ACCase point mutations, the presence of which is denoted by ✓.

Population	*Am*GSTF1	*Am*GSTU2	ALS mutation	ACCase mutation
Peldon 05	↑	↑	✓	X
Roth 09	-	-	X	X
Suffolk 09	↑	↑	X	✓
Kent 02	↑	↑	X	X
Warren 09	↑	↑	✓	✓
Pend 14	↑	-	X	X
Hor 08	↓	-	✓	✓
Notts 05	↓	-	X	✓

Each population was treated with flufenacet as previously described in 2.3.2. Two time points of 2 and 6 hours were selected, allowing enough time coverage to discern any difference in metabolism between populations. As can be seen in Table 17, multiple differences within populations were observed, both in terms of overall metabolite concentrations, and distribution of metabolites. In all instances there was a greater amount of metabolite detectable at 6 hours compared to 2 hours, resulting from progressively more flufenacet being available for metabolism, and early metabolites being processed further downstream. The WTS Roth 09 population was found to have a low level of detectable metabolites at both 2 and 6 hours compared to most populations, with 0.545 and 2.783 nmol extracted at each time point respectively. Although most resistant strains contained higher levels of conjugate than the WTS population by 2 hours, there were no statistically significant difference between the Suffolk, Kent, Warren, and Pend populations in terms of overall metabolite. Neither the Notts nor Roth population have been characterised as displaying enhanced herbicide metabolism. These two populations were found to have the lowest level of metabolite with 0.540 and 0.545 nmol at 2 hours, respectively.

By 6 hours, differences within the metabolic profiles of the populations had become much more apparent. There were no significant differences between levels of metabolite detected within the Roth and Notts populations 6 hours after treatment. This was to be expected as

these populations have not shown any degree of NTRS, and with Notts having been previously demonstrated as having lower levels of *Am*GSTF1. This decreased level of *Am*GSTF1 however did not seem to result in a decrease in the level of metabolite detected compared to the WTS Roth 09 population. Interestingly, the population deemed TSR, Hor 08, showed significantly higher levels of metabolite than both Notts and Roth populations, with 3.681 nmol of metabolite detected compared to the 2.7 nmol of both Roth and Notts. A number of these populations have been previously tested for susceptibility towards Atlantis (Actives: mesosulfuron-methyl and iodosulfuron-methyl, both ALS inhibitors) and Cheetah (Active: fenoxaprop-p-ethyl), an ACCase inhibitor (Sabbadin et al., 2017). The Kent population, although having previously been designated as showing "high" levels of NTSR, did not show significantly different levels of flufenacet metabolism from the WTS population. It has previously been demonstrated by Sabbadin, et al. (2017) that this population, despite increased levels of both *Am*GSTU2 and *Am*GSTF1, retained a large degree of susceptibility towards mesosulfuron. The population designated as TSR for both ALS and ACCase (Hor 08), showed a significantly higher level of flufenacet metabolites compared to the WTS population, indicating a degree of enhanced detoxification. Within other populations which have been demonstrated to display NTSR, higher levels of flufenacet metabolism were observed. Of the NTSR populations, Peldon contained the lowest level of total conjugate at 3.222 nmol within the extract. This proved to be significantly lower than levels seen within other NTSR populations of which Suffolk, Warren, and Pend populations had contents in excess of 3.8 nmol. It was shown that despite increases in metabolism of flufenacet within NTSR populations, that susceptibility to flufenacet was still maintained. Upon treatment with flufenacet at field rate, a 100% mortality rate was observed in all populations.

Table 17. The levels of each conjugate as well as total conjugate detected 2 and 6 hours after treatment with 165 nmol of flufenacet (approximate field rate). Trials were conducted on wild type (Roth 09), MHR (Kent 02, Pend 09), and NTSR (Hor 08, Notts 05) populations of blackgrass, with several populations (Peldon 05, Suffolk 09, Warren 09) demonstrating both MHR and NTSR type resistance

2 Hours post treatment

Population	Glutathione (nmol)	Cysteinyl-glycine (nmol)	Glutamyl-cysteine (nmol)	Cysteine (nmol)	Total conjugate (nmol)
Peldon 05	0.495	0.211	0.008	0.179	**0.893**
Roth 09	0.29	0.163	0.013	0.163	**0.545**
Suffolk 09	0.589	0.255	0.012	0.158	**1.015**
Kent 02	0.633	0.260	0.014	0.143	**1.050**
Warren 09	0.649	0.173	0.014	0.186	**1.023**
Pend 14	0.782	0.196	0.009	0.144	**1.131**
Hor 08	0.470	0.236	0.005	0.153	**0.865**
Notts 05	0.311	0.158	0.005	0.071	**0.540**

6 Hours post treatment

Population	Glutathione (nmol)	Cysteinyl-glycine (nmol)	Glutamyl-cysteine (nmol)	Cysteine (nmol)	Total conjugate (nmol)
Peldon 05	1.053	0.433	0.07	1.665	**3.222**
Roth 09	1.000	0.685	0.0178	1.080	**2.783**
Suffolk 09	1.226	0.907	0.036	1.689	**3.86**
Kent 02	1.155	0.615	0.015	1.036	**2.822**
Warren 09	1.356	0.704	0.034	1.76	**3.854**
Pend 14	1.644	0.680	0.018	1.629	**3.97**
Hor 08	1.19	0.757	0.033	1.701	**3.681**
Notts 05	0.929	0.777	0.029	1.022	**2.757**

4.6 Discussion

Looking at the results of the uptake studies, it has been clearly shown that the incorporation of adjuvants into the flufenacet formulation can result in a large increase in uptake within blackgrass, wheat, and ryegrass. Incorporation of both the Tween and Tween L series of adjuvants resulted in significantly higher levels of both parent and metabolites within plant extracts when compared to the non- adjuvant containing formulation. Although adjuvants had a large increase in uptake compared to the base SC formulation, there were minimal differences observed between the various adjuvant treatments within wheat. Within wheat, the addition of all adjuvants resulted in increased metabolite formation at a similar rate with the exception of Tween 22 and Tween L-0515 which were significantly lower. In contrast, differences in uptake were much more apparent in blackgrass and ryegrass. In both weed species there appeared to be a stepwise progression within the Tween series depending on the chain length of the polysorbate molecule, with Tween 22 (8) resulting in the greatest uptake and Tween 20 (20) resulting in the least. The progressive change in molecule length also results in a progressive change in physiochemical properties, with an increasing log P and decreasing HLB with shorter chain lengths. This would suggest that lowering the aqueous solubility of the adjuvants resulted in the greatest increase in uptake within the flufenacet formulation. Based simply on log P and HLB, Tween 22 and L15-05 would be expected to behave similarly. This was not found to be the case within both blackgrass and ryegrass however, suggesting additional factors influencing adjuvants effect on uptake. The Tween L-1505 adjuvant is both larger in molecular weight, as well as consisting a more branched structure which may reduce effectiveness in enhancing herbicide uptake when compared to Tween 22.

There were a few notable differences in the way by which flufenacet was metabolised within each plant species. Within wheat, catabolism of the glutathione conjugate occurs primarily through cleavage of the glycine residue to form a flufenacet glutamyl-cysteine conjugate. There have been two proposed pathways by which this may occur; Firstly, by sequestering of the glutathione conjugate into the vacuole by ATP-binding cassette transporters, where carboxypeptidase hydrolyses the glycine-cysteine bond to form a glutamyl-cysteine conjugate. The glutamyl residue is in turn cleaved by glutamyl-transpeptidase, resulting in the cysteine conjugate (Brazier-Hicks et al., 2008; J. Coleman et al., 1997). The second proposed

pathway occurs within the cytosol, with the carboxypeptidase activity of the phytochelatin synthase enzyme resulting in cleavage of the glycine residue. This is followed by catabolism to the cysteine conjugate by a γ-glutamyltranspeptidase isoenzyme localized to the plasma membrane (Blum et al., 2007). Within blackgrass and ryegrass, the formation of the cysteinyl-glycine conjugate appeared to be the primary intermediate in cysteine conjugate formation. The cleavage of the glutamate residue is mediated by a gamma-glutamyl transferase (GGT) enzyme, resulting in the cysteinyl-glycine conjugate, and free glutamate. GGT enzymes are thought to be present in both the vacuole as well as the cytosol. It has been found however that the rate of vacuole sequestering of the glutathione conjugate is much greater than the rate by which cytosolic GGT's are able to hydrolyse glutathione conjugates. It is therefore thought that the majority of this processing occurs in the vacuole (Hanigan, 2014; Ohkama-Ohtsu et al., 2007). However, based on the low levels of cysteine conjugate found within wheat when compared to the levels of glutamyl-cysteine, and the aforementioned low rate of cytosolic GGT activity, it could be theorised that majority of flufenacet metabolism in terms of flux is taking place within the cytosol of wheat, and within the vacuole of both blackgrass and ryegrass.

Enzyme activity assays were performed using crude extracts from each plant species to look for GST conjugating abilities towards CDNB and flufenacet. There was a notable decrease in CDNB conjugating ability of wheat when compared to both blackgrass and ryegrass which showed similar levels. Activity towards flufenacet however proved much different, with overall conjugating ability much lower towards flufenacet than CDNB in all instances. It was also observed that despite having similar activity towards CDNB, the ryegrass and blackgrass extracts had very different activity towards flufenacet. Ryegrass showed half the activity compared to blackgrass, with wheat showing less than a quarter. The low level of glutathione conjugation in wheat was highlighted when looking at the composition of extracted metabolites with significantly less glutathione-flufenacet in wheat than both blackgrass and ryegrass. The comparatively low levels of reduced glutathione and enzymatic activity observed within ryegrass compared to blackgrass would suggest a limited capacity to metabolise flufenacet. Where the levels of the glutathione conjugate and further downstream metabolites continue to increase with blackgrass, albeit at a reduced rate after

6 hours, the levels of each had reached a plateau within ryegrass further supporting the notion a maximum metabolic rate had been reached.

Based on the comparatively low levels of both flufenacet and the glutathione-flufenacet metabolite within wheat, as well as the higher levels of flufenacet retained within the leaf wash, it could be concluded that there was overall less uptake in wheat than was seen in either weed species. Despite the much lower rate of metabolism to the glutathione conjugate seen within enzyme activity assays, the level of glutathione-flufenacet conjugate was still much lower than the differences in enzymatic rate would be expected to produce with the same level of flufenacet present. There was however rapid metabolism of this glutathione conjugate to the glutamyl-cysteine conjugate which may give rise to the low level of flufenacet detected. Looking at the level of parent as well as the decrease in overall flufenacet in the wash extract however would support the claim that there was overall less flufenacet uptake within wheat than the two weed species. Despite large differences in enzymatic activity towards flufenacet, levels of the glutathione conjugate remained similar between the two weed species, with the initial rate of glutathione-flufenacet formation being greater in ryegrass than blackgrass at early time points. Considering the much lower enzymatic rate of conversation, and the much lower levels of glutathione present within ryegrass, this supported the notion that a higher level of flufenacet must be present within ryegrass to achieve similar levels of metabolite. It was also found that overall metabolite levels continued to increase from 6 to 16 hours within blackgrass as flufenacet present in the plant was metabolised. This however was not the case with ryegrass within which conjugate levels remained level between 6 and 16 hours. This showed that a maximum enzymatic rate had been attained as this pattern remained consisted throughout multiple higher performing adjuvants.

5 Formulation profiling and the leaf structure and wax composition of wheat, black grass, and ryegrass

5.1 Introduction

There are several factors which play a major role in herbicide uptake. Two variables are the physiochemical properties of the spray droplet, as well as the chemical and physical makeup of the leaf upon which the droplet is being applied (Calore et al., 2015; Ringelmann et al., 2009). It has been shown that any variations in leaf surface properties, physical and/or chemical, can drastically change how the same droplet will interact with the leaf surface and therefore have a large bearing on uptake (Kurokawa et al., 2018). Likewise, altering the properties of the droplet will alter how it interacts with the same plant.

The plant cuticle consists of two hydrophobic layers, the first of which being a soluble, continuous extracellular membrane consisting of various lipids and overlaying the cell wall of the epidermal cells, referred to as the cutin. The second upper layer, regarded as plant waxes, is a complex mixture of long chain aliphatic compounds such as alkanes, fatty acids, fatty alcohols, aldehydes, esters, and small amounts of minor cyclic compounds such as sterols (Heredia, 2003). This waxy layer consists of intracuticular waxes embedded within the cutin polymer matrix, and the epicuticular wax on the leaf surface. The epicuticular waxy layer acts as the first barrier between the plant and environment, the surface morphology and chemical structure of which can greatly influence leaf surface wettability (Buschhaus & Jetter, 2011; Koch et al., 2006). Waxy structures can vary greatly between plants and were first classified by Barthlott, (1998), who found the physical structure often corresponded to a dominant aliphatic compound. Wheat (*Triticum aestivum*) represents an important crop species as a human food source and as such the waxy composition has been studied extensively. Differences in both chemical composition and wax morphology have been found within several different *Triticum* variants with a platelet like structure being the most commonly encountered, stemming from a high level of primary alcohols (Koch et al., 2006). Conversely, the leaf properties of weed species are generally poorly characterised and offer a potential avenue for improved herbicide uptake by developing an understanding of chemical-leaf interactions.

The ability of herbicides to be absorbed into plants is dictated by their ability to penetrate the leaf cuticle, with such penetration mediated by a concentration gradient (Basi et al., 2013). As the waxy composition has such a profound effect on surface morphology and wettability, this represents one of the key parameters in herbicide deposition and uptake behaviour (Kraemer et al., 2009). As a potential avenue of improving herbicide efficacy and reducing impact on non-target organisms, it is important to better understand the interactions between herbicide formulations and the leaf characteristics of target plants. Foliar uptake however is a complex system with a number of factors that need to be taken into consideration. These factors include leaf surface characteristics, both chemical and structural, as well as physiochemical properties of the active and the types and concentration of any formulating components. Due to the number of variables their relation to plant uptake is only partially understood despite the need for greater herbicide efficiency (Fernández et al., 2015; Hunsche et al., 2012; C. J. Wang et al., 2007). Within post emergence application of herbicides, herbicide effectiveness is reliant on cuticular penetration of the active, as well as movement through the plant through short distance translocation to mesophyll cells, and further distances through the vascular tissues of the plant to sites of new growth (Satchivi & Myung, 2014). Upon removal of the waxy cuticle using organic solvents, there has been herbicide uptake serval orders of magnitude greater, indicating the importance of the leaf wax in acting as the uptake limiting barrier.

This chapter looks to explore the influences both the formulation properties as well as the leaf morphology and chemical composition have upon the wettability of herbicide droplets and how this might relate to uptake. It was hypothesised that leaves with shorter chain length aliphatics would be less hydrophobic and therefore, the wettability, and by extension herbicide uptake rates, would be greater than in leaf wax consisting of larger chain length aliphatics.

5.1 Formulation physical properties

5.1.1 Droplet dry down analysis

During the drying of particle carrying droplets, a phenomenon known as the “coffee ring” effect is often observed upon droplet drying. The coffee ring effect is characterised by the deposition of particulate matter from the droplet along the outer perimeter upon droplet drying. This pattern arises from capillary flow as a result of differential levels of evaporation across the droplet. Liquid evaporates at the droplet edge at a greater rate than the bulk of the droplet and is replenished by liquid from the interior of the droplet, drawing more particulate matter to the outer edge of the drop. The resulting capillary flow towards the edge of the droplet can carry a large percentage of particulate matter to the droplet edge (Hu et al., 2006; Mampallil et al., 2018). With the use of surfactants, it has been found to be possible to both enhance the degree of coffee ring formation, cause more evenly distributed drying or in some instances cause flow inversion. There are a number of mechanisms by which surfactants have been proposed to effect particle distribution; Marangoni flow, interactions at the contact line, particle-particle interactions within the droplet, particle interactions with the liquid-gas and liquid-solid interfaces, and suppression of evaporation (Karapetsas et al., 2016).

In terms of herbicide uptake, there is debate over whether a strong coffee ring effect will result in greater or lesser uptake. On one hand, a strong coffee ring effect will cause a greater concentration of active at the outer edge of the droplet and therefore create a greater concentration gradient over which the active can diffuse into the plant. On the other hand, the droplet edge dries at a quicker rate than the interior of the droplet potentially leaving a large concentration of the active with poor mobility and therefore bioavailability (Kraemer et al., 2009).

To check the effect of surfactants on herbicide uptake and any possible positive or negative effect, a range of adjuvants were used to determine droplet dry down distribution. This was performed upon a glass surface to determine the influence of each adjuvant on particle uniformity within a drying droplet. Four droplets for each formulation were imaged and the ratio of particulate matter at the edge of the droplet to that distributed throughout the centre was determined and displayed as the beta value. The closer this value is to 1, the more evenly distributed the particles are within the dry droplet. All formulations showed a significantly

lower beta value than the flufenacet SC, highlighting the adjuvants ability to promote more evenly distributed droplet drying (Figure 43). This data was then plotted as the respective beta values (Figure 44). The Tween L series, along with Tween 24 and Tween 20 showed more evenly distributed particulate matter within the droplet compared to that of the base SC formulation ($p \leq 0.05$). Both the Tween 22 and Tween 23 formulations showed no significant increase in particle distribution compared to the SC formulation. However, they were also not significantly different when compared to the Tween L and remaining Tween formulations. As each of the adjuvants provide a similar level of particulate distribution it would be reasonable to assume that this would not be the cause of any variations in uptake between formulations. This however does not take into consideration any variations that may arise from different leaf surfaces.

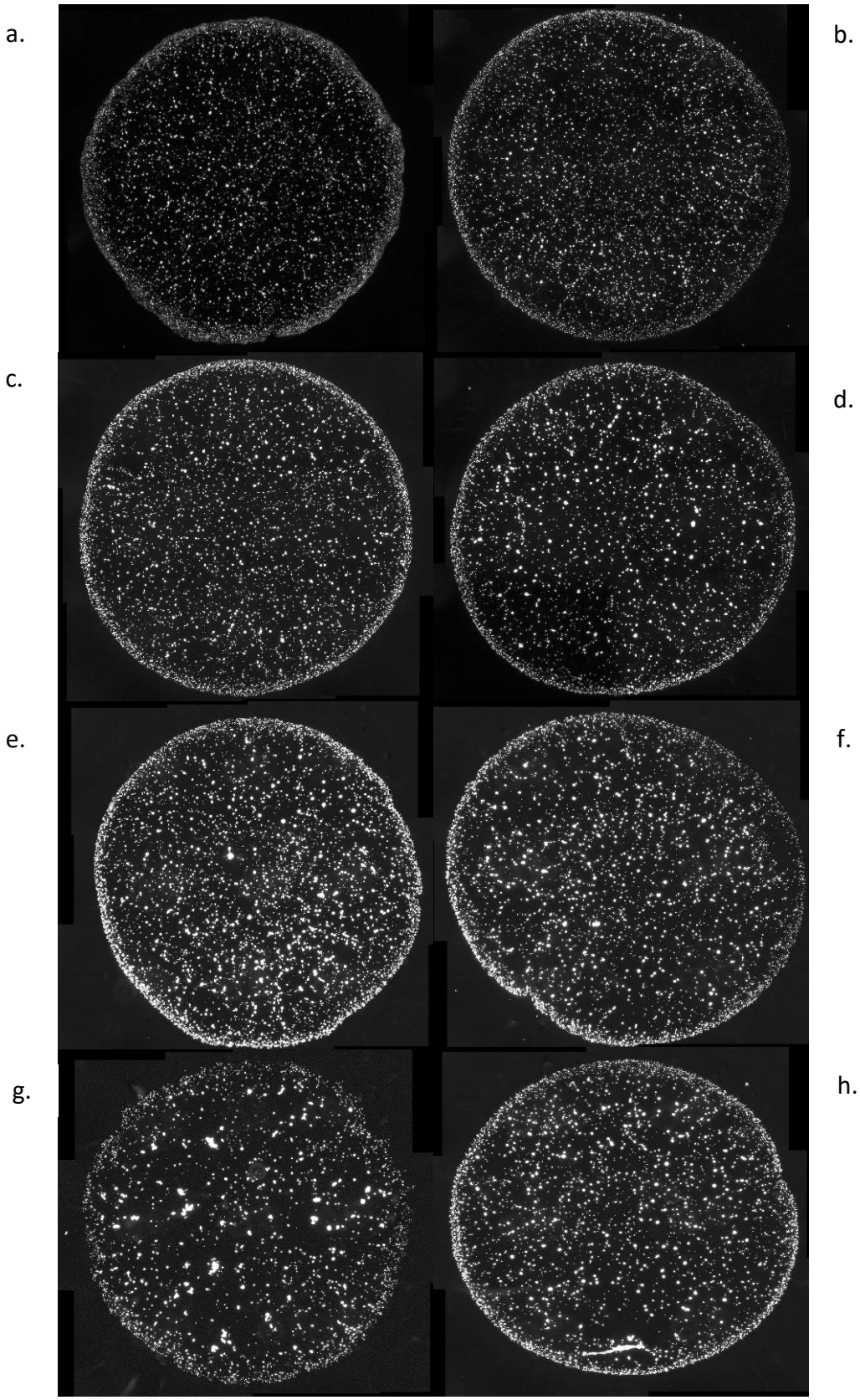

Figure 43.Fully dried droplets of flufenacet formulations on glass microscope slides on which droplet dry down analysis (DDA) was performed.The displayed images are representative of the 4 replicates on which analysis was performed. Droplet a. shows the base SC formulation, b. = Tween 20, c. = Tween 22, d. = Tween 23, e. = Tween 24, f. = Tween L-0515, g. = Tween L-1010, h. = Tween L-1505

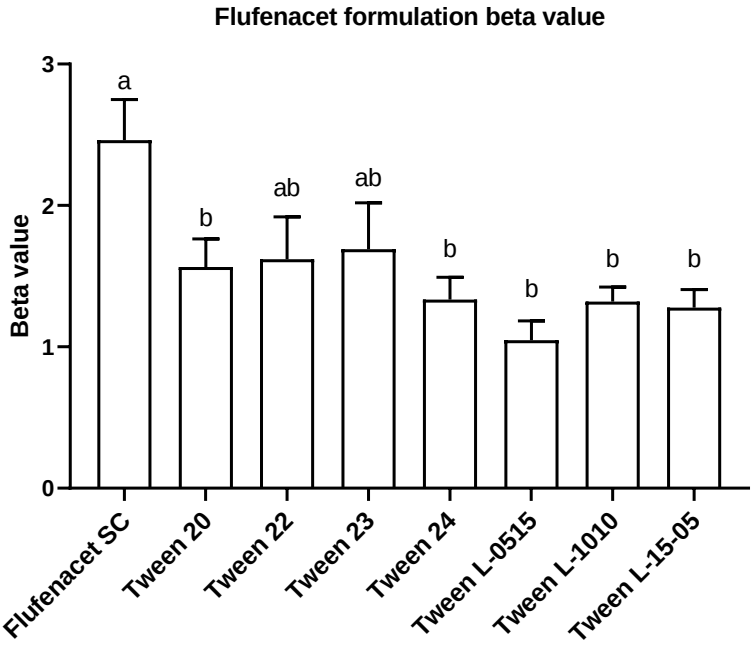

Figure 44. The beta value for each of the adjuvant containing formulations as well as the base SC formulation. The beta value is calculated based on the ratio of particles at the outer edge of the droplet compared to those within the centre, providing an indication of the uniformity of the droplets. Columns that do not share a common letter are statistically significantly different, with a P value of less than 0.05 as determined by multiple t-test.

5.1.2 Surface tension

Surface tension plays a significant role in the wetting and spreading abilities of a liquid and has a significant impact on the interaction between herbicide and leaf surface. Due to the relatively high surface tension of water (72.8 mN/m), it has low a capacity to wet and spread across hydrophobic surfaces such as that of a waxy leaf. It is therefore important in herbicide formulation to make use of chemicals that mitigate this poor wetting and spreading ability by reducing the surface tension (Castro et al., 2018; Damato et al., 2017).

Within the liquid, each solute molecule is surrounded by additional solute molecules, all of which exert a pulling force. If the molecule is completely immersed, this force is equal in all directions rendering a net energy of zero. At the liquids surface however, there are no liquid molecules above the surface molecule and this net force is broken, resulting in an inward pulling force exerted upon the surface molecules. The surface tension is caused by this imbalance of molecular force at the surface between the liquid droplet and air interface, and is defined as work required per unit of new surface area (Bruel et al., 2019).

Surface tension measurements were taken for the flufenacet SC formulation and those containing 10% w/w Tween and Tween L series adjuvants. This was done so by a Wilhelmy plate in which a thin, platinum plate was used to measure the interfacial tension between the air-liquid interface of each of the formulations. The plate was submerged in the solution and slowly retracted, with the force (F) at the point of detachment being measured and used to calculate the surface tension (γ) using the Wilhelmy equation:

$$\gamma = \frac{F}{l \cos \theta}$$

Where l is proportional to the wetted perimeter of the plate (2w + 2d) where w is the plate width and d the plate thickness, and θ is the contact angle between the liquid phase and the plate (H. Zhang, 2016). The contact angle is reduced to near zero by burning the plate using a bunsen burner in-between each measurement. This was confirmed by validating with water with which a surface tension close to 74 mN/m was attained with complete wetting. Wilhelmy's equation can therefore be simplified and used to calculate the surface tension of the various formulations as shown below in Figure 45.

$$\gamma = \frac{F}{l}$$

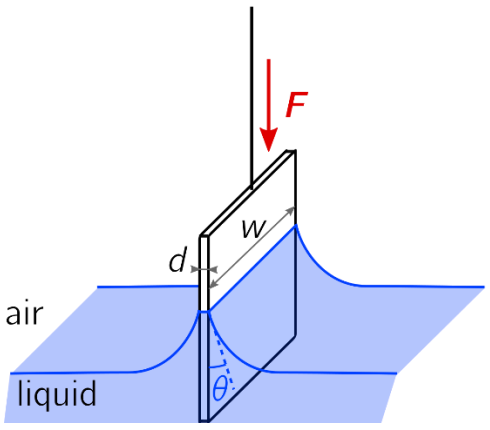

Figure 45. The Wilhelmy Plate is fully submerged into the solution of interest and the force required to break contact with the liquid per area of plate is determined. (Image: Dooley, 2018)

Overall, it was demonstrated that adjuvants can induce a significant impact on surface tension (Table 18). A reduction in surface tension would be expected to result in increased wetting and spreading of the formulation. In turn, this would be expected to translate to a lower contact angle and greater distribution of the formulation across the application surface. In all instances outside of the addition of Tween 20, there was a significant reduction in surface tension when compared to the base SC formulation (Table 19). Within the Tween series, there seemed to be a small incremental change in surface tension correlating to the level of ethoxylation. Tween 20 has the highest level of ethoxylation (20) and an average surface tension reading of 36.16 mN/m, yielding very little difference from the base SC formulation. Tween 22 however has the lowest ethoxylation level (8) and a surface tension of 33.87 mN/m, offering a significant reduction over the base formulation. The Tween L series did not appear to have an incremental change with changing chemical structure but was still found to give a significant reduction in contact angle over the base formulation.

Table 18. A table of the surface tension at the air-liquid interface with the adjuvant containing formulations, and the base SC formulation.

Adjuvant	Surface tension (mN/m)
Flufenacet SC	36.19 ± 0.35
Tween 20	36.16 ± 0.18
Tween 22	33.87 ± 0.22
Tween 23	34.53 ± 0.42
Tween 24	34.67 ± 0.18
Tween L-0515	35.35 ± 0.24
Tween L-1010	34.77 ± 0.34
Tween L-1505	35.07 ± 0.19

Table 19. Repeat measure ANOVA results when comparing the surface tension of various adjuvant containing formulations. Significance of variance was measured using a two-way ANVOA.

Surface tension	Flufenacet SC	Tween 20	Tween 22	Tween 23	Tween 24	Tween L-0515	Tween L-1010	Tween L-1505
Flufenacet SC		ns	**	**	*	*	**	*
Tween 20	ns		***	*	***	*	**	***
Tween 22	**	***		ns	**	***	*	***
Tween 23	**	*	ns		ns	ns	**	ns
Tween 24	*	***	**	ns		*	**	***
Tween L-0515	*	*	***	***	*		ns	ns
Tween L-1010	**	**	*	**	**	ns		ns
Tween L-1505	*	***	***	***	***	ns	ns	

*ns = not significant, * = P ≤ 0.05, ** = P ≤ 0.005, *** = P < 0.001*

5.1.3 Contact angle

The contact angle can be defined as the interfacial interaction at the contact line between all three phases, solid, liquid and vapour. The three phase point of interaction generates a contact angle based on the adhesive and cohesive forces and indicates the degree of wetting when a liquid and solid interact (Jiang et al., 2017). More specifically, for wetting to occur, liquid molecules close to the three phase contact point must break away from the bulk of the droplet, displace gas molecules adsorbed to the solid surface, and form bonds with the molecules of the solid surface. If the solid-liquid adhesive force is strong enough to overcome the liquid cohesive force as well as the solid-gas adhesive force, spontaneous wetting occurs (Lazghab et al., 2005). It is often considered that a contact angle of less than 90^{o} represents high wettability while those greater than 90^{o} are indicative of low wettability. The contact angle (θ) is depended on the surface tension of the liquid (liquid-gas interface, δ_{lg}), the interfacial tension between the solid and liquid (liquid-solid interface, δ_{sl}), and the surface free energy of the solid (solid-gas interface, δ_{sg}), and can be defined by Young's equation (Bruel et al., 2019; Jennissen, 2011; Jiang et al., 2017):

$$\delta_{sg} = \delta_{sl} + \delta_{lg} \times cos\theta$$

However, Young's equation relies on a number of assumptions, one of which being that the application surface is smooth and homogenous (Seo et al., 2015). This is not attainable within a leaf due to the wax structure, leaf trichome, stomata, and general uneven nature and distribution of plant leaf structures. Although not possible to define the surface free energy

of the leaves through Young's equation, contact angle can still provide a useful tool when observing the interaction between formulations and the leaf surface, and act as a means of measuring the wettability of the formulations upon differing plant species (Fernández & Khayet, 2015).

Contact angle measurements were taken for each of the adjuvant treated formulations as well as the base SC formulation. Due to the limitations of the syringe system used when performing contact angle readings, it was not possible to use the 0.4 µl droplet size which was used during spotting application of the formulations. Experimentally it was found that 7 µl was the lowest amount at which all droplets could fall from the syringe under the force of gravity alone and so was used throughout all contact angle readings. Droplets were applied to the leaf surface with one measurement being taken just after impact and settling of the droplet, and an additional measurement being taken after 1 minute to observe spreading over time.

Parafilm was used as an initial test surface due to its hydrophobic nature and to be sure contact angles were observable with a notable change detected across the 1-minute time frame. As parafilm provides a much more uniform surface than that of a leaf, it was also used in the first instance to try and observe the impact of surface tension upon the wettability of the formulations. As seen in Figure 46, it was observed in all instances that upon initial contact all adjuvant containing formulations resulted in a lower contact angle than the SC formulation. At the initial point of contact, there was no significant difference observed between most formulations, with Tween L-1505 being the only formulation to have a notably greater contact angle than Tween 20, Tween 22, and Tween L-1010 formulations. This would indicate that upon initial settling, all adjuvant treated formulations behave similarly on parafilm, irrespective of the variations in surface tension and chemical properties of the adjuvant. The contact angle was once again observed after 1 minute to see the progression of the droplet over time. All formulations showed a receding contact angle indicating spreading across the surface. In all instances, aside from Tween L-1505, the contact angle after 1 minute remained significantly lower than that observed in the base SC formulation, although the rate of angle recession was much lower in several instances, particularly in Tween 20 (Table 20). The contact angle of the Tween L-1010 formulation receded to the

greatest extent, and after 1 minute had a statistically significant lower contact angle than all other formulations.

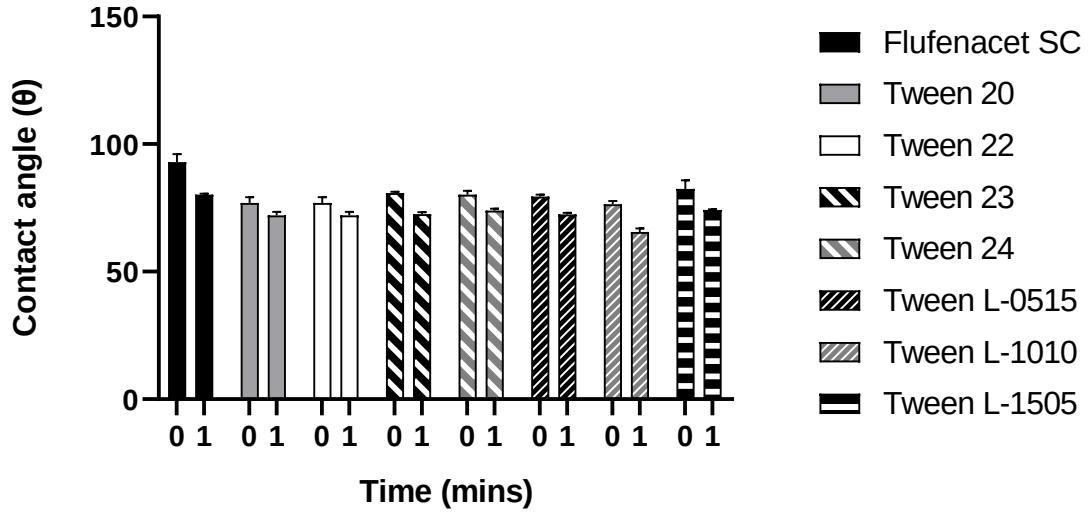

Figure 46. Contact angle of the various formulations applied to parafilm just after impact (0) and after 1 minute (1). This allowed for an indication of the level of droplet spreading over time, based on the contact angle recession after 1 minute.

In addition to observations using parafilm, leaves of wheat, blackgrass, and ryegrass were used as solid surfaces on which to observe contact angle (Figure 47, Figure 48, and Figure 49 respectively). This was to look for any links between contact angle and the uptake levels previously observed, as well as differences in formulation behaviour upon different species.

When formulations were applied to wheat leaves, it was observed that upon settling all formulations behaved similarly to that of the base SC formulation except for Tween L-1010 which showed a significantly lower contact angle. After 1 minute the contact angle was seen to recede at a similar rate in all formulations, including that of the L10-10 formulation. However, due to starting at a much lower contact angle upon application, the angle still remained significantly lower than that seen within the other formulations.

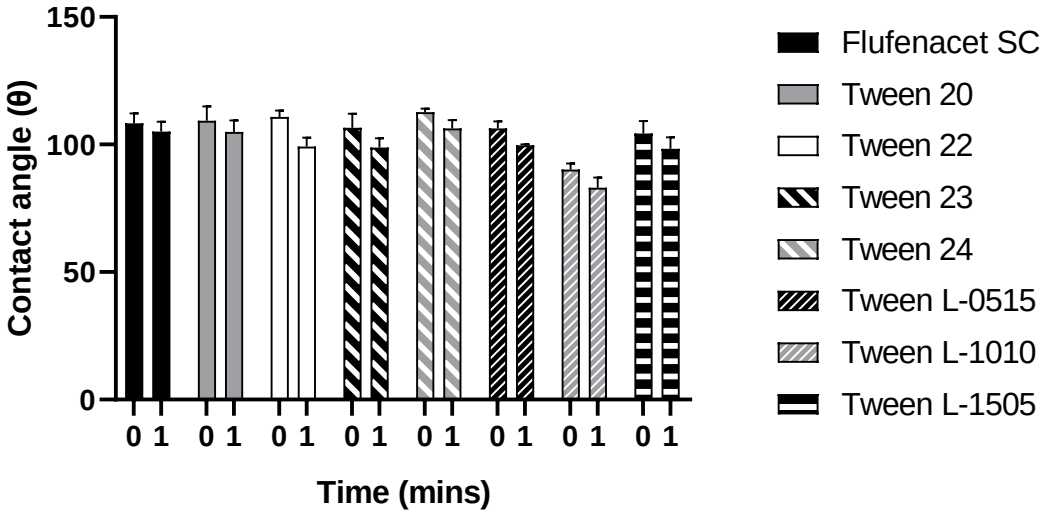

Figure 47. Contact angle observed from formulations applied to wheat upon initial droplet settling and after 1 minute.

Blackgrass showed a much greater range in contact angle when compared to parafilm, wheat, and ryegrass leaves. Tween 22 showed the lowest contact angle upon initial application and was significantly lower than all other formulations with the exception of Tween 23, the adjuvant with the second lowest level of ethoxylation (12 polyethylene glycol repeats). Within the Tween series, there appeared to be an incremental increase in contact angle with increasing levels of ethoxylation, with Tween 20 (20 units of polyethylene glycol) having the greatest angle of 108.7^{o} compared to the 76.4^{o} observed within the Tween 22 formulation (8 units of polyethylene glycol). The Tween L series demonstrated no significant decrease in contact angle when compared to that of the base SC formulation upon initial impact. After 1 minute, the observed contact angle for Tween 22, Tween 23 and Tween 24 had receded below 90^{o} indicating good wettability and spreading across the leaf surface, and a greater decrease in contact angle over this time frame than the base SC formulation. The Tween L series retained a high contact angle, on par with that of the base SC formulation, and was much greater than that seen with either Tween 22 or Tween 24. It was noted however that the rate of contact angle recession was much greater in Tween L-1010 than both Tween 20 and Tween 24, suggesting a longer exposure period would lead to a more reduced contact angle by comparison.

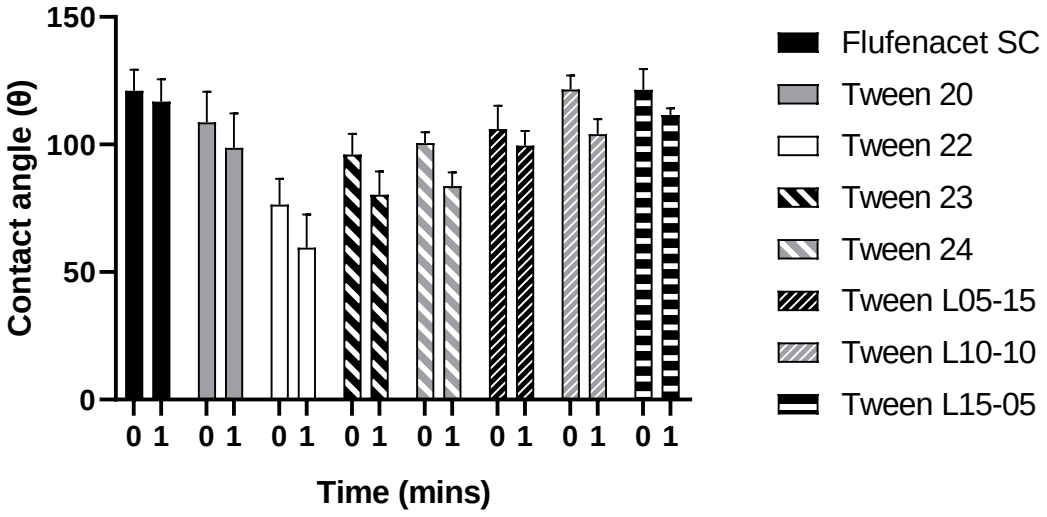

Figure 48. Contact angle observed upon formulation application to blackgrass leaves after initial droplet application and after 1 minute.

With droplet application to ryegrass leaves (Figure 49), it appeared that the addition of the Tween series had little impact on the initial contact angle, with no significant differences from that of the base SC formulation in all instances. Incorporation of the Tween L series resulted in a significantly lower contact angle compared to both the SC formulation and Tween series of adjuvants. After 1 minute it was observed that all adjuvant containing formulations had receded to an angle smaller than that of the base SC formulation, indicating a much greater rate of spreading. There was a further increase in spreading within the Tween L series, with all formulations having a significantly reduced contact angle when compared to the SC formulation and Tween series of adjuvants.

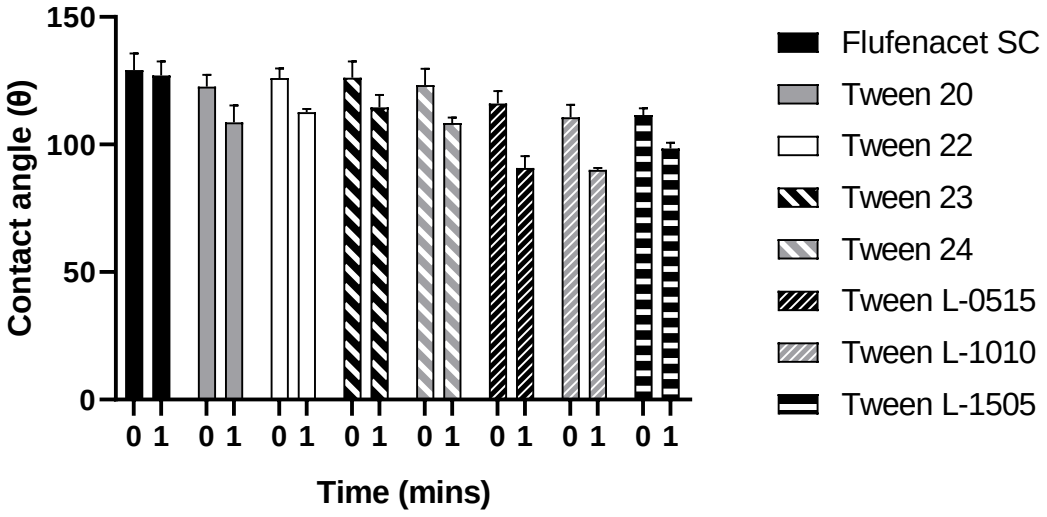

Figure 49. Contact angle upon formulation application to ryegrass after initial application and settling and after 1 minute.

The overview of the effects of the adjuvants upon the three types of leaf surface and parafilm were compared to see the influence of the leaf surface upon wetting (Figure 50). In most instances, both the flufenacet SC, as well the adjuvant containing formulations showed a significantly greater contact angle in each of the three plants tested compared to the parafilm, indicating a greater degree of hydrophobicity. The one exception to this was the contact angle of the Tween 22 formulation in blackgrass, which was comparable to its application upon parafilm. In addition to this, the difference between Tween 23's contact angle on parafilm and blackgrass was only marginally significant upon impact with no significant difference being observed after the contact angle had receded for 1 minute. On average, ryegrass had the greatest contact angle upon application of most formulations. The rate of contact angle recession observed in ryegrass was greater than that seen in wheat and comparable to that of blackgrass as summarised in Table 20.

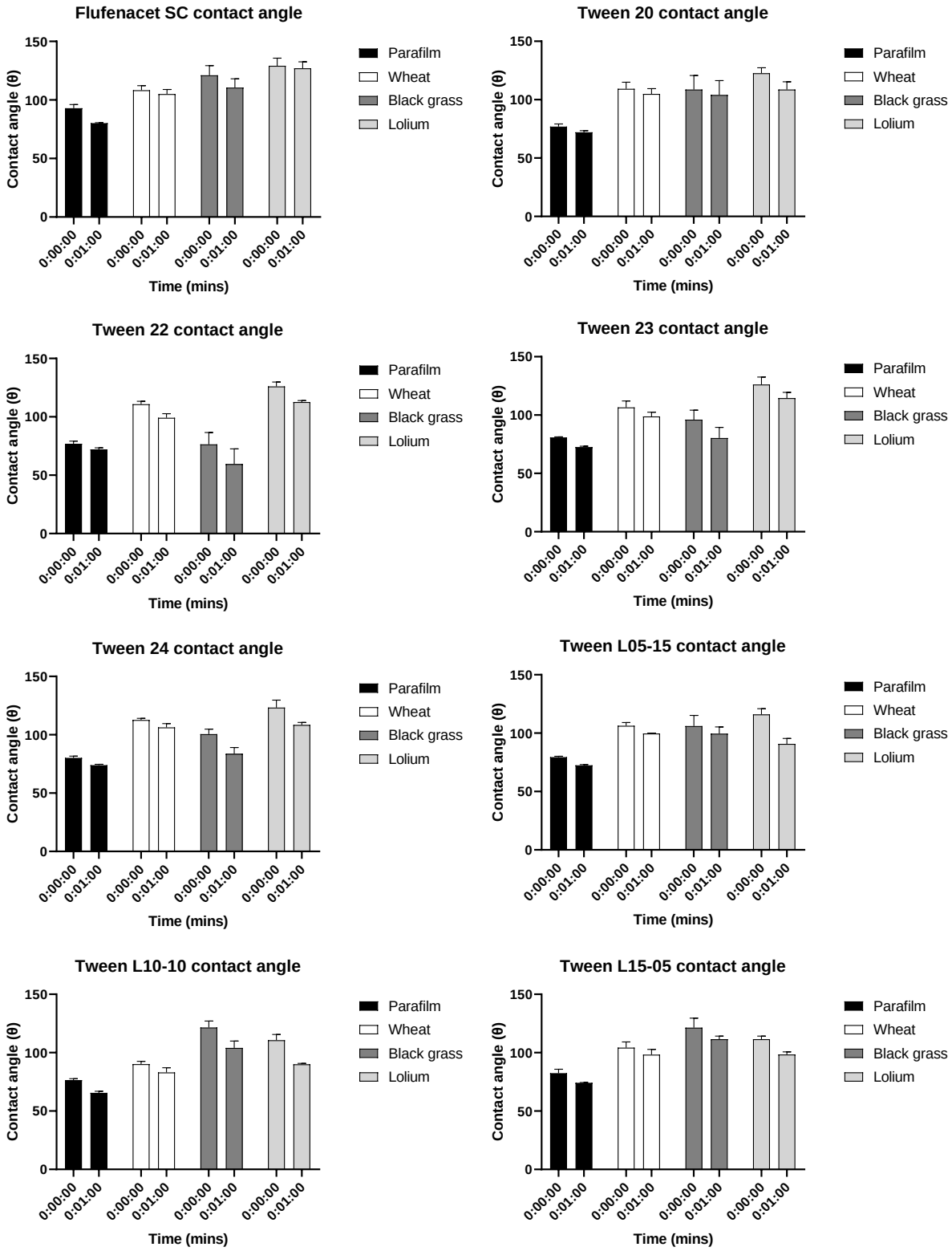

Figure 50. Each table shows the influence of the adjuvants on the contact angle of herbicide droplets applied to parafilm, wheat, blackgrass, and lolium (rye grass).

In general, trends in contact angle recession remained similar throughout each treatment regardless of the initial contact angle upon surface contact. The Tween series followed a stepwise increase in contact angle recession with decreasing polyethylene glycol chain length. The largest chain length, Tween 20, was shown to have the lowest degree of contact angle recession in all instances, while the shortest, Tween 22, showed the greatest decrease in contact angle over time. The Tween L series showed a greater degree of variation in how the droplet behaved on each of the application surfaces. Within the series, Tween L-0515 had a similar degree of recession upon parafilm, wheat, and blackgrass but proved to have a substantially greater effect on the contact angle of the ryegrass application. Tween L-1010 showed a significant decrease in contact angle upon both blackgrass and ryegrass, with a recession above 17.5 degrees across 1 minute in both instances. The effects of Tween L-1010 on wheat proved to be substantially less, with a decrease of only 7.12 degrees over 1 minute, similar to that seen with Tween 23 and Tween 24. Tween L-1505 proved to have the least effect upon contact angle of all the Tween L applications as well as the lowest change in contact angle.

Table 20. The change in contact angle across 1 minute for each of the formulations when applied to parafilm, wheat, blackgrass and ryegrass leaves is displayed. This allowed for comparison of droplet behaviour upon the various surfaces by observing the differences in contact angle recession rates, and thus the extent to which the droplet has spread across the surface. Data are presented as the mean with standard deviation indicating variance.

	Contact angle recession (Δθ/min)			
Adjuvant	**Parafilm**	**Wheat**	**Blackgrass**	**Ryegrass**
Flufenacet SC	12.77 ± 2.45	3.33 ± 1.80	4.63 ± 1.62	3.47 ± 1.15
Tween 20	4.9 ± 1.62	4.33 ± 1.63	10.53 ± 0.96	9.3 ± 1.56
Tween 22	8.05 ± 1.08	11.55 ± 2.01	16.88 ± 3.16	15.95 ± 2.61
Tween 23	8.23 ± 0.21	7.82 ± 2.95	15.85 ± 1.16	12.9 ± 1.17
Tween 24	6.27 ± 1.06	6.38 ± 2.71	13.07 ± 2.13	11.57 ± 2.15
Tween L-0515	7.07 ± 0.13	6.63 ± 1.98	6.52 ± 3.01	18.60 ± 3.16
Tween L-1010	10.9 ± 1.98	7.12 ± 2.53	17.55 ± 3.21	17.57 ± 2.96
Tween L-1505	8.25 ± 2.72	6.1 ± 0.29	9.95 ± 4.39	13.1 ± 1.31

As contact angle and surface tension are closely related, the change in contact angle was plotted in relation to the surface tension (Figure 51). A Pearson's correlation coefficient was calculated to determine the strength of the correlation between surface tension and recession of contact angle on each of the surfaces. Wheat showed the strongest degree of correlation with an r value of -0.931, demonstrating that a higher surface tension resulted in

less spreading of the applied droplet. The same trend was found within both blackgrass and ryegrass, although less strongly, with r values of -0.773 and -0.659 respectively, however still indicating significant correlation. There was no significant correlation between surface tension and contact angle found using parafilm as the application surface. Upon plotting a linear regression, there was a much greater influence of surface tension on the contact angle found within blackgrass and ryegrass than that found within wheat. Wheat was found to have a gradient of -2.869, compared to -4.652 in blackgrass and -4.041 in ryegrass. As there are several parallels between the leaf wax within ryegrass and blackgrass (section 5.3.3), this may explain the similar relationship between contact angle and surface tension observed within the two grass weeds.

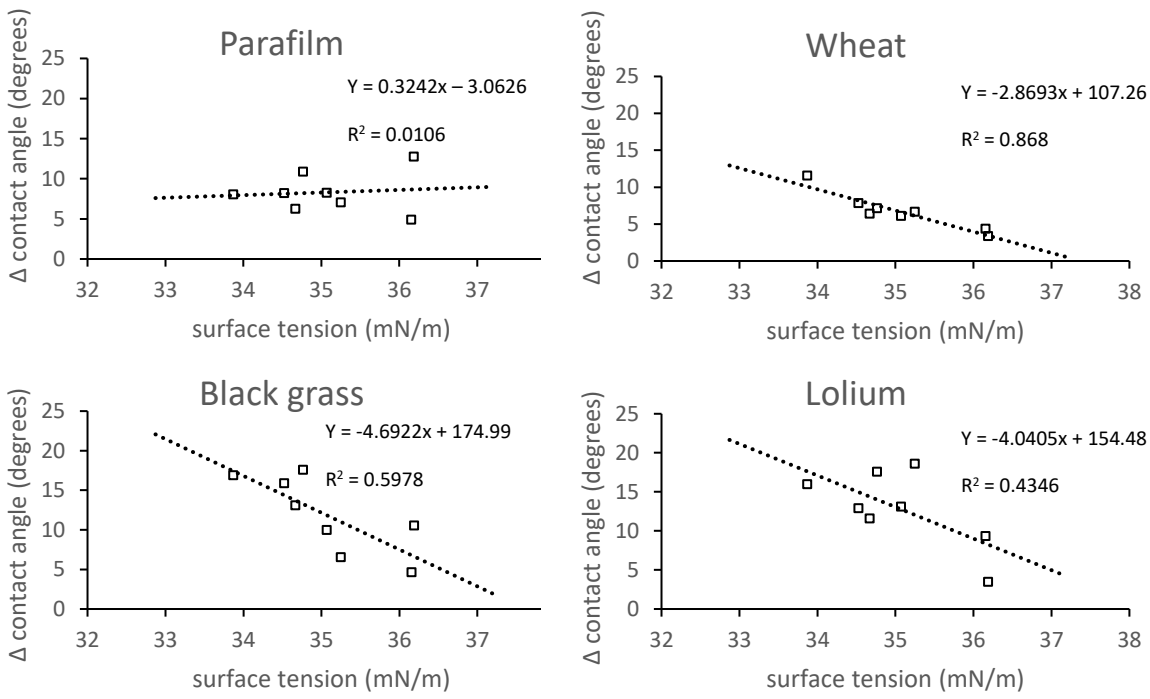

Figure 51. The change in contact angle over 1-minute relative to the surface tension of each formulation. The gradient of the line demonstrates the rate of increase in contact angle recession (and thereby greater spreadability) with decreasing surface tension of the formulation. It was shown that surface tension of the formulation is less impactful on the rate of spreading across wheat when compared to blackgrass and lolium, with no tangible impact noted on parafilm.

5.2 Leaf physical structure

In addition to the spray droplet properties, the physical and chemical characteristics of the leaf have a large impact upon the interaction between droplet and solid surface, as has been observed in section 5.22 (Papierowska et al., 2018). To investigate leaf surface structure, its physical characteristics were observed by scanning electron microscopy (SEM, Figure 52). With regards to imaging nanoscale objects, light microscopy has limited resolution, as objects can often be smaller than the wavelength of light. Microscopes which utilised electrons can therefore attain much better resolutions due to the use of a much shorter wavelength (Smith, 2008). This allows for high resolution observations of leaf wax crystal structures, as well as larger leaf structures such as stomata and trichomes to a definition that would otherwise be unattainable by light microscopy.

During sample preparation, tissue samples were dehydrated. Both sample coating and SEM imaging were performed under vacuum, which has a high propensity for causing distortion in water-containing samples. A number of techniques are available to dehydrate samples prior to analysis, all of which will cause some degree of alteration to the native structure of the plant which must be considered (Littlejohn et al., 2015; Pathan et al., 2010). In the first instance, critical point drying was used as a means of maintaining cellular structure across the leaf surface. This however resulted in a degree of surface wax being dissolved due to the use of solvent in the drying process. Simple air drying, despite possible sample shrinkage, was therefore used due to higher consistency and high-resolution imaging of the wax structure. As gold coating is required to produce an electrically conductive surface, this also has the potential to obscure very fine details depending on the thickness of the gold film (Golding et al., 2016). Due to the comparative size of the wax microstructure, this is unlikely to cause any great distortion but must still be taken into consideration.

Looking at each leaf at 200x magnification revealed some noticeable differences in surface composition (Figure 52). Blackgrass contained only small trichomes which were hard to visualise at 200x magnification and seemed ordered across ridges upon the leaf surface. Within both wheat and ryegrass, the trichomes were much larger and have a more sporadic distribution, as well as being more numerous within the set area of the image. At greater magnification, these variations in trichome were further highlighted. Within blackgrass, trichomes are comparatively much shorter than that of wheat and ryegrass with a length of

around 15 µm from tip to base, and a width around 10 µm at the widest point. Wheat possessed the longest trichomes with a length of 60 µm but these were thinner, with a width of less than 10 µm. Ryegrass trichome took on a much more “thorn” like appearance and had a length of around 40 µm and width of approximately 30 µm at the base.

Stomata of each species were also analysed, and differences in size were found within plant species (the stomata of ryegrass were around 20 µm, those in blackgrass 25 µm, and those in wheat 30 µm). The density of stomata was hard to accurately determine due to folding of the leaf often obscuring their position. When looking at the wax crystal structure, all three species were coated in a platelet wax structure with no differences observed within the crystalline structure. There were however potential differences in wax density across the leaf surfaces with wheat appearing to have a greater density of wax compared to both the blackgrass and ryegrass. A means of direct quantification of the leaf coverage would be needed to confirm this observation.

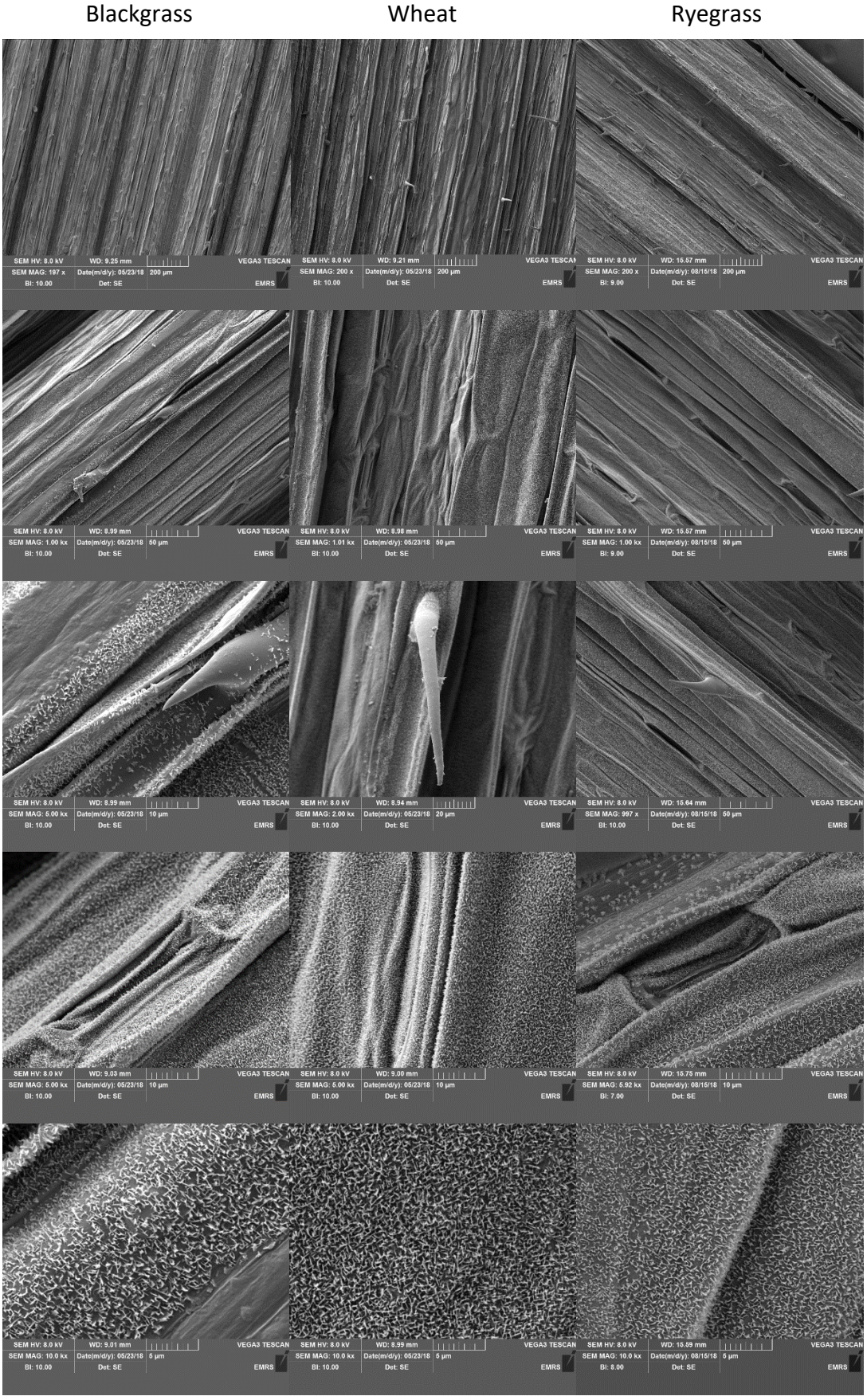

Figure 52.Images obtained by electron microscopy of the leaf surfaces of blackgrass, wheat, and ryegrass.

5.3 Leaf wax chemical composition

A semi crystalline layer of wax is present on the surface of all plant leaves and offers a protective barrier to external pressures, forming the first barrier for entry of herbicides. The waxy layer of plant leaves can vary greatly, not just in terms of physical structure but chemical composition within structurally similar wax crystals (Barthlott et al., 1998; Buschhaus & Jetter, 2011; Koch et al., 2006). Solvent based methods have been widely used for extraction of leaf waxes while minimising the removal of other contaminating plant matter. The role of the solvent is to selectively dissolve the wax components with the extent of solubility depending upon intermolecular interactions between solvent and the waxy components (Dunitz et al., 2009). Solvents of similar structure and properties to the intended solute often result in better dissolution. Chloroform was used for the extraction of wax from ryegrass, blackgrass, and wheat leaves, due to its reliable ability to dissolve wax hydroxyl components and the reproducibility of extractions (Loneman et al., 2017). Hydroxyl components, in the form of primarily alcohols have been shown to be the dominant waxy component within wheat and ryegrass (Ringelmann et al., 2009) and have also been highlighted as the major reason for the formation the platelet waxy crystals present in all tested plants (Koch et al., 2006).

Wax was extracted from 5 g of leaf tissue for all plants by submersion in 50 ml of chloroform for 30 seconds. This step was again repeated on the same tissue and the two 50 ml extracts combined, then the solvent evaporated. Upon evaporation, the mass of wax extracted was determined and the percentage crude yield was determined (Table 21):

$$\%\ crude\ yield = \left(\frac{mass\ of\ extract\ (g)}{biomass\ (g)}\right) \times 100$$

Table 21. Percentage crude yield attained by submersion of 5g of leaves from each species (wheat, blackgrass, ryegrass) in chloroform for 30 seconds on two occasions. Three extractions were performed per plant species.

	Wheat	**Blackgrass**	**Ryegrass**
% crude yield	2.07 ± 0.09	1.93 ± 0.09	2.1 ± 0.11

To both identify and quantity wax components in each extract, samples were analysed by gas chromatography-mass spectrometry (GC-MS) to identify components, and gas chromatography-flame ionisation detector (GC-FID) for quantification. GC chromatograms for each plant shared many similarities with regards to peak identity. However, the relative abundance of many components was significantly different despite the similar wax structure within each plant. Peaks were identified and quantified using representative standards, as well as a predictive library to look for similar MS spectra (NIST 98).

Due to the large variation in molecular response when using GC-MS, GC-FID was chosen as the means of quantifying wax compounds due to the uniformity in detector response to compounds of the same group. As the composition of each aliphatic group remained the same aside from a progressive increase in carbon chain length, the variation in response from one compound to the next will be minimal, provided they remain within the range free from high and low molecular weight discrimination (Schomburg et al., 1977; Tissot et al., 2012). Calibration curves were made up for the key wax components identified, alkanes, fatty alcohols, fatty acids, sterols, and aldehydes using representative standards for each chemical class (Table 22). Due to the poor resolution of the lower concentration fatty alcohols and fatty acids, these standards were derivatised using trimethylsilyl (TMS), allowing for their quantification. To check for high molecular weight discrimination resulting from the use of a split injector, a broad-spectrum alkane was run, as well as derivatised alcohol samples of C28 and C30. It was found that all identified alkanes remained within the mass range prior to the effects of high molecular weight discrimination and a reduced response factor. This was also found to be the case with alcohol, with both samples behaving the same upon derivatisation. Due to a lack of commercially available high chain length compounds, it was assumed that none of the aliphatics experienced molecular weight discrimination during testing.

Each standard curve consisted of six points with concentrations ranging from 1mg/ml down to $0.31x10^{-3}$ mg/ml using a 5 times dilution series. Standard curves were produced by calculating the ratio of the internal standard, n-tetracosane (C24), against the standard of interest. The area ratio and mass ratio were calculated as displayed in equations below,with the two values plotted against one another.. This was used to generate a line of best fit equating to the response factor of the standard against the internal standard.

$$Area\ ratio = \frac{area\ of\ standard\ peak}{area\ of\ internal\ standard\ peak}$$

$$Mass\ ratio = \frac{Mass\ of\ standard\ (\frac{mg}{ml})}{Mass\ of\ internal\ standard\ (\frac{mg}{ml})}$$

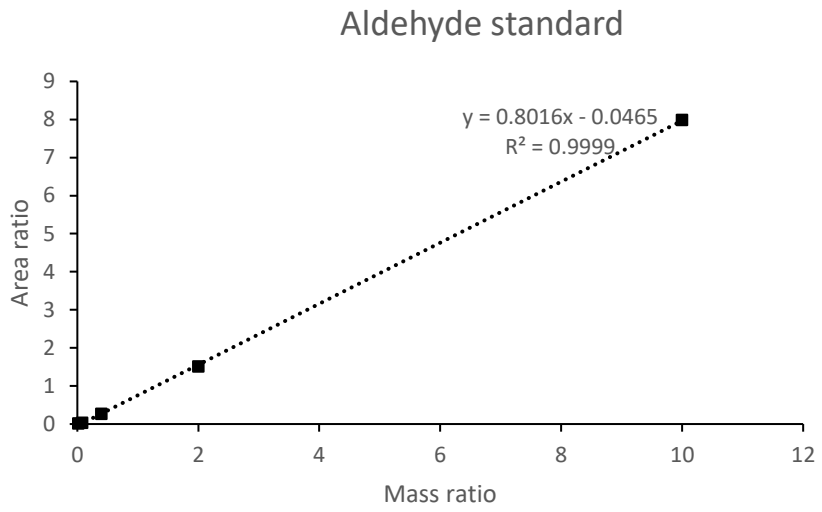

Figure 53. The mass to area ratio was used as the means of determining concentration of each of the component for a single chemical group (e.g. aldehyde). These ratios were based off comparisons between an internal standard and standard curve of the chemical group in question, providing a response factor. This figure shows the mass ratio vs area ratio of the aldehyde standard, dodecanal vs the internal standard, n-tetracosane, and the attained response factor (0.8016)

Table 22. Representative chemical standards for each wax group and the response factor when compared to the internal standard n-tetracosane (C24)

Wax group	Standard	Injection volume (µl)	Concentration range (mg/ml)	R2	Response factor
Alkane	*n*-Hentriacontane	1	0.2 - 0.78x10^{-3}	1.0000	1
Alcohol	1- Triacontanol	1	0.2 - 0.31x10^{-2}	0.9991	0.6655
Sitosterol	β-sitosterol	1	0.2 - 0.31x10^{-2}	0.9979	0.5747
Fatty acids	Octadecanoic acid	1	0.2 - 0.31x10^{-2}	0.9971	0.4879
Aldehyde	Dodecanal	1	0.2 - 0.31x10^{-2}	0.9999	0.8016

5.3.1 n-Alkanes

Identification of alkanes was relatively simple due to the unique fragmentation profile and comparison of the retention times to a broad-spectrum alkane standard. The diagnostic ion

for alkanes is of m/z 57 and was used to search the spectrum, with the fragmentation profile of potential alkanes being used to confirm identity. Within the low m/z region of alkane spectra, there are ions at intervals of 14 m/z indicating the loss of CH_2 as demonstrated in Figure 55. For each alkane, the largest ion had an m/z of C_nH_{2n} + 2, where n represents the length of the carbon chain. Additional smaller fragments were found of m/z C_nH_{2n} + 1 and C_nH_{2n}. Within long chain alkanes, the M^+ was always detectable but becomes less abundant the larger the molecule. The most intense peaks were generally found with a fragmentation length between C_3-C_5 forming as a result of α-cleavage. Table 23 shows the fragmentation ions of *n*-alkanes which were identified within each of the wax extracts, with each containing characteristic C_3-C_5 fragments of alkanes in the greatest abundance (m/z 57, m/z 71, m/z 85). Figure 54 a. shows the spectrum obtained within each wax sample with Figure 54 b. showing the predicted compound from within the database, further confirming identity as pentacosane.

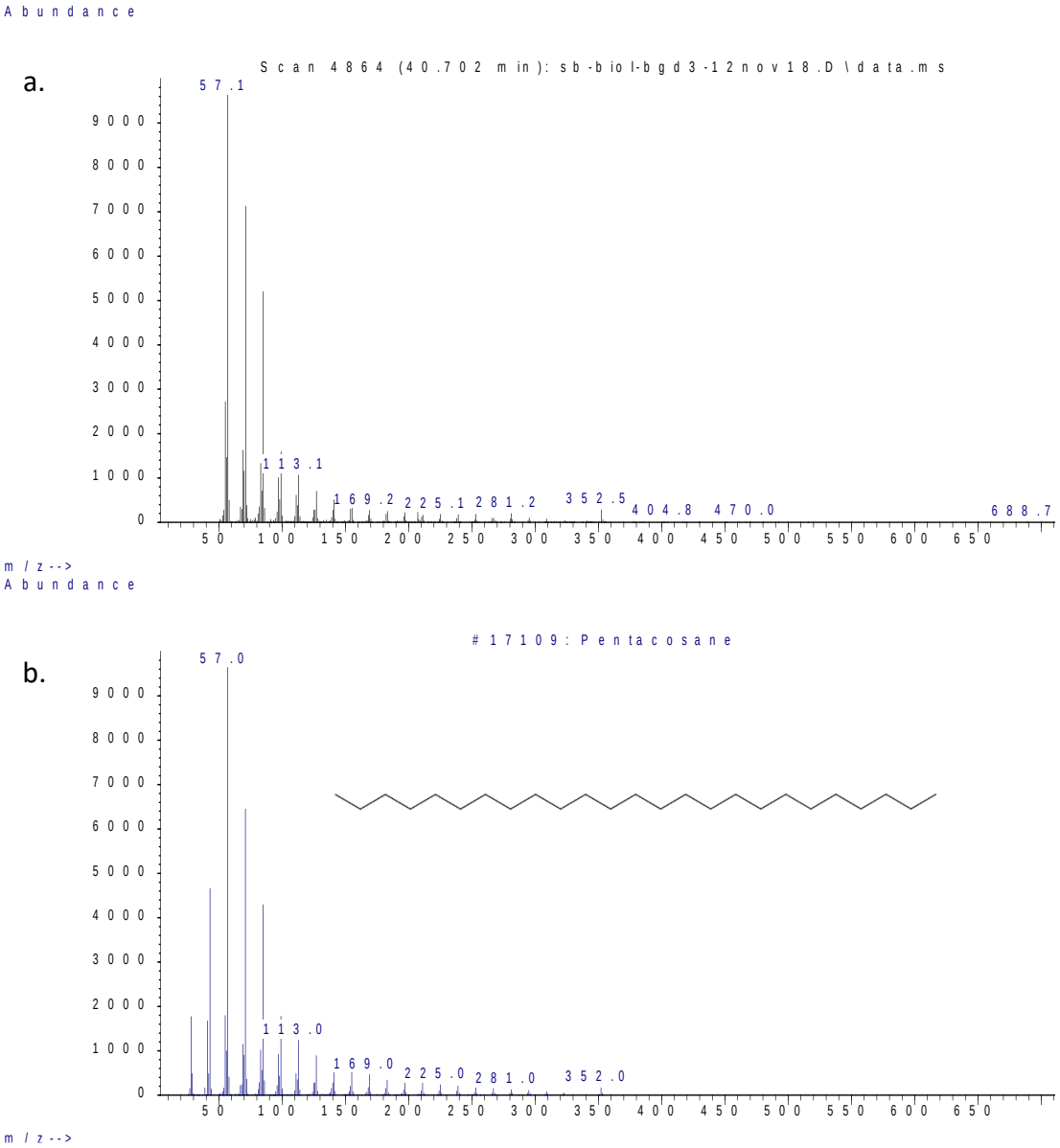

Figure 54. Example of the mass fragmentation profile obtained within blackgrass (a) alongside that predicted by the data base (b) and the fragmentation profile this would give for pentacosane (C25). The fragmentation profile and retention times were repeated across all other plant species.

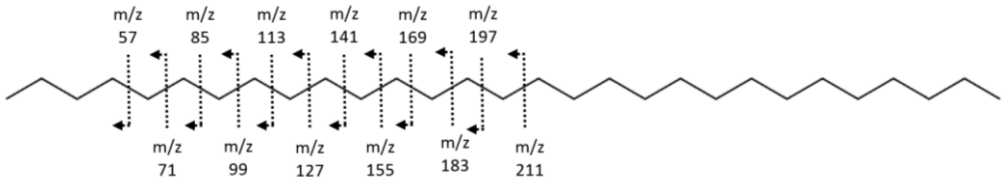

Figure 55. The ion fragmentation of n-nonacosane (C29). Alkane fragmentation occurs by α cleavage

Table 23. Shows the fragmentation ions for the alkanes identified within each plant extract

***n*-Alkanes**	**M^+**	**EI fragmentation**
n-henicosane (C21)	296	57, 71, 85, 99,113, 127, 296
n-tricosane (C23)	324	57, 71, 85, 99, 113, 127, 324
n-pentacosane (C25)	352	57, 71, 85, 99, 113, 127, 281, 352
n-heptacosane (C27)	380	57, 71, 85, 99, 113, 127, 380
n-nonacosane (C29)	408	57, 71, 85, 99, 113, 127, 408
n-hentriacontane (C31)	436	57, 71, 85, 99, 113, 127, 436

Initially, non-derivatisation of samples was found to result in coelution of 1-octocosanol (C28) and n-hentriacontane (C31). This issue was resolved however by TMS derivatisation of the alcohol causing a shift in retention time and allowing the two peaks to be resolved. Multiple hydrocarbons were then identified within each plant species in the form of long chain, straight alkanes (Figure 56). It has previously been shown that n-hentriacontane (C31) and n-nonacosane (C29) are often the most prominent n-alkanes within plant wax extracts, which exclusively contain odd chain length alkanes (Herbin et al., 1969). In general, wheat was found to have a higher abundance of longer chain length alkanes with the most prominent alkane found to be n-hentriacontane (C31) (highlighted in red), making up 5.5% of the wax extract. Seven additional odd chain length alkanes between C21-C35 were detected, with C33 being the second most prevalent within wheat (2.4%), and all other alkanes accounting for less than 2% of the total extract. Blackgrass and ryegrass presented n-nonacosane (C29) (highlighted in blue) as the most common alkane (3.8% and 5% respectively), with additional alkanes between C21-35 detected in blackgrass and C23-C35 in ryegrass. Despite the C29 alkane being the most abundant within ryegrass, C31 was also detected in high abundance, at a level comparable to the most abundant alkane in blackgrass (C29) and 30% less than the most abundant in wheat.

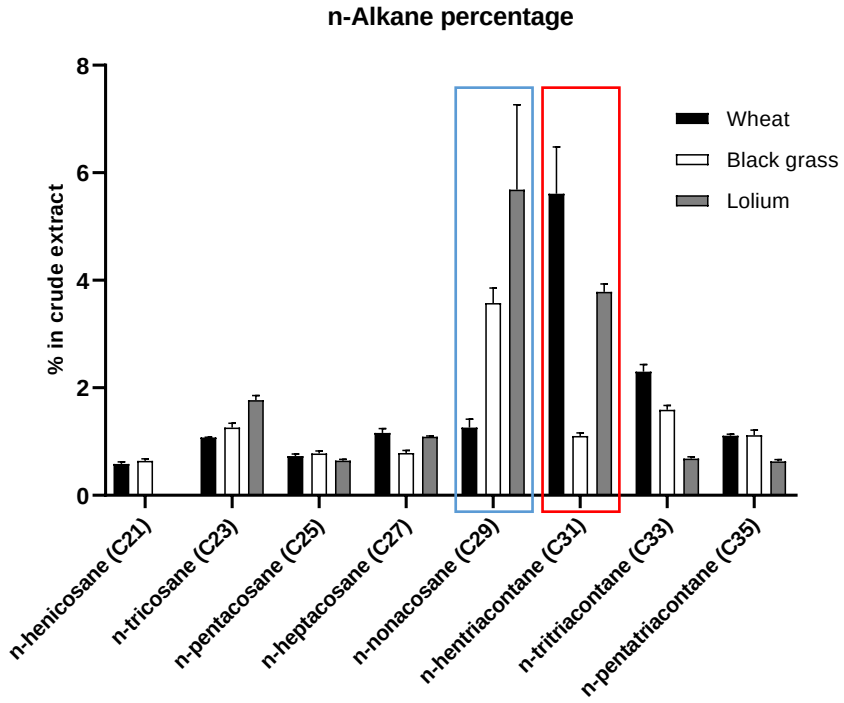

Figure 56. The percentage of total wax extract composed of each of the identified n-alkanes. The two highlighted alkanes (n-nonacosane in blue and n-hentriacontane in red) are of the greatest abundance and will therefore have the greatest influence on leaf surface properties

5.3.2 Primary alcohols

Primary alcohols have been found to be the most abundant chemicals within many waxes and result in the formation of the platelet structure seen in Figure 52. (Koch et al., 2006). This observation was consistent with the chemical composition of the wax extracts, with all plants having primary alcohols as the dominant extracted component.

The levels of these alcohols varied largely between the three plant species tested. Within wheat, the alcohol of greatest abundance was found to be 1-octocosanol (C28) which is consistent with previous observations made by Tulloch et al., (1973). It was also observed that wheat had a greater abundance of high chain length alcohols when compared to both blackgrass and ryegrass, with blackgrass showing a preference for comparatively shorter chain length alcohols, with 1-hexacosanol (C26) being the most abundant primary alcohol within samples.

Ryegrass was found to have a much lower abundance of primary alcohols when compared to both blackgrass and wheat, with no alcohol above a chain length of C30 found within the

extracts. Within ryegrass, C26 was again found to be the most abundant primary alcohol but was found at a lower quantity than in blackgrass. Although C28 and C26 were easily identifiable in the wheat and blackgrass/ryegrass GCMS spectra respectively, the lower abundance alcohols were more poorly resolved. TMS derivatisation of hydroxyl containing compounds was used to improve volatility and peak shape, allowing for the detection of lower

abundance alcohols. Alongside this, the primary alcohol standard used for quantification was also derivatised with TMS to allow for quantification of the now derivatised alcohols.

Identification of alcohols was performed by looking for the diagnostic m/z 75 ion formed as shown in Figure 58 b., with M^+-15 resulting from the loss of CH_3 (Figure 58 a.), both of which were the dominant fragmentation ions of TMS derivatised alcohol.

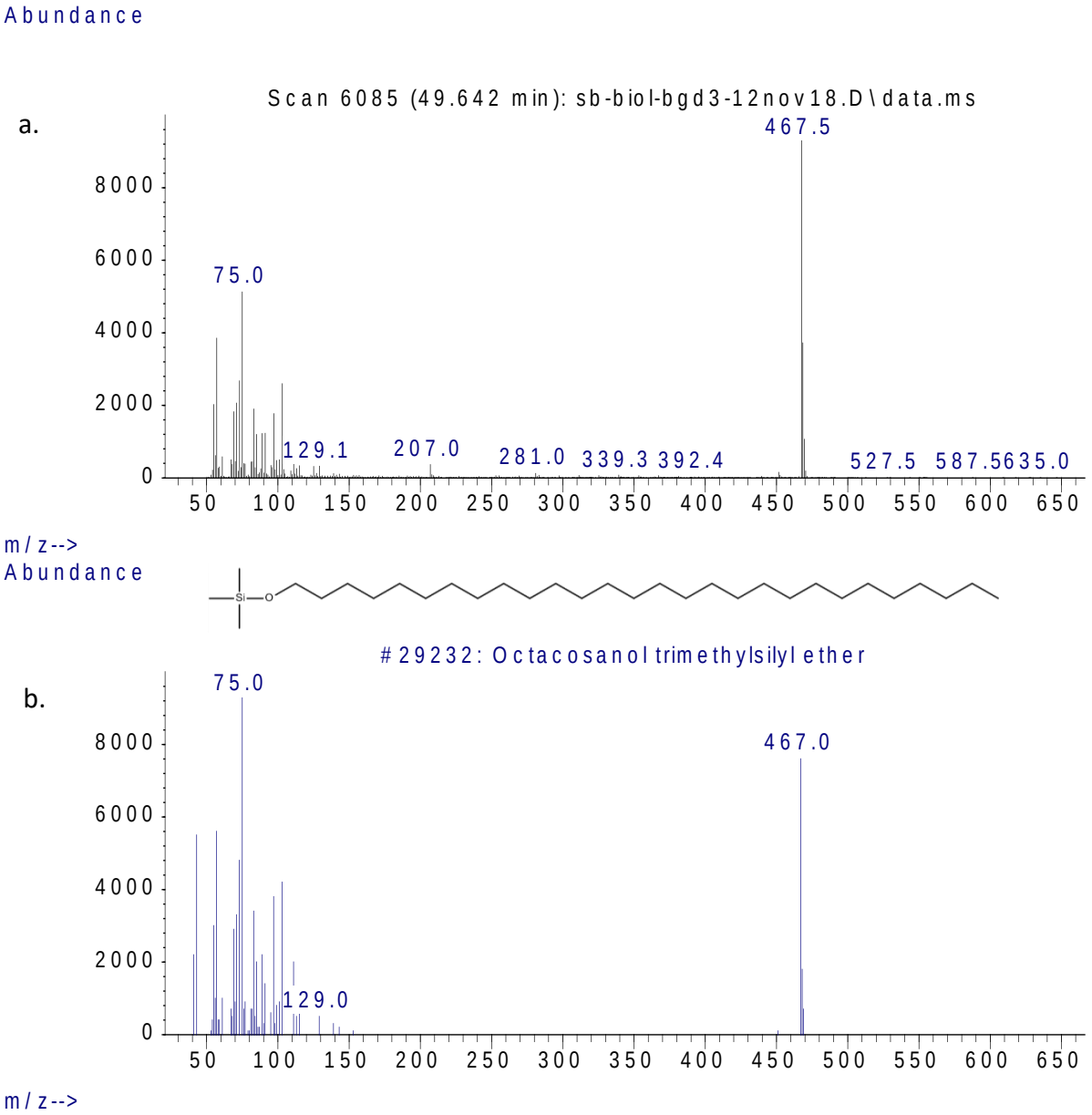

Figure 57.The fragmentation profile obtained from GC-MS of black grass samples for C28 TMS derivatised alcohol (a) and the closest matching MS spectrum found within the library (b).

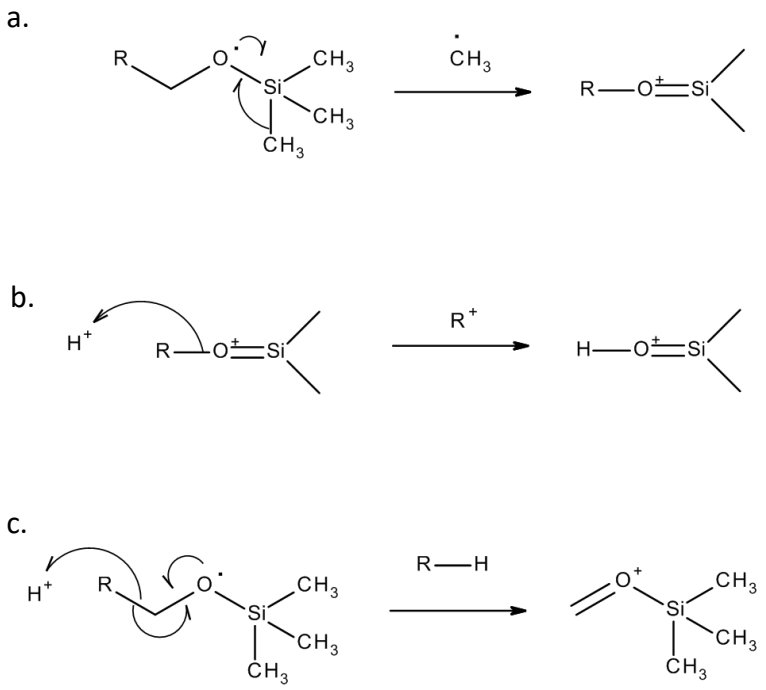

Figure 58. Formation of fragments M^+ – 15 (a), m/z 75 (b) and m/z 103 (c). Each of which are fragmentation ions of primary TMS derivatised alcohols.

Table 24. Fragmentation profile found within TMS derivatised alcohols.

TMS derived primary alcohol		M+	EI fragmentation
1-tetradecanol	(C14)	286	57, 75, 103, 271, 286
1-hexadecanol	(C16)	314	57, 75, 103, 117, 299, 314
1-octadecanol	(C18)	342	57, 75, 103, 311, 327, 342
1-eicosanol	(C20)	370	57, 75, 103, 340, 355, 370
1-docosanol	(C22)	398	57, 75, 103, 367, 383, 398
1-tetracosanol	(C24)	426	57, 75, 103, 281, 411, 426
1-hexacosanol	(C26)	454	57, 75, 103, 129, 423, 439, 454
1-octacosanol	(C28)	482	57, 75, 103, 125, 207,451, 467, 482
1-triacontanol	(C30)	510	57, 75, 103, 125, 479, 495, 510
1-Dotriacontanol	(C32)	538	57, 75, 103, 125, 523, 538
1-tetratriacontanol	(C34)	566	57, 75, 103, 125, 551

Within each species, the majority of the alcohol fraction was composed of one alcohol, as highlighted in Figure 59. In wheat, 1-octacosanol (C28) (highlighted in red) accounted for 37.57% of the total extract, while 1-hexaconsanol (C26) (highlighted in blue) accounted for 44.11% of the total alcohol extract in blackgrass and only accounting for 20.34% in ryegrass. A number of other alcohols were found ranging from C14 up to C34, with each representing less than 1.2% of the total extract. Once again wheat was found to have a greater percentage of higher molecular weight compounds, having a significantly greater amount of 1-

octaconsanol (C28), 1-tricantanol (C30), and 1-dotiacontanol (C32) compared to both blackgrass and ryegrass. In ryegrass extracts, all fatty alcohols outside of 1-hexaconsanol (C26) accounted for less than 0.2% of the total extract. This was also found to be the case within blackgrass with the addition of 1-tetracosanol (C24) and 1-octacosanol (C28) accounting for a higher percentage of the extract at 0.57% and 1.13% respectively. 1-tetracosanol (C24) was found to be in much higher abundance within the blackgrass extract than both wheat and ryegrass, with around five times the amount by comparison.

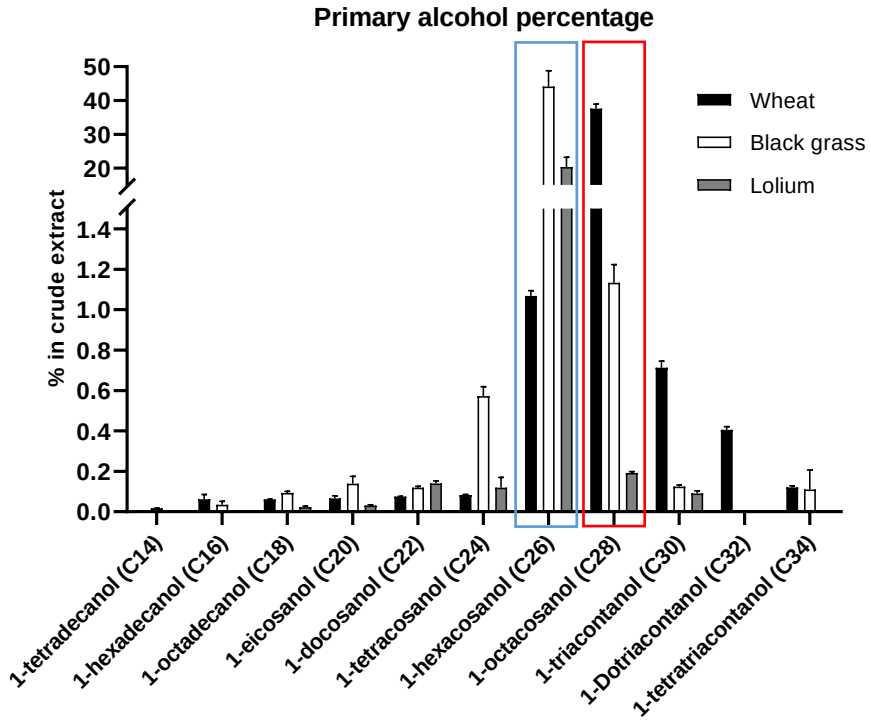

Figure 59. The composition of primary alcohols within the crude extract as a percentage of the total extract. The two highlighted alcohols (1-hexacosanol in blue and 1-octocosanol in red) comprise the greatest percentage of the leaf wax and as such have the greatest influence on the physiochemical properties.

5.3.3 Fatty acids

Fatty acids play a major role in waxy cuticle formation and as precursors to a number of other components (Samuels et al., 2008). Cuticular formation begins with the synthesis of C16 and C18 fatty acids within the plasmids of epidermal cells (Ohlrogge et al., 1995). The fatty acids then undergo elongation with the progressive addition of C_2 to form very long chain fatty acids, which act as the precursor for the synthesis of other wax components (Samuels et al., 2008). Reduction of the fatty acid can occur resulting in an aldehyde intermediate which can

be further reduced to form a primary alcohol (Chibnall et al., 1934; Kolattukudy, 1996; Samuels et al., 2008). As fatty acids are the precursor to many of the extracted wax components, a large number were identified within each species. Fatty acids ranging from C14 to C28 in chain length were identified (Table 25), with C26 being the most abundant in ryegrass and blackgrass and C28 the most abundant in wheat . This is not unsurprising as this corresponds to the chain lengths of the alcohols in the greatest abundance, for which the fatty acid is a precursor.

Identification of fatty acids was performed by looking for the diagnostic m/z 73 ion, as well as the M^+ - 15 which resulted from the loss of CH_3 and found to be the most abundant ions (Figure 60).

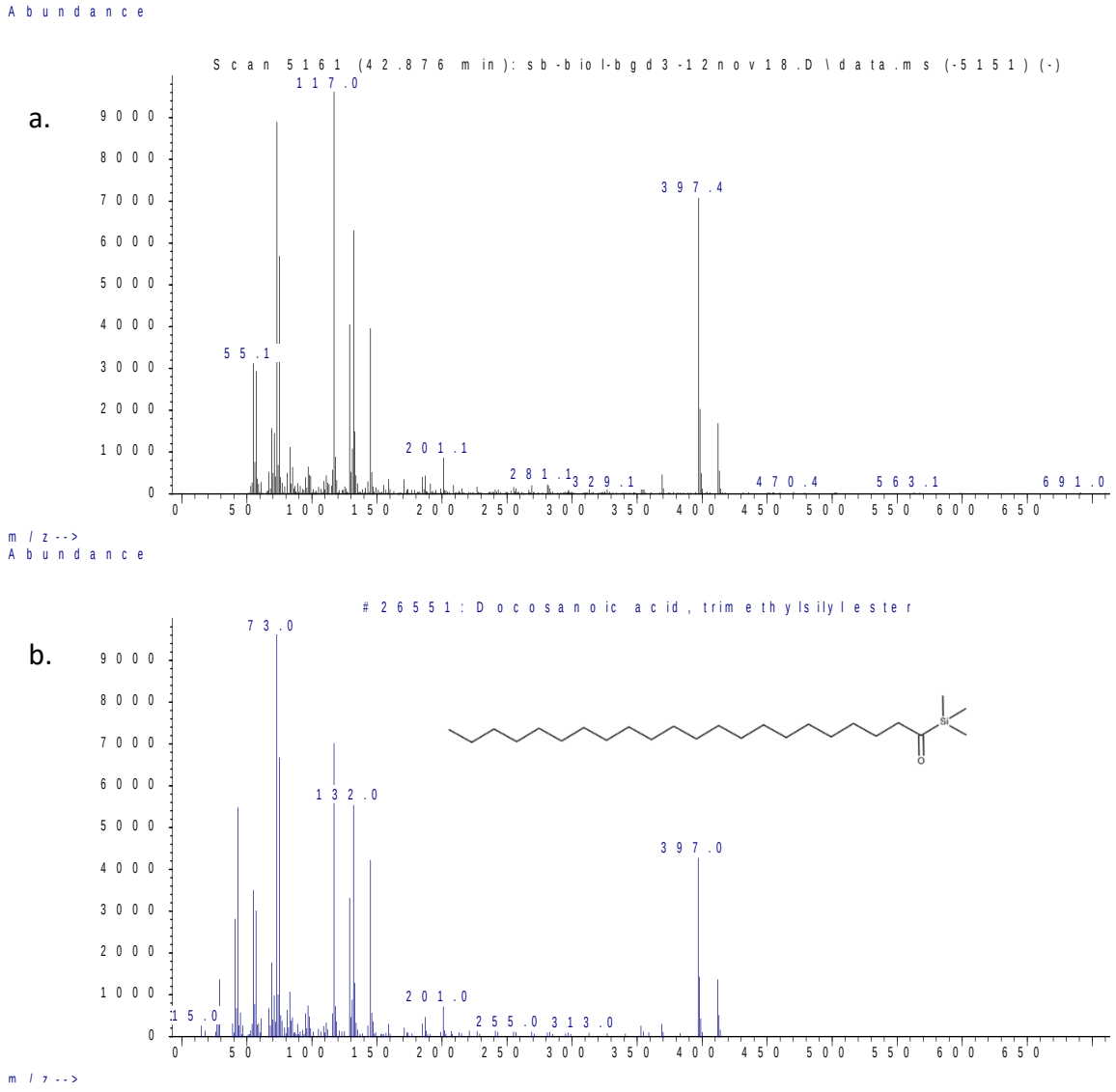

Figure 60. The fragmentation patter for docosanoic acid and the library equivalent spectrum from which the identification was determined.

Table 25. Identified fatty acids and their fragmentation profile after TMS derivatisation found within GC-MS spectra.

TMS derived fatty acids		M+	EI fragmentation
Tetradecanoic acid	(C14)	300	73, 97, 117, 132, 145, 285, 300
Hexadecanoic acid	(C16)	328	73, 95, 117, 132, 145, 269, 285, 313, 328
Octadecanoic acid	(C18)	356	73, 97, 117, 132, 145, 159, 201, 341, 356
Eicosanoic acid	(C20)	384	73, 97, 117, 132, 145, 165, 185, 201, 325, 341, 369
Docosanoic acid	(C22)	412	73, 97, 117, 132, 201, 353, 369, 397, 412
Tetracosanoic acid	(C24)	440	73, 97, 117, 132, 201, 425, 440
Hexacosanoic acid	(C26)	468	73, 97, 117, 132, 390, 437, 453, 468
Octacosanoic acid	(C28)	496	73, 97, 117, 281, 418, 434, 481, 496

Fatty acids, although making up a much smaller portion of the extracts than alcohol, followed a similar trend regarding chain lengths as demonstrated in Figure 61. Octacosanoic acid (C28) (highlighted in red) was found to be the most frequently occurring fatty acid in wheat making up 3.48% of the total crude extract. A very small portion was found within blackgrass however none could be detected within ryegrass. Both ryegrass and blackgrass contained hexacosanoic acid (C26) (highlighted in blue) as the dominant fatty acid, accounting for 2.17 and 2.10 % of the total extract respectively, with no significant difference determined between the two. Ryegrass was found to have the smallest range of detectable fatty acids with only trace amounts of hexadecanoic acid (C16) found and no detectable fatty acids of a chain length greater than C26. This was somewhat unexpected as both aldehydes and alcohols of C28 chain length were found within the ryegrass extract, for which a C28 fatty acid would be a precursor.

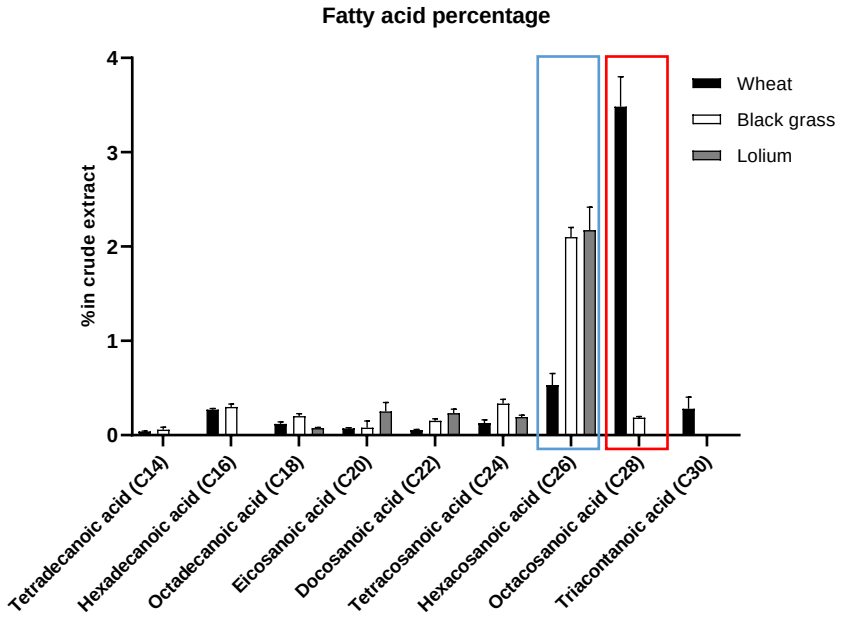

Figure 61. The percentage of each of the identified fatty acids within the total crude extract. The two highlighted fatty acids, hexacosanoic acid (blue) and octacosanoic acid (red) comprise the most abundant and therefore important fatty acids of the extracts.

5.3.4 Aldehydes

Aldehydes ranging from C24 to C32 were identified in varying quantities across all three plant species. Within wheat, the most abundant aldehyde was of chain length C28 whereas in both blackgrass and ryegrass this was found to be C26. As aldehydes are reduced to fatty alcohols, this would be expected, with C26 and C28 alcohols being the most abundant in ryegrass and blackgrass, and wheat respectively, as indicated by Samuels et al., 2008. In this case, due to limited aldehyde spectra within the database, predictions were made based on closely matching spectra. For example, the spectra in Figure 62 a. was not present within the database but was determined with the help of Figure 62 b (tetracosanal), being the closest matching in the database. Due to the presence of a characteristic aldehyde fragmentation, and the presence of an ion of *m/z* 362 resulting from the loss of water, Figure 62 a spectra was identified as hexacosanal.

Once the identification pattern for aldehydes became apparent, identification was relatively straight forward with a number of identifiable fragments resulting from both McLafferty rearrangement, as well as α-cleavage as shown in Figure 63. Major fragments occurred at M^+ -18 due to the loss of water, as well as at *m/z* 57, both of which occur as a result of McLaffery

rearrangement. Three less abundant peaks were also found at M^+ -44, M^+ -29 and M^+ -1 resulting from α-cleavage and allowing for easy confirmation of the identified aldehyde.

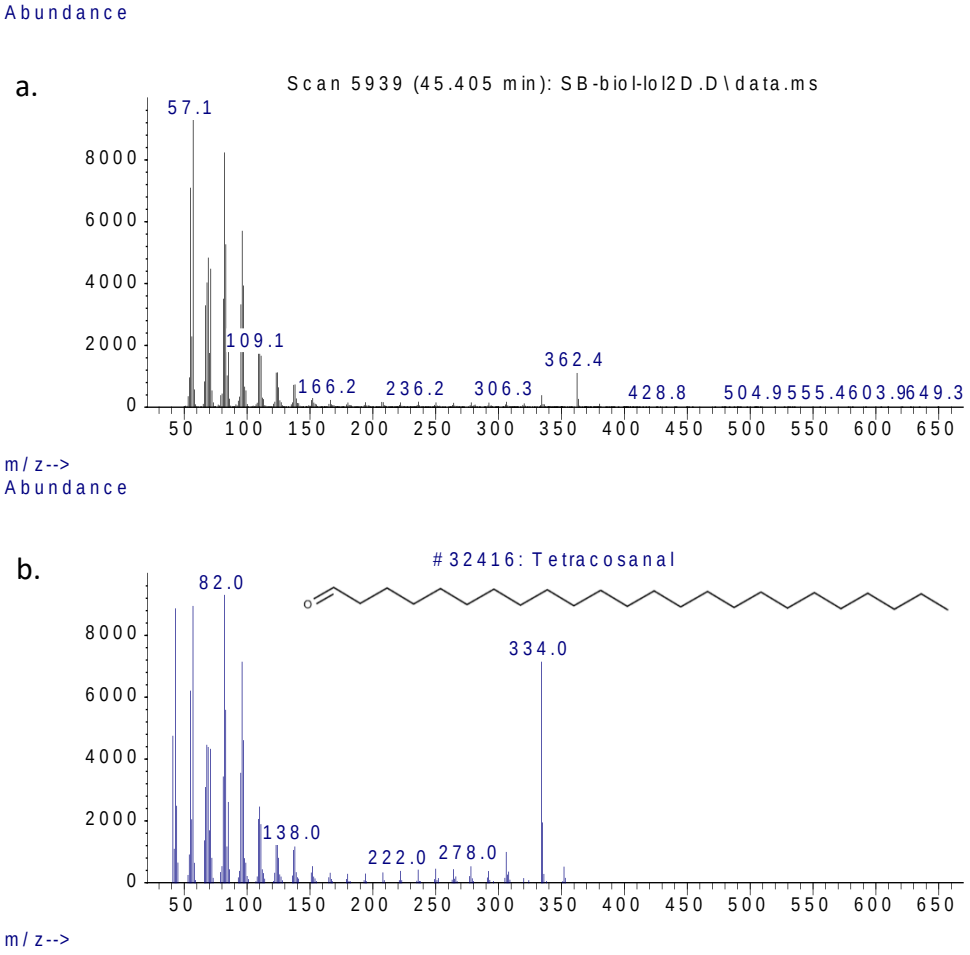

Figure 62.The fragmentation profile of Hexacosanal (a) and the library profile for Tetracosanal (Hexacosanal not present in library m/z 334 + C_2 equates to m/z 362)

Table 26. Fragmentation ions of all aldehydes detected within samples

Aldehyde		**M+**	**EI fragmentation**
Tetracosanal	(C24)	352	57, 71, 82, 96, 113, 334, 352
Hexacosanal	(C26)	380	57, 71, 82, 96, 123, 138, 334, 362, 380
Octacosanal	(C28)	408	57, 71, 82, 96, 110, 124, 138, 390, 408
Triacontanal	(C30)	436	57, 71, 82, 96, 156, 418, 436
Dotriacontanal	(C32)	464	57, 71, 82, 96, 446, 464

a.

b.

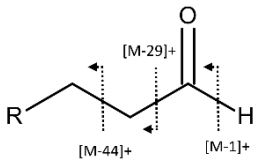

c.

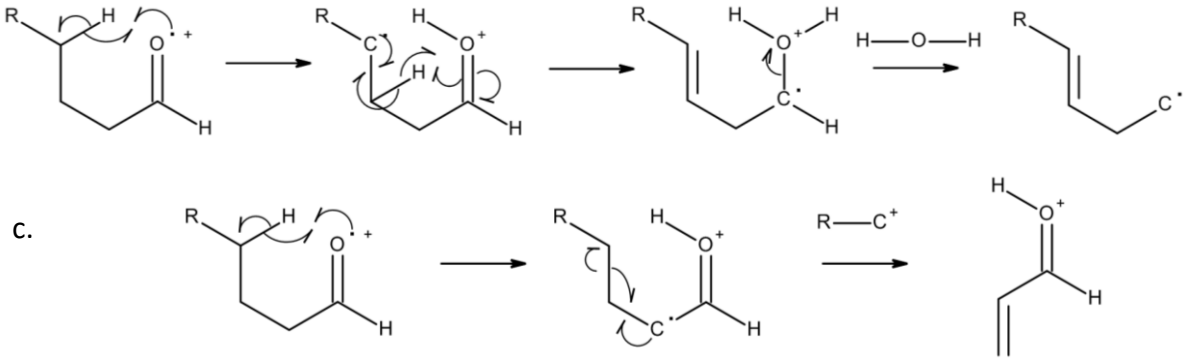

Figure 63.α- cleavage profile of aldehydes (a) as well as the formation of M^+ - 18 from loss of water (b) and formation of the base m/z 57 peak (c) within aldehydes resulting from McLafferty rearrangement.

A total of 5 even chain length aldehydes were identified across all extracts between C24 and C32 in length. As highlighted in Figure 64, hexacosanal (C26) (highlighted in blue) was found to be the most abundant aldehyde in blackgrass and ryegrass, with octacosanal (C28) (highlighted in red) being the most prevalent in wheat extracts. This was found to coincide with the synthesis pathway for alcohols, in which aldehydes are reduced to form long chain fatty alcohols. As hexacosanol (C26) and octacosanol (C28) are the dominant alcohols within the wax mixture, the same chain length aldehydes being the major aldehyde component was to be expected. Ryegrass was also found to consist of higher chain length aldehydes than both wheat and blackgrass, as well as containing an overall greater proportion of aldehyde within the extract.

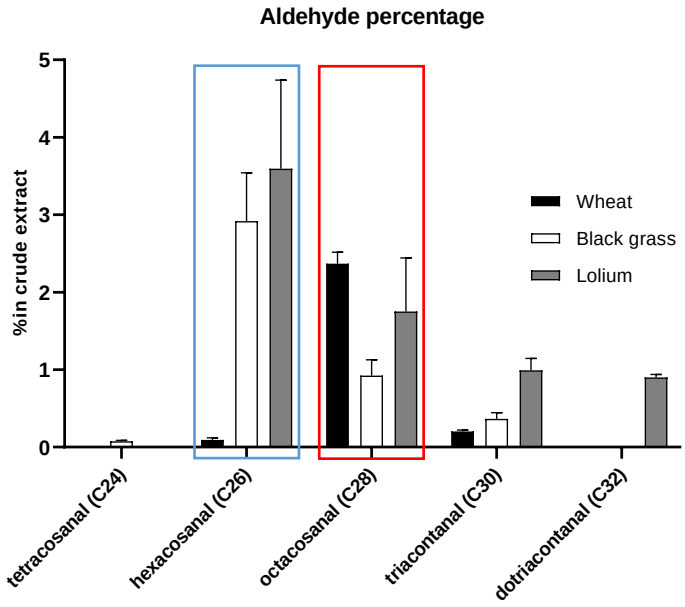

Figure 64.Aldehyde composition as a percentage of the total extract. Detectable aldehydes covered a shorter range of chain lengths compared to other aliphatics found within the leaf wax. The two most prominent wax components, Hexacosanal and octacosanal, are highlighted in blue and red, respectively.

5.3.5 Sterols

Sterols are a complex group of molecules all composed of four cyclic carbon rings and sharing structural similarities. Plant sterols are primarily found as free sterols within cell membranes where they regulate fluidity and permeability of the membrane. (Ferrer et al., 2017).

Sterols were found to be a very minor component of leaf wax with only wheat and blackgrass containing quantifiable amounts and ryegrass only small trace amounts. Sterols have previously been reported in wheat straw extracts, comprising in excess of 15% of the total waxes extracted (R. C. Sun et al., 2003). These studies reported cholesterol, stigmastanol and ergostanol, none of which were identified within this study. However, two sterols were found within the plant extracts to varying degrees, B-sitosterol and campersterol. B-sitosterol was found to be the most abundant sterol within wheat showing 4-fold higher levels than campersterol within ryegrass. It would not come as a surprise for β-sitosterol to be present in higher amounts in wheat due to its role as a precursor for the synthesis of a large number of other plant sterols in this cereal crop (Chappell, 1995). Campersterol is synthesised from the same precursors as β-sitosterol, 24-Methylenelophenol, with both being the major products of sterol biosynthesis. The ratio between each is determined by the activity of steryl

methyltransferases and ethyl transferases which catalyse the methyl (leading to campersterol formation) or ethylation (leading to β-sitosterol formation) of 24-Methylenelophenol. In blackgrass these levels were found to be near identical with no significant difference in the percentage of β-sitosterol or campersterol.

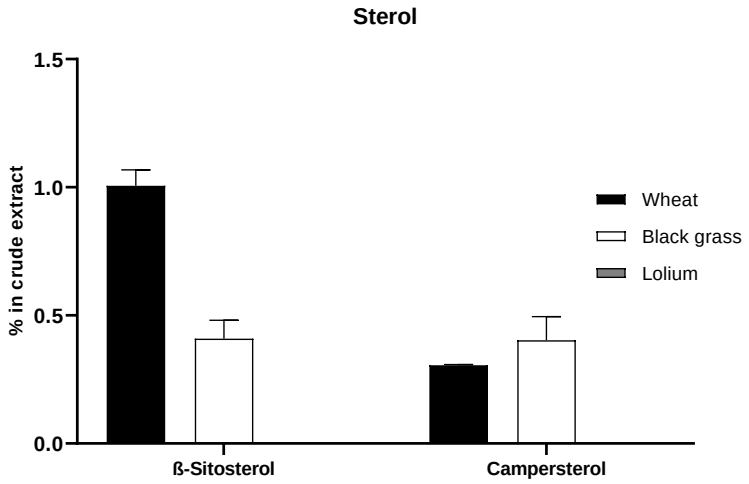

Figure 65. The percentage composition of ß-sitosterol and campersterol in wheat and blackgrass. None was detected within ryegrass extracts

5.3.6 Overall wax composition

Fatty alcohols were found to be the most abundant waxy component in all three species, making up over 40% of the total extract for wheat and blackgrass (Figure 66) and 21% in ryegrass. In each of the three plant species, alkanes accounted for more than 10% of the total extract, with blackgrass containing significantly less (10.9%) than both wheat (13.8%) and ryegrass (14.3%). Fatty acids were found at a much lower frequency than both alkanes and fatty alcohols, accounting for 5.1% of the total crude extract within wheat, 3.4% in blackgrass and 2.9% in lolium. Aldehydes were detectable in each species, comprising a significantly different percentage of the total extract in all three instances. Ryegrass was found to contain the greatest percentage, with aldehydes accounting for 7.24% of the total extract. Wheat was found to contain the lowest level of aldehydes, accounting for only 2.67% of the total extract while blackgrass contained 4.28%.

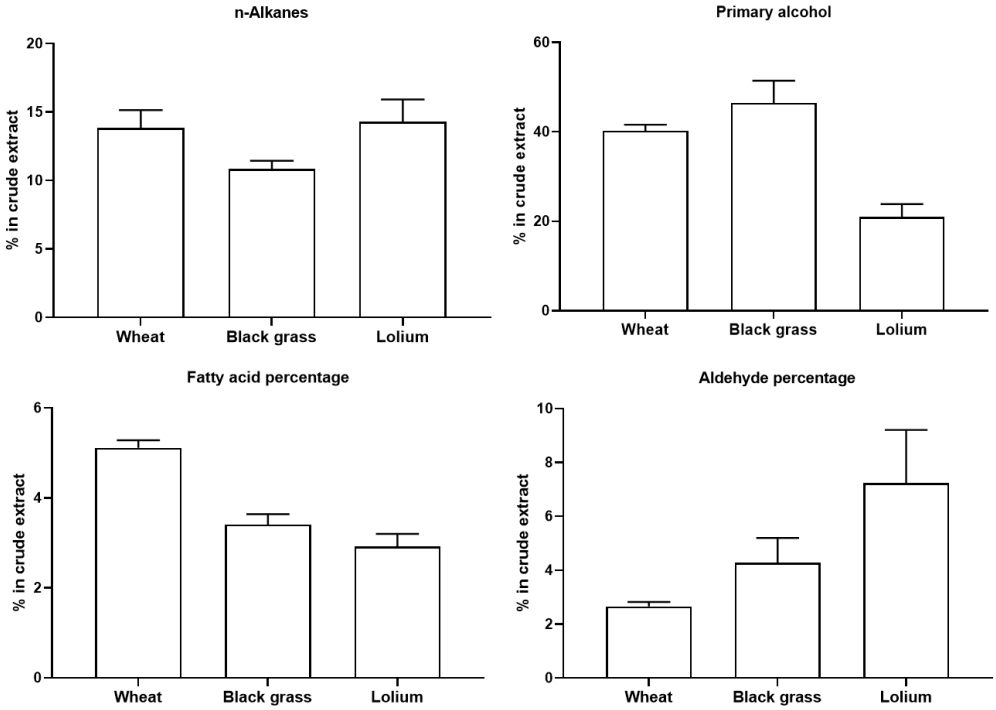

Figure 66. The total percentage composition of the four major wax components identified in wheat, blackgrass, and ryegrass

5.4 Discussion

In this chapter the effects of adjuvants on the physical properties of a base formulation were investigated, along with how these formulations interact with the plant surface in the form of contact angle. To help elucidate the reasons for the variations in contact angle, both the chemical and physical properties of the leaf surface were investigated through SEM and surface wax content analysis.

When looking at the physical properties of the droplet, it was found that outside of the base SC formulation, all formulations resulted in a similar level of particulate distribution upon drying of the drop. This would mean that there was no difference in coffee ring effect between formulations and thus all would maintain a similar concentration gradient across the droplet. The particulate distribution on the leaf surface however could not be investigated due to limitations with machinery and may be influenced by the leaf surface and the changes in contact angle that were observed. Assuming all particles still behave similarly across the leaf surfaces, variations in particulate distribution within the droplet would not be anticipated to be a driving force behind variations in herbicide uptake.

The surface tension of each formulation was investigated and was strongly linked to spreading and wetting, and therefore contact angle. There were small but significant variations in surface tension between formulations which seemed to have a notable impact on their spreadability across the various leaf surfaces. In all instances outside of Tween 20, the addition of an adjuvant reduced the surface tension of the base SC formulation. There were large variations within the behaviour of formulations upon initial contact with the leaf surface. However, similar rates of spreading were often observed. This change in contact angle over time correlated positively with the surface tension, with a greater surface tension resulting in a lesser ability of the herbicide to spread over time across each of the leaf surfaces. However, there were some outliers to this trend which may need further investigation, primarily within the Tween L series. The Tween L series is much less well defined than the Tween series and consists of a more complex change in chemical structure, with a decrease in polyethylene glycol chain length being mirrored by an increase in polypropylene oxide chain length. These deviations of the Tween L series from the correlation of surface tension and contact angle regression may be explained by the influence of Tween L on the

wax macrostructure. In order to confirm this, studies would need to be carried out investigating the adjuvants ability to dissolve and plasticise the leaf wax of each species.

Leaf wax was extracted from each species using chloroform, a solvent which has been reported on a number of occasions to provide good dissolution ability of leaf waxes (Bewick et al., 1993; Buschhaus et al., 2007). In all instances crude yields were similar, resulting in around 2 mg of extract per 5 g of leaf tissue. A qualitative analysis of the chemical composition of the wax of each species was carried out by GC-MS utilising the NIST 98 library to help with identification. Each of wheat, blackgrass, and ryegrass extracts were composed of primary alcohols, fatty acids, fatty aldehydes, and n-alkanes, with small amounts of sterols present. The main components in each class were successfully identified, where a notable percentage of each extract remained unidentified, possibly comprising of components in low concentrations, or fatty esters. The latter have been found in a number of studies but were not eluted off the column due to their large size and low volatility (Baker, 1982; Buschhaus & Jetter, 2011).

Due to the similarities within the chemical composition of each leaf extract, a quantitative analysis was required to investigate differences between each of the species. A comprehensive analysis of each extract was carried out using representative standards and TMS derivatisation of hydroxyl containing compounds to improve thermal stability, volatility, and peak shape. This allowed for detection of low abundance fatty alcohol and fatty acid components, as well as improved resolution of the high concentration alcohol groups. With each of n-alkanes, fatty alcohols, and fatty acids, wheat showed higher degrees of longer chain length compounds when compared to ryegrass and blackgrass. As longer chain length molecules result in greater degrees of hydrophobicity and long chain alkanes are inherently hydrophobic, this would explain the generally slower rate of contact angle recession witnessed in wheat when compared to both grasses. Ryegrass and blackgrass have much more similar chemical compositions with both nonacosane (C29), 1-hexacosanol (C26), hexacosinoic acid (C26), and hexacosanal (C26) as the highest occurring alkane, alcohol, fatty acid, and aldehyde respectively (highlighted in blue in each instance). It was noted however that ryegrass extracts contained the smallest range of detectable fatty acids, with none detectable of chain lengths greater than C26. This was unexpected as both C28 alcohols and

aldehydes were found within the lolium extract in relatively high abundance, for which a C28 fatty acids would be expected as the precursor.

It was found that despite the large differences in trichome concentration, size, and shape between ryegrass and wheat, the majority of adjuvants resulted in similar rates of contact angle recession, with only L05-15 and Tween 20 resulting in notably different rates. This would suggest that the influence of the chemical composition of leaf wax is having a greater degree of impact on the spreading of the herbicide droplets than the overall physical structure of the leaf. This can be especially seen when looking back to wheat, the wax of which is structurally the same as both blackgrass and ryegrass and yet generally results in significantly smaller rates of contact angle regression. Further confirmation of this might be achieved through the use of various mutant strains of the same species with notable variations in total wax content while maintaining the same physical surface structure.

6 General discussion and future work

6.1 Introduction

Herbicides were first discovered in the 1940's as a means of weed control in cropping areas. Due to their high level of effectiveness, major efforts were put into the discovery of new herbicides, with a new mode of action being discovered every 2 years between early 1950's to mid-1980's. This rate of discovery has slowed considerably, with no herbicide actions on new molecular targets commercialised in the last 30 years (Dayan, 2019). Several factors have resulted in this lapse in active research and discovery, including production cost for a single active ($286 million in 2016), the commercial success of genetically modified herbicide resistant crops, and increasing toxicological and environmental criteria which must be fulfilled for a product to be deemed safe (McDougall, 2010; Peters et al., 2018). Consequently, there has been an increasing emphasis placed upon herbicide formulation, both as a means of decreasing environmental impact, as well as extending the potential use of already discovered actives. Adjuvants are typically incorporated into herbicide formulations to improve properties such as wetting and spreading, stability, efficacy, and reduce environmental impact (Hazen, 2000; Tu & Randall, 2003). Adjuvants are particularly important within water-based formulations which are often less effective than their solvent-based counterparts. Despite the reduced efficacy of water-based formulations, the lower environmental impact and higher user safety have resulted in an increased interest in these formulations. Adjuvant selection is an important part of formulation and can greatly affect the effectiveness of herbicides. Factors such as the physiochemical properties of the active used, the intended weed target, and the crop to which the formulation will be applied must be considered for appropriate adjuvant-active pairing (Tu & Randall, 2003).

6.2 Overall conclusions

The work in this thesis aimed to establish a reliable means by which herbicide uptake could be studied without the use of radio-labelled chemicals. It was hypothesised that a biomarker such as gene induction, protein induction or metabolite accumulation, could be used as a proxy measure for herbicide uptake. Through this marker, the influence of adjuvants upon uptake could be measured in wheat, blackgrass and ryegrass as model crop and weed species respectively, with the level of metabolite present correlating to the level of bioavailable herbicide. It was found that glutathione conjugated flufenacet and downstream catabolites

served as a reliable indicator of the uptake of flufenacet, without the use of radiolabelled chemicals.

A variety of adjuvants were selected for incorporation into the flufenacet formulation in the form of the Tween and Twee L series. These adjuvants were selected due to the progressive stepwise change in chemical properties within each family of adjuvants. It was hypothesised that the progressive change in chemical nature would lead to a progressive change in uptake rate and shed light on the influence of the chemical properties of adjuvants on the uptake of an active within a formulation. This was found to be true within the Tween series of adjuvants in which a stepwise change in uptake was observed. Of the tween adjuvants, Tween 22 (the lowest HLB adjuvant of the Tween series) resulted in the highest level of uptake within blackgrass and ryegrass, with Tween 20 (the highest HLB of the Tween series) resulting in the lowest. This hypothesis however did not hold true for the Tween L series, with no clear link between the chemical properties and the uptake rates observed, suggesting influencing factors outside of just HLB.

Within the final experimental chapter of the thesis, the link between physiochemical properties of the leaf surface, chemical properties of the adjuvant containing formulations, and the uptake rates observed, was investigated. It was hypothesised that leaves with shorter chain length aliphatics would be less hydrophobic and therefore, the wettability, and by extension herbicide uptake rates, would be greater than in leaf wax consisting of larger chain length aliphatics. Experimental results supported this hypothesis, with wheat wax containing a greater concentration of higher chain length aliphatics when compared to both ryegrass and blackgrass. Uptake studies showed wheat to overall have lower uptake levels when compared to both blackgrass and lolium, confirming that influence of the leaf wax composition upon uptake.

The main conclusions established from this work were as follows: 1. Glutathione conjugated flufenacet and downstream catabolites serve as a reliable indicator of the uptake of the herbicide. 2. Decreasing surface tension of the herbicide formulation will increase spreading and improve uptake, the extent of which is dependent upon the physiochemical properties of the leaf surface. This provides a useful tool by which a herbicide formulation may be tailored based on the active used, the target weeds, and the crop on which the formulation is to be applied. The work in this thesis provides the groundwork through which herbicide

formulations may be designed to selectively enhance uptake within weed species while minimising uptake rates within the crop to be protected.

6.3 General discussion

6.3.1 Establishment of biomarkers

In establishing a reliable marker of herbicide uptake, a three tier "omics" approach was used looking at gene expression, protein expression, and metabolite levels. The formation of metabolites proved the most reliable of the tested approaches, with notable differences between different adjuvant treatments. It has been found in previous studies that gene induction occurs in waves, with many detoxifying genes being induced before the 5 hour time frame where initial herbicide damage occurs (Brazier-Hicks et al., 2019; Swindell, 2006). The work carried out within this thesis found was to be in line with previous findings, with most stress-induced genes reach a peak level of induction between 1 and 3 hours post treatment, before progressively declining back to base levels. *TaGSTU2* was found to be induced sooner than other selected markers, with a 13.5-fold increase 30 minutes after flufenacet application. Despite this early induction, *TaGSTU2* progressively decreased thereafter, despite continued herbicide uptake. By 3 hours, treatment with metolachlor resulted in a 1.9-fold increase in induction of *TaGSTU2* compared to the 8-fold determined with flufenacet. It has been previously shown in soybean (G*lycine max)* that *GmGSTU2* showed no changes in transcript levels upon treatment with atrazine, a herbicide which undergoes metabolism via glutathione conjugation (Skopelitou et al., 2017). On the other hand, phi class GSTs (GTSF) have been found to show catalytic activity towards chloroacetanilide, thiocarbamate, and chlorotriazine herbicides whereas Tau class GSTs (GSTU) show greater activity towards diphenyl ethers, aryloxyphenoxypropionates, chloracetamides and phenoxy propionic ester herbicides (Dixon et al., 2003; Thom et al., 2002). As neither atrazine (chlorotriazine) nor metolachlor (chloroacetanilide) showed a high level of induction of *GSTU2*, this would suggest a selective spectrum of inducibility. Although studies have not been performed looking at specific GSTs involved in the metabolism of flufenacet, structural similarities have been noted between flufenacet and fluorodifen, a diphenyl ether herbicide which undergoes GSTU2 mediated detoxification (Axarli et al., 2009). In conjunction with the high level of induction of GSTU2 upon flufenacet application in wheat, it would support the notion that flufenacet undergoes GSTU mediated glutathionylation. Despite the inducibility of GSTU2 upon treatment with

flufenacet, this did not correlate with metabolite formation and therefore uptake levels. As linking gene induction to the levels of herbicide presently in the plant would prove difficult, gene induction was not deemed suitable as a marker of uptake.

6.3.2 Adjuvant uptake studies

Due to previously mentioned results, flufenacet metabolism via glutathione conjugation and further downstream catabolism was chosen as the means through which to monitor herbicide uptake. Although flufenacet-glutathione and flufenacet-cysteine conjugates could be synthesised, no such standards were available for flufenacet-cysteinyl-glycine or flufenacet-γ-glutamyl-cysteine conjugates. Due to the similarities in the cysteine and glutathione conjugate standard curves attained by LCMS, it was assumed that the cysteinyl-glycine and glutamyl-cysteine conjugates would behave similarly and thus quantification was performed using the glutathione-conjugate standard curve.

Metolachlor-glutathione conjugation has previously been investigated in *Sorghum bicolor,* with crude protein extracts tested for their conjugating abilities (Gronwald et al., 1987). The authors found a linear dose response with increasing levels of the metolachlor-glutathione conjugate formation correlating with increasing concentrations of metolachlor, supporting the notion that metabolite concentration correlates to the amount of herbicide available for metabolism. However, it is well known that with many glutathione-conjugated xenobiotics, metabolism occurs both spontaneously and via enzymatic metabolism by GSTs (Campbell et al., 2008; Gronwald et al., 1987). Wheat has been shown to exhibit low constitutive GST activity towards dimethenamid despite showing much higher levels of activity towards the substrate CDNB, a general GST substrate (Habig et al., 1974; Riechers et al., 1997). In this thesis, it was confirmed that despite both wheat and blackgrass showing similar GST activity towards CDNB, activity towards flufenacet was found to be much higher in blackgrass compared to wheat. This would indicate differing GST involvement in flufenacet and CDNB conjugation, and therefore CDNB does not provide an accurate indication of flufenacet metabolising capability.

Previous studies have investigated the metabolism of flufenacet in susceptible and resistant populations of ryegrass. The susceptible population was found to metabolise the glutathione conjugate preferentially by cleavage of the glutamyl residue to form a cysteinyl-glycine conjugate (Dücker et al., 2019). This was consisted with the results shown in chapter 4, with

low levels of the alternative glutamyl-cysteine conjugate detected. Although the metabolism of flufenacet in blackgrass has yet to be documented in any great detail, it was found to be metabolised by similar means to herbicide susceptible ryegrass populations, preferentially catabolising the glutathione conjugate to the cysteinyl-glycine conjugate. Dücker (2019) also showed that flufenacet-resistant population of ryegrass were able to metabolise flufenacet via the formation of the glutamyl-cysteine conjugate to comparable levels to that determined with the cysteinyl-glycine conjugate. When NTSR populations of blackgrass were tested this was found not to be the case, with all tested populations still preferentially forming the cysteinyl-glycine conjugate. Upon treatment with flufenacet at field rate, it was found that all NTSR, TSR, and WTS blackgrass populations suffered a 100% mortality rate. This in combination with the work conducted by Dücker would suggest an alternative means through which flufenacet resistance has arisen, although was still demonstrated to result from enhanced metabolism. In contrast, wheat was found to metabolise flufenacet primarily via cleavage of the glycine residue to form a glutamyl-cysteine-flufenacet conjugate.

Herbicides have strict maximum rates at which they may be applied to be in line with environmental regulations, to limit spray drift, and cause minimal crop damage (Gitsopoulos et al., 2018). Several researchers have shown that the use of adjuvants can greatly increase herbicide uptake while maintaining the same application rate (Calore et al., 2015; O'Sullivan et al., 1980). As a result, the use of adjuvants is of great interest, though information concerning the impact of the use of differing chemistries remains limited (Gitsopoulos et al., 2018). Interaction between adjuvant, plant, and the environment present a complex system which must be optimised to improve herbicide efficiency. As a result there is no universal adjuvant that will improve performance of all herbicides against all weeds and under all environmental conditions (Pacanoski, 2014). The concentration at which the adjuvant is added must be considered. It has been found with multiple adjuvants, that the surface tension of a herbicide formulation will continue to decrease the higher the concentration of surfactant. In diluted formulations, this was found to be the case up until a concentration of 0.125% adjuvant, after which no further decrease in surface tension was observed. It has also been found that at concentrations above 0.5%, adjuvants have the potential to cause phytotoxicity to both crop and weed plants (Singh et al., 1984; Tu & Randall, 2003). For these reasons, adjuvants in the presented studies were incorporated at a rate of 10% w/w, resulting

in a concentration of 0.25% w/v adjuvant upon dilution in water. In general, it was found that reducing the surface tension of the herbicide formulation using adjuvants resulted in a decrease in contact angle and an increase in the rate of contact angle recession. Gitsopoulos (2018) showed with diquat that reducing the contact angle did not always proportionally result in an increase in herbicide efficiency. In the current study this was found to be the case with the Tween L series of adjuvants with flufenacet, which despite significant reductions in contact angle when applied to blackgrass and ryegrass, did not result in the same enhancement in uptake as seen with the Tween series of adjuvants. Although other studies have been conducted on Tween adjuvants, these have focused almost exclusively on the differing chemistries between Tween 20 (monolaurate), Tween 40 (monopalmitate), Tween 60 (monostearate), and Tween 80 (monooleate), with little work carried out investigating the effect of adjuvant chain length. That which has been conducted was consistent with the work within this thesis, showing a stepwise reduction in surface tension and contact angle with reducing polysorbate chain length (Tween 22 = 8, Tween 23 = 12, Tween 24 = 16, Tween 20 = 20) (Penfield et al., 2015). Penfield (2015) also demonstrated that uptake of imidacloprid through isolated leaf cuticles of apple (*Malus domestica*) was consistent between all adjuvants. This was also found to be the case within wheat, with no significant variations between herbicide uptake when using the different Tween adjuvants. When a glyphosate and clethodim tank mix was applied to the weed plant Canadian horseweed (*Erigeron Canadensis*) in conjunction with Tween series of adjuvants, results were consistent with those found in blackgrass and ryegrass. It was found that shorter chain length adjuvants resulted in increased control of Canadian horseweed*,* with a stepwise level of increased control with decreasing chain length (Penfield et al., 2015). The lack of variation in adjuvant treatments within wheat and apple leaves, as well as enhanced control or uptake within blackgrass, ryegrass, and Canadian horseweed would indicate plant surface properties having large effects on the efficacy of adjuvants.

6.3.3 Physiochemical properties

As blackgrass and ryegrass were shown to exhibit analogous trends in contact angle recession and were considerably different to wheat, it was hypothesised that this difference could be due to variations in the leaf surface of each plant. The physical structure of wax on the surface of the adaxial and abaxial leaf surfaces of wheat, blackgrass, and ryegrass was examined by

SEM. In each instance the structure was found to be a crystalline platelet structure as defined by Barthlott (1998). The importance of the crystalline structure in dictating leaf hydrophobicity has been previously demonstrated in rice. The *LGF1* gene was found to be responsible for the formation of fatty alcohols and dictated the ratio of C30 primary alcohols and C30 aldehydes. In rice mutants expressing significantly less LGF1, it was found that the levels of C30 alcohols markedly decreased with levels of C30 aldehyde increasing. The resulting leaf wax did not form the crystalline platelet structure, resulting in a decrease in hydrophobicity, and increase in contact angle of water applied to the surface (Kurokawa et al., 2018). Although the crystalline structure in each of blackgrass, ryegrass, and wheat was found to be the same, this is not the case for all plants, with the highest concentration aliphatic often dictating the crystalline structure formed. As such, further plant species would need to be investigated comprising a range of chemical and physical constituents to gain a deeper understanding of adjuvant-plant pairing. This however also adds difficulty in establishing if differences in application behaviour arise from differing chemical or physical structures.

As the physical structure of wax in wheat, blackgrass and ryegrass was found to be the same, it was thought the chemical composition may dictate the differences in contact angle and uptake observed. In each plant primary alcohols were found to be the most abundant compounds, and are one of the most critical components in forming the crystalline platelet structure (Barthlott et al., 1998). It has been found in multiple strains of wheat that octacosanol (C30) is the most abundant aliphatic, and that 1-hexacosanol (C28) is the most prevalent in ryegrass, consistent with the populations tested in this thesis (Feng et al., 2009; Ringelmann et al., 2009). Although limited studies have been performed on the composition of wax in blackgrass, it was found to share many parallels to ryegrass, also showing 1-hexacosanol as the most abundant compound. In general, both blackgrass and ryegrass were composed of shorter chain length aliphatics than wheat. It is therefore likely that the higher chain length compounds found within wheat wax would result in a more hydrophobic surface (Carignan et al., 2013; Negi, 2019). This is supported by contact angle reading which demonstrated a lesser degree of wettability of wheat leaves when compared to both blackgrass and ryegrass.

In conclusions, despite low levels of GST activity observed within wheat, it appeared that a degree of tolerance to flufenacet in the crop results from reduced uptake. Both the lesser wettability, lower overall conjugate, and higher flufenacet retention within the leaf wash would support this. Similar results were shown in maize (*Zea mays*) which was found to gain some of its tolerance towards the herbicide dicamba as a result of reduced foliar uptake when compared to the weeds goosegrass (*Galium aparine*) and redroot pigweed (*Amaranthus retroflexus*), despite showing lower levels of metabolism (Grossmann et al., 2002).

6.4 Limitations

Several limitations must be taken into account when interpreting the findings of this study. The primary means used for measuring herbicide uptake was to observe metabolite formation. Although notable differences were detected in metabolite levels from the various adjuvants incorporated into the formation, the method would have benefitted from further validation. This could have been performed by using radiochemicals to gain a more robust understanding of the herbicide metabolic pathways, and the ratios of metabolites found within each plant. Due to a lack of access to both radiochemicals and facilities in which to run such trials, this should be highlighted as a limitation of the method, and as such, a firm distinction cannot be made between parent herbicide inside the plant cells, trapped within the waxy cuticle, or on the leaf surface.

Secondly, no efficacy studies demonstrating the impact of adjuvants have been presented within this thesis. Several attempts were made at performing spray trials to highlight the impact of the various adjuvants on weed control. In each instance however, plants were infected with powdery mildew part ways through the trial. This resulted in unreliable data, where the effects of the herbicide and powdery mildew could not be distinguished and so the attained data could not be used. Although multiple attempts were made to attain such data, time constraints eventually meant this was not feasible.

Thirdly, flufenacet is often used a pre-emergence herbicide. Although there are some post-emergence uses, the majority of flufenacet use within the UK and Europe as a whole occurs pre-emergence. The assays developed only addressed foliar application and therefore are limited to only the lesser used post-emergence application of flufenacet.

6.5 Future work

Although initial studies have allowed for cross comparison of adjuvants within a single species, cross comparing between each species proves a much more difficult task. Flufenacet has been previously reported as undergoing both oxidative and glutathione mediated metabolism, however no oxidative metabolites were detectable in any tested species. The metabolism of metolachlor was shown to occur via both oxidation and glutathione conjugation in each sample indicating a possible inability to detect flufenacet oxidative metabolites by LCMS. Further screening by GCMS or refinement of the LCMS method may allow for oxidative metabolites to be detected and a more complete idea of the total herbicide within the plant. In addition, the testing of additional herbicides while maintaining formulation composition would be of great interest to examine the effects of herbicide physiochemical properties and their influence on uptake.

Several adjuvants have been demonstrated to disrupt the waxy cuticle of plants and facilitate uptake (Gitsopoulos et al., 2018). This was found to be the case with all tested adjuvants in all plants, though this proved hard to quantify. Although a firm method for quantification of adjuvant plasticisation has yet to be developed, establishing a method would allow for more in-depth study of the cause of uptake variations between differing adjuvants. This has the potential to shed light upon the differences between the Tween and Tween L series of adjuvants.

7 Appendix

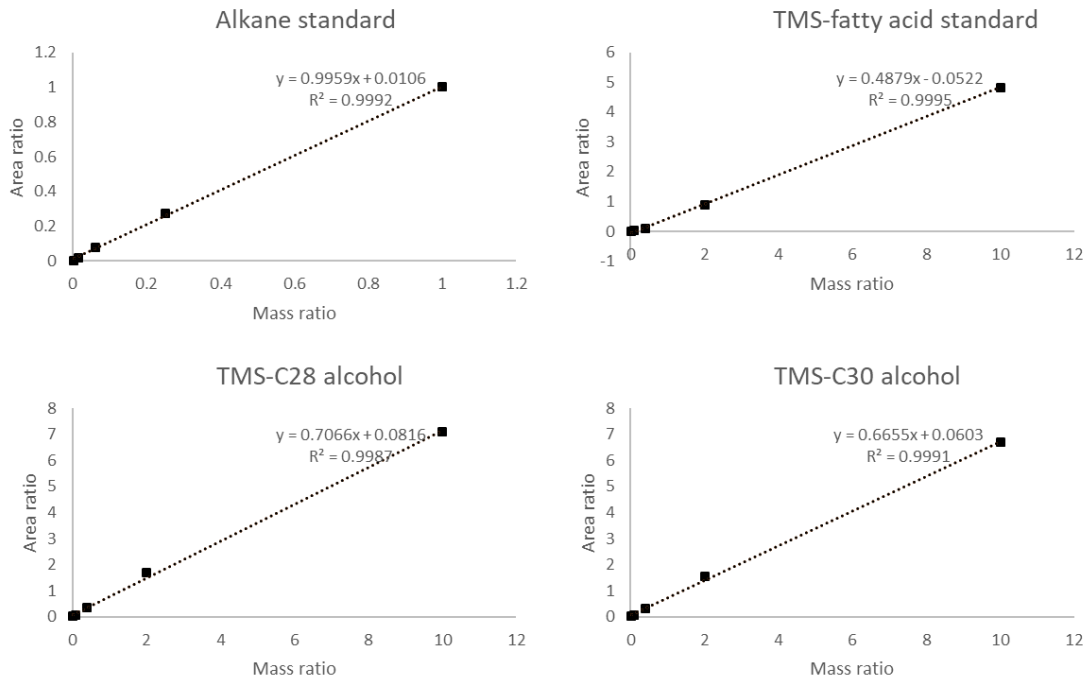

Figure A 1. Wax standards for alkanes (n-tetracosane), TMS derivitised fatty acid (octodecanoic acid), and TMS derivitised C28 and C30 alcohol.

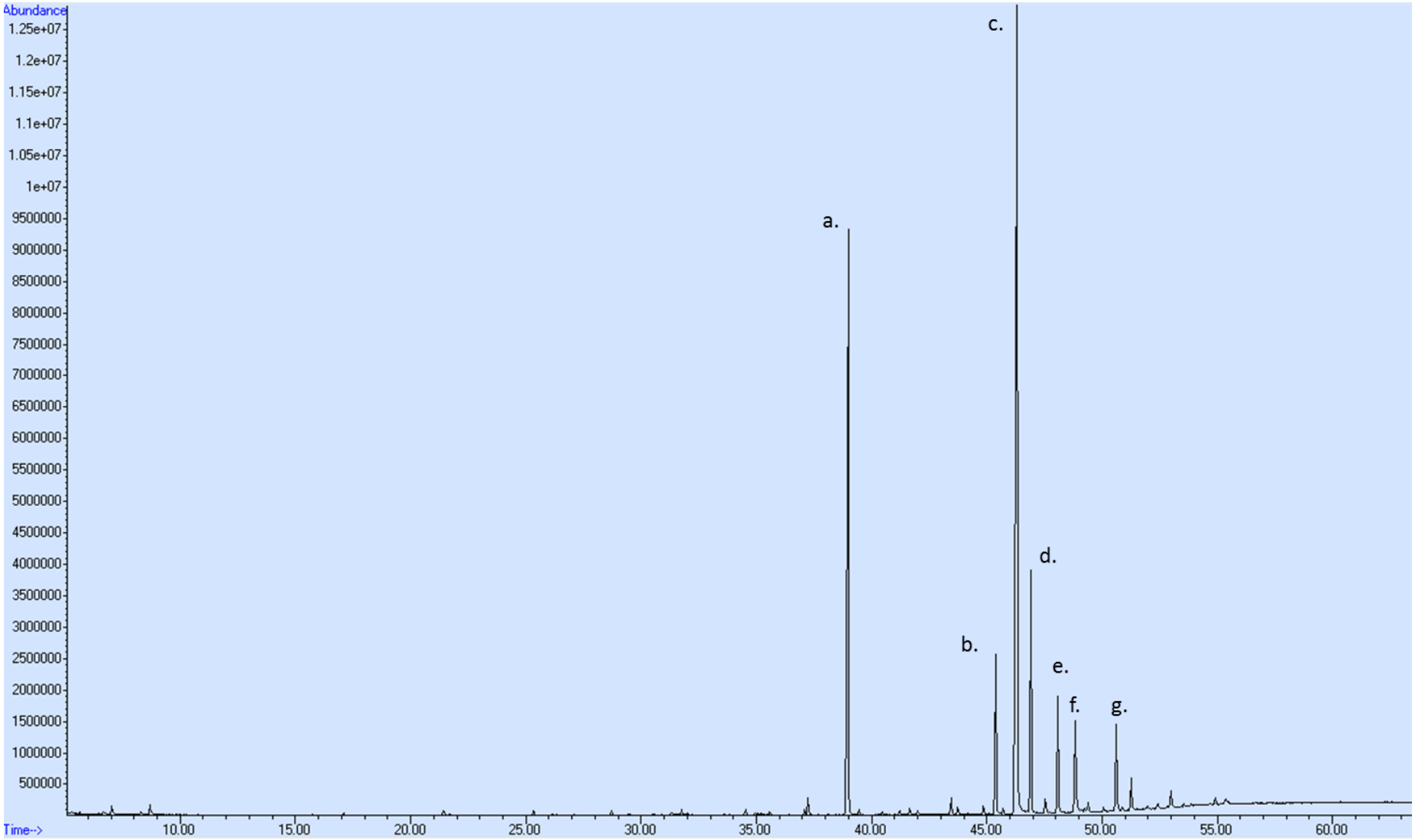

Figure A 2. GCMS spectrum of wax extracted from ryegrass showing the most prominent peaks. (peak identity: a. – C24 alkane internal standard, b. - C29 alkane, c. – C26 alcohol, d. – C26 aldehyde, e. – C31 alkane, f. – C28 alcohol, g. – C33 alkane)

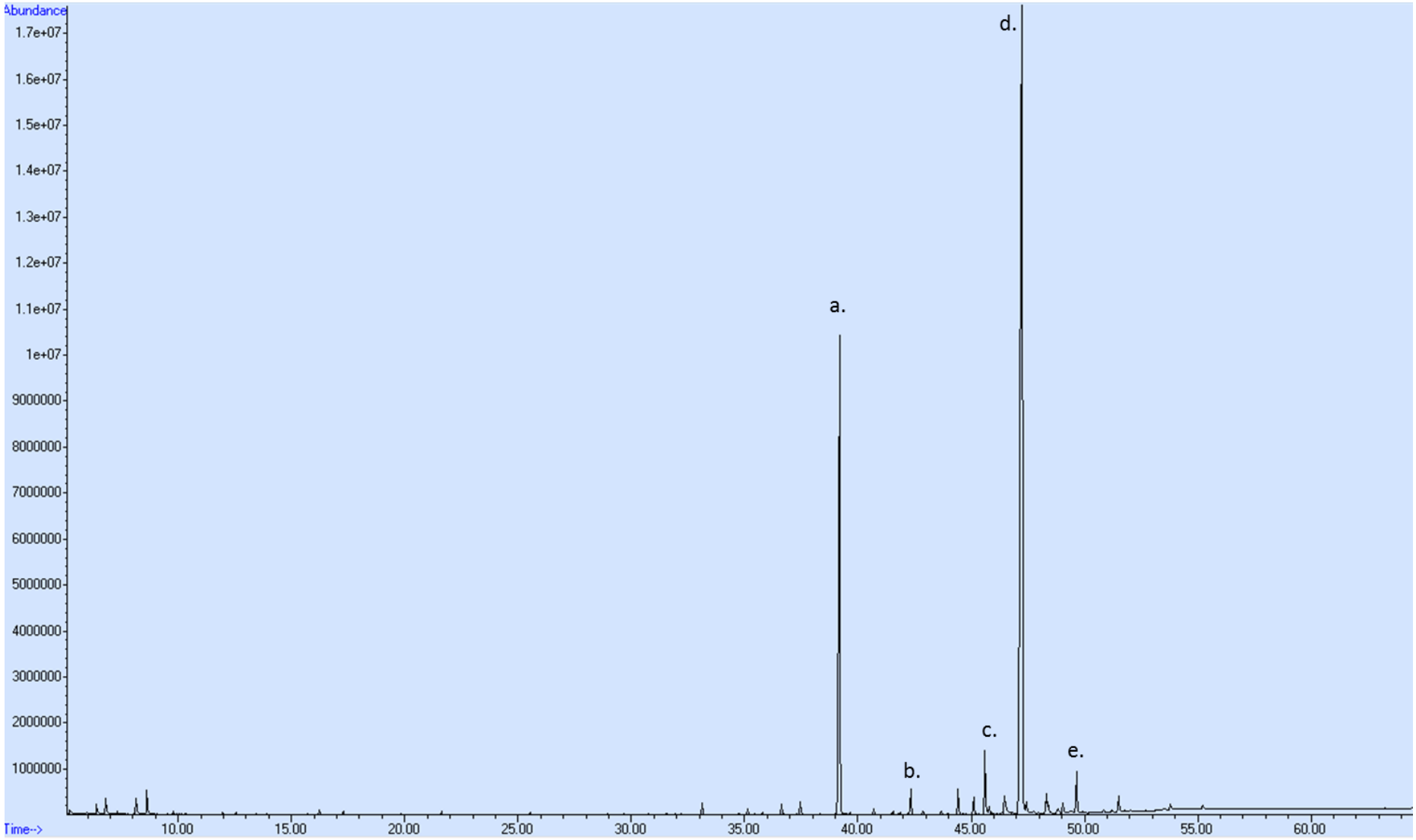

Figure A 3. GCMS spectrum of wax extracted from blackgrass showing the most prominent peaks. (peak identity: a. – C24 alkane internal standard, b. – C24 alcohol, c. - C29 alkane, , d. – C26 alcohol, e. – C26 aldehyde)

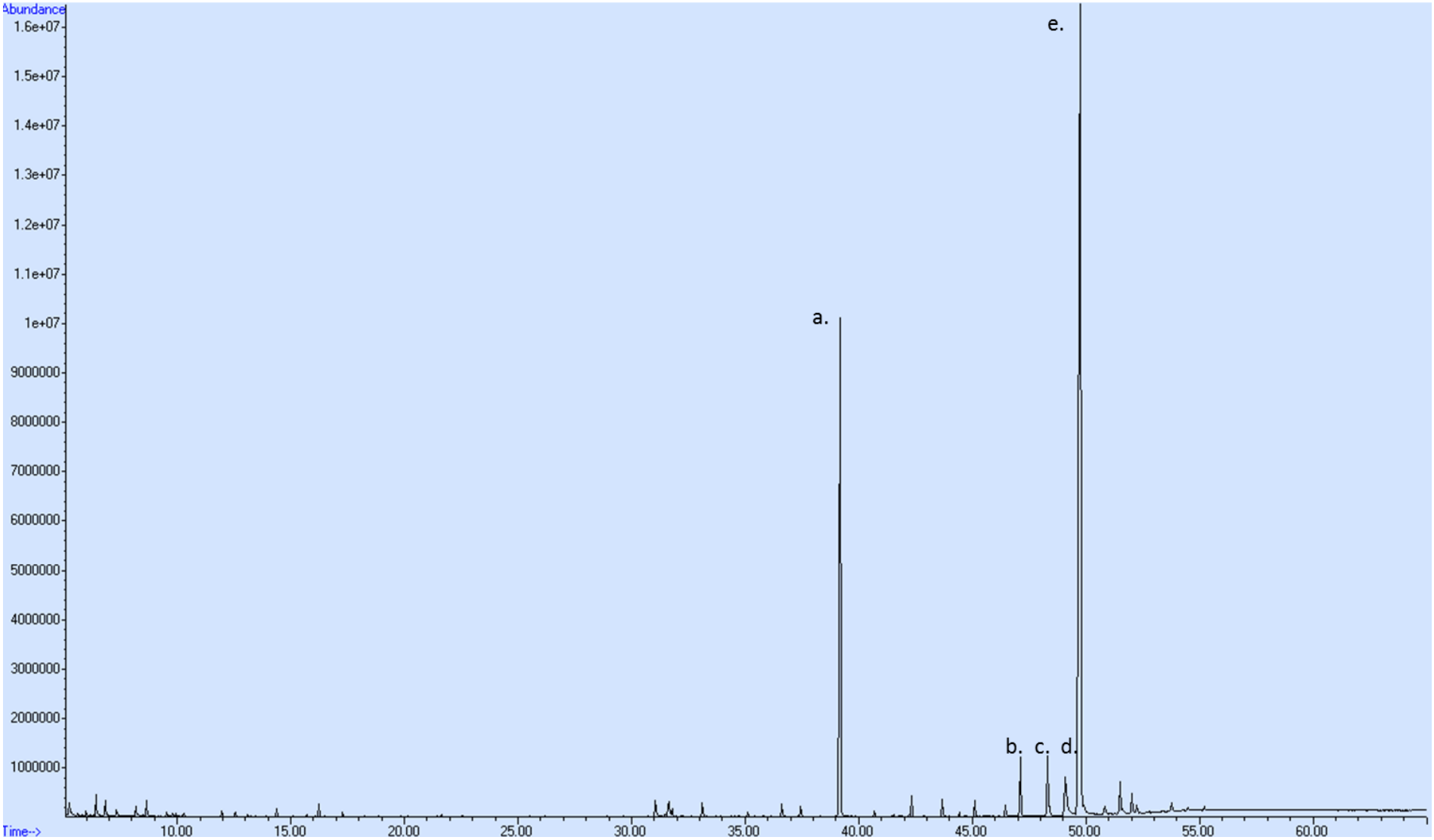

Figure A 4. GCMS spectrum of wax extracted from wheat showing the most prominent peaks. (peak identity: a. – C24 alkane internal standard, b. – C29 alkane, c. - C26 alcohol, , d. – C28 aldehyde, e. – C28 alcohol)

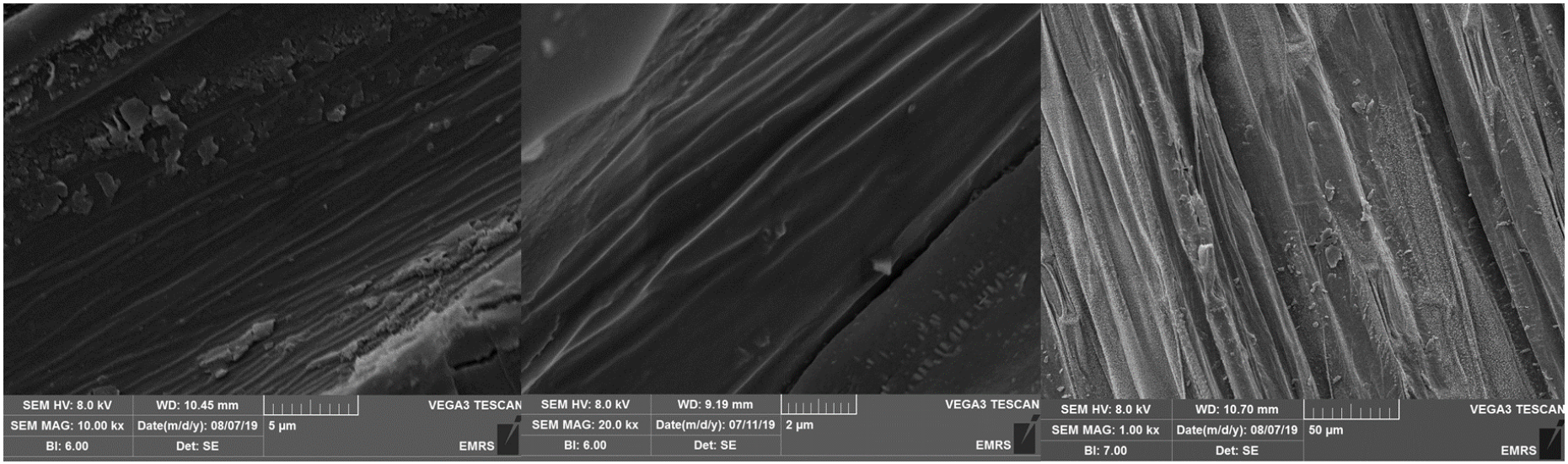

Figure A 5. The plasticising effects of Tween L-1010, Tween 22, and Tween 23 on wheat. These disruptions in wax could be seen across all tested plant species across all adjuvant treatments however proved difficult to quantify

Abbreviations

ABC	ATP-binding cassette
ACCase	Acetyl-CoA carboxylase
ACS	Acetyl-CoA synthetase
ALS	Acetolactate synthase
amu	atomic mass unit
ATP	Adenosine triphosphate
CAT	Catalase
CBF	C-repeat/DRE-Binding Factor
cDNA	Complementary Diribonucleic acid
CDNB	1-Chloro-2,4-dinitrobenzene
CoA	Coenzyme A
Cq	Cycle quantification
CYP	Cytochrome P450
d.i.	De-ionized
Da	Dalton
DDA	Dried Droplet Analysis
dNTP	Deoxyribonucleotide triphosphate
DTT	Dithiothreitol
EC	Emulsifiable concentrate
EDTA	Ethylenediaminetetraacetic acid
EO	Ethylene oxide
EW	Oil in water emulsion
FA	Fatty acid
FAS	Fatty acid synthase
g	gram or relative centrafugal force (context specific)
GC-FID	Gas chromatography flame ionisation detection
GCMS	Gas chromatography mass spectroscopy
gFw	Gram of fresh weight
GGT	Gamma-glutamyl transferase
GSH	Reduced glutathione
GSSG	Oxidised glutathione
GST	Glutathione-S-transferase
GSTF1	Glutathione-S-transferase, Phi class
GSTU	Glutathione-S-transferase, Tau class
GT	Glycosyl transferase
HCl	Hydrochloric acid
HLB	Hydrophilic-lipophilic balance
HSP	Heat shock protein
KHz	Kilohertz
LEA	Late embryogenesis abundant
log P	Partition coefficient
M	Molar

m/z	Mass to charge ratio
min	Minute
ml	milliliter
mM	Milimolar
mN/m	Millinewtons per meter
MSMS	Tandem mass spectrometry
NADPH	Nicotinamide adenine dinucleotide phosphate
nKat	Nanokatal
nm	Nanometer
nmol	Nanomol
NTSR	Non-target site resistance
PDC	Pyruvate dehydrogenase complex
PkA	Peak area units
PO	Propylene oxide
POD	Peroxidase
PPFD	Photosynthetic photon flux density
ppm	Parts per million
PPO	Protoporphyrinogen oxidase
PS II	Photosystem II
PVDF	Polyvinylidene difluoride
PVPP	Polyvinylpolypyrollidone
QDa	Quadrupole dalton
qPCR	Quantitative polymerase chain reaction
QTOF	Quadrupole time of flight
RNA	Ribonucleic acid
rpm	Revolutions per minute
SC	Suspension concentrate
SDS-PAGE	Sodium dodecyl sulfate polyacrylamide gel electrophoresis
SEM	Scanning electron microscopy
SOD	Superoxide dismutase
TBS	Tris buffered saline
TEMED	Tetramethylethylenediamine
TSR	Target site resistance
UV	Ultra violet
V	Voltage
v/v	Volume to volume
VLCFA	Very long chain fatty acid
W/O	Water in oil emulsion
w/v	Weight to volume
w/w	Weight to weight
θ	Contact angle
°C	Degrees celsius
µg	Microgram

µl	Microlitre
µm	Micrometer

8 References

Agnello, A. C., Huguenot, D., Van Hullebusch, E. D., & Esposito, G. (2015). Phytotoxicity of citric acid and Tween® 80 for potential use as soil amendments in enhanced phytoremediation. *International journal of phytoremediation, 17*(7), 669-677.

Al-Khatib, K., Unland, J. B., Olson, B. L. S., & Graham, D. W. (2002). Alachlor and metolachlor transformation pattern in corn and soil. *Weed science, 50*(5), 581-586.

Alici, E. H., & Arabaci, G. (2016). Determination of SOD, POD, PPO and cat enzyme activities in Rumex obtusifolius L. *Annual Research & Review in Biology, 11*(3), 1-7.

Andersen, E., Ali, S., Byamukama, E., Yen, Y., & Nepal, M. (2018). Disease resistance mechanisms in plants. *Genes, 9*(7), 339.

Anderson, J., Ellsworth, P., Faira, J., Head, G., Owen, M., Pilcher, C., Shelton, A., Meissle, M. (20190). Genetically engineered crops: Importance of diversified integrated pest management for agriculture and sustainability. *Frontiers in Bioengineering and Biotechnology, 7* (24).

Axarli, I., Dhavala, P., Papageorgiou, A. C., & Labrou, N. E. (2009). Crystallographic and functional characterization of the fluorodifen-inducible glutathione transferase from Glycine max reveals an active site topography suited for diphenylether herbicides and a novel L-site. *Journal of molecular biology, 385*(3), 984-1002.

Baker, E. A. (1982). *Chemistry and morphology of plant epicuticular waxes.* Paper presented at the Linnean Society symposium series.

Barthlott, W., Neinhuis, C., Cutler, D., Ditsch, F., Meusel, I., Theisen, I., & Wilhelmi, H. (1998). Classification and terminology of plant epicuticular waxes. *Botanical journal of the Linnean society, 126*(3), 237-260.

Basi, S., Hunsche, M., & Noga, G. (2013). Effects of surfactants and the kinetic energy of monodroplets on the deposit structure of glyphosate at the micro-scale and their relevance to herbicide bio-efficacy on selected weed species. *Weed research, 53*(1), 1-11.

Baucom, R. S. (2019). Evolutionary and ecological insights from herbicide-resistant weeds: what have we learned about plant adaptation, and what is left to uncover? *New Phytologist*.

Bewick, T. A., Shilling, D. G., & Querns, R. (1993). Evaluation of epicuticular wax removal from whole leaves with chloroform. *Weed Technology, 7*(3), 706-716.

Blum, R., Beck, A., Korte, A., Stengel, A., Letzel, T., Lendzian, K., & Grill, E. (2007). Function of phytochelatin synthase in catabolism of glutathione-conjugates. *The Plant Journal, 49*(4), 740-749.

Bowles, D., Isayenkova, J., Lim, E.-K., & Poppenberger, B. (2005). Glycosyltransferases: managers of small molecules. *Current opinion in plant biology, 8*(3), 254-263.

Brazier-Hicks, M., Evans, K. M., Cunningham, O. D., Hodgson, D. R. W., Steel, P. G., & Edwards, R. (2008). Catabolism of Glutathione Conjugates in Arabidopsis thaliana ROLE IN METABOLIC REACTIVATION OF THE HERBICIDE SAFENER FENCLORIM. *Journal of Biological Chemistry, 283*(30), 21102-21112.

Brazier-Hicks, M., Howell, A., Cohn, J., Hawkes, T., Hall, G., McIndoe, E., & Edwards, R. (2019). Chemically induced herbicide tolerance in rice by the safener metcamifen is associated with a phased stress response. *Journal of experimental botany*.

Brazier-Hicks, M., Gershater, M., Dixon, D., & Edwards, R. (2018). Substrate specificity and safener inducibility of the plant UDP-glucose-dependent family 1 glycosyltransferase super-family. *Plant biotechnology journal, 16*(1), 337-348.

Bruel, C., Queffeulou, S., Darlow, T., Virgilio, N., Tavares, J. R., & Patience, G. S. (2019). Experimental methods in chemical engineering: Contact angles. *The Canadian Journal of Chemical Engineering, 97*(4), 832-842.

Burghardt, M., Friedmann, A., Schreiber, L., & Riederer, M. (2006). Modelling the effects of alcohol ethoxylates on diffusion of pesticides in the cuticular wax of Chenopodium album leaves. *Pest Management Science: formerly Pesticide Science, 62*(2), 137-147.

Burns, E. E., Keith, B. K., Refai, M. Y., Bothner, B., & Dyer, W. E. (2018). Constitutive redox and phosphoproteome changes in multiple herbicide resistant Avena fatua L. are similar to those of systemic acquired resistance and systemic acquired acclimation. *Journal of plant physiology, 220*, 105-114.

Buschhaus, C., Herz, H., & Jetter, R. (2007). Chemical composition of the epicuticular and intracuticular wax layers on the adaxial side of Ligustrum vulgare leaves. *New Phytologist, 176*(2), 311-316.

Buschhaus, C., & Jetter, R. (2011). Composition differences between epicuticular and intracuticular wax substructures: how do plants seal their epidermal surfaces? *Journal of experimental botany, 62*(3), 841-853.

Cajka, T., & Fiehn, O. (2014). Comprehensive analysis of lipids in biological systems by liquid chromatography-mass spectrometry. *Trends Analyt Chem, 61*, 192-206. doi:10.1016/j.trac.2014.04.017

Calore, R. A., Ferreira, M. d. C., Rodrigues, N. E. L., & Otuka, A. K. (2015). Distribution pattern, surface tension and contact angle of herbicides associated to adjuvants on spraying and control of Ipomoea hederifolia under rainfall incidence. *Engenharia Agrícola, 35*(4), 756-768.

Campbell, A., Holstege, D., Swezey, R., & Medina-Cleghorn, D. (2008). Detoxification of molinate sulfoxide: comparison of spontaneous and enzmatic glutathione conjugation using human and rat liver cytosol. *Journal of Toxicology and Environmental Health, Part A, 71*(19), 1338-1347.

Carignan, D., Désy, O., Ghani, K., Caruso, M., & de Campos-Lima, P. O. (2013). The size of the unbranched aliphatic chain determines the immunomodulatory potency of short and long chain n-alkanols. *Journal of Biological Chemistry, 288*(34), 24948-24955.

Carvalho, S. J. P. d., Nicolai, M., Ferreira, R. R., Figueira, A. V. d. O., & Christoffoleti, P. J. (2009). Herbicide selectivity by differential metabolism: considerations for reducing crop damages. *Scientia agrícola, 66*(1), 136-142.

Case, L. T., Mathers, H. M., & Senesac, A. F. (2005). A review of weed control practices in container nurseries. *HortTechnology, 15*(3), 535-545.

Castro, E. B., Carbonari, C. A., Velini, E. D., Gomes, G., & Belapart, D. (2018). Influence of Adjuvants on the Surface Tension, Deposition and Effectiveness of Herbicides on Fleabane Plants. *Planta Daninha, 36*.

Césari, S., Kanzaki, H., Fujiwara, T., Bernoux, M., Chalvon, V., Kawano, Y., . . . Kroj, T. (2014). The NB-LRR proteins RGA4 and RGA5 interact functionally and physically to confer disease resistance. *The EMBO journal, 33*(17), 1941-1959.

Chappell, J. (1995). Biochemistry and molecular biology of the isoprenoid biosynthetic pathway in plants. *Annual review of plant biology, 46*(1), 521-547.

Chibnall, A. C., & Piper, S. H. (1934). The metabolism of plant and insect waxes. *Biochemical Journal, 28*(6), 2209.

Coleman, J., Blake-Kalff, M., & Davies, E. (1997). Detoxification of xenobiotics by plants: chemical modification and vacuolar compartmentation. *Trends in plant science, 2*(4), 144-151.

Coleman, S., Linderman, R., Hodgson, E., & Rose, R. L. (2000). Comparative metabolism of chloroacetamide herbicides and selected metabolites in human and rat liver microsomes. *Environmental health perspectives, 108*(12), 1151-1157.

Comont, D., Knight, C., Crook, L., Hull, R., Beffa, R., & Neve, P. (2019). Alterations in life-history associated with non-target-site herbicide resistance in Alopecurus myosuroides. *Frontiers in plant science, 10*, 837.

Cornuault, V., Posé, S., & Knox, J. P. (2018). Disentangling pectic homogalacturonan and rhamnogalacturonan-I polysaccharides: Evidence for sub-populations in fruit parenchyma systems. *Food chemistry, 246*, 275-285.

Cummins, I., Cole, D. J., & Edwards, R. (1999). A role for glutathione transferases functioning as glutathione peroxidases in resistance to multiple herbicides in black-grass. *The Plant Journal, 18*(3), 285-292.

Cummins, I., Dixon, D. P., Freitag-Pohl, S., Skipsey, M., & Edwards, R. (2011). Multiple roles for plant glutathione transferases in xenobiotic detoxification. *Drug metabolism reviews, 43*(2), 266-280.

Cummins, I., Wortley, D. J., Sabbadin, F., He, Z., Coxon, C. R., Straker, H. E., . . . Hughes, D. (2013). Key role for a glutathione transferase in multiple-herbicide resistance in grass weeds. *Proceedings of the National Academy of Sciences, 110*(15), 5812-5817.

Curran, W. S., McGlamery, M. D., Liebi, R. A., & Lingenfelter, D. D. (1999). Adjuvants for enhancing herbicide performance.

Cush, R. (2006). Back to basics: A review of pesticide formulation types. *Golf Course Manag, 74*(1), 143-145.

Czarnota, M., & Thomas, P. A. (2010). Using surfactants, wetting agents, and adjuvants in the greenhouse.

Damato, T. C., Carrasco, L. D. M., Carmona-Ribeiro, A. M., Luiz, R. V., Godoy, R., & Petri, D. F. S. (2017). The interactions between surfactants and the epicuticular wax on soybean or weed leaves: Maximal crop protection with minimal wax solubilization. *Crop protection, 91*, 57-65.

Dayan, F. E. (2019). Current Status and Future Prospects in Herbicide Discovery. *Plants, 8*(9), 341.

de Ruiter, H., & Meinen, E. (1998). Influence of water stress and surfactant on the efficacy, absorption, and translocation of glyphosate. *Weed science, 46*(3), 289-296.

Délye, C., Zhang, X.-Q., Michel, S., Matéjicek, A., & Powles, S. B. (2005). Molecular bases for sensitivity to acetyl-coenzyme A carboxylase inhibitors in black-grass. *Plant physiology, 137*(3), 794-806.

Devine, M. D., & Shukla, A. (2000). Altered target sites as a mechanism of herbicide resistance. *Crop protection, 19*(8-10), 881-889.

DiTomaso, J. M. (1999). *Barriers to foliar penetration and uptake of herbicides.* Paper presented at the Proceedings of the California Weed Science Society.

Dixon, D. P., McEwen, A. G., Lapthorn, A. J., & Edwards, R. (2003). Forced evolution of a herbicide detoxifying glutathione transferase. *Journal of Biological Chemistry, 278*(26), 23930-23935.

Dücker, R., Zöllner, P., Lümmen, P., Ries, S., Collavo, A., & Beffa, R. (2019). Glutathione transferase plays a major role in flufenacet resistance of ryegrass (Lolium spp.) field populations. *Pest management science*.

Dunitz, J. D., & Gavezzotti, A. (2009). How molecules stick together in organic crystals: weak intermolecular interactions. *Chemical Society Reviews, 38*(9), 2622-2633.

Ebringerová, A. (2005). *Structural diversity and application potential of hemicelluloses.* Paper presented at the Macromolecular Symposia.

Feng, J., Wang, F., Liu, G., Greenshields, D., Shen, W., Kaminskyj, S., . . . Zou, J. (2009). Analysis of a Blumeria graminis-secreted lipase reveals the importance of host epicuticular wax components for fungal adhesion and development. *Molecular plant-microbe interactions, 22*(12), 1601-1610.

Fenn, J. B., Mann, M., Meng, C. K., Wong, S. F., & Whitehouse, C. M. (1989). Electrospray Ionization for Mass-Spectrometry of Large Biomolecules. *Science, 246*(4926), 64-71. doi:DOI 10.1126/science.2675315

Fernández, V., & Khayet, M. (2015). Evaluation of the surface free energy of plant surfaces: toward standardizing the procedure. *Frontiers in plant science, 6*, 510.

Ferrell, M. A. (2004). Basic guide to weeds and herbicides. *http://www. uwyo. edu/plants/wyopest/TrainingManuals/Weedctrl. pdf*.

Ferrer, A., Altabella, T., Arró, M., & Boronat, A. (2017). Emerging roles for conjugated sterols in plants. *Progress in lipid research, 67*, 27-37.

Flors, C., Fryer, M. J., Waring, J., Reeder, B., Bechtold, U., Mullineaux, P. M., . . . Baker, N. R. (2006). Imaging the production of singlet oxygen in vivo using a new fluorescent sensor, Singlet Oxygen Sensor Green®. *Journal of experimental botany, 57*(8), 1725-1734.

Gage, K. L., Krausz, R. F., & Walters, S. A. (2019). Emerging Challenges for Weed Management in Herbicide-Resistant Crops. *Agriculture, 9*(8), 180.

Gershater, M. C., Cummins, I., & Edwards, R. (2007). Role of a carboxylesterase in herbicide bioactivation in Arabidopsis thaliana. *Journal of Biological Chemistry, 282*(29), 21460-21466.

Gitsopoulos, T. K., Damalas, C. A., & Georgoulas, I. (2018). Optimizing diquat efficacy with the use of adjuvants. *Phytoparasitica, 46*(5), 715-722.

Golding, C. G., Lamboo, L. L., Beniac, D. R., & Booth, T. F. (2016). The scanning electron microscope in microbiology and diagnosis of infectious disease. *Scientific reports, 6*, 26516.

Grant, C., Twigg, P., Bell, G., & Lu, J. R. (2008). AFM relative stiffness measurement of the plasticising effect of a non-ionic surfactant on plant leaf wax. *Journal of colloid and interface science, 321*(2), 360-364.

Gray, E. W., & Fusco, R. (2017). Microbial control of black flies (Diptera: Simuliidae) with Bacillus thuringiensis subsp. israelensis *Microbial Control of Insect and Mite Pests* (pp. 367-377): Elsevier.

Gronwald, J. W., Fuerst, E. P., Eberlein, C. V., & Egli, M. A. (1987). Effect of herbicide antidotes on glutathione content and glutathione S-transferase activity of sorghum shoots. *Pesticide Biochemistry and Physiology, 29*(1), 66-76.

Grossmann, K., Caspar, G., Kwiatkowski, J., & Bowe, S. J. (2002). On the mechanism of selectivity of the corn herbicide BAS 662H: a combination of the novel auxin transport inhibitor diflufenzopyr and the auxin herbicide dicamba. *Pest Management Science: formerly Pesticide Science, 58*(10), 1002-1014.

Habig, W. H., Pabst, M. J., & Jakoby, W. B. (1974). Glutathione S-transferases the first enzymatic step in mercapturic acid formation. *Journal of Biological Chemistry, 249*(22), 7130-7139.

Hagedorn, O., Fleute-Schlachter, I., Mainx, H. G., Zeisler-Diehl, V., & Koch, K. (2017). Surfactant-induced enhancement of droplet adhesion in superhydrophobic soybean (Glycine max L.) leaves. *Beilstein journal of nanotechnology, 8*(1), 2345-2356.

Hanigan, M. H. (2014). Gamma-glutamyl transpeptidase: redox regulation and drug resistance *Advances in cancer research* (Vol. 122, pp. 103-141): Elsevier.

Hao, Y., Zhang, N., Xu, W., Gao, J., Zhang, Y., & Tao, L. (2019). A natural adjuvant shows the ability to improve the effectiveness of glyphosate application. *Journal of Pesticide Science, 44*(2), 106-111.

Harholt, J., Suttangkakul, A., & Scheller, H. V. (2010). Biosynthesis of pectin. *Plant physiology, 153*(2), 384-395.

Hartzler, B. (2019). Absorption of foliar-applied herbicides. *Integrated Crop Management*.

Hazen, J. L. (2000). Adjuvants—terminology, classification, and chemistry. *Weed Technology, 14*(4), 773-784.

Heap, I. (2014). Global perspective of herbicide-resistant weeds. *Pest management science, 70*(9), 1306-1315.

Herbin, G. A., & Robins, P. A. (1969). Patterns of variation and development in leaf wax alkanes. *Phytochemistry, 8*(10), 1985-1998.

Heredia, A. (2003). Biophysical and biochemical characteristics of cutin, a plant barrier biopolymer. *Biochimica et Biophysica Acta (BBA)-General Subjects, 1620*(1-3), 1-7.

Hess, F. D., & Foy, C. L. (2000). Interaction of surfactants with plant cuticles. *Weed Technology, 14*(4), 807-813.

Hilz, E., & Vermeer, A. W. P. (2013). Spray drift review: The extent to which a formulation can contribute to spray drift reduction. *Crop protection, 44*, 75-83.

Hu, H., & Larson, R. G. (2006). Marangoni effect reverses coffee-ring depositions. *The Journal of Physical Chemistry B, 110*(14), 7090-7094.

Hull, H. M. (1982). Action of adjuvants on plant surfaces. *Adjuvants for herbicides*, 26-67.

Hunsche, M., & Noga, G. (2012). Effects of relative humidity and substrate on the spatial association between glyphosate and ethoxylated seed oil adjuvants in the dried deposits of sessile droplets. *Pest management science, 68*(2), 231-239.

Iqbal, N., Manalil, S., Chauhan, B. S., & Adkins, S. W. (2019). Investigation of alternate herbicides for effective weed management in glyphosate-tolerant cotton. *Archives of Agronomy and Soil Science*, 1-15.

Izadi-Darbandi, E., Aliverdi, A., Anabestani, M., & Shamsabadi, A. (2019). Adjuvants to Improve Phenmedipham+ Desmedipham+ Ethofumesate Efficacy Against Weeds in Sugar Beet (Beta vulgaris). *Planta Daninha, 37*.

Jain, N., Vergish, S., & Khurana, J. P. (2018). Validation of house-keeping genes for normalization of gene expression data during diurnal/circadian studies in rice by RT-qPCR. *Scientific reports, 8*(1), 3203.

Jang, S., Marjanovic, J., & Gornicki, P. (2013). Resistance to herbicides caused by single amino acid mutations in acetyl-C o A carboxylase in resistant populations of grassy weeds. *New Phytologist, 197*(4), 1110-1116.

Jeffree, C. E. (2006). The fine structure of the plant cuticle. *Biology of the plant cuticle, 23*, 11-125.

Jemal, M., & Xia, Y. Q. (1999). The need for adequate chromatographic separation in the quantitative determination of drugs in biological samples by high performance liquid chromatography with tandem mass spectrometry. *Rapid communications in mass spectrometry, 13*(2), 97-106.

Jennissen, H. P. (2011). Redefining the Wilhelmy and Young equations to imaginary number space and implications for wettability measurements. *Materialwissenschaft und Werkstofftechnik, 42*(12), 1111-1117.

Jiang, H., Müller-Plathe, F., & Panagiotopoulos, A. Z. (2017). Contact angles from Young's equation in molecular dynamics simulations. *The Journal of chemical physics, 147*(8), 084708.

Karapetsas, G., Sahu, K. C., & Matar, O. K. (2016). Evaporation of Sessile Droplets Laden with Particles and Insoluble Surfactants. *Langmuir, 32*(27), 6871-6881. doi:10.1021/acs.langmuir.6b01042

Keegstra, K. (2010). Plant cell walls. *Plant physiology, 154*(2), 483-486.

Khan, R., Inam, M. A., Khan, S., Jiménez, A. N., Park, D. R., & Yeom, I. T. (2019). The Influence of Ionic and Nonionic Surfactants on the Colloidal Stability and Removal of CuO Nanoparticles from Water by Chemical Coagulation. *International journal of environmental research and public health, 16*(7), 1260.

Khare, R. R., & Sondhia, S. (2014). Cyhalofop-p-butyl mobility and distribution of residues in soil at various depths. *Journal of Environmental Science and health, Part B, 49*(6), 391-399.

Kirkwood, R. C. (1999). Recent developments in our understanding of the plant cuticle as a barrier to the foliar uptake of pesticides. *Pesticide Science, 55*(1), 69-77.

Knowles, A. (2006). Adjuvants and additives: 2006 edition. *Agrow Reports*.

Koch, K., Barthlott, W., Koch, S., Hommes, A., Wandelt, K., Mamdouh, W., . . . Broekmann, P. (2006). Structural analysis of wheat wax (Triticum aestivum, cv.'Naturastar'L.): from the molecular level to three dimensional crystals. *Planta, 223*(2), 258-270.

Kolattukudy, P. E. (1996). Biosynthetic pathways of cutin and waxes, and their sensitivity to environmental stress. *Plant cuticles: an integrated functional approach*.

Kraemer, T., Hunsche, M., & Noga, G. (2009). Surfactant-induced deposit structures in relation to the biological efficacy of glyphosate on easy-and difficult-to-wet weed species. *Pest Management Science: formerly Pesticide Science, 65*(8), 844-850.

Kreuz, K., Tommasini, R., & Martinoia, E. (1996). Old enzymes for a new job (herbicide detoxification in plants). *Plant physiology, 111*(2), 349.

Kumada, H.-O., Koizumi, Y., & Sekiya, J. (2007). Purification and characterization of dipeptidase hydrolyzing L-cysteinylglycine from radish cotyledon. *Bioscience, biotechnology, and biochemistry, 71*(12), 3102-3104.

Kurokawa, Y., Nagai, K., Huan, P. D., Shimazaki, K., Qu, H., Mori, Y., . . . Aiga, S. (2018). Rice leaf hydrophobicity and gas films are conferred by a wax synthesis gene (LGF 1) and contribute to flood tolerance. *New Phytologist, 218*(4), 1558-1569.

Lazghab, M., Saleh, K., Pezron, I., Guigon, P., & Komunjer, L. (2005). Wettability assessment of finely divided solids. *Powder Technology, 157*(1-3), 79-91.

Lechelt-Kunze, C., Meissner, R. C., Drewes, M., & Tietjen, K. (2003). Flufenacet herbicide treatment phenocopies the fiddlehead mutant in Arabidopsis thaliana. *Pest Management Science: formerly Pesticide Science, 59*(8), 847-856.

Li, X., & Nicholl, D. (2005). Development of PPO inhibitor-resistant cultures and crops. *Pest Management Science: formerly Pesticide Science, 61*(3), 277-285.

Li, X., Qin, Y., Liu, C., Jiang, S., Xiong, L., & Sun, Q. (2016). Size-controlled starch nanoparticles prepared by self-assembly with different green surfactant: The effect of electrostatic repulsion or steric hindrance. *Food chemistry, 199*, 356-363.

Li, Y., & Xiang, D. (2019). Stability of oil-in-water emulsions performed by ultrasound power or high-pressure homogenization. *PloS one, 14*(3), e0213189.

Li, Z., Van Acker, R., Robinson, D., Soltani, N., & Sikkema, P. (2017). Managing weeds with herbicides in white bean in Canada: a review. *Canadian journal of plant science, 97*(5), 755-766.

Lichtenthaler, H. K., Langsdorf, G., & Buschmann, C. (2013). Uptake of diuron and concomitant loss of photosynthetic activity in leaves as visualized by imaging the red chlorophyll fluorescence. *Photosynthesis research, 116*(2-3), 355-361.

Littlejohn, G. R., Mansfield, J. C., Parker, D., Lind, R., Perfect, S., Seymour, M., . . . Moger, J. (2015). In vivo chemical and structural analysis of plant cuticular waxes using stimulated Raman scattering microscopy. *Plant physiology, 168*(1), 18-28.

Loneman, D. M., Peddicord, L., Al-Rashid, A., Nikolau, B. J., Lauter, N., & Yandeau-Nelson, M. D. (2017). A robust and efficient method for the extraction of plant extracellular surface lipids as applied to the analysis of silks and seedling leaves of maize. *PloS one, 12*(7), e0180850.

Mampallil, D., & Eral, H. B. (2018). A review on suppression and utilization of the coffee-ring effect. *Advances in Colloid and Interface Science, 252*, 38-54.

Manthey, F. A., Nalewaja, J. D., & Szelezniak, E. F. (1989). Herbicide-oil-water emulsions. *Weed Technology, 3*(1), 13-19.

Martin, A., Whitford, F., & Jordan, T. (2011). Pesticides and Formulation Technology. *Perdue Extension, 31*.

Martinez, D. A., Loening, U. E., & Graham, M. C. (2018). Impacts of glyphosate-based herbicides on disease resistance and health of crops: a review. *Environmental Sciences Europe, 30*(1), 2.

Matallana-González, M. C., & Morales, P. (2019). Dietary fiber sources and human benefits: The case study of cereal and pseudocereals. *Functional Food Ingredients from Plants*, 83.

Matsunaga, T., Ishii, T., Matsumoto, S., Higuchi, M., Darvill, A., Albersheim, P., & O'Neill, M. A. (2004). Occurrence of the primary cell wall polysaccharide rhamnogalacturonan II in pteridophytes, lycophytes, and bryophytes. Implications for the evolution of vascular plants. *Plant physiology, 134*(1), 339-351.

McDougall, P. (2010). The cost of new agrochemical product discovery, development and registration in 1995, 2000 and 2005-8. *Final Report. Verfügbar in: http://www.*

croplife. org/files/documentspublished/1/enus/REP/5344_REP_2010_03_04_Phillips_McDougal_Research_and_Development_study. pdf [Abfrage am 24.04. 2010].

Mesnage, R., & Antoniou, M. N. (2018). Ignoring adjuvant toxicity falsifies the safety profile of commercial pesticides. *Frontiers in public health, 5*, 361.

Moss, S. (2017). Black-grass (Alopecurus myosuroides): why has this weed become such a problem in Western Europe and what are the solutions? *Outlooks on Pest Management, 28*(5), 207-212.

Moss, S. R., Cocker, K. M., Brown, A. C., Hall, L., & Field, L. M. (2003). Characterisation of target-site resistance to ACCase-inhibiting herbicides in the weed Alopecurus myosuroides (black-grass). *Pest management science, 59*(2), 190-201.

Moss, S. R., Tatnell, L. V., Hull, R., Clarke, J. H., Wynn, S., & Marshall, R. (2010). Integrated management of herbicide resistance. *HGCA project report*(466).

Nakka, S., Jugulam, M., Peterson, D., & Mohammad, A. (2019). Herbicide resistance: Development of wheat production systems and current status of resistant weeds in wheat cropping systems. *The Crop Journal*.

Nandi, A., Yan, L.-J., Jana, C. K., & Das, N. (2019). Role of Catalase in Oxidative Stress-and Age-Associated Degenerative Diseases. *Oxidative Medicine and Cellular Longevity, 2019*.

Naot, D., Ben-Hayyim, G., Eshdat, Y., & Holland, D. (1995). Drought, heat and salt stress induce the expression of a citrus homologue of an atypical late-embryogenesis Lea5 gene. *Plant molecular biology, 27*(3), 619-622.

Negi, J. S. (2019). Nanolipid Materials for Drug Delivery Systems: A Comprehensive Review *Characterization and Biology of Nanomaterials for Drug Delivery* (pp. 137-163): Elsevier.

Neve, P., Busi, R., Renton, M., & Vila-Aiub, M. M. (2014). Expanding the eco-evolutionary context of herbicide resistance research. *Pest management science, 70*(9), 1385-1393.

Novák, A., Boldizsár, Á., Ádám, É., Kozma-Bognár, L., Majláth, I., Båga, M., . . . Galiba, G. (2015). Light-quality and temperature-dependent CBF14 gene expression modulates freezing tolerance in cereals. *Journal of experimental botany, 67*(5), 1285-1295.

O'Sullivan, P. A., & O'Donovan, J. T. (1980). Influence of various herbicides and Tween 20 on the effectiveness of glyphosate. *Canadian journal of plant science, 60*(3), 939-945.

Ohkama-Ohtsu, N., Zhao, P., Xiang, C., & Oliver, D. J. (2007). Glutathione conjugates in the vacuole are degraded by γ-glutamyl transpeptidase GGT3 in Arabidopsis. *The Plant Journal, 49*(5), 878-888.

Ohlrogge, J., & Browse, J. (1995). Lipid biosynthesis. *The Plant Cell, 7*(7), 957.

Ottis, B. V., Mattice, J. D., & Talbert, R. E. (2005). Determination of antagonism between cyhalofop-butyl and other rice (Oryza sativa) herbicides in barnyardgrass (Echinochloa crus-galli). *Journal of agricultural and food chemistry, 53*(10), 4064-4068.

Pacanoski, Z. (2014). Herbicides and Adjuvants. *Herbicides, Physiology of Action, and Safety*. doi:10.5772/60842

Pan, X.-l., Dong, F.-s., Wu, X.-h., Xu, J., Liu, X.-g., & Zheng, Y.-q. (2019). Progress of the discovery, application, and control technologies of chemical pesticides in China. *Journal of Integrative Agriculture, 18*(4), 840-853.

Pansook, S., Incharoensakdi, A., & Phunpruch, S. (2019). Effects of the Photosystem II Inhibitors CCCP and DCMU on Hydrogen Production by the Unicellular Halotolerant Cyanobacterium Aphanothece halophytica. *The Scientific World Journal, 2019*.

Papierowska, E., Szporak-Wasilewska, S., Szewińska, J., Szatyłowicz, J., Debaene, G., & Utratna, M. (2018). Contact angle measurements and water drop behavior on leaf surface for several deciduous shrub and tree species from a temperate zone. *Trees, 32*(5), 1253-1266.

Paria, S., & Khilar, K. C. (2004). A review on experimental studies of surfactant adsorption at the hydrophilic solid–water interface. *Advances in Colloid and Interface Science, 110*(3), 75-95.

Parr, J., & Norman, A. G. (1965). Considerations in the use of surfactants in plant systems: A review. *Botanical Gazette, 126*(2), 86-96.

Parween, T., Jan, S., Mahmooduzzafar, S., Fatma, T., & Siddiqui, Z. H. (2016). Selective effect of pesticides on plant—A review. *Critical reviews in food science and nutrition, 56*(1), 160-179.

Pascal-Lorber, S., Alsayeda, H., Jouanin, I., Debrauwer, L., Canlet, C., & Laurent, F. o. (2010). Metabolic fate of [14C] Diuron and [14C] linuron in wheat (Triticum aestivum) and radish (Raphanus sativus). *Journal of agricultural and food chemistry, 58*(20), 10935-10944.

Pasquali, R. C., Taurozzi, M. P., & Bregni, C. (2008). Some considerations about the hydrophilic–lipophilic balance system. *International journal of pharmaceutics, 356*(1-2), 44-51.

Pathan, A. K., Bond, J., & Gaskin, R. E. (2010). Sample preparation for SEM of plant surfaces. *Materials Today, 12*, 32-43.

Patzoldt, W. L., Hager, A. G., McCormick, J. S., & Tranel, P. J. (2006). A codon deletion confers resistance to herbicides inhibiting protoporphyrinogen oxidase. *Proceedings of the National Academy of Sciences, 103*(33), 12329-12334.

Penfield, K., Young, B., Young, J., Kruger, G., Henry, R., & Lindner, G. (2015). Physical and Biological Effects of Modified Polysorbate 20 *Pesticide Formulation and Delivery Systems: 34th Volume, Translating Basic Science into Products*: ASTM International.

Peters, B., & Strek, H. J. (2018). Herbicide discovery in light of rapidly spreading resistance and ever-increasing regulatory hurdles. *Pest management science, 74*(10), 2211-2215.

Pollard, M., Beisson, F., Li, Y., & Ohlrogge, J. B. (2008). Building lipid barriers: biosynthesis of cutin and suberin. *Trends in plant science, 13*(5), 236-246.

Pontzen, R. (2007). Designing the best-Getting the most out of agrochemicals. *PFLANZENSCHUTZ NACHRICHTEN-BAYER-ENGLISH EDITION, 59*(1), 63.

Popp, C., Burghardt, M., Friedmann, A., & Riederer, M. (2005). Characterization of hydrophilic and lipophilic pathways of Hedera helix L. cuticular membranes: permeation of water and uncharged organic compounds. *Journal of experimental botany, 56*(421), 2797-2806.

Powles, S. B., & Preston, C. (1995). Herbicide cross resistance and multiple resistance in plants. *Herbic. Resist. Action Committee Monogr, 2*.

Raman, R. (2017). The impact of Genetically Modified (GM) crops in modern agriculture: A review. *GM Crops & Food, 8* (4), 195-208.

Rasool, R., Bhullar, M. S., Singh, M., & Gill, G. S. (2019). Flufenacet controls multiple herbicide resistant Phalaris minor Retz. in wheat. *Crop protection, 121*, 127-131.

Rea, P. A. (2007). Plant ATP-binding cassette transporters. *Annu. Rev. Plant Biol., 58*, 347-375.

Richter, A. S., & Grimm, B. (2013). Thiol-based redox control of enzymes involved in the tetrapyrrole biosynthesis pathway in plants. *Frontiers in plant science, 4*, 371.

Richter, L. H. J., Jacobs, C. M., Mahfoud, F., Kindermann, I., Bohm, M., & Meyer, M. R. (2019). Development and application of a LC-HRMS/MS method for analyzing

antihypertensive drugs in oral fluid for monitoring drug adherence. *Anal Chim Acta, 1070*, 69-79. doi:10.1016/j.aca.2019.04.026

Riechers, D. E., Irzyk, G. P., Jones, S. S., & Fuerst, E. P. (1997). Partial characterization of glutathione S-transferases from wheat (Triticum spp.) and purification of a safener-induced glutathione S-transferase from Triticum tauschii. *Plant physiology, 114*(4), 1461-1470.

Ringelmann, A., Riedel, M., Riederer, M., & Hildebrandt, U. (2009). Two sides of a leaf blade: Blumeria graminis needs chemical cues in cuticular waxes of Lolium perenne for germination and differentiation. *Planta, 230*(1), 95-105.

Roechling, A. (2018). Herbicide formulation: How we maximise effectiveness in the field. Retrieved from https://cropscience.bayer.co.uk

Ruiz-Santaella, J. P., Heredia, A., & De Prado, R. (2006). Basis of selectivity of cyhalofop-butyl in Oryza sativa L. *Planta, 223*(2), 191-199.

Sabbadin, F., Glover, R., Stafford, R., Rozado-Aguirre, Z., Boonham, N., Adams, I., . . . Edwards, R. (2017). Transcriptome sequencing identifies novel persistent viruses in herbicide resistant wild-grasses. *Scientific reports, 7*, 41987.

Sadler, C., Schroll, B., Zeisler, V., Waßmann, F., Franke, R., & Schreiber, L. (2016). Wax and cutin mutants of Arabidopsis: quantitative characterization of the cuticular transport barrier in relation to chemical composition. *Biochimica et Biophysica Acta (BBA)-Molecular and Cell Biology of Lipids, 1861*(9), 1336-1344.

Samuels, L., Kunst, L., & Jetter, R. (2008). Sealing plant surfaces: cuticular wax formation by epidermal cells. *Annu. Rev. Plant Biol., 59*, 683-707.

Satchivi, N. M., & Myung, K. (2014). Modeling xenobiotic uptake and movement: A review. *Retention, uptake, and translocation of agrochemicals in plants*, 41-74.

Schmitt, V., Destribats, M., & Backov, R. (2014). Colloidal particles as liquid dispersion stabilizer: Pickering emulsions and materials thereof. *Comptes Rendus Physique, 15*(8-9), 761-774.

Schmittgen, T. D., & Zakrajsek, B. A. (2000). Effect of experimental treatment on housekeeping gene expression: validation by real-time, quantitative RT-PCR. *Journal of biochemical and biophysical methods, 46*(1-2), 69-81.

Schomburg, G., Behlau, H., Dielmann, R., Weeke, F., & Husmann, H. (1977). Sampling techniques in capillary gas chromatography. *Journal of Chromatography A, 142*, 87-102.

Schuler, M. A., & Werck-Reichhart, D. (2003). Functional genomics of P450s. *Annual review of plant biology, 54*(1), 629-667.

Schulz, B., & Kolukisaoglu, H. Ü. (2006). Genomics of plant ABC transporters: the alphabet of photosynthetic life forms or just holes in membranes? *FEBS letters, 580*(4), 1010-1016.

Seo, K., & Kim, M. (2015). Re-derivation of Young's equation, Wenzel equation, and Cassie-Baxter equation based on energy minimization *Surface Energy*: InTechOpen.

Sherwani, S. I., Arif, I. A., & Khan, H. A. (2015). Modes of action of different classes of herbicides. *Herbicides, Physiology of Action, and Safety, InTech*, 165-186.

Shukla, A., & Devine, M. D. (2008). Basis of crop selectivity and weed resistance to triazine herbicides. *The triazine herbicides, 50*, 111-118.

Shi, C., Zheng, Y., Geng, J., Liu, C., Pei, H., Ren, Y., Dong, Z., Zhao, L., Zhang, N., Chen, F,. Identification of herbicide resistance loci using a genome-wide association study and linkage mapping in Chinese common wheat. *The Crop Journal, 8* (4), 666-675

Singh, M., Orsenigo, J. R., & Shah, D. O. (1984). Surface tension and contact angle of herbicide solutions affected by surfactants. *Journal of the American Oil Chemists' Society, 61*(3), 596-600.

Sinha, K. K., Choudhary, A. K., & Kumari, P. (2016). Entomopathogenic fungi *Ecofriendly Pest Management for Food Security* (pp. 475-505): Elsevier.

Skopelitou, K., Muleta, A. W., Papageorgiou, A. C., Chronopoulou, E. G., Pavli, O., Flemetakis, E., . . . Labrou, N. E. (2017). Characterization and functional analysis of a recombinant tau class glutathione transferase GmGSTU2-2 from Glycine max. *International journal of biological macromolecules, 94*, 802-812.

Smith, D. J. (2008). Ultimate resolution in the electron microscope? *Materials Today, 11*, 30-38.

Spiridon, I., & Popa, V. I. (2005). Hemicelluloses: structure and properties. *Polysaccharides: structural diversity and functional versatility, 2*.

Stara, A., Kubec, J., Zuskova, E., Buric, M., Faggio, C., Kouba, A., & Velisek, J. (2019). Effects of S-metolachlor and its degradation product metolachlor OA on marbled crayfish (Procambarus virginalis). *Chemosphere, 224*, 616-625.

Sterling, T. M. (1994). Mechanisms of herbicide absorption across plant membranes and accumulation in plant cells. *Weed science, 42*(2), 263-276.

Sun, R. (2010). *Cereal straw as a resource for sustainable biomaterials and biofuels: chemistry, extractives, lignins, hemicelluloses and cellulose*: Elsevier.

Sun, R. C., & Tompkinson, J. (2003). Comparative study of organic solvent and water-soluble lipophilic extractives from wheat straw I: yield and chemical composition. *Journal of wood science, 49*(1), 0047-0052.

Svec, D., Tichopad, A., Novosadova, V., Pfaffl, M. W., & Kubista, M. (2015). How good is a PCR efficiency estimate: Recommendations for precise and robust qPCR efficiency assessments. *Biomolecular detection and quantification, 3*, 9-16.

Svyantek, A. W., Aldahir, P., Chen, S., Flessner, M. L., McCullough, P. E., Sidhu, S. S., & McElroy, J. S. (2016). Target and nontarget resistance mechanisms induce annual bluegrass (Poa annua) resistance to atrazine, amicarbazone, and diuron. *Weed Technology, 30*(3), 773-782.

Swindell, W. R. (2006). The association among gene expression responses to nine abiotic stress treatments in Arabidopsis thaliana. *Genetics, 174*(4), 1811-1824.

Taiz, L., Zeiger, E., Møller, I. M., & Murphy, A. (2015). Plant physiology and development.

Terescenco, D., Hucher, N., Savary, G., & Picard, C. (2019). From interface towards organised network: Questioning the role of the droplets arrangements in macroscopically stable O/W emulsions composed of a conventional non-ionic surfactant, TiO2 particles, or their mixture. *Colloids and Surfaces A: Physicochemical and Engineering Aspects, 578*, 123630.

Tétard-Jones, C., Sabbadin, F., Moss, S., Hull, R., Neve, P., & Edwards, R. (2018). Changes in the proteome of the problem weed blackgrass correlating with multiple-herbicide resistance. *The Plant Journal, 94*(4), 709-720.

Thellin, O., Zorzi, W., Lakaye, B., De Borman, B., Coumans, B., Hennen, G., . . . Heinen, E. (1999). Housekeeping genes as internal standards: use and limits. *Journal of biotechnology, 75*(2-3), 291-295.

Thom, R., Cummins, I., Dixon, D. P., Edwards, R., Cole, D. J., & Lapthorn, A. J. (2002). Structure of a tau class glutathione S-transferase from wheat active in herbicide detoxification. *Biochemistry, 41*(22), 7008-7020.

Tissot, E., Rochat, S., Debonneville, C., & Chaintreau, A. (2012). Rapid GC-FID quantification technique without authentic samples using predicted response factors. *Flavour and fragrance journal, 27*(4), 290-296.

Tominack, R. L., & Tominack, R. (2000). Herbicide formulations. *Journal of Toxicology: Clinical Toxicology, 38*(2), 129-135.

Tranel, P. J., & Wright, T. R. (2002). Resistance of weeds to ALS-inhibiting herbicides: what have we learned? *Weed science, 50*(6), 700-712.

Travlos, I. S., Gkotsi, T., Roussis, I., Kontopoulou, C.-K., Kakabouki, I., & Bilalis, D. J. (2017). Effects of the herbicides benfluralin, metribuzin and propyzamide on the survival and weight of earthworms (Octodrilus complanatus). *Plant, Soil and Environment, 63*(3), 117-124.

Trivedi, P., Karppinen, K., Klavins, L., Kviesis, J., Sundqvist, P., Nguyen, N., . . . Väänänen, J. (2019). Compositional and morphological analyses of wax in northern wild berry species. *Food chemistry, 295*, 441-448.

Tu, M., & Randall, J. M. (2003). Adjuvants. *TU, M. et al. Weed control methods handbook the nature conservancy. Davis: TNC*, 1-24.

Tulloch, A. P., & Hoffman, L. L. (1973). Leaf wax of Triticum aestivum. *Phytochemistry, 12*(9), 2217-2223.

Van Eerd, L. L., Hoagland, R. E., Zablotowicz, R. M., & Hall, J. C. (2003). Pesticide metabolism in plants and microorganisms. *Weed science, 51*(4), 472-495.

Vieira, B.C., Luck, J.D., Amundsen, K.L., Werle, R., Gaines, T.A., & Kruger, G.R. (2020). Herbicide drift exposure leads to reduced herbicide sensitivity in Amaranthus spp. *Scientific Reports, 10 (2146)*.

Vila-Aiub, M. M., Neve, P., & Powles, S. B. (2009). Fitness costs associated with evolved herbicide resistance alleles in plants. *New Phytologist, 184*(4), 751-767.

Voragen, A. G. J., Coenen, G.-J., Verhoef, R. P., & Schols, H. A. (2009). Pectin, a versatile polysaccharide present in plant cell walls. *Structural Chemistry, 20*(2), 263.

Wang, C. J., & Liu, Z. Q. (2007). Foliar uptake of pesticides—present status and future challenge. *Pesticide Biochemistry and Physiology, 87*(1), 1-8.

Wang, G. F., Wei, X., Fan, R., Zhou, H., Wang, X., Yu, C., . . . Kang, Z. (2011). Molecular analysis of common wheat genes encoding three types of cytosolic heat shock protein 90

(Hsp90): functional involvement of cytosolic Hsp90s in the control of wheat seedling growth and disease resistance. *New Phytologist, 191*(2), 418-431.

Wang, J.-D., Bao, H.-J., Shi, H.-Y., & Wang, M.-H. (2010). Development of an enzyme-linked immunosorbent assay for quantitative determination of cyhalofop-butyl. *Pesticide Biochemistry and Physiology, 98*(1), 68-72.

Westra, P. M. a. P. (1998). Herbicide Surfactants and Adjuvants. *Crop Series*.

Whistler, R. L. (1993). Hemicelluloses *Industrial gums* (pp. 295-308): Elsevier.

Wiwattanapatapee, R., Sae-Yun, A., Petcharat, J., Ovatlarnporn, C., & Itharat, A. (2009). Development and evaluation of granule and emulsifiable concentrate formulations containing Derris elliptica extract for crop pest control. *Journal of agricultural and food chemistry, 57*(23), 11234-11241.

Wu, J., Wang, K., Zhang, Y., & Zhang, H. (2014). Determination and study on dissipation and residue determination of cyhalofop-butyl and its metabolite using HPLC-MS/MS in a rice ecosystem. *Environmental monitoring and assessment, 186*(10), 6959-6967.

Wu, P., Han, Z., Mo, W., Wu, X., Chen, Z., Zhang, Y., . . . Sun, H. (2019). Soybean processing wastewater supported the removal of propyzamide and biochemical accumulation from wastewater by Rhodopseudomonas capsulata. *Bioprocess and biosystems engineering*, 1-10.

Xu, L.-y., Zhu, H.-p., Ozkan, H. E., Bagley, W. E., Derksen, R. C., & Krause, C. R. (2010). Adjuvant effects on evaporation time and wetted area of droplets on waxy leaves. *Transactions of the ASABE, 53*(1), 13-20.

Ye, F., Zhai, Y., Guo, K.-L., Liu, Y.-X., Li, N., Gao, S., . . . Fu, Y. (2019). Safeners improve maize tolerance under herbicide toxicity stress by increasing the activity of enzymes in vivo. *Journal of agricultural and food chemistry*.

Zhang, C., Wohlhueter R., Zhang, H., Genetically modified foods: A critical review of their promise and problems. *Food Science and Human Wellness, 5* (3), 116-123.

Zhang, H. (2016). Surface characterization techniques for polyurethane biomaterials *Advances in polyurethane biomaterials* (pp. 23-73): Elsevier.

Zhang, W., Jiang, F., & Ou, J. (2011). Global pesticide consumption and pollution: with China as a focus. *Proceedings of the International Academy of Ecology and Environmental Sciences, 1*(2), 125.

Zhao, B., Hua, X., Wang, F., Dong, W., Li, Z., Yang, Y., . . . Wang, M. (2015). Biodegradation of propyzamide by Comamonas testosteroni W1 and cloning of the propyzamide hydrolase gene camH. *Bioresource technology, 179*, 144-149.

Zimdahl, R. L. (2018). *Fundamentals of weed science*: Academic press.

Ziv, C., Zhao, Z., Gao, Y. G., & Xia, Y. (2018). Multifunctional roles of plant cuticle during plant-pathogen interactions. *Frontiers in plant science, 9*, 1088.